Defect Correction Methods for the Solution of Singularly Perturbed Convection-Diffusion Problems

A Thesis
Submitted for the award of degree of
Doctor of Philosophy
in Mathematics

by

Monika Choudhary
(2K18/PHD/AM/03)

Under the supervision of
Prof. Aditya Kaushik

Department of Applied Mathematics
Delhi Technological University
Bawana Road, Delhi 110042 (India)

3 December 2023

To my parents.

Certificate

Department of Applied Mathematics
Delhi Technological University, Delhi

This is to certify that the research work embodied in the thesis entitled "Defect Correction Methods for the Solution of Singularly Perturbed Convection-Diffusion Problems" submitted by Monika Choudhary (2K18/PHD/AM/03) is the result of her original research carried out in the Department of Applied Mathematics, Delhi Technological University, Delhi, for the award of **Doctor of Philosophy** under the supervision of **Prof. Aditya Kaushik**.

It is further certified that this work is original and has not been submitted in part or fully to any other university or institute for the award of any degree or diploma.

This is to certify that the above statement made by the candidate is correct to the best of our knowledge.

Date: 3 December 2023
Place: Delhi , India

Prof. Aditya Kaushik
(Supervisor)

Prof. S. Siva Prasad Kumar
(Head of Department)

Declaration

I declare that the research work in this thesis entitled "**Defect Correction Methods for the Solution of Singularly Perturbed Convection-Diffusion Problems**" for the award of the degree of ***Doctor of Philosophy in Mathematics*** has been carried out by me under the supervision of ***Prof. Aditya Kaushik***, Department of Applied Mathematics, Delhi Technological University, Delhi, India, and has not been submitted by me earlier in part or full to any other university or institute for the award of any degree or diploma.

I declare that this thesis represents my ideas in my own words and where others' ideas or words have been included, I have adequately cited and referenced the original sources. I also declare that I have adhered to all principles of academic honesty and integrity and have not misrepresented or fabricated or falsified any idea/data/fact/source in my submission.

Monika Choudhary
(2K18/PHD/AM/03)

Date: 3 December 2023

Acknowledgements

First and foremost, I would like to express my sincere and profound gratitude to my PhD supervisor, Prof. Aditya Kaushik, for his invaluable guidance, scholarly contributions, and consistent encouragement throughout the PhD. His tireless work ethic, patience, and dedication have strongly encouraged me. I could not have imagined a better advisor and mentor for my PhD work.

Next, I want to convey my sincere thanks to the Head of the Department and other department faculty members for their constant support and for encouraging me to pursue a PhD. I would also like to express my appreciation to the departmental staff members for their assistance during the period.

I am indebted to my parents for all their love and support. I would like to express my heartfelt gratitude towards my parents for everything they have done for me over the years. I would also like to express my gratitude to my sister and my close friends for their encouragement and support during my research.

Finally, I express my gratitude to the almighty God for his blessings and help throughout the PhD.

Monika Choudhary
DTU Delhi

Abstract

This thesis provides efficient and higher-order methods for solving singular convection-diffusion perturbation problems. A differential equation is singularly perturbed when some or all of its highest-order derivatives are multiplied by a small parameter, known as the perturbation parameter. When limiting the perturbation parameter to a value of zero, the solution to such problems reveals a multiscale character, which adds stiffness to the problem. This results in the formation of boundary layers. In these layers, the physical variable varies rapidly across small domains. As a result of the presence of layer phenomena, theoretical methods cannot accurately approximate the solution. These methods are only pertinent to a subset of problems, and prior knowledge of the solution's behaviour is required. Consequently, it is an intriguing task to develop uniform numerical methods for solving such problems.

This thesis aims to develop higher-order defect correction methods for the solution of four distinct kinds of convection-diffusion problems. Combining a stable, low-order, precise, and computationally inexpensive upwind difference scheme with a higher-order, less stable modified central difference operator is possible in these methods. In addition to being free of directional bias, the process is also unconditionally stable and converges uniformly. This technique can be utilised in an adaptive procedure to refine the mesh in non-smooth regions. For a convection-diffusion problem, a defect correction method over an adaptive mesh produces uniform second-order convergence. For a convection-diffusion problem with a discontinuous coefficient and point source, a defect correction method combining a simple upwind scheme and a central difference scheme at all mesh points over the Bakhvalov Shishkin mesh is studied. A posteriori error estimates are established, yielding second-order convergence at all mesh points. Then, a parabolic convection-diffusion problem with a large shift is solved by utilising an implicit Euler scheme in time variable on a uniform mesh and a defect correction method comprised of the upwind scheme and the modified central difference scheme in space variable on a non-uniform mesh. The second order of spatial convergence and the first order of temporal convergence are obtained. Finally, a parabolic convection-diffusion problem with

a discontinuous convection coefficient and a source is solved using an implicit difference scheme in time on a uniform mesh and a defect correction scheme based on a finite difference discretisation over an adaptive mesh in space. Estimates of parameter uniform error reveal uniform convergence of first-order in time and second-order in space. Based on the contribution of this study, we suggest future research directions for analysing more complex problems.

Table of Contents

List of Figures

List of Tables

Chapter 1

Introduction

1.1 Perturbation Theory

Differential equations are ubiquitous in mathematical modelling and describe various physical processes in science and engineering. By expressing the relationship between the rate of change of a variable and the variable itself, differential equations provide a powerful tool for understanding and predicting how systems evolve over time and space. They allow us to solve and analyse complex problems associated with the underlying physical phenomena and provide insight into the behaviour and dynamics of the corresponding systems. Their significance spans various disciplines, making them an indispensable tool for scientific inquiry and technological advancement.

In scientific disciplines, when dealing with mathematical models of physical phenomena, we often attempt to deal with the essential quantities while ignoring the negligible ones that involve small parameters. However, a natural question concerning the role of the omitted terms arises. Does the presence or omission of such terms affect the solution or the information obtained from the mathematical model? Perturbation theory helps us answer this. It is a mathematical framework employed to analyse and understand the effects of disturbances or changes in a system due to these small parameters known as perturbation parameters. It allows researchers to refine their understanding of systems by considering both the simplified, unperturbed models and the more complex, perturbed counterparts. This approach plays a crucial role in fields such as physics, engineering, and applied mathematics, offering a nuanced perspective on the behaviour of systems in the presence of subtle influences. The perturbation problems are categorised broadly into regular and singular perturbation problems.

Let $\mathcal{D}$ be an open bounded set with smooth boundary Γ and $\bar{\mathcal{D}}$ denotes its closure. Consider the boundary value problem

$$\mathcal{P}_\varepsilon : \mathcal{L}_\varepsilon u := \mathcal{L}_0 + \varepsilon \mathcal{L}_1 = f(x, \varepsilon); \quad x \in \mathcal{D} \text{ and } u(\Gamma) \text{ is given.} \tag{1.1.1}$$

Here ε is a small parameter such that $0 < \varepsilon \ll 1$, $\mathcal{L}_\varepsilon$ is a differential operator, and $f(x, \varepsilon)$ is a given real-valued smooth function. We assume that, for each ε, $\mathcal{P}_\varepsilon$ has a unique smooth solution $u := u_\varepsilon(x)$. Denote by $\mathcal{P}_0$ the corresponding degenerate equation obtained by setting $\varepsilon = 0$ in (1.1.1) and by u_0 the smooth solution of $\mathcal{P}_0$.

Definition 1.1.1. Problem $\mathcal{P}_\varepsilon$ is called regularly perturbed with respect to some norm $\| \cdot \|$ if there exists a solution u_0 of problem $\mathcal{P}_0$ such that

$$\| u_\varepsilon - u_0 \| \to 0 \text{ as } \varepsilon \to 0.$$

Otherwise, $\mathcal{P}_\varepsilon$ is said to be singularly perturbed with respect to the same norm.
Here $\| \cdot \|$ is the supremum norm (or maximum norm) defined for every continuous function $g : \bar{\Omega} \to \mathbb{R}$ as

$$\| g \|_{\bar{\Omega}} = \sup \left\{ |g(x)| : x \in \bar{\Omega} \right\}.$$

Example 1.1.2. Consider the algebraic problem $\mathcal{P}_\epsilon$:

$$5x_\epsilon^2 + \epsilon x_\epsilon - 3 = 0, \quad 0 < \epsilon \ll 1. \tag{1.1.2}$$

The roots of $\mathcal{P}_\epsilon$ reads

$$x_\epsilon = \frac{-\epsilon \pm \sqrt{\epsilon^2 + 60}}{10}. \tag{1.1.3}$$

It follows from (1.1.3) that as $\epsilon \to 0$, the roots x_ϵ become $\pm\sqrt{\frac{3}{5}}$. Clearly, $x_\epsilon = \pm\sqrt{\frac{3}{5}}$ are the roots of the corresponding degenerate problem $\mathcal{P}_0$. Thus, $\mathcal{P}_\epsilon$ is a regular perturbation problem.

Example 1.1.3. Consider the boundary value problem $\mathcal{P}_\epsilon$:

$$u_\epsilon''(x) + 2\epsilon u_\epsilon'(x) - 4u_\epsilon(x) = 0 \text{ with } u_\epsilon(0) = 0,\ u_\epsilon(1) = 1 \text{ and } 0 < \epsilon \ll 1. \tag{1.1.4}$$

The solution of $\mathcal{P}_\epsilon$ reads

$$u(x) := u_\epsilon(x) = \frac{e^{\lambda_1 x} - e^{\lambda_2 x}}{e^{\lambda_1} - e^{\lambda_2}}, \text{ where } \lambda_1 = -\epsilon + \sqrt{\epsilon^2 + 4},\ \lambda_2 = -\epsilon - \sqrt{\epsilon^2 + 4}. \tag{1.1.5}$$

Moreover, note that $\lim_{\epsilon \to 0} u_\epsilon = \dfrac{\sinh(2x)}{\sinh(2)} := u_0$. Clearly, u_0 is the solution of the corresponding degenerate problem $\mathcal{P}_0$. Thus, $\mathcal{P}_\epsilon$ is a regular perturbation problem.

Example 1.1.4. Consider the boundary value problem $\mathcal{P}_\epsilon$:

$$-\epsilon u_\epsilon''(x) + u_\epsilon'(x) = 1,\ x \in (0,1) \text{ with } u(0) = u(1) = 1 \text{ and } 0 < \epsilon \ll 1. \tag{1.1.6}$$

The solution of $\mathcal{P}_\epsilon$ reads

$$u(x) := u_\epsilon(x) = x - \frac{e^{\left(-\frac{1-x}{\epsilon}\right)} - e^{\left(-\frac{1}{\epsilon}\right)}}{1 - e^{\left(-\frac{1}{\epsilon}\right)}}. \tag{1.1.7}$$

The solution u_ϵ considered as function of two variables $u_\epsilon : [0,1] \times (0,1) \to u(x,\epsilon)$ satisfies

$$\lim_{x\to p}\lim_{\epsilon\to 0} u(x,\epsilon) = p = \lim_{\epsilon\to 0}\lim_{x\to p} u(x,\epsilon),\ \forall p \in [0,1).$$

Although

$$\lim_{x\to 1}\lim_{\epsilon\to 0} u(x,\epsilon) = 1 \neq 0 = \lim_{\epsilon\to 0}\lim_{x\to 1} u(x,\epsilon).$$

The solution u_ϵ as a function of two variables exhibits a singularity at the point $(1,0)$ in the (x,ϵ)-plane. Since, $\|u_\epsilon - u_0\| \nrightarrow 0$ uniformly throughout the entire domain as ϵ approaches zero, $\mathcal{P}_\epsilon$ is a singular perturbation problem.

Perturbation theory becomes a powerful ally when navigating the complexities of convection-diffusion problems, where the interplay of transport phenomena poses a unique set of challenges. In mathematical modelling for fluid dynamics and heat transfer, convection and diffusion are key players, each influencing the system in distinct ways. In this context, perturbation theory allows us to dissect these complex problems by introducing small parameters that capture nuances in the convective and diffusive processes. The tailored approach proves invaluable in fields ranging from environmental science to engineering, offering a lens through which we can unravel the layered dynamics of fluid flow and heat transfer.

1.2 Singular Perturbation Problems

Singular perturbation problems (SPPs) are of common occurrence in nature. Typically these problems arise in modelling of various complex phenomena such as chemical-reactor theory [187], bio-chemical kinetics [157], gas porous electrodes theory [251], quantum mechanics [37], Reissner-Mindlin plate theory [11], Michaelis-Menton theory for enzyme reactions [197], drift diffusion equation of semiconductor device [250], diffraction theory [55], usimulation of oil extraction from underground reservoirs [73], magneto-hydrodynamics duct problems at Hartman number [91], atmospheric pollution [226], water quality crisis in river networks [34], mathematical model of liquid crystal material [203], heat transportation problems with large Peclet numbers [193], financial

modelling of option pricing and corporate liabilities [33], predator-prey population dynamics [153], optimum control problems in certain resistance-capacitor electrical circuits [136]. The study of singular perturbation problems is imperative because of their great practical value.

1.2.1 Historical Overview

Fluid mechanics in the 19th century developed in two directions: theoretical hydrodynamics and hydraulics. The former originated from Euler's equations for inviscid flows, reaching a high level of comprehensiveness. However, the results of this classical science starkly contrasted with experimental findings, illustrated by the famous contradiction of d'Alembert. The d'Alembert paradox was only resolved in a revolutionary 1904 paper by L. Prandtl, who showed that no matter how small the viscosity, viscous effects can never be neglected [10, 222]. More precisely, the determining factor is the Reynolds number *Re*, a dimensionless measure of the relative importance of inertial to viscous forces in the flow. Prandtl postulated that for certain kinds of high Reynolds numbers or nearly frictionless flows, for example, the flow past a streamlined body like an airfoil, the viscous effects would be confined to thin regions called boundary layers. In specific high *Re* flows, like the flow around a bluff body like a sphere, viscous effects aren't limited to thin layers. In these cases, the impact of viscosity is more dramatic than its low value might initially suggest.

However, the aerodynamic boundary layer was first defined by Prandtl [222]. Friedrichs and Wasow coined the term singular perturbation in their work [80]. In 1957, in a fundamental paper [284], M. I. Vishik and L .A. Lyusternik studied linear partial differential equations with singular perturbations, introducing the famous Vishik-Lyusternik method. From that moment on, an entire literature has been devoted to this subject [150, 138, 122, 117, 241]. The critical concept of boundary layers has now spread to many other fields; boundary layers often arise in what is known as singular perturbation problems [10, 222]. For a deeper dive into the historical overview, an introduction to Prandtl's resolution of the paradox concerning flow past a thin plate, and other classical examples, the interested reader is encouraged to explore an exciting general article "*Ludwig Prandtl and boundary layers in fluid flow-How a small viscosity can cause large effects*" by J. H. Arakeri and P. N. Shankar [10].

1.2.2 Classification of Singular Perturbation Problems

The singular perturbation problems are further classified into the following two broad categories:

1. **Singular perturbation problem of cumulative type:** These problems are characterised by a small perturbation parameter ϵ whose effect becomes apparent after a substantial period, generally after an interval of order $O\left(\frac{1}{\epsilon}\right)$. For example, consider the motion of a satellite orbiting the Earth, where the spherically symmetric gravitational field is the dominating force. The satellite's motion would be periodic if the gravitational field were the sole factor acting on it. However, small influencing forces from factors such as the thin atmosphere, moon, distant sun, and other stars significantly alter the satellite's motion after many orbital revolutions due to their cumulative effect.

2. **Singular perturbation problem of layer type:** Characterised by a small perturbation parameter ϵ, these problems exhibit small spatial regions known as layer regions where the solution undergoes abrupt variations. The solution unveils a multiscale character, introducing stiffness to the problem over a short interval. Meanwhile, away from these layers, the solution behaves regularly and varies gradually. The classification of these problems further depends on the location of the layers, leading to different categories.

   (a) **Singular perturbation problems of boundary layer type:** In these problems, the layer region is adjacent to the boundary of the domain. Researchers commonly refer to this region as the boundary layer, a term Prandtl originally introduced in fluid mechanics. Shock waves are another term for these phenomena in gas dynamics. These layers are typically known as skin layers in electric applications. On the other hand, in mathematics, it sometimes goes by the name of Stoke's surfaces.

   (b) **Singular perturbation problems of interior layer or free layer type:** In these problems, the layers are located within the domain, away from the borders. Therefore, these layers are sometimes known as interior layers or free layers. Several factors might cause the occurrence of these interior layers, including turning points, non-smooth coefficients, non-smooth initial/boundary conditions, non-linearities, or a lack of borders.

In this thesis, we consider singular perturbation problems of layer type. It is crucial to determine the actual location, width and strength of all the existing layers within the solution to determine the solution to the problem [212]. The characteristics of the layers, including their strength, width, and location, depend on whether the singular perturbation problem is of convection-diffusion or reaction-diffusion type. The coefficients and ini-

tial/boundary conditions stated in the problem also play an essential role. We will now, therefore, look at the classification of singular perturbation problems as follows:

1. **Convection-diffusion problems:** Convection-diffusion problems model physical phenomena involving convection, reaction, and diffusion processes. In these problems, the order of the degenerate equation reduces by one. Let us consider a two-point boundary value problem on a unit interval $\Omega = (0, 1)$

$$\begin{cases} -\varepsilon u_\varepsilon''(x) + u_\varepsilon'(x) = 0, \ x \in \Omega \\ u_\varepsilon(0) = u_0, \quad u_\varepsilon(1) = u_1, \end{cases}$$

where $u_0, u_1 \in \mathbb{R}$ are some given constants and $0 < \varepsilon \ll 1$. The exact solution of the problem is $u_\varepsilon(x) = \dfrac{u_1 e^{-1/\varepsilon} - u_0}{e^{-1/\varepsilon} - 1} + \dfrac{u_0 - u_1}{e^{-1/\varepsilon} - 1} e^{-(1-x)/\varepsilon}$. The corresponding degenerate equation is of order one, and we can impose only one boundary condition. It needs to be clarified which of the two possible boundary conditions we can impose. Since the characteristic direction aligns with the positive x-axis, we cannot impose a boundary condition at $x = 1$. The corresponding degenerate problem reads

$$\begin{cases} v_0'(x) = 0, \ x \in \Omega \\ v_0(0) = u_0, \end{cases}$$

and its solution is $v_0(x) = u_0$. Therefore, a boundary layer will form near $x = 1$ unless the boundary value of u_ε at $x = 1$ agrees with the value of the reduced solution v_0 at $x = 1$. Thus we may say that the solution exhibit only one boundary layer of width ε in the neighbourhood of $x = 1$.

2. **Reaction-diffusion problems:** Reaction-diffusion problem models physical phenomena involving both reaction and diffusion processes. In these types of problems, the order of the degenerate equation reduces by two. Let us consider a two-point boundary value problem defined on a unit interval $\Omega = (0, 1)$

$$\begin{cases} -\varepsilon u_\varepsilon''(x) + u_\varepsilon(x) = 0, \ x \in \Omega \\ u_\varepsilon(0) = u_0, \quad u_\varepsilon(1) = u_1, \end{cases}$$

where $u_0, u_1 \in \mathbb{R}$ are the given constants and $0 < \varepsilon \ll 1$. The exact solution of the problem is $u_\varepsilon(x) = \dfrac{u_1 - u_0 e^{-1/\sqrt{\varepsilon}}}{1 - e^{-2/\sqrt{\varepsilon}}} e^{-(1-x)/\sqrt{\varepsilon}} + \dfrac{u_0 - u_1 e^{-1/\sqrt{\varepsilon}}}{1 - e^{-2/\sqrt{\varepsilon}}} e^{-x/\sqrt{\varepsilon}}$. Note that the corresponding degenerate equation has order zero. Consequently, we cannot impose any boundary conditions on its solution. The exact solution of the degenerate equation is $v_0(x) = 0$. Therefore, a boundary layer will appear at $x = 0$ unless $u_0 = 0$.

Similarly, a boundary layer will occur at $x = 1$ unless $u_1 = 0$. The layer correction function $e^{-x/\sqrt{\varepsilon}}$ in the solution suggests that the solution has a steep gradient in $(0, \sqrt{\varepsilon})$ but not in $(\sqrt{\varepsilon}, 1)$. The behaviour of $e^{-(1-x)/\sqrt{\varepsilon}}$ is analogous. Therefore, we may have two boundary layers of width $\sqrt{\varepsilon}$, each at outflow boundary regions. However, one or no boundary layer may occur for special choices of boundary conditions.

In this thesis, we study singular perturbation problems of convection-diffusion type. To gain an understanding of the strength and location of layers in the solution of convection-diffusion problems, consider the model convection-diffusion problem defined on a unit interval $(0, 1)$

$$-\epsilon u''(x) + a(x)u'(x) + b(x)u(x) = g(x), \ x \in (0, 1) \tag{1.2.1}$$

where $0 < \epsilon \ll 1$ is the perturbation parameter and appropriate boundary conditions are specified. The rules presented in Table 1.1 serve as a valuable resource for inferring information regarding the strength and location of boundary and interior layers appearing in the solution of the problem (1.2.1). If $a(x) = 0$, the problem (1.2.1) transforms into a reaction-diffusion problem. In that case, Table 1.2 provides helpful information regarding the strength and location of the interior and boundary layers in the solution for reaction-diffusion equations.

1.3 Methods for Solving Singular Perturbation Problems

To solve singularly perturbed problems, researchers commonly employ two principal methods: asymptotic methods and numerical methods.

1.3.1 Asymptotic Methods

The asymptotic methods are widely used in mathematics to obtain precise approximations for solving singular perturbation problems. These methods offer a straightforward approach to accurately determining an approximation for the solution. In this study, the analysis of the problem's limiting behaviour is conducted through asymptotic expansion methods. The solution is then approximated by constructing an asymptotic series, which is expressed in terms of the small perturbation parameter ϵ, such as

$$u = u_0 + \epsilon u_1 + \epsilon^2 u_2 + \cdots .$$

Table 1.1: **Strength and location of boundary and interior layers for singularly perturbed convection-diffusion problems**

Smoothness of functions			**Value of the function**	**Strength and location of**	
$b(x)$	$a(x)$	$f(x)$	$a(x)$	**Boundary Layer**	**Interior Layer**
Smooth			$< 0, \forall x \in \overline{\Omega}$	Strong, at $x = 0$	—
Smooth			$> 0, \forall x \in \overline{\Omega}$	Strong, at $x = 1$	—
Smooth		Discontinuous at $x = d \in \Omega$	$< 0, \forall x \in \overline{\Omega}$	Strong, at $x = 0$	Weak, on right side of $x = d$
Smooth		Discontinuous at $x = d \in \Omega$	$> 0, \forall x \in \overline{\Omega}$	Strong, at $x = 1$	Weak, on left side of $x = d$
Smooth	Discontinuous at $x = d \in \Omega$		$< 0, \forall x \in \overline{\Omega}$	Strong, at $x = 0$	Weak, on right side of $x = d$
Smooth	Discontinuous at $x = d \in \Omega$		$> 0, \forall x \in \overline{\Omega}$	Strong, at $x = 1$	Weak, on left side of $x = d$
Smooth	Discontinuous at $x = d \in \Omega$		$> 0, x \in (0, d)$ and $< 0, x \in (d, 1)$	—	Strong, on both side of $x = d$
Smooth	Discontinuous at $x = d \in \Omega$		$< 0, x \in (0, d)$ and $> 0, x \in (d, 1)$	Solution is unbounded	
—			$= 0$	SPP is of reaction-diffusion type	

Table 1.2: **Strength and location of boundary and interior layers for singularly perturbed reaction-diffusion problems**

Smoothness of functions		**Strength and location of**	
$b(x)$	$f(x)$	**Boundary Layer**	**Interior Layer**
Smooth		Strong, at both endpoints $x = 0$ and $x = 1$	—
Smooth	Discontinuous at $x = d \in \Omega$	Strong, at both endpoints $x = 0$ and $x = 1$	Strong, on both sides of $x = d$

Here u_0, u_1, $u_2, \cdots$ are sufficiently smooth functions. The values of u_0, u_1, $u_2, \cdots$ can be obtained by substituting u into the given equation after doing term-by-term differentiation. After substitution, the first few terms are solved to get $u_0,\ u_1,\ u_2, \cdots$ and form an approximate solution to the problem. The asymptotic solution accurately approximates the solution to the problem over a large portion of the domain, i.e., the outer region, but is inaccurate over the small region, i.e., the layer region, because the effect of the perturbation term in the problem is not negligible in this region. However, the straightforward asymptotic expansion leads to a differential equation of lower order than the original differential equation, and the solution fails to satisfy all the boundaries or the initial conditions.

Thus, the method of asymptotic expansion fails to adequately approximate the exact solution of the singular perturbation problem. This limitation of the asymptotic expansion method is removed by using the following methods:

1. **Method of matched asymptotic expansions:** This methodology involves obtaining two complementary solutions within their respective regions, namely inner solution and outer solution, by treating a specific portion of the domain as a distinct perturbation problem. In subsequent steps, the solutions obtained from various regions within the domain are patched or matched to obtain an approximate solution that encompasses the entire domain. The process of matching the inner and outer solutions was initiated through the utilisation of a stretching transformation [79]. In the 1950s, researchers refined and implemented this method to address various physical problems [155, 151, 208, 125, 126, 285, 286]. One can refer to the following literature to gain a deeper understanding of this method: [280, 210, 135].

2. **Method of multiple scales:** This method focuses on developing uniformly valid approximations for solving singular perturbation problems by applying multiple scales for the independent variable. Including additional terms involves introducing new independent variables to eliminate secular terms and ascertain a uniformly approximate solution. Cole [31] introduced this idea in the late 1950s, and has since been thoroughly investigated and analysed in various examples. After that, this approach has been extensively applied in solving a number of singular perturbation problems, as documented in various studies [134, 110, 152, 259, 60, 54, 28]. The multiple scales method has been found to provide a notable advantage when solving nonlinear problems [148]. However, introducing additional slow scales can lead to potential ambiguities in the perturbation series solution, which must be carefully addressed, as demonstrated in [31].

3. **WKB approximation:** This method is employed to obtain a global approximation for solving linear singular perturbation problems. The proposed methodology suggests an exponential dependence of the solution on the boundary layer, a valid assumption for linear singular perturbation problems. This assumption greatly simplifies obtaining an asymptotic approximation for the solution. The methodology entails first identifying an approximate set of linearly independent solutions combined using the superposition principle to generate a general solution. In contrast to other asymptotic approaches, such as matched asymptotic expansions or multiple scales, the boundary conditions are generally solved exactly at the end of the process rather than being approximated. This method, known as the Wentzel-Kramers-Brillouin (WKB) method, was first utilised in the 1920s to approximate solutions to the Schrödinger equation. The method's historical development is documented in [104], whereas reference [249] provides extensive mathematical details. The WKB method has been widely employed in quantum and solid mechanics, as shown by its applications in the respective fields [37] and [266]. Moreover, this approach has been extensively employed in solving various singular perturbation problems [92, 143, 2].

4. **Other Methods:** In addition to the aforementioned prominent asymptotic methods, several other asymptotic methods can be applied to both linear and nonlinear problems. For linear problems, some of these methods include the Poincaré-Lindstedt method [137, 214, 30, 181, 44, 201], the method of strained parameters [202, 258, 265], the method of periodic averaging [53, 124, 4], and the linearised perturbation method. For nonlinear problems, there are methods such as the variational iteration method [100, 103], the modified Poincaré-Lindstedt method [101, 174, 227, 6], the homotopy perturbation method [207, 102, 1], the parameter expansion method [239, 291] and the perturbation-iteration methods [12, 184, 203]. Books [282, 263, 31, 209] contain more information on the progressive developments in the asymptotic theory of singular perturbations.

The asymptotic expansion method applies to a limited range of problems and necessitates the user's knowledge of the location and width of the boundary layer. Furthermore, this method must be optimally designed to solve two-dimensional problems efficiently. The validity of the asymptotic approximation for complex one-dimensional nonlinear problems is limited to small perturbation parameter values. One must thoroughly understand the expected solution behaviour to implement these methods successfully. This serves as

a source of motivation for individuals to employ numerical methods to solve such problems.

1.3.2 Numerical Methods

Numerical methods are employed to obtain an approximate solution for problems that are typically unsolvable using closed-form solutions. These methods are designed to solve a wide range of problems and offer quantitative information about the problem. Because these methods are quantitative, their solutions differ significantly from the qualitative solutions provided by asymptotic methods.

Over the last few decades, researchers have developed several numerical approaches for solving singular perturbation problems. Computational methods and parameter uniform numerical methods are two broad categories for these methods. When the perturbation parameter is set to a critical value, the standard finite difference, finite element, or finite volume methods, collectively called classical computational methods, are found to be insufficient on uniform meshes and require an extremely large number of mesh points to generate accurate numerical solutions [99]. The reason behind this limitation of the computational methods is the presence of steep gradients in the boundary layer(s) of the analytical solution. These methods fail to reduce the maximum point-wise error until the mesh size and the singular perturbation parameter have the same order of magnitude. On the other hand, refining the mesh size to the order of the perturbation parameter increases the number of mesh points and the related computing cost. Hence, the major constraint of the computational method is the domain discretization's dependency on the perturbation parameter. Therefore, to construct robust computational methods that are independent of the perturbation parameter in terms of discretization, error, and order of convergence is desirable. These methods are known as parameter uniform numerical methods. The parameter uniform methods are broadly classified into two main categories: the fitted finite difference operator and the fitted mesh method.

A brief survey enumerating the chronological developments in both classical computational methods and parameter-uniform numerical methods is as follows.

1. **Finite Difference Methods :** The finite difference method (FDM) is a widely recognised and commonly used approach for estimating the solution of a singular perturbation problem. It is a straightforward technique that has been extensively studied and applied in various fields of research. The introduction of numerical applications can be traced back to the late 1960s, aligning with the minicomputers. These minicomputers offered a convenient platform for tackling complex problems. The

discretization technique employed in this method involves partitioning the domain of interest into a mesh or grid. In the process, the differential equation is transformed by substituting all the derivatives with algebraic differential quotients. For example, the derivative $\frac{dz}{dx}$ may be replaced by first-order forward difference quotient

$$\left.\frac{dz}{dx}\right|_i \approx \frac{z_{i+1} - z_i}{h}$$

or by a second-order central difference quotient

$$\left.\frac{dz}{dx}\right|_i \approx \frac{z_{i+1} - z_{i-1}}{2h}$$

where u_i is the value of u at the mesh point i and h is the mesh spacing. By substituting the derivatives at all interior mesh points with their corresponding values, a system of algebraic equations is formed, where $u_i's$ represent the unknowns. After implementing the boundary conditions, the system will exhibit a correspondence between the number of unknowns and interior nodes within the mesh. The values of these unknowns can be obtained by solving the system of equations by direct methods or iterative methods such as the Gauss-Seidel method, Jacobi method, Successive over-relaxation method, or other advanced techniques.

The development of a three-point difference scheme on a uniform mesh for a one-dimensional two-point singular perturbation boundary value problem was first introduced in [218]. The approach employed consisted of finding mesh regions where the difference between the computed solution and its adjacent value exceeded a predetermined threshold value. An iterative procedure was applied to increase the concentration of mesh points at these identified locations. Additionally, a smoothing approach was applied to mitigate the accuracy loss resulting from sudden changes in mesh spacing. The Gauss elimination method was employed to solve the system of linear algebraic equations that were derived from the difference scheme. The numerical results obtained, demonstrate that the computed solution converged to the exact solution. Later, this method is extended to solve a class of nonlinear problems [219]. These methods require strict constraints on the mesh spacing to maintain stability when the perturbation parameter is very small. For example, consider the following singular perturbation boundary value problem:

$$-\epsilon u''(x) + a(x)u'(x) + b(x)u(x) = g(x),\ x \in (0,1),\ u(0) = u_0,\ u(1) = u_1.$$

Here ϵ is a perturbation parameter, $a(x)$, $b(x)$ and $g(x)$ are smooth functions satisfying $a(x), b(x) \geq 0$ on $(0, 1)$. It was discovered that the central difference scheme, implemented on a uniform mesh $\{x_i = ih\}$ with mesh spacing $(h = 1/N)$, becomes

unstable and oscillates when $a(x_i)h/2\epsilon > 1$ [62]. The authors proposed implementing an upwind scheme to solve the stability problem [113]. In this proposed scheme, the conventional first derivative is substituted with a one-sided difference method, either forward or backward, instead of the central difference approach. The selection between forward or backward difference depends upon the sign of $a(x)$ at a specific mesh point x_i. The scheme is referred to as the Il'in-Allen-Southwell scheme [5]. It was observed that the upwind scheme demonstrated stability and exhibited better convergence in comparison to the central difference scheme. The scheme under consideration is widely recognised as the first fitted operator scheme. However, it is important to note that this scheme does have certain limitations, it exhibits first-order uniform convergence in the outer region.

In [63], a class of SPPs is solved by using an upwind finite difference method. The author compared the asymptotic behaviour of the solution obtained from the difference scheme with the exact solution. Later, the authors extended this method to solve second-order ordinary differential equations [64]. They obtained elementary estimates for the solution and its derivatives by using the maximum principle [225]. In [3], the upwind method is further refined and used to solve SPPs with systems of equations. In this method, a parameter was introduced in the difference equation, and it was chosen in such a way that an accurate approximation for the reduced problem is obtained in the interior region as well. Later, this method is extended to solve SPPs with internal turning points [24].

In [13], the authors modified the upwind scheme to enhance its accuracy for convection-diffusion SPPs. This modified scheme achieved second-order accuracy, similar to the central difference scheme, while preserving the stability properties of the upwind scheme. This modification improved the accuracy of the solution and provided better convergence properties.

In [84], the author developed a family of uniformly accurate finite difference schemes for convection-diffusion SPPs using the high-order differences with identity expansion (HODIE) framework [177, 61]. The discretization error analysis was carried out using the stability results from [205]. The theoretical analysis showed that the uniform convergence of any order could be achieved, depending on the smoothness of the data. Achieving higher-order convergence with this scheme required additional evaluations of the data.

In [70], the exponential box scheme is introduced to solve singularly perturbed convection-diffusion problems. This scheme combined the exponential difference

operator [5] with Keller's box scheme [132] to achieve a stable and second-order accurate approximation of the solution. Later in [32], the authors proved that the exponential difference, when applied on a uniform mesh with a mesh size of h, provides uniformly second-order accuracy for solving convection-diffusion problems. This result demonstrated that the exponential box scheme is reliable and accurate across the entire computational domain, ensuring consistent second-order accuracy of the approximation.

In [75], it is shown that for convection-diffusion SPPs, the fitted finite difference operator is only necessary for the layer region, while the solution in the outer region can be accurately approximated using the standard fitted operator. This observation allowed for more efficient computation by reducing the computational cost in the outer region. In [76], the author investigated a variety of finite difference schemes to derive sufficient conditions for uniform convergence. He showed that these conditions are not only satisfied by uniformly convergent schemes but also by a more general class of upwind schemes.

In [17], the authors solved a singularly perturbed reaction-diffusion problem using the finite difference method on a non-uniform mesh. The non-uniform mesh was constructed by using a continuous mesh generating function $\psi : \bar{\Omega} \to [0, 1]$, which is defined as

$$\psi(t) = \begin{cases} \chi(t) := -\frac{\sigma\epsilon}{\beta} \ln(1 - t/q), & t \in [0, \tau], \\ \phi(t) := \chi(\tau) + \psi'(\tau)(t - \tau), & t \in [\tau, 1/2], \\ 1 - \psi(1 - t), & t \in (1/2, 1], \end{cases}$$

where the transition point τ is the solution of the nonlinear problem $(1 - 2\tau)\phi'(t) = 1 - 2\chi(\tau)$. The mesh generated by this method is known as the Bakhvalov mesh. This mesh is considered to have a complicated structure, and extending the mesh to solve the singularly perturbed partial differential equations (PDEs) is difficult.

In [255], the author developed a scheme based on the integro-interpolation method [246] to solve a class of singularly perturbed differential equations of ordinary type and parabolic type. The scheme was developed on a mesh similar to the Bakhvalov mesh and exhibited third-order convergence for ordinary differential equations and first-order convergence for partial differential equations. In [287], the author generalised the Bakhvalov mesh for the finite-difference discretization of one-dimensional nonlinear reaction-diffusion SPPs. This generalisation extended the use of the Bakhvalov mesh to handle nonlinear problems and achieved a uniform second-order convergence.

In [85], an exponentially graded mesh was employed for two-point singularly perturbed boundary value problems. The graded mesh divided the domain into three regions: the inner region with an extremely fine mesh, the transit region where the mesh geometry changes from fine to coarse, and the outer region with a uniform mesh. The number of mesh points in the inner region was significantly higher (approximately k times) than the number of mesh points in the outer region. Various finite difference schemes were applied on the graded mesh and uniform convergence of fourth-order was achieved. However, the complexity involved in creating the graded mesh made it challenging to extend the mesh to higher dimensions. Considering this limitation, in [256] G. I. Shishkin introduced a relatively simple mesh known as the Shishkin mesh, which could be conveniently extended to higher dimensions. For convection-diffusion problems, he proposed a piecewise uniform mesh with a transition point defined as $\tau = \min\left(\frac{1}{2}, \epsilon\tau_0 \ln N\right)$, where $\tau_0 \geq p/\alpha$. The parameter p characterises the order of convergence of the numerical method. The mesh $\bar{\Omega} = \{x_i\}_{i=0}^{N}$ is constructed by dividing both subintervals $[0, \tau]$ and $[\tau, 1]$ into $N/2$ equal subintervals if a boundary layer is present near the left endpoint of the domain. When $\epsilon\tau_0 \ln N > \frac{1}{2}$, (for sufficiently large N compared to $1/\epsilon$), this mesh transforms into a uniform mesh. Similarly, if there is a boundary layer near the right endpoint, the domain $\bar{\Omega}$ divided into $[0, 1-\tau]$ and $[1-\tau, 1]$ each with $N/2$ equal subintervals, to obtain a piecewise uniform mesh. For reaction-diffusion problems, the transition parameter τ is defined as $\tau = \min\left(\frac{1}{4}, \sqrt{\epsilon}\tau_0 \ln N\right)$, where $\tau_0 \geq p/\alpha$. A piecewise uniform mesh is constructed by discretizing the domain $\bar{\Omega} = [0, 1]$ into $[0, \tau]$, $[\tau, 1-\tau]$, $[1-\tau, 1]$, where the subintervals contain $N/4$, $N/2$ and $N/2$ equally spaced mesh points, respectively. It is important to note that one limitation of the Shishkin mesh is that it requires prior knowledge about the location and width of the boundary layers. All these meshes, Bakhvalov [17], Vulanović [287], Gartland [85], and Shishkin [256], are constructed based on a priori information about the width and location of the layers in the exact solution and are thus known as apriori meshes.

In [179], the author introduced a posteriori mesh, which does not require prior information about the width and location of the layers in the exact solution. The method involves computing an approximate solution on an arbitrary mesh and then using the error estimate, based on the difference derivatives of the computed solution to determine a monitor function. This monitor function helps in achieving mesh equidistribution. Authors in [26] further developed this idea by proposing a monitor function that combines a constant term with an appropriate power of the second

derivative of the singular component of the solution. This choice of monitor function improved the mesh equidistribution and enhanced the accuracy of the numerical solution. In [141, 162], the authors utilised the arc-length monitor function for mesh equidistribution to solve convection-diffusion problems. In [220], the author introduced numerical methods based on exponential finite difference approximations with fourth-order accuracy for solving one and two-dimensional convection-diffusion problems. A nonlinear two-point SPP is considered in [120]. The authors employed quasi-linearisation to linearise the original nonlinear equation for each linear case. Then, they used a cubic spline difference scheme on a variable mesh to approximate the linear equations. Continuing their work, the authors in [121] developed an exponentially fitted difference scheme using spline in compression for solving twopoint singularly perturbed boundary value problems. In [163], the author presented a survey on layer-adapted meshes for convection-diffusion problems, emphasising the importance of using appropriate grids to achieve uniform convergence.

In [252], the authors introduced a finite difference scheme for discretizing singularly perturbed boundary value problems. The presented scheme is a combination of the simple upwind scheme and the central difference scheme on a Shishkin mesh. It is observed that the proposed scheme exhibited higher-order convergence compared to the simple upwind scheme alone.

In [82], the authors presented defect correction scheme based on finite difference discretizations over Shishkin mesh to solve a singularly perturbed convection diffusion problem. The method combines the stability of the upwind difference scheme and the higher-order convergence of the central difference scheme and results in a higher order stable scheme. Authors in [81] solved a singularly perturbed linear convection–diffusion problem using defect correction scheme over some Shishkin type of meshes. The method is shown to be convergent, uniformly in the diffusion parameter, of second order in the discrete maximum norm. In [94], authors presented defect correction method by combining first order upwind scheme and second order modified central difference scheme to solve a singularly perturbed convection-diffusion problem in one-dimension.

In [133], the author analysed a defect correction method for a one-dimensional convection-diffusion problem without turning points. He showed that the kth approximation obtained using the defect correction method converges uniformly with

a rate of $O((\epsilon_0 - \epsilon)^k + h^2)$, where ϵ_0 is of the order $O(h)$ in outer regions. However, the error estimates degrade to $O(1)$ in the inner regions.

In [247], the authors presented an adaptive finite difference method to solve singularly perturbed convection-diffusion problems. The authors combined a first-order upwind and a second-order central scheme to achieve a higher order of convergence. In [164], the author discretized a singularly perturbed convection-diffusion problem using a simple first-order upwind difference scheme on general meshes. He derived an expansion of the error of the scheme that enables uniform error bounds with respect to the perturbation parameter in the discrete maximum norm for both a defect correction method and the Richardson extrapolation technique.

In [217], the authors considered a self-adjoint two-point singularly perturbed boundary value problem. They employ a fitted finite difference scheme on a Shishkin mesh for solving the problem by reducing it to normal form. While the authors in [176] proposed a non-standard finite difference scheme for solving self-adjoint two-point singularly perturbed boundary value problems using Micken's finite difference method.

In [274], the authors introduced a spline difference scheme that uses quadratic and cubic splines for discretizing reaction-diffusion problems on a non-uniform mesh. In [275], the authors discretized reaction-diffusion problems using quadratic splines on a piecewise uniform Shishkin mesh and achieved an almost second-order accuracy in the discrete maximum norm. In [109], the authors used a cubic spline difference scheme on Bakhvalov mesh to solve reaction-diffusion problems. The result obtained using the Bakhvalov mesh was found to be superior to that achieved with the Shishkin mesh.

In [25], the author presented a cubic spline in compression to solve two-point singularly perturbed boundary value problems. In [139], the author analysed that the arc-length monitor function does not yield satisfactory numerical approximations for reaction-diffusion problems. It has been observed that an optimal choice of the monitor function not only depends on the discretization technique and the norm of the error to be minimised but also on the nature of the problem.

Authors in [233] applied exponential splines to generate an almost second-order uniformly convergent difference scheme on standard Shishkin mesh for semi-linear reaction-diffusion problems. The method exhibits uniform convergence of almost second-order in discrete maximum norm. Later, they devised an exponential spline difference scheme on piecewise uniform Shishkin mesh [234].

In [235], the authors used spline in compression to generate second and fourth-order uniformly convergent numerical techniques for singularly perturbed boundary value problems. To deal with Robin-type boundary conditions, authors in [200] applied the central difference method on the regular region of standard Shishkin mesh and cubic splines to discretize the layer region.

In [9], the authors considered a one-dimensional steady-state convection-diffusion problem with Robin boundary conditions. To discretize the problem, they use standard upwind finite difference operators on Shishkin meshes. Furthermore, the authors in [51] developed a finite difference scheme for solving a one-dimensional time-dependent convection-diffusion problem with initial-boundary conditions. They employed the classical Euler implicit method for time discretization and the simple upwind scheme on a Shishkin mesh for spatial discretization.

In [196], the authors investigated the effect of Richardson extrapolation on two fitted operator finite difference methods (FOFDM), (FOFDM-I) [217] and (FOFDM-II) [176]. They found that FOFDM-I achieved fourth-order accuracy for moderate values of the perturbation parameter, while it attained second-order accuracy for small values of the perturbation parameter. However, they observed that Richardson extrapolation did not improve the order of convergence for FOFDM-I. For FOFDM-II, which is uniformly second-order convergent, the order of convergence can be improved up to fourth-order by using Richarson extrapolation. In [166], the author proposed a compact fourth-order finite difference scheme for solving two-point reaction-diffusion SPPs on a Shishkin mesh.

In [116], the authors proposed a numerical approach to solve the singularly perturbed time-dependent convection-diffusion problem in one spatial dimension. They employed a semi-discretization technique by applying the backward Euler finite difference method in the temporal direction. To discretize the resulting set of ordinary differential equations, they utilised the midpoint upwind finite difference scheme on a non-uniform mesh of Shishkin type in the spatial direction. In [95], the authors proposed a method in which domain decomposition was combined with higher-order difference discretization for solving two-point singularly perturbed boundary value problems of convection-diffusion type. In [59], the authors used the same scheme combination as in [200] on an equidistributed grid. Their approximation scheme uses cubic splines for the mixed-boundary conditions and the classical central scheme elsewhere.

In [96], the author proposes a higher-order numerical scheme to solve singularly perturbed reaction-diffusion problems. The proposed scheme is a combination of a fourth-order numerical difference method and a classical central difference method. In [146], the authors presented a parameter-uniform numerical method on equidistributed meshes for solving a class of singularly perturbed parabolic problems with Robin boundary conditions. The discretization consists of a modified Euler scheme in time, a central difference scheme in space, and a special finite difference scheme for the Robin boundary conditions.

In [88], a parameter-uniform numerical method is constructed for singularly perturbed Robin type parabolic convection-diffusion problems having boundary turning points. The problem is discretized by means of the implicit Euler method in time and the non-standard finite difference method in space on a uniform mesh. Moreover, the non-standard finite difference method is used to discretize the Robin boundary conditions. While in [254], the authors deal with a singularly perturbed two-dimensional steady-state convection-diffusion problem with Robin boundary conditions.

In [195], the authors considered a time-dependent singularly perturbed reaction diffusion problem. They employ the classical backward Euler method to discretize the problem in time and a fitted operator finite difference method in space. In [93], the authors proposed a classical upwind finite difference scheme on layer-adapted nonuniform meshes to solve singularly perturbed parabolic convection-diffusion problem. In [194], the authors proposed a uniformly convergent FDM for a coupled system of singularly perturbed ordinary differential equations of convection-diffusion type. It was proved that the proposed discrete operator satisfies the stability property in the maximum norm. In [228], the author presented a survey of non-standard FDMs.

In [86], the authors proposed an adaptive finite difference technique using the central difference scheme on a layer-adapted mesh for a linear second-order singularly perturbed boundary value problem. It was shown that the proposed technique has fourth-order convergence. In [180], the authors considered singularly perturbed degenerate parabolic convection-diffusion problems in two-dimension. They used an alternating direction implicit finite difference scheme to discretize the time derivative and an upwind finite difference scheme to discretize the spatial derivative.

In [206], the authors introduced a hybrid difference scheme for solving singularly perturbed convection-diffusion problems. Their scheme combined the up-

wind scheme on the coarse part of the Shishkin mesh with the central difference scheme on the fine part. In [87], the authors considered a singularly perturbed fourth-order differential equation with a turning point. They used the classical finite difference scheme on an appropriate piecewise uniform Shishkin mesh to solve the problem. In [58], the authors proposed a second-order uniformly convergent numerical method for a singularly perturbed parabolic convection-diffusion initial-boundary-value problem in two-dimension. They used a fractional-step method in the time direction, while a finite difference scheme was used in the spatial direction. In [260], a higher-order Richardson extrapolation scheme is presented for solving a singularly perturbed system of parabolic convection-diffusion problems. Whereas in [175], a septic B-spline method is presented for solving a self-adjoint singularly perturbed two-point boundary value problem.

In [115], the authors presented a second-order robust method for solving singularly perturbed Burgers' equation. In [83], a specific class of parabolic singularly perturbed convection-diffusion problems is investigated. The problem is discretized using the backward Euler scheme in the temporal direction and the upwind scheme on a Harmonic mesh in the spatial direction. In [147], the authors introduce a high-order convergent numerical method for singularly perturbed time dependent problems using mesh equidistribution. The discretization is based on the backward Euler scheme in time and a high-order non-monotone scheme in space. In [198], numerical approximations are computed for the solution of a system of two reaction-convection-diffusion equations by a fitted mesh finite difference method. In [261], authors conducted a numerical investigation of an initial-boundary-value problem for a singularly perturbed system of two equations of convection-diffusion type. The authors proposed a numerical method that combined a spline-based scheme with a Shishkin mesh and achieved second-order uniform convergence. While in [262], the authors present a uniformly convergent numerical technique for a time dependent singularly perturbed system of two equations of reaction-diffusion type. The proposed numerical technique consists of the Crank–Nicolson scheme in the temporal direction over a uniform mesh and the quadratic B-splines collocation technique over an exponentially graded mesh in the spatial direction. In [204], the authors considered singularly perturbed elliptic convection-diffusion differential equations in two-dimensions. They discretized the problem by using an upwind difference scheme on a modified exponentially graded Bakhvalov mesh. Further, in [296], the authors analysed a higher order numerical method for a class of two-dimensional parabolic singularly perturbed problem of convection-diffusion type

for the case when the convection coefficient is vanishing inside the domain. The Peaceman–Rachford scheme is used on a uniform mesh for time discretization, and a hybrid scheme is applied on the Bakhvalov–Shishkin mesh for spatial discretization. In [52], the authors deal with one-dimensional linear parabolic singularly perturbed systems of convection-diffusion type. The diffusion term in each equation is affected by a small positive parameter of different magnitudes. The numerical algorithm combines the classical upwind finite difference scheme to discretize in space and the fractional implicit Euler method together with an appropriate splitting by components to discretize in time.

In [215], the authors considered a second-order singularly perturbed Volterra integro-differential equation. On a layer adapted Shishkin mesh, the problem is solved using finite difference schemes. Whereas in [216] author presents a fitted mesh finite difference method for solving a singularly perturbed Fredholm integro-differential equation.

2. **Finite element methods:** The finite element method (FEM) is a widely employed numerical approach for approximating solutions to ordinary differential equations and partial differential equations. In this method, the dependent variable u in the differential equation is approximated by a function u_h that is constructed as a linear combination of basis functions S as $u \approx u_h = \sum_i u_i S_i$. The basis functions, S_i, are chosen such that they form a set of functions that span the solution space. The coefficients of the basis functions, u_i, represent the unknowns that need to be determined. These coefficients correspond to the values of the solution at specific mesh points, i. By substituting the approximation u_h into the original differential equation, the problem is transformed into a system of algebraic equations. This system is then solved to determine the values of the coefficients u_i, which in turn define the approximate solution u_h. The finite element method offers flexibility in choosing the shape and size of the basis functions, allowing for adaptability to complex geometries and varying solution behaviour. It is widely used in various fields of engineering and applied sciences for solving a wide range of problems governed by differential equations.

   In the late 1970s, researchers initiated the use of Petrov-Galerkin techniques, a modified version of the Finite Element Method (FEM), for the purpose of resolving singular perturbation problems (SPPs). In [301], the authors acknowledged the necessity of employing distinct methodologies to tackle SPPs through the use of finite element analysis. A Finite Element Method technique resembled the up-

wind scheme by integrating upwinding into the test function. The objective of this change was to achieve a solution for SPPs that is free from oscillations. In [185], the author presented a Finite Element Method formulation that reduces to a simple upwind scheme in the asymptotic scenario. This formulation was specially designed for the numerical solution of singularly perturbed Ordinary Differential Equations (ODEs).

In [268], the authors applied the FEM with a Petrov-Galerkin approach using exponential basis elements to solve conservative non self-adjoint singularly perturbed boundary value problems. The method has first-order convergence in L_∞ and second-order convergence at the nodes. The Authors in [71] introduced an adaptive streamline diffusion finite element method for solving stationary convection-diffusion problems by using shock capturing artificial viscosity technique.

In [47], the authors introduced a FEM that utilised piecewise linear and quadratic basis functions to solve second-order differential equations. Further, in [106], the authors used an upwind finite element scheme for two-dimensional convective transport equations. Author in [281] proposed a FEM technique employing piecewise polynomials of degree at most k to solve two-point singularly perturbed boundary value problems. The proposed method provided parameter-uniform error estimates of $O(h^{k+1})$ in the maximum norm, indicating convergence rates that depended on the mesh size h. In [107], the authors conducted a survey summarising various FEMs and upwind schemes employed to solve convection-dominated flow problems.

In [272], the authors applied Galerkin FEMs using a piecewise polynomial basis functions on a Shishkin mesh to obtain optimal convergence results for high-order elliptic two-point singularly perturbed boundary value problem of reaction-diffusion type. They also achieved uniform convergence results for a family of Galerkin FEMs on a Shishkin mesh for high-order elliptic two-point singularly perturbed boundary value problems of convection-diffusion type [273].

In [159], the author utilised Galerkin FEM on a Bakhvalov-Shishkin mesh to solve a linear two-dimensional convection-diffusion problem. It was shown that better error estimates were obtained on the Bakhvalov-Shishkin mesh compared to the Shishkin mesh. Further, in [299], the author studied superconvergence approximations of singularly perturbed boundary value problems of reaction-diffusion type and convection-diffusion type. He obtained superconvergence with an error bound

of $O((N^{-1}\log(N+1))^{p+1})$ in a discrete energy norm by applying the standard finite element method of any fixed order p on a modified Shishkin mesh.

In [78], the authors applied Galerkin FEM to solve elliptic convection-diffusion problems. They analysed the superconvergence property of the method on a Shishkin mesh and determined that it was almost first-order accurate in the energy norm. In [48], the authors proposed a multiscale FEM to approximate the solution to elliptic SPPs with high contrast coefficients using coarse quasi-uniform meshes. The method achieved first-order convergence in the energy norm and second-order convergence in the L_2 norm. Authors in [114] compared the performance of He's homotopy perturbation method with that of FEM for solving the two-dimensional heat conduction equation. Results proved that there was excellent agreement between the analytical results obtained using the homotopy perturbation method and the numerical results obtained using FEM, proving the accuracy and reliability of FEM in solving heat conduction problems.

In[178], authors proposed the direct discontinuous Galerkin (DDG) finite element method, using piecewise polynomials of degree $k \geq 1$ on a Shishkin mesh to solve convection-dominated singularly perturbed two-point boundary value problems. Authors proved the consistency, stability and convergence of order k (up to a logarithmic factor) in an energy-type norm. In [45], authors proposed the local discontinuous Galerkin (LDG) method with piecewise polynomials of degree at most $k > 0$ over three families of layer-adapted meshes: Shishkin-type, Bakhvalov-Shishkin-type and Bakhvalov-type to solve singularly perturbed convection-diffusion problem posed on the unit square in $\mathbb{R}^2$. In [46], authors solved a singularly perturbed convection–diffusion problem, posed on the unit square in ($\mathbb{R}^2$) whose solution has both exponential and characteristic boundary layers using the local discontinuous Galerkin (LDG) method on Shishkin meshes.

In [298], the authors solved a singularly perturbed convection-diffusion equation using linear FEM on a Shishkin mesh. They utilised symmetries in the convective term of the bilinear form over adjacent intervals to achieve superconvergence of almost second-order accuracy in general cases. This research highlighted the potential for improving the accuracy and efficiency of FEM through the exploitation of specific problem structures and symmetries. In [293], the authors construct a finite volume element method on the Shishkin mesh for solving a singularly perturbed reaction-diffusion problem. In [231], the authors introduce numerical methods for singularly perturbed convection-diffusion problems with a turning point. As a re-

sult of the turning point, the problem typically exhibits exponential-type boundary layers or a cusp-type interior layer. They develop non-symmetric discontinuous Galerkin FEM with interior penalties for both cases. Usual Shishkin mesh is invoked for the problem with boundary layers, whereas generalised Shishkin type mesh is used to tackle the interior layer of cusp-type.

In [105], the author proposed a FEM that utilised a combination of quadratic trial and cubic test functions to solve the steady-state convection-diffusion equation. A series of papers were published investigating the selection of test spaces to symmetrize the associated bilinear form; see, e.g., [20, 22, 21, 23]. The goal was to obtain an optimal approximate solution similar to the ones achieved by applying Galerkin methods to symmetric problems.

In [267], the author presented a FEM approach for solving a non self-adjoint SPP. In [240], the author achieved optimal convergence results for the two-point singularly perturbed boundary value problem of convection-diffusion type in the energy norm. The analysis was conducted on a Bakhvalov mesh.

In [65], a convection-dominated diffusion problem is solved by combining the FEM or FDM with the method of characteristics. The authors derived optimal order errorestimates in L^2 and $W^{1,2}$ for the FEM and various error estimates for a variety of FDMs. The concept of hinged elements was introduced in [211]. These elements were essentially piecewise linear finite elements that could vary according to problem data and were used to solve one-dimensional linear non self-adjoint two-point singularly perturbed boundary value problems.

Comprehensive discussions on the theoretical foundations and practical implementations of FEM for various problems can be found in several books; see, e.g. [40, 35, 15]. These references extensively cover the theory and applications of FEM.

3. **Finite volume methods:** The finite volume method (FVM) is a numerical technique used to approximate the solution to partial differential equations (PDEs). In this method, the domain is discretized into mesh elements known as control volumes. The PDE is integrated over each control volume to obtain a set of balance equations. These balance equation are then discretized into a set of algebraic equations, resulting in a system of equations with discrete unknowns. The system of equations can be solved either exactly or approximately using direct or iterative methods such as the Gauss-Seidel method and the Jacobi method. Iterative methods iteratively update the values of the unknowns until a desired level of accuracy

is achieved. Direct methods, on the other hand, solve the system of equations in one step but may be computationally expensive for large systems. The FVM is an integral scheme, similar to the FEM, whereas FDM is a differential scheme. In FVM, the integral form of the PDEs is used to construct the discrete equations, whereas FDM approximates the derivatives directly using finite difference approximations. Differential schemes are generally faster than integral schemes, but integral schemes, such as FVM, have the advantage of being more accurate than their differential counterparts when dealing with irregular meshes. For a detailed description of FVM, several books are available as references. [190] provides a detailed description of cell-vertex FVMs, [154] focuses on FVMs for hyperbolic problems, and [182] covers FVMs for general PDEs, providing a comprehensive overview of the method and its applications.

1.4 Plan of the Thesis

In this thesis, we study, analyse and develop the numerical methods for solving various models of singularly perturbed convection-diffusion boundary value problems. As discussed in the preceding sections, an adaptive discretization approach may adapt to situations with different physical and dynamic properties by varying the resolution, order, and type of discretization. It is generally used with an adaptive numerical method that balances the solution accuracy and the associated computational cost. Therefore, an appropriate numerical method and the discretization technique accurately solve the problem and improve convergence. Taking this into account, in this thesis, we propose higher-order defect correction methods to solve singularly perturbed convection-diffusion problems. We apply the proposed methods to solve four different convection-diffusion problems of varying complexity.

The thesis is organized as follows: Chapter 2 presents a higher-order defect correction method to solve a class of singularly perturbed convection diffusion equations that reads

$$\left.\begin{aligned} &Lu(x) = -\epsilon u''(x) + a(x)u'(x) + b(x)u(x) = g(x), \quad x \in (0,1), \\ &u(0) = u(1) = 0, \end{aligned}\right\} \tag{1.4.1}$$

where $0 < \epsilon \ll 1$ is the perturbation parameter, $a(x) \geq 2\alpha > 0$ and $b(x) \geq \beta \geq 0$. The function $a(x)$, $b(x)$ and $g(x)$ are sufficiently smooth functions. The defect correction method is presented over polynomial-Shishkin mesh to solve the problem. The method combines an inexpensive, lower-order stable, upwind difference scheme and a higher-order, less stable central difference scheme. The mesh is designed in such a way so that

most of the mesh points remain in the regions with rapid transitions. The proposed numerical method is analysed for consistency, stability and convergence. An extensive theoretical analysis is presented, which establishes that the method is second-order uniformly convergent and highly stable. The convergence obtained is optimal because it is free from any logarithmic term. The rigorous numerical analysis of the proposed method on Shishkin, Bakhvalov Shishkin, Vulanovic-Improved Shishkin and polynomial Shishkin mesh establishes the supremacy of the proposed scheme.

Chapter 3 presents defect correction method to solve singularly perturbed convection-diffusion problem with discontinuous coefficient and point source which is given as

$$\left.\begin{aligned} &Lu(x) = -\epsilon u''(x) - (a(x)u(x))' + b(x)u(x) = g(x) + \gamma\delta_c,\ x \in (0,1), \\ &u(0) = u(1) = 0, \end{aligned}\right\} \tag{1.4.2}$$

where δ_c is the shifted Dirac-delta function $\delta_c(x) = \delta(x-c)$ with $c \in \Omega$. Assume that $\epsilon \in (0,1]$, $a(x) \geq \alpha_1 > 0$ for $x \in (0,c)$, and $a(x) \geq \alpha_2 > 0$ for $x \in (c,1)$. Let $\alpha = \min\{\alpha_1, \alpha_2\}$. The function $b(x)$ is assumed to be sufficiently smooth and satisfies

$$b(x) \geq 0 \text{ and } b(x) - (a(x))' \geq 0,\ x \in [0,1]. \tag{1.4.3}$$

A higher-order defect correction methods consists of upwind difference scheme and central difference scheme at all mesh points over Bakhvalov Shishkin mesh is proposed to solve the problem. A posteriori error alaysis is presented in L_∞-norm. The error estimates of the proposed numerical method satisfy parameter-uniform second-order convergence on the layer-adapted grid. The numerical analysis confirms the theoretical error analysis and reveals parameter-uniform second-order convergence in discrete maximum-norm.

Chapter 4 proposes the defect correction method to solve a class of singularly perturbed parabolic convection-diffusion problem with a large shift that reads

$$\left.\begin{aligned} &u_t(x,t) - \epsilon u_{xx}(x,t) + a(x)u_x(x,t) + b(x)u(x,t) + c(x)u(x-1,t) = g(x,t), \\ &u(x,t) = r_0(x),\ (x,t) \in [0,2] \times \{t=0\}, \\ &u(x,t) = r_1(x,t),\ (x,t) \in [-1,0] \times [0,T], \\ &u(x,t) = r_2(t),\ (x,t) \in \{x=2\} \times [0,T], \end{aligned}\right\} \tag{1.4.4}$$

where $0 < \epsilon \ll 1$, a, b, c and g are sufficiently smooth functions such that $a(x) > \alpha > 0$, $c(x) > 0$, $b(x) \geq 0$. The solution to the problem considers the present state of the physical system and its history. The proposed method combines an inexpensive, lower-order stable, upwind difference scheme and a higher-order, less stable central difference scheme at some grid points. The mesh has been chosen so that most of the mesh points remain in the regions with rapid transitions. Whereas an implicit finite difference scheme is used

to discretize the time variable. The proposed numerical method has been analysed for consistency, stability and convergence. Theoretical analysis is performed to obtain consistency and error estimates. The method is uniformly convergent and second-order accurate in space and first-order in time. We do not use asymptotic expansions of discretization errors in our analysis. Numerical results agree with the theoretical estimates and indicate that the defect correction technique can improve accuracy for singular perturbation problems.

Chapter 5 presents defect correction method to solve a class of singularly perturbed parabolic convection-diffusion problem with discontinuous convection coefficient and source which is given as

$$\left.\begin{aligned} &Lu(x,t) = \epsilon u_{xx}(x,t) + a(x)u_x(x,t) - b(x)u(x,t) - u_t(x,t) = g(x,t), \\ &(x,t) \in (0,c) \times (0,T] \cup (c,1) \times (0,T], \\ &u(x,0) = r_0(x), \ \ x \in [0,1], \\ &u(0,t) = r_1(t), \ \ t \in [0,T], \\ &u(1,t) = r_2(t), \ \ t \in [0,T], \end{aligned}\right\} \tag{1.4.5}$$

where $0 < \epsilon \ll 1$ is the perturbation parameter, $b(x)$ is a sufficiently smooth function such that $b(x) \geq \beta \geq 0$ on $[0,1]$, the convection coefficient $a(x)$ and the source term $g(x)$ are sufficiently smooth functions on $(0,c) \cup (c,1)$ satisfying

$$|[a](c)| \leq C, \quad |[g](c)| \leq C. \tag{1.4.6}$$

The problem is discretized using defect correction method over non-uniform Bakhvalov Shishkin mesh in space. Moreover, the time variable is discretized using an implicit finite difference method. The error analysis indicates that the numerical solution is uniformly stable and shows parameter-uniform second-order convergence in space and first-order in time. The results of numerical experiments corroborate the theoretical findings and verify the optimal accuracy of the proposed scheme.

Finally, Chapter 6 concludes the thesis with a summary of the work highlighting its significant contributions. It opens the discussion about future research directions and points out the challenging steps towards analysing more complicated problems.

Chapter 2

Convection-Diffusion Problems

2.1 Introduction

Singularly perturbed convection-diffusion problems constitute a class of mathematical models that arise in various fields of science and engineering. These problems involve the simultaneous interaction of convection and diffusion phenomena, and a small parameter characterizes them, which multiplies the highest-order derivative term in the governing equations. This small parameter introduces a significant disparity in the scales of the convection and diffusion processes leading to boundary layers. The solution of these equations exhibits a multiscale character since the corresponding degenerate system fails to satisfy the given boundary data. There are narrow regions across which the solution changes rapidly and displays layer behaviour.

Standard numerical methods on uniform meshes fail to consistently approximate solutions in these layer regions. The classical finite difference or finite element methods constructed on uniform meshes are unsuitable for solving singularly perturbed convection-diffusion problems [253]. The stable upwind difference scheme is first-order uniformly convergent in the discrete maximum norm on a layer-adapted grid. On the other hand, the formally second-order convergent central difference scheme oscillates in domains where the perturbation parameter is small compared to the local step size [99]. In fact, for problems with a strongly asymmetric differential operator, the usual discretizations are either unstable, inaccurate or direction-dependent. For example, the higher-order accurate differences based on Petrov-Galerkin weighting are strongly direction-dependent because they depend on the equation's flow direction [111]. Symmetric schemes, like the finite difference method or the usual Galerkin methods with symmetric weighting functions, are either unstable or only first-order accurate [99, 19, 89].

The search for a uniform numerical approximation led to the advent of fitted mesh methods defined on layer-adapted grids [230, 173]. Bakhvalov first proposed layer-adapted meshes in the context of reaction-diffusion problems [17, 240, 39]. Later on, special meshes were investigated extensively for convection-diffusion problems. That includes Shishkin's piecewise equidistant meshes [140], meshes that are based on equidistribution [27, 98, 97], Gartland type meshes [85], Bakhvalov-Shishkin mesh [159, 300] and Vulanović improved Shishkin mesh [288, 290]. Further development leads to the layer-adapted meshes defined using a recursive formula. Examples are the Gartland-Shishkin meshes [243] or the graded meshes analysed in [66, 127, 161, 38, 294] and others. The two major classifications of layer-adapted meshes are a priori and posteriori. A priori mesh depends on advanced knowledge of the width and location of layers present in the solution. A priori grid appears an attractive choice being easy to generate and less expensive in terms of computational cost. Nevertheless, the prerequisites for the same are too restrictive.

In this context, Bakhvalov [18] was the first to propose a mesh for a class of reaction-diffusion problems. However, the process of mesh construction is too complex to consider. A relatively simple piecewise uniform mesh proposed by Shishkin [257] too had a drawback of waning the order of convergence by a logarithmic factor. Indeed, mesh generation depends heavily on a priori information about the location and width of the layers. Typically, the information required is not available in advance. The upwind schemes are one of the most straightforward and stable discretization schemes. However, they are more dissipative according to the flow. It uses the values upstream to evaluate the property on the boundaries and depends on the flow direction. First-order upwind schemes are easily convergent but are at most first-order convergent [168, 156].

In contrast, higher-order upwind methods are highly accurate but more difficult to converge [283]. In addition to convergence and accuracy, numerical diffusion can be a significant problem with upwind schemes. It may produce false results, particularly mass diffusion problems with high Peclet numbers, i.e. singular perturbation problems [248]. An essential challenge in the numerical solution of the singular perturbation problem is the different approximations required in the smooth part of the solution and the boundary or interior layers.

Many researchers have tried to provide consistent numerical approximations to singularly perturbed convection-diffusion equations using a defect correction method [108, 168]. In [72], the singularly perturbed convection-diffusion problem is solved using an iterative method based on defect correction. A convection-diffusion problem is also studied in [14]. In [94], authors used a defect-correction parameter-uniform numeri-

cal method for solving a convection-diffusion equation. Furthermore, the time-dependent Navier-Stoke equation was solved using the defect correction method [149, 188]. This method is also suitable for singularly perturbed delay differential equations [189].

The analysis of the special methods for singularly perturbed convection-diffusion problems is a growing area of research and has yet to see much development in the literature. This chapter presents a defect correction method to overcome some of the limitations of numerical methods and obtain higher-order accurate solutions for convection-diffusion problems. Besides, the chapter presents rigorous consistency, stability and convergence analysis of the proposed scheme and illustrates numerical results.

2.2 Problem description

Consider the non-homogeneous boundary value problem

$$\left.\begin{aligned} &Lu(x) = -\epsilon u''(x) + a(x)u'(x) + b(x)u(x) = g(x), \quad x \in (0,1), \\ &u(0) = u(1) = 0, \end{aligned}\right\} \tag{2.2.1}$$

where $0 < \epsilon \ll 1$ is the small perturbation parameter, $a(x) \geq 2\alpha > 0$ and $b(x) \geq \beta \geq 0$. The function $a(x)$, $b(x)$ and $g(x)$ are sufficiently smooth functions. The operator L satisfies the maximum principle [225] and the problem (2.2.1) has a unique solution [166]. Moreover, the solution of (2.2.1) admits a decomposition into regular and singular components that reads

$$u(x) = \upsilon(x) + \omega(x). \tag{2.2.2}$$

The regular component υ satisfies $L\upsilon = g(x)$ and the singular component ω satisfies $L\omega = 0$ where $|\omega(0)| \leq Ce^{-\alpha/\epsilon}$ and $|\omega(1)| \leq C$ [99, pp. 23]. Further, we may obtain

Lemma 2.2.1. *Let $x \in (0,1)$ and $q \in N$. Then*

$$|\upsilon^{(k)}(x)| \leq C \quad \text{and} \quad |\omega^{(k)}(x)| \leq C\epsilon^{-k}e^{-\alpha((1-x)/\epsilon)} \quad \text{for} \quad 0 \leq k \leq q.$$

Proof. The proof follows from [186]. □

The derivatives of the solution to problem (2.2.1) depend on the negative powers of the perturbation parameter. Moreover, the error estimates generated by classical schemes depend on bounds for these derivatives. Consequently, it fails to hold for arbitrarily small values of the perturbation parameter. It is indeed the principal layer function $\omega_0(x) = \gamma e^{(-\alpha(1-x)/\epsilon)}$ which causes the trouble. As in [82], the singular component is split into two parts written as $\omega := \omega_0 + \omega_1$ where $\omega_1^k = O(\epsilon^{-k+1})$ and ω_0 satisfies a constant-coefficient differential equation.

Remark 2.2.2. (a) In general, one can assume homogeneous boundary conditions by substracting from u a smooth function κ that satisfies the original boundary conditions [99]. For example, given Drichlet boundary conditions $u(a) = \rho_a$ and $u(b) = \rho_b$, take

$$\kappa(x) = \rho_a \frac{x-b}{a-b} + \rho_b \frac{x-a}{b-a}$$

and set $\tilde{u}(x) = u(x) - \kappa(x)$. Then $\tilde{u}$ is the solution of a differential equation of the same type but with homogeneous boundary conditions.
(b) Also, one can assume without loss of generality that $x \in [0, 1]$ by means of the linear transformation $x \to \dfrac{x-a}{b-a}$.

2.3 Mesh description

Let $N \in \mathbb{N}$ be an even integer. Consider the mesh $\Gamma_N := \{0 = x_0 \leq x_1 \ldots x_{N-1} \leq x_N = 1\}$, which is equidistant in $[0, x_{N/2}]$ and graded in $[x_{N/2}, 1]$. Let $\tau = \dfrac{2\epsilon\phi \ln N}{\alpha} \leq 1/2$ and $\epsilon \leq CN^{-1}$. Partition $[0, 1]$ into two mesh subintervals so that $\Gamma_N = [0, 1-\tau] \cup [1-\tau, 1]$. Here, $x_{N/2} = 1-\tau$ is the mesh transition point separating the coarse and fine mesh regions. The mesh takes $N/2$ points in interval $[0, 1-\tau]$ such that $x_0 = 0$ and $x_{N/2} = 1-\tau$. The remaining $N/2$ points lie in the interval $[1-\tau, 1]$ such that each step size $h_i = x_i - x_{i-1}$ satisfies $h_i \geq h_{i+1}$ for $i = N/2+1, \cdots, N-1$. The mesh turns dense as we move towards the layer region and capture the exponential boundary layers in the solution, and one can stimulate the solution precisely. The layer-adapted mesh generated on $[1-\tau, 1]$ is based on a mesh-generating function [242]. Let λ be the mesh-generating function that is monotonically increasing satisfying $\lambda(1) = 1$ and $\lambda(1/2) = \ln N$. Then, for $t_i = i/N$, the mesh points are given by

$$x_i = \begin{cases} \left(1 - \dfrac{2\epsilon \log N}{\alpha}\right)\dfrac{2i}{N} & \text{for } 0 \leq i \leq \dfrac{N}{2}, \\ 1 - \dfrac{2\epsilon}{\alpha}\lambda(t_i) & \text{for } \dfrac{N}{2}+1 \leq i \leq N. \end{cases}$$

Define mesh-characterising function ψ such that $\psi = e^{-\lambda}$. Here, we are omitting indices for mere simplicity. Table 2.4 illustrates the mesh-characterising feature for different classes of layer-adapted meshes [166, 242, 158]. The polynomial-Shishkin mesh is the generalised mesh and lies in the centre of this work. One can obtain the original Shishkin class of mesh by setting m=1. The resulting mesh reads

$$x_i = \begin{cases} \left(1 - \dfrac{2\epsilon \log N}{\alpha}\right)\dfrac{2i}{N} & \text{for } 0 \leq i \leq \dfrac{N}{2}, \\ 1 - \dfrac{2\epsilon}{\alpha}(2t)^m \log N & \text{for } \dfrac{N}{2}+1 \leq i \leq N. \end{cases}$$

Table 2.1: Mesh generating and characterising functions of different layer adapted meshes [166].

Mesh	$\psi(t)$	$\max \lvert\psi'\rvert$	$\max \lambda'$
Shishkin-type meshes	N^{-2t}	$C \log N$	$C \log N$
Bakhvalov-Shishkin meshes	$1 - 2(1 - N^{-1})t$	C	CN
Polynomial-Shishkin meshes	$N^{-(2t)^m}$	$C(\log N)^{1/m}$	$Cm \log N$

Lemma 2.3.1. *The step size h_i of Γ_N satisfies $h_i \leq CN^{-1}$ for all $i = 1, 2, \ldots N$.*

Proof. For $1 \leq i \leq N/2$ the proof is trivial. In the case $N/2 + 1 \leq i \leq N$, we have

$$h_i = \frac{2\epsilon}{\alpha} N^{-1} \max \lambda'(t_i).$$

Since $\lambda(t_i) = \log N(2t_i)^m$, $\lambda'(t_i) = m \log N(2t_i)^{m-1}$. Consequently, we obtain

$$h_i = \frac{2\epsilon}{\alpha} m \log N(2t_i)^{m-1} = \frac{2\epsilon}{\alpha} m \log N 2^{m-1} \left(\frac{i}{N}\right)^{m-1} \leq CN^{-1} \text{ for } m \geq 2.$$

□

2.4 The difference scheme

For $i \geq 1$, a function Z_i and step size h_i define [264]

$$D_+ Z_i := \frac{Z_{i+1} - Z_i}{h_{i+1}}, \quad D_- Z_i := \frac{Z_i - Z_{i-1}}{h_i} \text{ and } D_0 Z_i := \frac{Z_{i+1} - Z_{i-1}}{h_{i+1} + h_i}$$

as the forward, backward and central difference approximation to first-order derivatives. A difference approximation for a second-order derivative is defined [264] to be

$$D_+ D_- Z_i := \frac{2}{h_{i+1} + h_i} \left(\frac{Z_{i+1} - Z_i}{h_{i+1}} - \frac{Z_i - Z_{i-1}}{h_i} \right).$$

The upwind operator for problem (2.2.1) takes the form

$$L_N^1 Z_i = \begin{cases} Z_i & \text{for } i = 0, N, \\ -\epsilon D_+ D_- Z_i + a_i D_- Z_i + b_i Z_i & \text{for } 1 \leq i \leq N - 1, \end{cases} \tag{2.4.1}$$

and the modified central difference operator for problem (2.2.1) reads

$$L_N^0 Z_i = \begin{cases} Z_i & \text{for } i = 0 \text{ and } i = N, \\ L_N^2 Z_i & \text{for } 1 \leq i \leq N/2, \\ L_N^1 Z_i & \text{for } N/2 \leq i \leq N - 1, \end{cases} \tag{2.4.2}$$

where $L_N^2 Z_i = -\epsilon D_+ D_- Z_i + a_i D_0 Z_i + b_i Z_i$.

The method based on defect correction allows us to combine low-order stabilised schemes with higher-order, less stable schemes. We can outline the two-stage process as

1. Compute initial approximation U^1 by solving $L_N^1 U^1 = g$ using an upwind difference scheme.

2. Estimate the defect τ_h by solving $\tau_h = g - L_N^0 U^1$ using the central difference scheme.

3. Compute the defect-correction δ using $L_N^1 \delta = \tau_h$.

4. The final corrected solution reads $U = U^1 + \delta$.

The consistency error $\hat{E}$ satisfies

$$\begin{aligned}
\hat{E} &= L_N^1(Ru - U) \\
&= L_N^1(Ru - U^1) + L_N^1 U^1 - L_N^1 U^1 + L_N^0 U^1 - g \\
&= L_N^1(Ru - U^1) + L_N^0 U^1 - g \\
&= L_N^1(Ru - U^1) + L_N^0 U^1 + L_N^0 Ru - L_N^0 Ru - RLu \\
&= (L_N^1 - L_N^0)(Ru - U^1) + (L_N^0 R - RL)u, \qquad (2.4.3)
\end{aligned}$$

where R is the restriction of continuous function over $[0, 1]$ to the defined mesh. The above representation for the consistency error is advantageous while performing the error analysis. To estimate relative consistency error $|(L_N^1 - L_N^0)(Ru - U^1)|$, we can apply operator L_N^1 to it. Moreover, in the following Lemma, we prove that L_N^1 and $L_N^1 - L_N^0$ commute.

Lemma 2.4.1. *The difference operator L_N^1 and $L_N^1 - L_N^2$ defined for* (2.2.1) *satisfies*

$$L_N^1(L_N^1 - L_N^2)Z_i = (L_N^1 - L_N^2)L_N^1 Z_i$$

iff $h_{i-1} = h_i = h_{i+1}$, $a_{i-1} = a_i = a_{i+1}$ and $b_{i-1} = b_i = b_{i+1}$.

Proof. Let us consider

$$\begin{aligned}
(L_N^1 - L_N^2)Z_i &= a_i(D_- - D_0)Z_i \\
&= -a_i h_{i+1}\left(\frac{D_+ Z_i - D_- Z_i}{h_{i+1} + h_i}\right) \\
&= -\frac{a_i h_{i+1}}{2} D_+ D_- Z_i. \qquad (2.4.4)
\end{aligned}$$

Apply L_N^1 to (2.4.4) and assume that $h_{i+1} = h_i = h_{i-1}$ also because the coefficients a_i and b_i are constants we obtain

$$\begin{aligned}
L_N^1(L_N^1 - L_N^2)Z_i &= -\frac{\epsilon}{2} D_+ D_- \left(a_i h_{i+1} D_+ D_- Z_i\right) + \frac{a_i}{2} D_- \left(a_i h_{i+1} D_+ D_- Z_i\right) \\
&\quad + \frac{b_i}{2}\left(a_i h_{i+1} D_+ D_- Z_i\right) \\
&= \frac{a_i h_{i+1}}{2}\left[-\epsilon D_+ D_-(D_+ D_- Z_i) + D_+ D_-(a_i Z_i)\right. \\
&\quad \left. + (D_+ D_-(b_i Z_i))\right]. \qquad (2.4.5)
\end{aligned}$$

Reverse the order of the operators, and we find

$$\begin{aligned}(L_N^1 - L_N^2)L_N^1 Z_i &= \frac{-a_i h_{i+1}}{2} D_+ D_- \left[-\epsilon D_+ D_- Z_i + a_i D_- Z_i + b_i Z_i\right] \\ &= \frac{a_i h_{i+1}}{2} \left[-\epsilon D_+ D_-(D_+ D_- Z_i) + D_+ D_-(a_i Z_i)\right. \\ &\quad \left. +(D_+ D_-(b_i Z_i))\right]. \end{aligned} \tag{2.4.6}$$

Hence, the proof follows. □

The mesh is uniform in the first half and graded in the remaining half of the domain. Thus, the above property holds only in the first half of the domain, and the relative consistency error vanishes in the remaining half due to the assumption that our operator L_N^0 vanishes. We require the following result from [186] to obtain a bound for relative consistency error.

Lemma 2.4.2. *Let $k \geq 4$ and $Z \in C^{(k)}[0,1]$. Then*

(i) $D_-(RZ)_i - Z'(x_i) = -\dfrac{1}{h_i}\displaystyle\int_{x_{i-1}}^{x_i} Z''(\xi)(\xi - x_{i-1})d\xi.$

(ii) $$\begin{aligned} D_0(RZ)_i - Z'(x_i) = {} & (h_{i+1} - h_i)Z''(x_i) + \frac{1}{2(h_i + h_{i+1})}\left(\int_{x_i}^{x_{i+1}} Z^{(3)}(\xi)(x_{i+1} - \xi)^2 d\xi \right. \\ & \left. - \int_{x_{i-1}}^{x_i} Z^{(3)}(\xi)(\xi - x_{i-1})^2 d\xi\right). \end{aligned}$$

(iii) $$\begin{aligned} D_+ D_-(RZ)_i - Z''(x_i) = {} & \frac{1}{(h_i + h_{i+1})}\left(\frac{1}{h_{i+1}}\left[\int_{x_i}^{x_{i+1}} Z^{(3)}(\xi)(x_{i+1} - \xi)^2 d\xi\right]\right. \\ & \left. -\frac{1}{h_i}\left[\int_{x_{i-1}}^{x_i} Z^{(3)}(\xi)(\xi - x_{i-1})^2 d\xi\right]\right). \end{aligned}$$

Proof. For proof, see [186]. □

Moreover, for all grid points x_i and smooth function Z, as in Lemma 2.4.2, it is easy to follow that

$$\begin{aligned} L_N^1(RZ)_i - (RLZ)_i = {} & \frac{-a_i}{h_i}\int_{x_i}^{x_i} Z^{(2)}(\xi)(\xi - x_{i-1})d\xi - \frac{\epsilon}{(h_i + h_{i+1})}\left(\frac{1}{h_{i+1}}\int_{x_i}^{x_{i+1}} Z^{(3)}(\xi)\right. \\ & \left. \times(x_{i+1} - \xi)^2 d\xi - \frac{1}{h_i}\int_{x_{i-1}}^{x_i} Z^{(3)}(\xi)(\xi - x_{i-1})^2 d\xi\right) \end{aligned} \tag{2.4.7}$$

and for grid points x_i with $h_i = h_{i+1}$

$$
\begin{aligned}
(i)\ L_N^1(RZ)_i - (RLZ)_i &= \frac{a_i}{h_i}\int_{x_{i-1}}^{x_i} Z^{(2)}(\xi)(\xi - x_{i-1})d\xi - \frac{\epsilon}{2h_i^2}\Big(\int_{x_i}^{x_{i+1}} Z^{(3)}(\xi)(x_{i+1}-\xi)^2 d\xi - \\
&\quad \int_{x_{i-1}}^{x_i} Z^{(3)}(\xi)(\xi - x_{i-1})^2 d\xi\Big) \\
&= \frac{a_i}{h_i}\int_{x_{i-1}}^{x_i} Z^{(2)}(\xi)(\xi - x_{i-1})d\xi - \frac{\epsilon}{6{h_i}^2}\Big(\int_{x_i}^{x_{i+1}} Z^{(4)}(\xi)(x_{i+1}-\xi)^3 d\xi \\
&\quad - \int_{x_{i-1}}^{x_i} Z^{(4)}(\xi)(\xi - x_{i-1})^3 d\xi\Big), \qquad (2.4.8) \\
(ii)\ L_N^0(RZ)_i - (RLZ)_i &= \frac{a_i}{4h_i}\Big(\int_{x_i}^{x_{i+1}} Z^{(3)}(\xi)(x_{i+1}-\xi)^2 d\xi - \int_{x_{i-1}}^{x_i} Z^{(3)}(\xi)(\xi - x_{i-1})^2 d\xi\Big) \\
&\quad -\frac{\epsilon}{6h_i^2}\Big(\int_{x_i}^{x_{i+1}} Z^{(4)}(\xi)(x_{i+1}-\xi)^3 d\xi \\
&\quad - \int_{x_{i-1}}^{x_i} Z^{(4)}(\xi)(\xi - x_{i-1})^3\Big). \qquad (2.4.9)
\end{aligned}
$$

The initial approximation U_i^1 of problem (2.2.1) admits a representation $U_i^1 = V_i^1 + W_i^1$ for $i = 0, \ldots N$ where V_i^1 satisfies

$$L_N^1 V_i^1 = g_i; \quad V_0^1 = \upsilon(0), \quad V_N^1 = \upsilon(1), \qquad (2.4.10)$$

and W_i^1 satisfies

$$L_N^1 W_i^1 = 0; \quad W_0^1 = \omega(0), \quad W_N^1 = \omega(1). \qquad (2.4.11)$$

Similarly, for $i = 0, \ldots N$, the corrected approximation U_i admits a representation that reads $U_i = V_i + W_i$ where,

$$L_N^1 V_i = (L_N^1 - L_N^0)V_i^1 + g_i; \quad V_0 = V_0^1, V_N = V_N^1, \qquad (2.4.12)$$

and

$$L_N^1 W_i = -L_N^0 W_i^1; \quad W_0 = W_0^1, \quad W_N = W_N^1. \qquad (2.4.13)$$

Consequently, we obtain

$$\|Ru - U\|_{\infty,d} \leq \|R\nu - V\|_{\infty,d} + \|R\omega - W\|_{\infty,d}\,. \qquad (2.4.14)$$

Later, we will employ this formula to obtain error estimates. Next, we define the mesh function $Q_i = \prod_{j=i+1}^{N}\left(1 + \frac{\alpha h_j}{\epsilon}\right)^{-1}$ for $i = 0, \ldots, N$ with the usual convention [269, 49]. It is straightforward to obtain that $Q_i - Q_{i-1} = \frac{\alpha h_i}{\epsilon} Q_{i-1}$.

Lemma 2.4.3. *There exist a positive constant C such that*

$$L_N^1 Q_i \geq \frac{C}{\max(\epsilon, h_i)} Q_i, \quad i = 1, \ldots, N-1. \qquad (2.4.15)$$

Proof. For $1 \leq i \leq N-1$, it is easy to follow that

$$D_+Q_i = \frac{\alpha}{2\epsilon}Q_i,\ D_-Q_i = \frac{\alpha}{2\epsilon+\alpha h_i}Q_i \text{ and } -\epsilon D_+D_-Q_i = \frac{-\alpha^2 h_i}{2\hbar_i(2\epsilon+\alpha h_i)}Q_i.$$

Consequently, we compute

$$\begin{aligned} L_N^1 Q_i &= -\epsilon D_+D_-Q_i + a_iD_-Q_i + b_iQ_i \\ &= \frac{-2\epsilon}{h_i+h_{i+1}}\left(\frac{Q_{i+1}-Q_i}{h_{i+1}} - \frac{Q_i-Q_{i-1}}{h_i}\right) + a_i\left(\frac{Q_i-Q_{i-1}}{h_i}\right) + b_iQ_i \\ &= \frac{\alpha}{\epsilon}\left(a_i - 2\frac{h_i}{h_i+h_{i+1}}\alpha\right)Q_{i-1} + b_iQ_i \\ &= \frac{\alpha}{h_i\alpha+\epsilon}\left(a_i - 2\frac{h_i}{h_i+h_{i+1}}\alpha + \frac{b_ih_i\alpha+\epsilon}{\alpha}\right)Q_i \\ &\geq \frac{C}{\max(\epsilon,h_i)}Q_i. \end{aligned}$$

□

Lemma 2.4.4. *For each i and mesh function Q_i*

$$\exp\left(-\frac{\alpha(1-x_i)}{\epsilon}\right) \leq \prod_{j=i+1}^{N}\left(1+\frac{\alpha h_j}{\epsilon}\right)^{-1}. \tag{2.4.16}$$

Furthermore, Q_i is monotonically increasing and for polynomial-Shishkin mesh Γ_N

$$Q_{N/2} \leq CN^{-\phi}. \tag{2.4.17}$$

Proof. For each i, note that

$$\exp\left(-\frac{\alpha(1-x_i)}{\epsilon}\right) \leq \left(1+\frac{\alpha h_{i+1}}{\epsilon}\right)^{-1}\cdots\left(1+\frac{\alpha h_N}{\epsilon}\right)^{-1} \leq \prod_{j=i+1}^{N}\left(1+\frac{\alpha h_j}{\epsilon}\right)^{-1}.$$

Moreover, for $i = \frac{N}{2}$

$$Q_{N/2} = \prod_{j=\frac{N}{2}+1}^{N}\left(1+\frac{\alpha h_j}{\epsilon}\right)^{-1} \leq \exp\left(\frac{-\alpha(1-x_{N/2})}{\epsilon+\alpha h}\right) \leq \exp\left(\frac{-\phi\log N}{1+8N^{-1}}\right) \leq CN^{-\phi}.$$

□

The discrete operator L_N^1 satisfies the discrete comparison principle, as we next prove.

Lemma 2.4.5. *Let v_i and ω_i be the grid functions satisfying $L_N^1v_i \leq L_N^1\omega_i$ for $i = 1,2,\ldots,N-1$ and $v_0 \leq \omega_0$, $v_N \leq \omega_N$. Then $v_i \leq \omega_i$ for $i = 0,1,\ldots,N$.*

Proof. The matrix associated with operator L_N^1 is an M-matrix, therefore, has a positive inverse. Hence, the result follows from [225]. □

Next, we prove that operator L_N^1 of (2.4.1) is $(\|.\|_{\infty,d}, \|.\|_{1,d})$-stable, where $\|.\|_{\infty,d}$ and $\|.\|_{1,d}$ are the discrete analogues of $L^\infty[0,1]$ and $L^1[0,1]$ norms. Discrete Green's functions are helpful while establishing the L_1-norm stability. Define Green's function $\mathcal{G}(x_i, \xi_j)$ associated with the operator L_N^1 and grid points $\xi_j = \{x_0, x_1 \dots x_N\}$ as

$$L_N^1 \mathcal{G}(x_i, \xi_j) = \delta_{i,j}(x_i, \xi_j); \quad \mathcal{G}(0, \xi_j) = \mathcal{G}(1, \xi_j) = 0, \tag{2.4.18}$$

where $\delta_{i,j}$ is the Kronecker delta and $i, j = 1, \dots N-1$.

Lemma 2.4.6. *There exists a positive constant C independent of ϵ such that*

$$0 \le |\mathcal{G}(x_i, \xi_j)| \le C, \quad i, j = 1, \dots N-1.$$

Proof. Fix $k \in \{0, 1, \dots, N\}$ and define a mesh function w_i as below

$$w_i = C \min \left\{ \prod_{j=i+1}^{k} \left(1 + \frac{\alpha h_j}{\epsilon}\right)^{-1}, 1 \right\}, \ i = 0, 1, \cdots N.$$

It is easy to follow that $w_i < C$ for $i < k$ and $w_i = C$ for $i \ge k$. If $0 < i < k$, we compute

$$\begin{aligned}
(L_N^1 w)_i &= \frac{-2\epsilon}{h_i + h_{i+1}} \frac{\alpha}{\epsilon} (w_i - w_{i-1}) + a_i \frac{\alpha}{\epsilon} w_{i-1} + b_i w_i \\
&= \frac{\alpha}{\epsilon} w_{i-1} \left[a_i - \frac{2\alpha h_i}{h_i + h_{i+1}} + b_i w_i \right] \\
&= \frac{\alpha}{\alpha h_i + \epsilon} w_i \left[a_i - \frac{\alpha h_i}{\hbar_i} + b_i \frac{h_i \alpha + \epsilon}{\alpha} \right] \ge \frac{C}{\max(\epsilon, h_i)} w_i > 0,
\end{aligned}$$

and if $i = k$

$$\begin{aligned}
(L_N^1 w)_i &= \frac{C\alpha}{\alpha h_k + \epsilon} \left(\frac{\epsilon}{\hbar_k} + a_k \right) \\
&= \frac{C\alpha}{\hbar_k} \left[\frac{\epsilon}{\alpha h_k + \epsilon} + \frac{a_k \hbar_k}{\alpha h_k + \epsilon} \right] \\
&= \frac{C\alpha}{\hbar_k} \left[\left(\frac{\epsilon + \alpha \hbar_k}{\alpha h_k + \epsilon} \right) + \left(\frac{(a_k - \alpha)\hbar_k}{\alpha h_k + \epsilon} \right) \right] \\
&= \frac{C\alpha}{\hbar_k} \left[\frac{1}{2} \left(\frac{\alpha h_k + \alpha h_{k+1} + 2\epsilon}{\alpha h_k + \epsilon} \right) \right] + \hbar_k \left[\frac{a_k - \alpha}{\alpha h_k + \epsilon} \right] = \frac{C}{2} \frac{\alpha}{\hbar_k}.
\end{aligned}$$

Also, $(L_N^1 w)_i = 0$ if $k < i < N$. Moreover, $\mathcal{G}(x_0, \xi_j) = 0 \le w_0$ and $\mathcal{G}(x_N, \xi_j) = 0 \le w_N$. Consequently, the required result follows from Lemma 2.4.5. □

If S denotes the space of grid functions s with $s_0 = s_N = 0$. Then, for $s \in S$

$$s_i = \sum_{j=1}^{N-1} \hbar_j \mathcal{G}_{ij} [L_N^1 s]_j, \quad i = 0, \dots, N,$$

and

$$\|s\|_{\infty,d} = max \left| \sum_{j=1}^{N-1} \hbar_j \mathcal{G}_{ij} [L_N^1 s]_j \right| \le C \left| \sum_{j=1}^{N-1} \hbar_j [L_N^1 s]_j \right| \le C \left\| L_N^1 s \right\|_{1,d}.$$

2.5 Error analysis

In this section, we calculate the consistency error for regular and singular components separately. Then, we combine both the results and find the error $\|Ru - U\|_{\infty,d}$. We begin our analysis with the regular component. To obtain consistency error on regular component $L_N^1(v - V)$, we will calculate the consistency error $(L_N^1 - L_N^0)(Rv - V^1)$ and relative consistency error $L_N^0(Rv) - (RLv)$. We assume $\hbar$ denotes H for $2 \le i \le N/2$ and h_i for $N/2 + 1 \le i \le N - 1$.

Lemma 2.5.1. *The regular component v of the solution u and its initial approximation V_i^1 satisfy*

$$\left|(L_N^1 - L_N^0)(Rv - V^1)_i\right| \le C\hbar^2. \tag{2.5.1}$$

Proof. For $\dfrac{N}{2} + 1 \le i \le N - 1$, $L_N^0 = L_N^1$. Thus

$$(L_N^1 - L_N^0)(Rv - V^1)_i = 0. \tag{2.5.2}$$

Now, for $1 \le i \le \dfrac{N}{2}$, Lemma 2.4.1 and the fact that $h_i = h_{i+1} = \hbar$ leads to

$$\begin{aligned}
L_N^1(L_N^1 - L_N^0)(Rv - V^1)_i &= \left(L_N^1 - L_N^0\right) L_N^1 \left(Rv - V^1\right)_i \\
&= a_i \left[D_- \left(L_N^1 Rv - L_N^1 V^1\right) - D_0 \left(L_N^1 Rv - L_N^1 V^1\right)\right] \\
&= a_i \left[D_-(L_N^1 Rv - Lv(x)) - D_0(L_N^1 Rv - Lv(x))\right] \\
&= a_i \left[\left(\frac{L_N^1(Rv)_i - L_N^1(Rv)_{i-1}}{h_i}\right) - \left(\frac{Lv(x_i) - Lv(x_{i-1})}{h_i}\right)\right] \\
&\quad -a_i \left[\left(\frac{L_N^1(Rv)_{i+1} - L_N^1(Rv)_{i-1}}{h_i + h_{i+1}}\right) + \left(\frac{Lv(x_{i+1}) - Lv(x_{i-1})}{h_i + h_{i+1}}\right)\right] \\
&= \frac{a_i}{2\hbar}\left[2\left(L_N^1(Rv)_i - L_N^1(Rv)_{i-1}\right) - 2\left(Lv(x_i) - Lv(x_{i-1})\right)\right] \\
&\quad -\frac{a_i}{2\hbar}\left[\left(L_N^1(Rv)_{i+1} - L_N^1(Rv)_{i-1}\right) + \left(Lv(x_{i+1}) - Lv(x_{i-1})\right)\right] \\
&= \frac{-\alpha}{\hbar}\left[(L_N^1(Rv)_{i+1} - Lv(x_{i+1})) - 2(L_N^1(Rv)_i - Lv(x_i))\right. \\
&\quad \left. + \left(L_N^1(Rv)_{i-1} - Lv(x_{i-1})\right)\right].
\end{aligned} \tag{2.5.3}$$

Now, we use (2.4.8) to obtain

$$\begin{aligned}
&|L_N^1(L_N^1 - L_N^0)(Rv - V^1)_i| \\
&\quad = \left|\frac{-\alpha}{\hbar}\left[\frac{-\epsilon}{6\hbar^2}\left[\int_{x_i}^{x_{i+1}} \left(v^{(4)}(\xi + \hbar) - 2v^{(4)}(\xi) + v^{(4)}(\xi - \hbar)(x_{i+1} - \xi)^3 d\xi\right)\right.\right. \\
&\qquad \left. - \int_{x_{i-1}}^{x_i} \left(v^{(4)}(\xi + \hbar) - 2v^{(4)}(\xi) + v^{(4)}(\xi - \hbar)(\xi - x_{i-1})^3 d\xi\right)\right] \\
&\qquad \left. + \frac{\alpha}{\hbar}\int_{x_{i-1}}^{x_i} (v^{(2)}(\xi + \hbar) - 2v^{(2)}(\xi) + v^{(2)}(\xi - \hbar)(\xi - x_{i-1}) d\xi)\right]\Bigg|.
\end{aligned} \tag{2.5.4}$$

An application of the fundamental theorem of calculus leads to

$$|L_N^1(L_N^1 - L_N^0)(Rv - V^1)_i| \le C\hbar^2 \left(\epsilon \left\|v^{(6)}\right\|_\infty + \left\|v^{(4)}\right\|_\infty\right). \tag{2.5.5}$$

Now on the coarse part, we apply the discrete maximum principle. Consider the barrier function $\bar{w}_i := C\hbar^2(1 + x_i)$. Then (2.4.1) leads to

$$\begin{aligned}
L_N^1\bar{w}_i &= -\epsilon D_+D_-\bar{w}_i + a_iD_-\bar{w}_i + b_i\bar{w}_i \\
&= \frac{-2\epsilon}{h_i + h_{i+1}}\left[\frac{\bar{w}_{i+1} - \bar{w}_i}{h_{i+1}} - \frac{\bar{w}_i - \bar{w}_{i-1}}{h_i}\right] + a_i\left[\frac{\bar{w}_i - \bar{w}_{i-1}}{h_i}\right] + b_i\bar{w}_i \\
&= \frac{-2\epsilon}{h_i + h_{i+1}}\left[\frac{C\hbar^2(1 + x_{i+1}) - C\hbar^2(1 + x_i)}{h_{i+1}} - \frac{C\hbar^2(1 + x_i) - C\hbar^2(1 + x_{i-1})}{h_i}\right] \\
&\quad + a_i\left[\frac{C\hbar^2(1 + x_i) - C\hbar^2(1 + x_{i-1})}{h_i}\right] + b_i(C\hbar^2(1 + x_i)) \\
&= \frac{-2\epsilon}{h_i + h_{i+1}}\left[\frac{C\hbar^2(1 + x_{i+1} - 1 - x_i)}{h_{i+1}} - \frac{C\hbar^2(1 + x_i - 1 - x_{i-1})}{h_i}\right] \\
&\quad + a_i\left[\frac{C\hbar^2(1 + x_i - 1 - x_{i-1})}{h_i}\right] + b_i(C\hbar^2(1 + x_i)) \\
&\ge C\hbar^2.
\end{aligned}$$

The required assertion thus follows from (2.5.2), (2.5.5) and Lemma 2.4.5. □

Lemma 2.5.2. *The error associated with the regular component v of the solution u of* (2.2.1) *satisfies*

$$\left|Lv(x_i) - L_N^0(Rv)_i\right| \le \begin{cases} CH^2\left(\epsilon\left\|v^{(4)}\right\|_\infty + \left\|v^{(3)}\right\|_\infty\right) & \text{for } 1 \le i \le \frac{N}{2}, \\ Ch_i\left(\epsilon\left\|v^{(3)}\right\|_\infty + \left\|v^{(2)}\right\|_\infty\right) & \text{for } \frac{N}{2} + 1 \le i \le N - 1. \end{cases} \tag{2.5.6}$$

Proof. For $1 \le i \le \dfrac{N}{2}$,

$$\begin{aligned}
L_N^0(Rv)_i - (RLv)_i &= \frac{-a_i}{4H}\left(\int_{x_i}^{x_{i+1}} v^{(3)}(\xi)(x_{i+1} - \xi)^2 d\xi - \int_{x_{i-1}}^{x_i} v^{(3)}(\xi)(\xi - x_{i-1})^2 d\xi\right) \\
&\quad - \frac{\epsilon}{6H^2}\left(\int_{x_i}^{x_{i+1}} v^{(4)}(\xi)(x_{i+1} - \xi)^3 d\xi - \int_{x_{i-1}}^{x_i} v^{(4)}(\xi)(\xi - x_{i-1})^3 d\xi\right) \\
&= \left|\frac{a_i}{4H}\left[\left\|v^{(3)}\right\|_\infty \frac{(x_{i+1} - x_i)^3}{3} + \left\|v^{(3)}\right\|_\infty \frac{(x_i - x_{i-1})^3}{3}\right]\right. \\
&\quad \left. + \frac{\epsilon}{6H^2}\left[\left\|v^{(4)}\right\|_\infty \frac{(x_{i+1} - x_i)^4}{4} + \left\|v^{(4)}\right\|_\infty \frac{(x_i - x_{i-1})^4}{4}\right]\right| \\
&\le CH^2\left(\epsilon\left\|v^{(4)}\right\|_\infty + \left\|v^{(3)}\right\|_\infty\right),
\end{aligned}$$

and for $\frac{N}{2}+1 \le i \le N-1$,

$$\begin{aligned}
\left|Lv(x_i) - L_N^0(Rv)_i\right| &= \left|\frac{-a_i}{h_i}\int_{x_{i-1}}^{x_i} v^{(2)}(\xi)(\xi - x_{i-1})d\xi - \frac{\epsilon}{h_i + h_{i+1}}\left[\frac{1}{h_{i+1}}\times\right.\right. \\
&\quad \left.\left.\int_{x_i}^{x_{i+1}} v^{(3)}(\xi)(x_{i+1}-\xi)^2 d\xi - \frac{1}{h_i}\int_{x_{i-1}}^{x_i} v^{(3)}(\xi)(\xi - x_{i+1})^2 d\xi\right]\right| \\
&= \left|\frac{-a_i}{h_i}\left\|v^{(2)}\right\|_\infty \frac{(x_i - x_{i-1})^2}{2} - \frac{\epsilon}{6(h_i+h_{i+1})}\left(\frac{1}{h_{i+1}}\left\|v^{(3)}\right\|_\infty\right.\right. \\
&\quad \left.\left.\times\frac{(x_{i+1}-x_i)^3}{3} - \frac{1}{h_i}\left\|v^{(3)}\right\|_\infty \frac{(x_i - x_{i-1})^3}{3}\right)\right| \\
&\le Ch_i\left(\epsilon\left\|v^{(3)}\right\|_\infty + \left\|v^{(2)}\right\|_\infty\right).
\end{aligned}$$

Thus, we find

$$\left|Lv(x_i) - L_N^0(Rv)_i\right| \le \begin{cases} CH^2\left(\epsilon\left\|v^{(4)}\right\|_\infty + \left\|v^{(3)}\right\|_\infty\right) & \text{for } 1 \le i \le \frac{N}{2}, \\ Ch_i\left(\epsilon\left\|v^{(3)}\right\|_\infty + \left\|v^{(2)}\right\|_\infty\right) & \text{for } \frac{N}{2}+1 \le i \le N-1. \end{cases}$$

□

Lemma 2.5.3. *The regular component v of the solution u and its corrected approximation V satisfy*

$$\|Rv - V\|_{\infty,d} \le CN^{-2}.$$

Proof. Combining inequalities from Lemma 2.5.1 and Lemma 2.5.2 to obtain

$$L_N^1(Rv - V) \le \begin{cases} CH^2 & \text{for } 1 \le i \le \frac{N}{2}, \\ Ch_i^2 & \text{for } \frac{N}{2}+1 \le i \le N. \end{cases}$$

Since $\|Rv - V\|_{\infty,d}$ vanishes at boundary, it follows that

$$\begin{aligned}
\|Rv - V\|_{\infty,d} &\le C\left\|L_N^1(v - V)\right\|_{1,d} \\
&\le CH^2 + \sum_{k=2}^{\frac{N}{2}} CH^3 + CH\frac{H + h_{\frac{N}{2}+1}}{2} + \sum_{k=\frac{N}{2}+2}^{N-1} h_i^3 \\
&\le C\left(H^2 + Hh_{\frac{N}{2}+1} + h_i^2\right) \le CN^{-2}.
\end{aligned}$$

□

The approach based on barrier functions is unsuitable for estimating the consistency error in analysing the singular component of the solution u. This term is complex when analysing the defect correction method, particularly on layer-adapted meshes. Therefore, we analyse the error estimates for singular components using the mesh function argument [133, 269].

Lemma 2.5.4. *The singular component ω of the solution u and its corrected approximation W satisfy*

$$L_N^1(\omega(x_i) - W) \leq \begin{cases} CN^{-(\phi-1)} & \text{for } 1 \leq i < \frac{N}{2}, \\ CN^{-(\phi-2)} & \text{for } i = \frac{N}{2}, \\ C\epsilon^{-1}N^{-1} & \text{for } \frac{N}{2}+1 \leq i \leq N-1. \end{cases} \tag{2.5.7}$$

Proof. For $1 \leq i \leq \dfrac{N}{2}$, we can write

$$\left|L_N^1(R\omega - W)_i\right| = \left|L_N^1(R\omega - W^1)_i\right| + \left|L_N^1(W^1 - W)_i\right|,$$

and consider both addends separately. From (2.4.11) and Lemma 2.4.4

$$\begin{aligned} \left|L_N^1(R\omega - W^1)_i\right| &= \left|L_N^1(R\omega)_i\right| \leq Q_{i+1}\left|\frac{4\epsilon}{H^2} + \frac{4\alpha}{H} + b_i\right| \\ &\leq CNQ_{i+1} \\ &\leq CN^{-(\phi-1)}. \end{aligned} \tag{2.5.8}$$

For $i = \dfrac{N}{2}$, we compute

$$\begin{aligned} \left|L_N^1(R\omega - W^1)_{\frac{N}{2}}\right| &\leq Q_{\frac{N}{2}+1}\left|\frac{2\epsilon}{h_i(H+h_i)} + \frac{2\epsilon}{H(H+h_i)} + \frac{4\alpha}{H} + b_i\right| \\ &\leq Q_{\frac{N}{2}+1}\left|\frac{4\epsilon}{Hh_i} + \frac{4\alpha}{H} + b_i\right| \\ &\leq CN^{-\phi}N^2 \\ &\leq CN^{-(\phi-2)}. \end{aligned} \tag{2.5.9}$$

Proceeding in a similar manner, we obtain

$$\left|L_N^1(W^1 - W)_i\right| = \left|L_N^0 W^1\right| \leq Q_{i+1}\left|\frac{4\epsilon}{H^2} + \frac{2\alpha}{H} + b_i\right| \leq CN^{-(\phi-1)}. \tag{2.5.10}$$

Thus, we find that

$$\left|L_N^1(\omega(x_i) - W)\right| \leq \begin{cases} CN^{-(\phi-1)} & \text{for } 1 \leq i < \frac{N}{2}, \\ CN^{-(\phi-2)} & \text{for } i = \frac{N}{2}. \end{cases} \tag{2.5.11}$$

Again, for $\dfrac{N}{2} + 1 \leq i \leq N-1$,

$$\left|L_N^1(R\omega - W)\right| = \left|(L_N^1 - L_N^0)(R\omega - W^1)\right| + \left|(L_N^0 R - RL)\omega\right|.$$

Then, the definition of L_N^0 leads to

$$\begin{aligned}
\left|L_N^1(R\omega - W)\right| &= \left|\frac{a_i}{h_i}\int_{x_{i-1}}^{x_i}\omega^{(2)}(\xi)(\xi - x_{i-1})d\xi - \frac{\epsilon}{h_i + h_{i+1}}\left[\frac{1}{h_{i+1}}\int_{x_i}^{x_{i+1}}\omega^{(3)}(\xi)\right.\right.\\
&\quad \left.\left.\times(x_{i+1} - \xi)^2 d\xi - \frac{1}{h_i}\int_{x_{i-1}}^{x_i}\omega^{(3)}(\xi)(\xi - x_{i-1})^2 d\xi\right]\right|\\
&\leq \left|C\epsilon^{-2}\int_{x_{i-1}}^{x_i} e^{-\frac{\alpha(1-\xi)}{2\epsilon}}d\xi + \frac{\epsilon}{h_i + h_{i+1}}\left[h_{i+1}\epsilon^{-3}\int_{x_i}^{x_{i+1}} e^{-\frac{\alpha(1-\xi)}{2\epsilon}}d\xi\right.\right.\\
&\quad \left.\left.-h_i\int_{x_{i-1}}^{x_i} e^{-\frac{\alpha(1-\xi)}{2\epsilon}}d\xi\right]\right|\\
&\leq \left|C\epsilon^{-2}\left[\frac{e^{-\alpha(1-\xi)/2\epsilon}}{-\alpha/2\epsilon}\right]_{x_{i-1}}^{x_i} + \frac{\epsilon}{h_i + h_{i+1}}\left[h_{i+1}\epsilon^{-3}\left[\frac{e^{-\alpha(1-\xi)/2\epsilon}}{-\alpha/2\epsilon}\right]_{x_i}^{x_{i+1}}\right.\right.\\
&\quad \left.\left.-h_i\epsilon^{-3}\left[\frac{e^{-\alpha(1-\xi)/2\epsilon}}{-\alpha/2\epsilon}\right]_{x_{i-1}}^{x_i}\right]\right|\\
&\leq \left|\frac{-C\epsilon^{-1}}{\alpha}e^{\frac{-\alpha}{2\epsilon}}\left(e^{\frac{-\alpha x_i}{2\epsilon}} - e^{\frac{-\alpha x_{i-1}}{2\epsilon}}\right) + \frac{\epsilon^{-1}}{2h_i}\left(-h_i e^{\frac{-\alpha}{2\epsilon}}\left(e^{\frac{-\alpha x_{i+1}}{2\epsilon}} - e^{\frac{-\alpha x_i}{2\epsilon}}\right)\right)\right.\\
&\quad \left.-\left(-h_i e^{\frac{-\alpha}{2\epsilon}}\left(e^{\frac{-\alpha x_i}{2\epsilon}} - e^{\frac{-\alpha x_{i-1}}{2\epsilon}}\right)\right)\right|\\
&\leq \left|\frac{-C\epsilon^{-1}}{\alpha}e^{\frac{-\alpha}{2\epsilon}}e^{\frac{\alpha x_i}{2\epsilon}}e^{\frac{-\alpha h_i}{4\epsilon}}sinh\left(\frac{h_i\alpha}{4\epsilon}\right) - C\epsilon^{-1}e^{\frac{-\alpha}{2\epsilon}}e^{\frac{\alpha x_i}{2\epsilon}}\left(e^{\frac{\alpha h_{i+1}}{2\epsilon}} - e^{\frac{\alpha h_i}{2\epsilon}}\right)\right|\\
&\leq \left|\frac{-C\epsilon^{-1}}{\alpha}e^{\left(\frac{-\alpha}{2\epsilon}\left(1-\left(x_i+\frac{h_i}{4}\right)\right)\right)}sinh\left(\frac{h_i\alpha}{4\epsilon}\right) - \frac{\epsilon^{-1}}{2}e^{\left(\frac{\alpha}{2\epsilon}(1+x_i)\right)}sinh\left(\frac{h_i\alpha}{2\epsilon}\right)\right|\\
&\leq C\epsilon^{-1}N^{-1}. \qquad (2.5.12)
\end{aligned}$$

Combining (2.5.8), (2.5.9), (2.5.10), (2.5.11) and (2.5.12) to obtain

$$L_N^1(\omega(x_i) - W) \leq \begin{cases} CN^{-(\phi-1)} & \text{for } 1 \leq i < \dfrac{N}{2}, \\ CN^{-(\phi-2)} & \text{for } i = \dfrac{N}{2}, \\ C\epsilon^{-1}N^{-1} & \text{for } \dfrac{N}{2} + 1 \leq i \leq N-1. \end{cases}$$

□

Lemma 2.5.5. *The singular component ω of the solution u and its corrected approximation W on Γ_N satisfy*

$$\|R\omega - W\|_{\infty,d} \leq CN^{-2}.$$

Proof. Proceeding in the similar manner as in Lemma 2.4.11, we can obtain

$$\begin{aligned}
\|R\omega - W\|_{\infty,d} &\leq C\left\|L_N^1(R\omega - W)\right\|_{1,d}\\
&\leq C\sum_{k=1}^{\frac{N}{2}-1} HN^{-(\phi-1)} + \left(\frac{H + h_{\frac{N}{2}}}{2}\right)N^{-(\phi-2)} + \sum_{k=\frac{N}{2}+1}^{N-1} Ch_i\left(\epsilon^{-1}N^{-1}\right)\\
&\leq CN^{-2}.
\end{aligned}$$

□

We can now state the main result of this section, the principle convergence theorem. The proof follows immediately from Lemma 2.5.3 and Lemma 2.5.5.

Theorem 2.5.6. *The approximate solution U on Γ_N and the continuous solution u of* (2.2.1) *satisfies*

$$\|Ru - U\|_{\infty,d} \leq CN^{-2}.$$

2.6 Numerical results

In this section, we consider two test examples from [99, 123] and put to test the effectiveness of the proposed method. Test problems are solved using the higher-order defect correction method suggested over an adaptive mesh. We compare the results over some adaptive meshes available in literature like Shishkin mesh [244], Vulanovic-Improved Shishkin mesh [160], Bakhvalov-Shishkin mesh [158] and polynomial-Shishkin mesh [166]. Moreover, we compare the results of the proposed method with the B-spline collocation method [123].

For a given value of N, the maximum absolute error (E_N) and numerical rate of convergence (P_N) is calculated using the formula given below

$$E_N = \max_{\epsilon} \|u - U\|_{\Gamma_N} \text{ and } P_N = \log_2\left(\frac{E_N}{E_{2N}}\right).$$

Example 2.6.1. *Consider the following convection-diffusion problem [99]*

$$-\epsilon u''(x) + u'(x) = g(x), \quad u(0) = u(1) = 0.$$

Here $g(x)$ is chosen so that the exact solution of the problem reads

$$u(x) = \frac{1}{1+\epsilon}\left(-e^{-x} + \frac{(e^{-1}-1)e^{-(1-x)/\epsilon} + 1 - e^{-1-1/\epsilon}}{1 - e^{-1/\epsilon}}\right).$$

Example 2.6.2. *Consider the following convection-diffusion problem [123]*

$$-\epsilon u''(x) + u'(x) + u(x) = g(x), \; u(0) = u(1) = 0.$$

Here $g(x)$ is chosen so that the exact solution of the problem reads

$$u(x) = a\cos\pi x + b\sin\pi x + Ae^{\lambda_1 x} + Be^{-\lambda_2(1-x)},$$

where $a = \dfrac{\epsilon\pi^2 + 1}{\pi^2 + (\epsilon\pi^2+1)^2}$, $b = \dfrac{\pi}{\pi^2 + (\epsilon\pi^2+1)^2}$, $A = \dfrac{-a(1+e^{-\lambda_2})}{1 - e^{\lambda_1 - \lambda_2}}$, $B = \dfrac{a(1+e^{\lambda_1})}{1 - e^{\lambda_1 - \lambda_2}}$, *$\lambda_1(x) < 0$ and $\lambda_2(x) > 0$ are the solutions of $-\epsilon\lambda''(x) + \lambda'(x) + 1 = 0$.*

Table 2.2: Maximum absolute error (E_N) and order of convergence (P_N) for Example 2.6.1 for $m = 2$.

	$\epsilon = 2 \times 10^{-5}$		$\epsilon = 2 \times 10^{-6}$		$\epsilon = 2 \times 10^{-7}$	
N	E_N	P_N	E_N	P_N	E_N	P_N
16	0.02926078	2.22	0.02926309	2.22	0.02926332	2.22
32	0.00627276	2.44	0.00627324	2.44	0.00627329	2.44
64	0.00114921	2.58	0.00114931	2.57	0.00114933	2.58
128	1.913998e-04	2.67	1.914124e-04	2.67	1.914179e-04	2.67
256	3.004118e-05	2.72	3.004308e-05	2.72	3.004433e-05	2.72
512	4.536608e-06	2.76	4.537018e-06	2.76	4.537061e-06	2.76

Table 2.3: Maximum absolute error (E_N) and order of convergence (P_N) for Example 2.6.1 for $m = 3$.

	$\epsilon = 2 \times 10^{-5}$		$\epsilon = 2 \times 10^{-6}$		$\epsilon = 2 \times 10^{-7}$	
N	E_N	P_N	E_N	P_N	E_N	P_N
16	0.004112682	3.34	0.004113024	3.34	0.004113058	3.34
32	4.041751e-04	3.51	4.042070e-04	3.51	4.042102e-04	3.51
64	3.524795e-05	3.63	3.525091e-05	3.63	3.525117e-05	3.63
128	2.840703e-06	3.70	2.840961e-06	3.70	2.841127e-06	3.70
256	2.174327e-07	3.75	2.174606e-07	3.75	2.174776e-07	3.76
512	1.608364e-08	3.79	1.608370e-08	3.79	1.608425e-08	3.83

Test problems are solved using the proposed defect correction method over the polynomial-Shishkin mesh. For Example 2.6.1, the maximum absolute error and order of convergence are obtained numerically and tabulated in Table 2.2 and Table 2.3 for $m = 2$ and 3, respectively. Besides, Table 2.4 presents a comparative analysis of maximum absolute error for Example 2.6.1 when $m = 2$ over a variety of adaptive meshes available in literature. For Example 2.6.2, the maximum absolute error and order of convergence are obtained numerically and tabulated in Table 2.4 when $m = 2$. Moreover, Table 2.6 compares the result obtained using the proposed defect correction method for different values of perturbation parameters over a polynomial-Shishkin mesh with the B-spline collocation method [123]. Figures 2.3 and 2.4 show the mesh density in the layer regions for Example 2.6.1 for different values of N. Figures 2.1 and 2.2 illustrate a comparison of maximum absolute error obtained using the proposed defect correction method over a polynomial-Shishkin mesh with the upwind scheme over a Bakhvalov-Shiskin mesh and

Table 2.4: Comparison of maximum absolute error (E_N), for Example 2.6.1, using the proposed defect correction method on various layer adapted meshes when $\epsilon = 2 \times 10^{-07}$.

Shishkin mesh [244]	Vulanovic-Improved Shishkin mesh [160]	Bakhvalov-Shishkin mesh [158]	polynomial-Shishkin mesh [166]
0.01638513	0.02609376	0.0061189	3.525117e-05
6.365040e-03	9.863050e-03	1.746604e-03	2.841127e-06
2.259211e-03	3.290856e-03	4.944540e-04	2.841127e-06
7.504937e-04	1.009660e-03	1.453690e-04	2.174776e-07
2.378557e-04	2.934636e-04	4.626797e-05	1.608425e-08

Table 2.5: Maximum absolute error (E_N) and order of convergence (P_N), for Example 2.6.2, for $m = 2$.

	$\epsilon = 2 \times 10^{-3}$		$\epsilon = 2 \times 10^{-5}$		$\epsilon = 2 \times 10^{-7}$	
N	E_N	P_N	E_N	P_N	E_N	P_N
32	2.903882e-04	3.42	3.176081e-04	3.26	3.178090e-04	3.26
64	2.697840e-05	3.17	3.297016e-05	3.41	3.301339e-05	3.26
128	2.986647e-06	3.23	3.013666e-06	3.14	3.112148e-06	3.14
256	3.164733e-07	2.14	3.402792e-07	2.53	3.529333e-7	2.52
512	5.951543e-08	2.60	5.981563e-08	2.61	6.034316e-08	2.60

the results obtained using other meshes available in the literature, respectively. Furthermore, Figures 2.5 and 2.6 show the solution plot for different values of ϵ for Example 2.6.1 and 2.6.2, respectively.

2.7 Conclusion

A higher-order accurate adaptive finite difference method based on a defect correction method is presented over a non-uniform polynomial-Shishkin mesh to solve singularly perturbed convection-diffusion problems. The underlying technique combines an inexpensive, lower-order stable, upwind difference scheme and a higher-order, less stable central difference scheme. The procedure starts with a stable, low-order, computationally inexpensive upwind method. Then, the defect correction proceeds by computing a sequence of approximations to the solution using a higher-order central difference method. Each successive approximation is of higher accuracy than the previous one. The approximations are sought on the same mesh to increase a numerical solution's accuracy

Table 2.6: Comparison of maximum absolute error (E_N), for Example 2.6.2, using the proposed defect correction method on a polynomial-Shishkin mesh with $m = 3$ and B-spline collocation method [123].

	B-spline collocation method [123]		Proposed method	
N	$\epsilon = 10^{-2}$	$\epsilon = 10^{-4}$	$\epsilon = 10^{-2}$	$\epsilon = 10^{-4}$
32	1.6438e-02	2.4642e-02	1.2374e-05	1.9838e-05
64	6.6001e-03	1.2649e-02	1.7802e-06	2.2779e-06
128	2.4825e-03	6.5826e-03	1.7109e-07	3.8653e-07
256	6.4332e-04	3.3112e-03	1.3427e-08	2.4679e-08
512	1.613e-04	1.6136e-03	9.0647e-10	9.3278e-10

without applying any grid refinement. The method yields highly accurate results for singular perturbation problems avoiding prevalent numerical oscillation in the numerical approximation. The method is unconditionally stable and free from directional bias. The convergence obtained is optimal because it is free from the logarithmic term. Numerical results and illustrations support the theoretical estimates. The results obtained using the proposed method over the polynomial-Shishkin mesh are superior to other adaptive meshes in the literature and spline collocation methods. The method presented is easy to implement and, with a bit of modification, can easily be extended to even more general situations like problems in higher dimensions and nonlinear evolution equations.

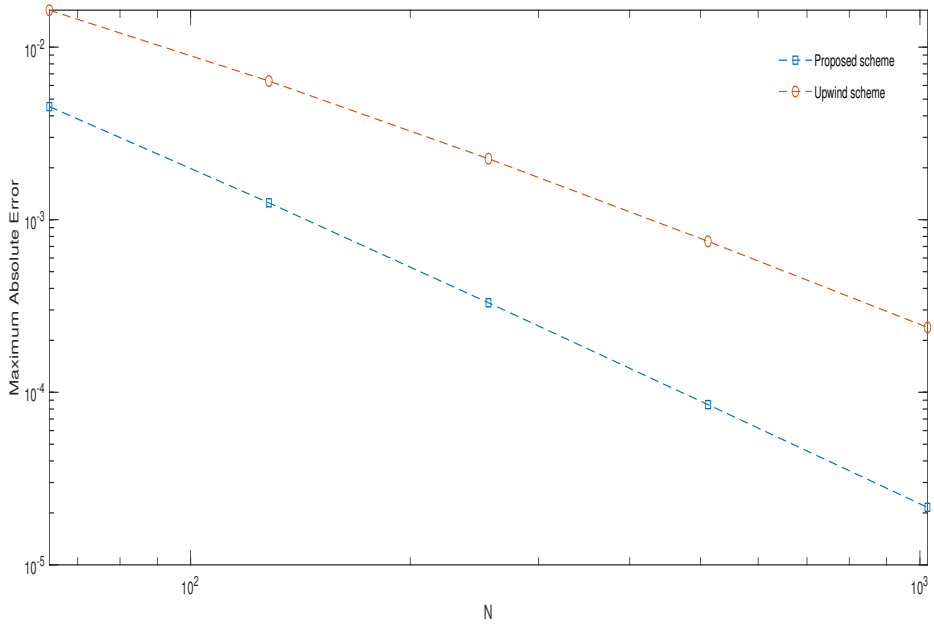

Figure 2.1: Comparison of maximum absolute error (E_N), for Example 2.6.1, with an upwind scheme defined over a Bakhvalov-Shishkin mesh.

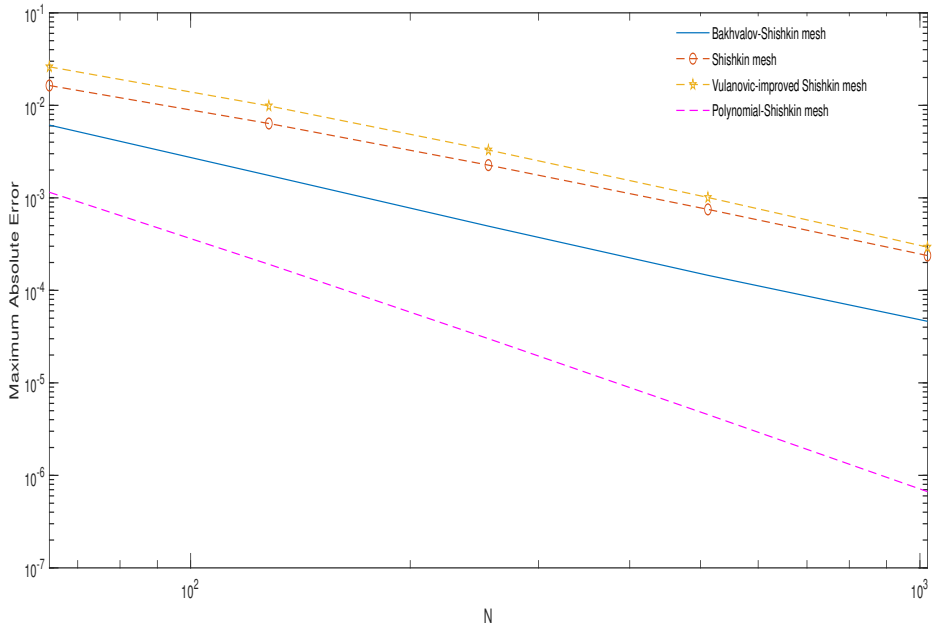

Figure 2.2: Comparison of maximum absolute error (E_N), for Example 2.6.1, using proposed method over various layer adapted meshes.

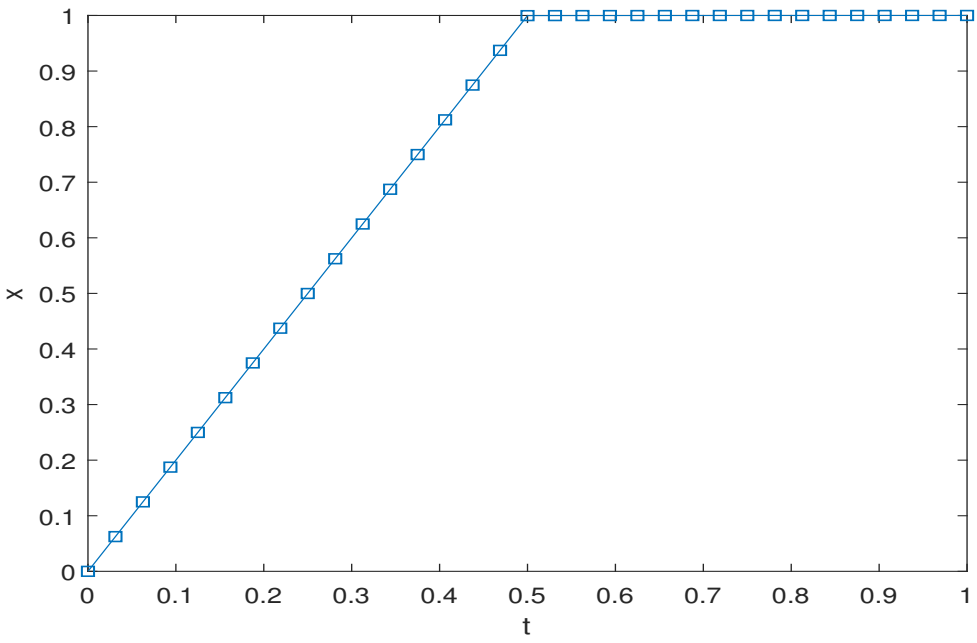

Figure 2.3: The mesh density towards the boundary layer $x = 1$ when $\epsilon = 10^{-05}$ and $N = 32$.

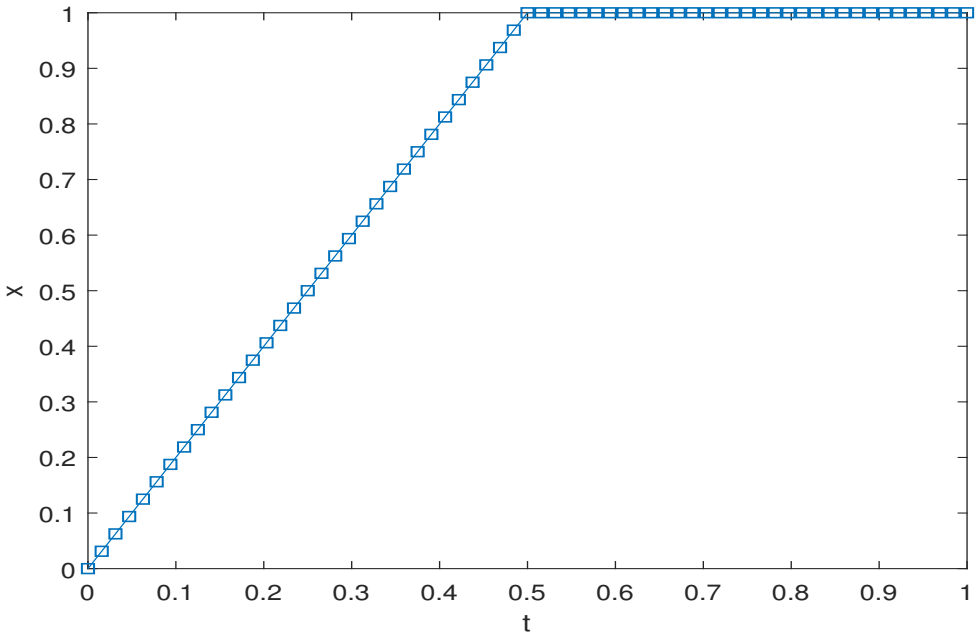

Figure 2.4: The mesh density towards the boundary layer $x = 1$ when $\epsilon = 10^{-05}$ and $N = 64$.

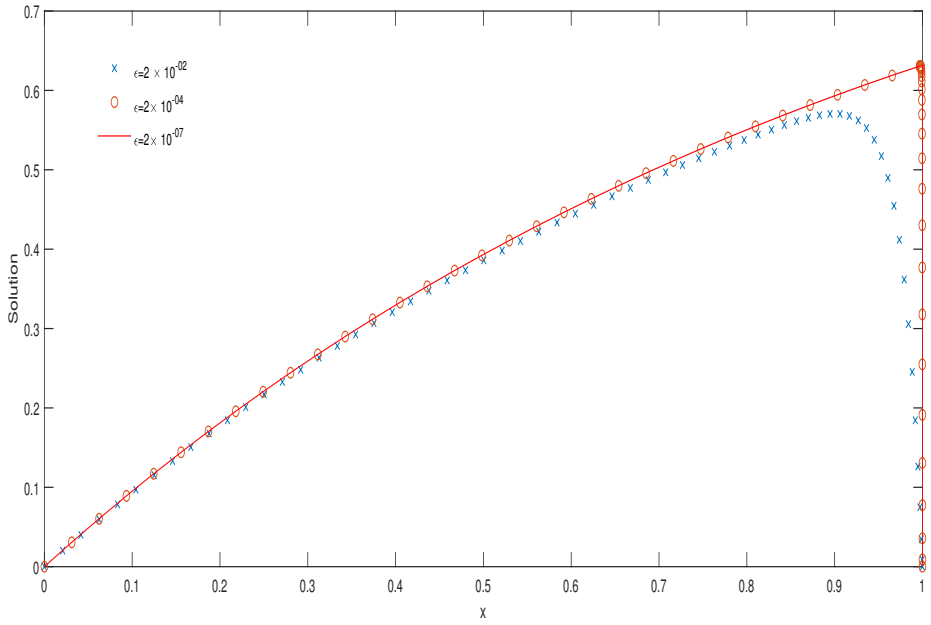

Figure 2.5: Numerical solution for Example 2.6.1 for different values of ϵ when $N = 64$.

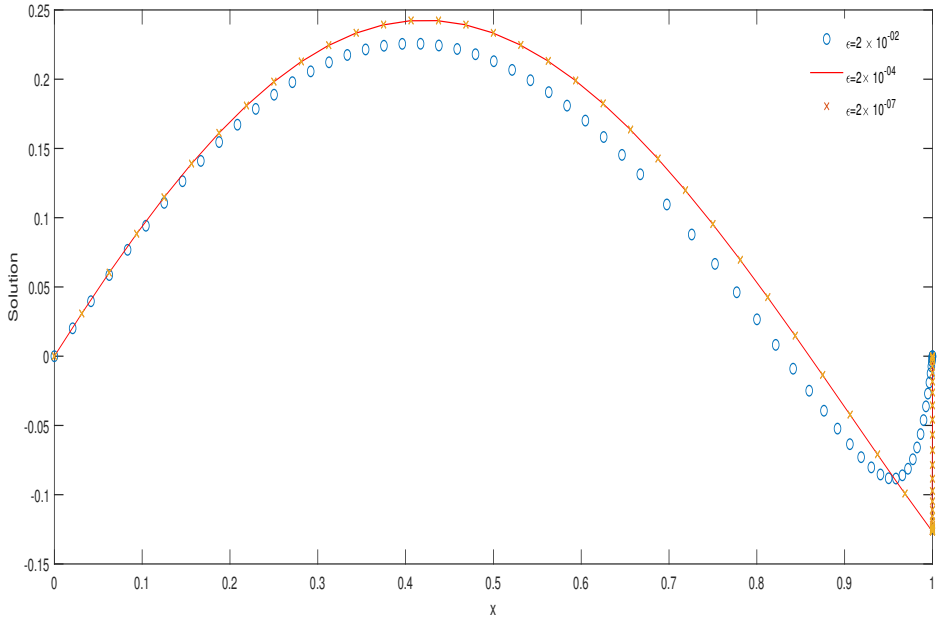

Figure 2.6: Numerical solution for Example 2.6.2 for different values of ϵ and $N = 64$.

Chapter 3

Convection-Diffusion Problems with Discontinuous Coefficient and Point Source

3.1 Introduction

In Chapter 2, we proposed a defect correction scheme for a class of singularly perturbed convection-diffusion problems. This chapter extends our study to singularly perturbed convection-diffusion problems with discontinuous coefficients and a point source.

Singularly perturbed convection-diffusion problems with discontinuous coefficients and point sources constitute a challenging class of mathematical models that arise in various fields, including physics, engineering and biology. These problems are stiff as they have a small parameter multiplying the highest-order differential coefficient and exhibit sensitivity to small perturbations in the system parameter. The presence of discontinuous coefficients and point sources adds complexity to the problem.

Discontinuous coefficients introduce abrupt changes or jumps in the system's material properties or physical characteristics. Moreover, the problem being singularly perturbed, the solution of these equations exhibits a multiscale character since the corresponding degenerate system fails to satisfy the given boundary data. There are narrow regions across which the solution changes rapidly and displays layer behaviour. Standard numerical methods on uniform meshes fail to consistently approximate solutions in these layer regions. Consequently, traditional solution techniques may not be directly applicable, requiring specialised methods to handle the discontinuities appropriately.

Many researchers have worked to provide estimation strategies for the discretization errors in numerical solutions of singular perturbation problems. Essentially, there are two

distinct categories of error estimation strategies. Instead of estimating the errors for a particular mesh, a priori error estimators provide information about the asymptotic behaviour of discretization errors. In contrast, posteriori error estimators directly determine actual solution error estimates from the numerical solution. The authors attempted to provide posteriori error estimates for different singular perturbation problems. Considerable attempts are seen in literature providing posteriori error estimates for different singular perturbation problems. In [167], authors solved a two-point boundary-value problem for a singularly perturbed convection-diffusion problem using a defect correction method. They obtained a robust posteriori error estimate of second-order in maximum norm.

In [172], authors considered a two-parameter singularly perturbed two-point boundary-value problem of reaction-convection-diffusion type. The problem was solved using a streamline-diffusion finite element method, and the author obtained a posteriori error estimate in the maximum norm. In [118], authors examined a two-parameter singular perturbation problem using the defect correction method over a Bakhvalov-Shishkin mesh. A posteriori error estimate they obtained is of second-order in maximum norm. In [112], a parameterised singular perturbation problem was solved using a hybrid difference method on an arbitrary mesh. A second-order accurate solution-adaptive algorithm based on the a posteriori error estimation was designed by equidistributing a monitor function. In [142], a singularly perturbed quasi-linear two-point boundary value problem with an exponential boundary layer was discretised on arbitrary non-uniform meshes using finite difference schemes. The authors gave first and second-order maximum norm a posteriori error estimates based on different derivatives of the numerical solution. Later, in [289], authors generalised and improved these results using the upwind finite difference discretization. In [238], authors considered two types of singularly perturbed, linear partial differential equations, namely time-dependent convection-diffusion problems and a two-dimensional elliptic equation having a first-order unperturbed operator and constructed finite element approximations via modifications of classical methods of lines and established a-posteriori estimates for the error between the solutions of the finite element methods and the boundary value problems arising from the line methods. In [237], authors proposed the Crank-Nicolson-Galerkin method of solving a singularly perturbed parabolic initial value problem. They derived posteriori error estimates for the finite element solution of the given parabolic problem on every discrete time level, providing a basis for adaptive mesh refinement. In [292], the author presents a posteriori error estimator for approximating the solution to an advection-diffusion equation with a non-constant, vector-valued diffusion coefficient in a conforming finite element space. Based on the complementary variational principle, they show that the error of an approximate solution

in an associated energy norm is bounded by the sum of the weighted L^2-norms of solutions to a set of independent complementary variational problems, each defined on only one element of the partition. The error bound guarantees the overestimation of the actual error and does not depend unfavourably on ϵ. Although the original equation is a non-self-adjoint problem, the strong form of each local variational problem is always a Poisson equation with Neumann boundary conditions. In [297], authors derived posteriori error estimates for the nonconforming finite element approximations on anisotropic meshes for a singularly perturbed reaction-diffusion problem.

The analysis of posteriori error estimates has yet to see much development in the literature. This chapter presents a defect correction method to solve a singularly perturbed convection-diffusion problem with a discontinuous coefficient and a point source over a Bakhvalov Shishkin mesh. We establish a posteriori error estimate of second-order in the maximum norm. Moreover, the chapter illustrates numerical results to support theoretical estimates.

3.2 Problem Description

Let $\Omega = (0, 1)$, $\Omega^- = (0, c)$ and $\Omega^+ = (c, 1)$. Consider the non-homogeneous boundary value problem

$$\left.\begin{aligned} &Lu(x) = -\epsilon u''(x) - (a(x)u(x))' + b(x)u(x) = g(x) + \gamma\delta_c,\ x \in (0, 1), \\ &u(0) = u(1) = 0, \end{aligned}\right\} \tag{3.2.1}$$

where $0 < \epsilon \ll 1$ is the small perturbation parameter, $\delta_c(x) = \delta(x - c)$ with $c \in \Omega$ is the Dirac-delta function, $a(x) \geq \alpha_1 > 0$ for $x \in (0, c)$ and $a(x) \geq \alpha_2 > 0$ for $x \in (c, 1)$. Let $\alpha = \min\{\alpha_1, \alpha_2\}$, $a(x)$ and $b(x)$ are sufficiently smooth functions such that

$$b(x) \geq 0 \text{ and } b(x) - (a(x))' \geq 0,\ x \in [0, 1]. \tag{3.2.2}$$

Thus, we may write

$$Lu = \begin{cases} -\epsilon u''(x) - (a(x)u(x))' + b(x)u(x) = g(x), & x \in (0, c) \cup (c, 1), \\ -\epsilon[u'](c) - [a](c)u(c) = \gamma, \end{cases} \tag{3.2.3}$$

where $[\eta](c) = \eta(c + 0) - \eta(c - 0)$ denotes the jump.

The operator L satisfies the maximum principle [225], and the problem (3.2.1) has a unique solution, $u \in C[0, 1] \cap C^2((0, c) \cup (c, 1))$ [166]. Moreover, from [169], we have

$$\|u\|_\infty \leq \frac{2}{\alpha} \sup_{x\in(0,1)} \left| \int_x^1 (g + \gamma\delta_c)(s)ds \right| \leq \frac{2}{\alpha} \left(\|g\|_{L^1(0,1)} + |\gamma| \right). \tag{3.2.4}$$

For $x \in (0, c)$, the solution of (3.2.1) satisfies

$$Lu = g,\ x \in (0, c), \quad u(0) = 0,\ u(c) = \rho.$$

From (3.2.4), note that $|\rho| \leq C$. Therefore, it follows from [133] that

$$|u^{(k)}(x)| \leq C\left\{1 + \epsilon^{-k}\exp\left(-\frac{\alpha_1 x}{\epsilon}\right)\right\},\ x \in (0, c),\ k = 0, 1, \cdots q, \tag{3.2.5}$$

where q depends on the smoothness of a, b and g on $(0, c)$. For $x \in (c, 1)$, the solution of (3.2.1) satisfies

$$Lu = g,\ x \in (c, 1), \quad u(c) = \rho,\ u(1) = 0,$$

and

$$|u^{(k)}(x)| \leq C\left\{1 + \epsilon^{-k}\exp\left(-\frac{\alpha_2(x-c)}{\epsilon}\right)\right\},\ x \in (c, 1),\ k = 0, 1, \cdots q. \tag{3.2.6}$$

Combining (3.2.5) and (3.2.6) to find

$$|u^{(k)}(x)| \leq C\left\{1 + \epsilon^{-k}\left\{\exp\left(-\frac{\alpha_1 x}{\epsilon}\right) + H_c(x)\exp\left(-\frac{\alpha_2(x-c)}{\epsilon}\right)\right\}\right\}, \tag{3.2.7}$$

where $H_c(x) = \begin{cases} 0, & x < c \\ 1, & x > c \end{cases}$ is the Heaviside step function.

3.3 Mesh Description

The solution to the problem (3.2.1) exhibits an interior layer at $x = c$ and a boundary layer at $x = 0$. Thus, we construct a non-uniform mesh that condenses points around $x = 0$ and $x = c$. For that, we use Bakhvalov-Shishkin mesh. Let $N \geq 8$ and τ_1, τ_2 be the mesh transition parameters such that

$$\tau_1 = \min\left\{\frac{c}{2}, \tau_0\epsilon\log N\right\},\ \tau_2 = \min\left\{\frac{1-c}{2}, \tau_0\epsilon\log N\right\},\ \tau_0 \geq 1.$$

Let $\tau_1 = \tau_2 = \tau_0\epsilon\log N$. Otherwise, N^{-1} is exponentially small compared to ϵ. We construct a mesh Γ_N such that

$$\Gamma_N = [0, c-\tau_1] \cup [c-\tau_1, c] \cup [c, 1-\tau_2] \cup [1-\tau_2, 1]. \tag{3.3.1}$$

The subintervals $(0, c-\tau_1)$ and $(c, 1-\tau_2)$ contain $N/4$ mesh points, and subintervals $(c-\tau_1, c)$ and $(1-\tau_2, 1)$ contain the same number of mesh points placed uniformly such that $x_0 = 0$, $x_{N/4} = c - \tau_1$, $x_{3N/4} = 1 - \tau_2$ and $x_N = 1$. The mesh is generated using a continuous, monotonically increasing, piecewise differentiable mesh-generating function

$$\Phi(t) = \begin{cases} \Phi_1(t) = -\log(1 - 4(1 - N^{-1})t), & t \in \left[0, \frac{1}{4}\right], \\ \Phi_2(t) = -\log(1 - 2(1 - N^{-1})(2t - 1)), & t \in \left[\frac{1}{2}, \frac{3}{4}\right]. \end{cases}$$

The resulting mesh reads

$$x_i = \begin{cases} \epsilon\tau_0\Phi_1(t_i), & i = 0, \cdots, N/4, \\ \tau_1 + 4\left(i - \dfrac{N}{4}\right)\left(\dfrac{1-\tau_1}{N}\right), & i = N/4+1, \cdots, N/2, \\ c + \epsilon\tau_0\Phi_2(t_i), & i = N/2+1, \cdots, 3N/4, \\ (c+\tau_2) + 4\left(i - \dfrac{3N}{4}\right)\left(\dfrac{1-c-\tau_2}{N}\right), & i = 3N/4+1, \cdots, N, \end{cases} \tag{3.3.2}$$

where $t_i = \dfrac{i}{N}$. As in Lemma 2.3.1, the step size satisfies $h_i \leq CN^{-1}$ for all $i = 0, \ldots, N$.

3.4 The Difference Scheme

For $i \geq 1$, a function ω_i and step size h_i, the forward, backward and central difference approximation to first-order derivatives are defined as

$$\omega_{x,i} = \frac{\omega_{i+1} - \omega_i}{h_{i+1}},\ \omega_{\bar{x},i} = \omega_{x,i-1} = \frac{\omega_i - \omega_{i-1}}{h_i},\ \omega_{\dot{x},i} = \frac{\omega_{i+1} - \omega_{i-1}}{2\hbar_i}, \text{and } \omega_{\hat{x},i} = \frac{\omega_{i+1} - \omega_i}{\hbar_i},$$

with the weighted mesh increment $\hbar$ defined by

$$\hbar_i = \begin{cases} \frac{h_1}{2}, & i = 0, \\ \frac{h_{i+1}+h_i}{2}, & i = 1, \cdots, N-1, \\ \frac{h_N}{2}, & i = N. \end{cases}$$

The upwind operator L_N^1 for problem (3.2.1) takes the form

$$L_N^1\omega_i = -\epsilon\omega_{\bar{x}x,i} - (a^-\omega)_{x,i} + (b\omega)_i = g_i + \Delta_{c,i}, \tag{3.4.1}$$

and the central difference operator L_N^2 results in

$$L_N^2\omega_i = -\epsilon\omega_{\bar{x}\hat{x},i} - (a^-\omega)_{\dot{x},i} + (b\omega)_i = g_i + \Delta_{c,i}, \tag{3.4.2}$$

where $\Delta_{c,i} = \begin{cases} h_{i+1}^{-1}, & c \in [x_i, x_{i+1}), \\ 0, & \text{otherwise.} \end{cases}$ The defect correction method takes the form

1. Compute initial approximation $\hat{U}^N$ using an upwind difference scheme

$$[L_N^1\hat{U}^N]_i = g_i + \Delta_{c,i},\ i = 1, 2, \cdots N-1. \tag{3.4.3}$$

2. Estimate the defect σ using the central difference scheme

$$\sigma_i = [L_N^2\hat{U}^N]_i - (g_i + \Delta_{c,i}),\ i = 1, 2, \cdots N-1. \tag{3.4.4}$$

3. Compute the defect-correction ∇ by solving

$$[L_N^1 \nabla]_i = \kappa_i \sigma_i, \quad \kappa_i = \frac{\hbar_i}{h_{i+1}}, \ i = 1, 2, \cdots, N-1. \tag{3.4.5}$$

4. The final corrected solution is given by

$$U_i^N = \hat{U}_i^N - \nabla_i, \ i = 1, 2, \cdots, N. \tag{3.4.6}$$

Next, let us define continuous and discrete operators to help us find the posteriori error bounds. Following [166], we define

$$\begin{aligned} (\mathcal{A}\omega)(x) &= \epsilon\omega'(x) + (a^-\omega)(x) + \int_x^1 (b\omega)(s)ds, \\ \mathcal{F}(x) &= \int_x^1 g(s)ds + \begin{cases} \gamma, & x \le c, \\ 0, & \text{otherwise}, \end{cases} \end{aligned} \tag{3.4.7}$$

$$[A^u\omega]_i = \epsilon\omega_{\bar{x},i} + (a^-\omega)_i + \sum_{k=i}^{N-1} h_{k+1}(b\omega)_k, \quad F_i^u = \sum_{k=i}^{N-1} h_{k+1}g_k + \begin{cases} \gamma, & x_i \le c, \\ 0, & \text{otherwise}, \end{cases} \tag{3.4.8}$$

and

$$[A^c\omega]_i = \epsilon\omega_{\bar{x},i} + \left(\frac{(a\omega) + (a\omega)_{-1}}{2}\right)_i + \sum_{k=i}^{N} \hbar_k(b\omega)_k, \ F_i^c = \sum_{k=i}^{N} \hbar_k g_k + \begin{cases} \gamma, & x_i \le c, \\ 0, & \text{otherwise}, \end{cases} \tag{3.4.9}$$

where $(b\omega)_{-1} = (b\omega)_{i-1}$ and $\hbar = \dfrac{h_N}{2}$. Note that $L\omega = -(\mathcal{A}\omega)'$ and $g = -(\mathcal{F})'$ on $(0, 1)$. It follows from (3.2.1) that $(\mathcal{A}\omega - \mathcal{F})'(x) = 0$. Consequently, integration yields

$$(\mathcal{A}\omega - \mathcal{F})(x) = \vartheta, \ x \in (0, 1), \tag{3.4.10}$$

where ϑ is some constant. From (3.4.3) and (3.4.8)

$$[L_N^1\omega] = -(A^u\omega)_x \quad \text{and} \quad g = -F_x^u.$$

Thus, we get

$$(\mathcal{A}u - \mathcal{F})(x) = c \text{ for } x \in (0, 1). \tag{3.4.11}$$

From (3.4.3), (3.4.4), (3.4.5) and (3.4.6), we obtain

$$[A^c U - (A^u - A^c)\Delta - F^c]_i = \hat{c} \ \text{ for } \ i = 1, 2, \cdots, N. \tag{3.4.12}$$

3.5 Error Analysis

In this section, we perform an error analysis. The analysis we perform employs the stability properties of the differential operator [7, 170]. Given an arbitrary function ω with $\omega(0) = \omega(1) = 0$, we have

$$\omega(x) = \int_0^1 \mathcal{G}(x,\xi)(L\omega)(\xi)d\xi \text{ for } x \in [0,1],$$

where $\mathcal{G}$ is the Green's function associated with L and Dirichlet boundary conditions, solves for fixed $\xi \in [0,1]$

$$\left.\begin{aligned}(L\mathcal{G}(\cdot,\xi))(x) = \delta(x-\xi) \text{ for } \ x \in (0,1),\\ \mathcal{G}(0,\xi) = \mathcal{G}(1,\xi) = 0,\end{aligned}\right\} \tag{3.5.1}$$

where δ is the Dirac-delta function. Moreover, $\mathcal{G}$ can also be defined using the adjoint operator $\mathcal{L}^*\omega = -\epsilon\omega'' + a\omega' + b\omega$ for fixed ξ as

$$\left.\begin{aligned}(\mathcal{L}^*\mathcal{G}(x,\cdot))(\xi) = \delta(\xi - x) \text{ for } \xi \in (0,1),\\ \mathcal{G}(x,0) = \mathcal{G}(x,1) = 0.\end{aligned}\right\} \tag{3.5.2}$$

Next, we define

$$\|\omega\|_\infty = \sup_{x\in[0,1]} |\omega(x)|, \ \ \|\omega\|_1 = \int_0^1 |\omega(x)|dx$$

and the $W^{-1,\infty}$ norm as

$$\|\omega\|_{-1,\infty} := \sup_{u\in W_0^{1,1}:|u|_{1,1}=1} \langle u,\omega\rangle = \min_{V:V'=\omega} \|V\|_\infty = \min_{C\in\mathbb{R}} \left\| \int_0^1 \omega(s)ds + C \right\|_\infty .$$

For an arbitrary $x \in (0,1)$ the reader is referred to [166, 165] to see the bounds on various norms of $\mathcal{G}(x,\cdot)$.

Lemma 3.5.1. *The Greeen's function $\mathcal{G}$ associated with the discrete operator L satisfies*

$$\|\mathcal{G}(x,\cdot)\|_1 \le \|\mathcal{G}(x,\cdot)\|_\infty \le \alpha^{-1}, \ \left\|\mathcal{G}_\xi(x,\cdot)\right\|_1 \le 2\alpha^{-1}, \ \left\|\mathcal{G}_{x\xi}(x,\cdot)\right\|_1 \le 2\epsilon^{-1}.$$

Moreover, for all $\omega \in W_0^{1,\infty}(0,1)$, the operator L satisfies

$$\|\omega\|_{\epsilon,\infty} = \max\left\{\frac{\alpha}{2}\|\omega\|_\infty, \frac{\epsilon}{2}\|\omega\|_\infty\right\} \le \|L\omega\|_{-1,\infty}.$$

Proof. For proof, see [166]. □

Theorem 3.5.2. *Let u be the solution of the boundary value problem*

$$Lu = -\mathcal{F}' \text{ on } (0,1); \ u(0) = u(1) = 0,$$

where

$$\mathcal{F} = A_{i-1/2}(x - x_{i-1/2}) \text{ for } x \in (x_{i-1}, x_i).$$

Then,

$$\|u\|_\infty \leq \max_{i=1,\cdots,N} \left\{ |A|_{i-1/2} \min\left[\frac{h_i}{2}, \frac{h_i^2}{8\epsilon}\right]\right\} \left(\frac{2 + 2\,\|a\|_\infty + \|b\|_\infty + \alpha}{\alpha}\right). \tag{3.5.3}$$

Proof. Let $x \in (0, 1)$ be arbitrary but fixed. The Green's function representation yields

$$\begin{aligned}
u(x) &= \int_0^1 \mathcal{G}(x,\xi) Lu(\xi) d\xi \\
&= -\int_0^1 \mathcal{G}(x,\xi)\mathcal{F}'(\xi) d\xi \\
&= \int_0^1 \mathcal{G}_\xi(x,\xi)\mathcal{F}(\xi) d\xi + \mathcal{G}(x,0)\mathcal{F}(0) - \mathcal{G}(x,1)\mathcal{F}(1) \\
&= \sum_{i=1}^N \int_{x_{i-1}}^{x_i} \mathcal{G}_\xi(x,\xi)\mathcal{F}(\xi) d\xi \\
&= \sum_{i=1}^N \int_{x_{i-1}}^{x_i} \mathcal{G}_\xi(x,\xi) A_{i-1/2}\,(\xi - x_{i-1/2})\, d\xi \\
&= \sum_{i=1}^N A_{i-1/2} \int_{x_{i-1}}^{x_i} \mathcal{G}_\xi(x,\xi)(\xi - x_{i-1/2}) d\xi \\
&= \sum_{i=1}^N A_{i-1/2} I_i,
\end{aligned}$$

where

$$\begin{aligned}
I_i &= \int_{x_{i-1}}^{x_i} \mathcal{G}_\xi(x,\xi)(\xi - x_{i-1/2}) d\xi \\
&= \frac{h_i^2}{8} \int_{x_{i-1}}^{x_i} \mathcal{G}_{\xi\xi}(x,\xi) d\xi - \int_{x_{i-1}}^{x_i} \mathcal{G}_{\xi\xi}(x,\xi) \frac{(\xi - x_{i-1/2})^2}{2} d\xi \\
&= \int_{x_{i-1}}^{x_i} \mathcal{G}_{\xi\xi}(x,\xi) d\xi \left[\frac{h_i^2}{8} - \frac{(\xi - x_{i-1/2})^2}{2}\right] d\xi.
\end{aligned} \tag{3.5.4}$$

Thus, we have

$$|I_i| \leq \frac{h_i}{2} \int_{x_{i-1}}^{x_i} |\mathcal{G}_\xi(x,\xi)| d\xi \;\text{ and }\; |I_i| \leq \frac{h_i^2}{8} \int_{x_{i-1}}^{x_i} |\mathcal{G}_{\xi\xi}(x,\xi)| d\xi.$$

Hence

$$|I_i| \leq \min\left\{\frac{h_i}{2}, \frac{h_i^2}{8\epsilon}\right\} \int_{x_{i-1}}^{x_i} \left(\epsilon \left|\mathcal{G}_{\xi\xi}(x,\xi)\right| + \left|\mathcal{G}_\xi(x,\xi)\right|\right) d\xi.$$

Therefore, it follows that

$$\begin{aligned}
|u(x)| &\leq \sum_{i=1}^N \left|A_{i-1/2} I_i\right| \leq \max_{i=1,\cdots,N} \left(\left|A_{i-1/2}\right| \min\left\{\frac{h_i}{2}, \frac{h_i^2}{8\epsilon}\right\}\right) \\
&\quad \times \left(\int_{x_{i-1}}^{x_i} \epsilon |\mathcal{G}_{\xi\xi}(x,\xi)| d\xi + \int_{x_{i-1}}^{x_i} |\mathcal{G}_\xi(x,\xi)| d\xi\right).
\end{aligned} \tag{3.5.5}$$

From (3.5.2), we get

$$\int_{x_{i-1}}^{x_i} \epsilon \mathcal{G}_{\xi\xi}(x,\xi) = -\int_{x_{i-1}}^{x_i} \delta(\xi - x) + \|a\|_\infty \int_{x_{i-1}}^{x_i} |\mathcal{G}_\xi(x,\xi)| d\xi + \|b\|_\infty \int_{x_{i-1}}^{x_i} |\mathcal{G}(x,\xi)| d\xi. \quad (3.5.6)$$

Thus, from (3.5.5) and (3.5.6), we obtain

$$\begin{aligned} |u(x)| &\leq \max_{i=1,\cdots,N} \left\{ |A_{i-1/2}| \min\left(\frac{h_i}{2}, \frac{h_i^2}{8\epsilon}\right)\right\} \times \left(-\int_{x_{i-1}}^{x_i} \delta(\xi - x) + \|a\|_\infty \right. \\ &\quad \left. \times \int_{x_{i-1}}^{x_i} |\mathcal{G}_\xi(x,\xi)| d\xi + \|b\|_\infty \int_{x_{i-1}}^{x_i} |\mathcal{G}(x,\xi)| d\xi + \int_{x_{i-1}}^{x_i} |\mathcal{G}_\xi(x,\xi)| d\xi \right) \\ &\leq \max_{i=1,\cdots,N} \left\{ |A_{i-1/2}| \min\left(\frac{h_i}{2}, \frac{h_i^2}{8\epsilon}\right)\right\} \left(\frac{2 + 2\|a\|_\infty + \|b\|_\infty + \alpha}{\alpha} \right). \end{aligned}$$

□

With these stability results, we now derive posteriori error estimates which is the main result of this paper. Let (3.2.2) holds true and $x \in (x_{i-1}, x_i)$. From (3.4.11) and (3.4.12), we obtain

$$\begin{aligned} \mathcal{A}(u-U)(x) &= \mathcal{F}(x) + \hat{c} - (\mathcal{A}U)(x) \\ &= \mathcal{F}(x) + \hat{c} - (\mathcal{A}U)(x) + [A^c U - (A^u - A^c)\Delta - F^c] - c \\ &= (\mathcal{F}(x) - F_i^c) + ([A^c U]_i - (\mathcal{A}U)(x)) - [(A^u - A^c)\Delta]_i + c - \hat{c} \\ &= \left(\int_x^1 (g - bU)(s) ds - \sum_{k=i}^{N} \hbar_k (g_k - (bU)_k) + [\epsilon[U_{\bar{x},i} - (U)'(x)]] \right. \\ &\quad + \left[\frac{(aU) + (aU)_{-1}}{2} - (a^- U)(x) \right] - \left[-\frac{(a\Delta) + (a\Delta)_{-1}}{2} + (a^-\Delta)(x) \right]_i \\ &\quad \left. - \sum_{k=i}^{N-1} h_{k+1}(b\Delta)_k + \sum_{k=i}^{N} \hbar_k (b\Delta)_k + c - \hat{c} \right). \end{aligned} \quad (3.5.7)$$

Put $\Upsilon = g - bU$ in (3.5.7) to obtain

$$\begin{aligned} \mathcal{A}(u-U)(x) &= \left(\int_x^1 \Upsilon(s) ds - \sum_{k=i}^{N} \hbar_k (\Upsilon_k) \right) + \epsilon \left[U_{\bar{x},i} - (U)'(x) \right] \\ &\quad + \left[\frac{(aU) + (aU)_{-1}}{2} - (a^- U)(x) \right] - \frac{h_i}{2} (a\Delta)_{\bar{x},i} \\ &\quad - \sum_{k=i}^{N-1} \frac{h_{k+1} - h_k}{2} (c\Delta)_k + \frac{h_N (c\Delta)_N}{2} + c - \hat{c}. \end{aligned} \quad (3.5.8)$$

Let Υ^I be the piecewise linear interpolant of Υ, then by using the definition of nodal linear interpolant, we get

$$\begin{aligned}
\int_x^1 \Upsilon(s)ds - \sum_{k=i}^{N} \hbar_k(\upsilon_k) &= \int_x^1 (\Upsilon - \Upsilon^I)(s)ds + \int_x^1 \Upsilon^I(s)ds - \sum_{k=i}^{N} \hbar_k(\upsilon_k) \\
&= \int_x^1 (\Upsilon - \Upsilon^I)(s)ds + \int_x^{x_i} \Upsilon^I(s)ds + \int_{x_i}^1 \Upsilon^I(s)ds - \sum_{k=i}^{N} \hbar_k(\Upsilon_k) \\
&= \int_x^1 (\Upsilon - \Upsilon^I)(s)ds + \int_x^{x_i} \Upsilon^I(s)ds + \sum_{k=1}^{N-1} \int_{x_k}^{x_{k+1}} \Upsilon^I(s)ds - \sum_{k=i}^{N} \hbar_k(\Upsilon_k) \\
&= \int_x^1 (\Upsilon - \Upsilon^I)(s)ds + (x_{i-1/2} - x)\Upsilon_{i-1/2} + \hat{\Psi}(x), \qquad (3.5.9)
\end{aligned}$$

where $\left\|\hat{\Psi}\right\|_{\infty,[x_{i-1},x_i]} \leq Ch_i^2 \left\|\Upsilon'\right\|_{\infty,[x_{i-1},x_i]}$.
Following [171] and the Taylor expansion to write

$$\begin{aligned}
U_{\bar{x},i} - (U)'(x) &= \frac{U_i - U_{i-1}}{h_i} - (U)'(x_i + x - x_i) \\
&= (x_{i-1/2} - x)(U_i)'' + \bar{\Psi}_i(x), \qquad (3.5.10)
\end{aligned}$$

where $\left\|\bar{\Psi}\right\|_\infty \leq Ch_i^2 \left\|(U)^{(3)}\right\|_\infty$. Similarly, we can write

$$\frac{(aU)_i - (aU)_{i-1}}{2} - (aU)(x) = (x_{i-1/2} - x)(aU)_{\bar{x},i} + \widetilde{\Psi}_i(x), \qquad (3.5.11)$$

where $\left\|\widetilde{\Psi}\right\|_{\infty,[x_{i-1,x_i}]} \leq Ch_i^2 \left\|(aU)''\right\|_{\infty,[x_{i-1},x_i]}$. Hence, (3.5.8) becomes

$$\begin{aligned}
\mathcal{A}(u-U)(x) &= \int_x^1 (\Upsilon - \Upsilon^I)(s)ds + (x_{i-1/2} - x)\Upsilon_{i-1/2} + \hat{\Psi}_i(x) + \epsilon\Big[(x_{i-1/2} - x)(u_i^N)'' \\
&\quad + \bar{\Psi}_i(x)\Big] + (x_{i-1/2} - x)(aU)_{\bar{x},i} + \widetilde{\Psi}_i(x) - \frac{h_i}{2}(b\Delta)_{\bar{x},i} \\
&\quad - \sum_{k=i}^{N-1} \frac{h_{k+1} - h_k}{2}(b\Delta)_k + \frac{h_N(c\Delta)_N}{2} + c - \hat{c}. \qquad (3.5.12)
\end{aligned}$$

Also, from [119]

$$\left| \int_x^1 (\Upsilon - \Upsilon^I)(s)ds \right| \leq \frac{1}{12} \sum_{i=1}^{N} h_i^3 \left\|\Upsilon''\right\|_{\infty,I_i}. \qquad (3.5.13)$$

Theorem 3.5.3. *The solution u of* (3.2.1) *and the solution U of* (3.4.6) *satisfies*

$$\|u - U\|_\infty \leq \theta := \theta_1 + \theta_2 + \theta_3 + \theta_4 + \theta_5, \qquad (3.5.14)$$

where

$$\begin{aligned}
\theta_1 &= \max_{i=1,\cdots,N}\left\{\left|\Upsilon_{i-1/2}+(aU)_{\bar{x},i}+\epsilon(U_i)''\right|\min\left\{\frac{h_i}{2},\frac{h_i^2}{8\epsilon}\right\}\left(\frac{2+2\|a\|_\infty+\|b\|_\infty}{\alpha}+1\right)\right\},\\
\theta_2 &= \frac{1}{\alpha}\max_{i=1,\cdots,N} h_i\left|(a\Delta)_{\bar{x},i}\right|,\\
\theta_3 &= \frac{2}{\alpha}\max_{i=1,\cdots,N}\left|\sum_{k=i}^{N-1}\frac{h_{k+1}-h_k}{2}(b\Delta)_k-\frac{(b\Delta)_N h_N}{2}\right|,\\
\theta_4 &= \frac{1}{6\alpha}\sum_{i=1}^{N} h_i^3\,\|\Upsilon''\|_{\infty,I_i},\\
\theta_5 &= \frac{2}{\alpha}\max_{i=1,\cdots,N} h_i^2\left\{\|\upsilon'\|_{\infty,I_i}+\|(aU)'\|_{\infty,I_i}+\epsilon\,\|U\|^{(3)}_{\infty,I_i}\right\},
\end{aligned}$$

and $I_i=[x_{i-1},x_i]$.

Proof. Using the fact that $L\omega=-(\mathcal{A}\omega)'$ and the Green's function repersentation of the solution, we calculate

$$\begin{aligned}
(u-U)(x) &= \int_0^1 \mathcal{G}(x,\xi)L(u-U)(\xi)d\xi\\
&= -\int_0^1 \mathcal{G}(x,\xi)(\mathcal{A}(u-U))'(\xi)d\xi\\
&= \int_0^1 \mathcal{G}_\xi(x,\xi)(\mathcal{A}(u-U))'(\xi)d\xi+\mathcal{G}(x,0)\mathcal{A}(0)-\mathcal{G}(x,1)\mathcal{A}(1).
\end{aligned}$$

From (3.5.12) it follows that

$$\begin{aligned}
(u-U)(x) &= \int_0^1 \mathcal{G}_\xi(x,\xi)\left[\Upsilon_{i-1/2}+\epsilon(u_i^N)''+(aU)_{\bar{x},i}+\hat{\Psi}_i(x)+\bar{\Psi}_i(x)+\widetilde{\Psi}_i(x)\right.\\
&\quad\left.+(c-\hat{c})\right]d\xi+\sum_{i=1}^{N}\int_{x_{i-1}}^{x_i}\mathcal{G}_\xi(x,\xi)\left(-\frac{h_i}{2}(a\Delta)_{\bar{x},i}-\sum_{k=i}^{N-1}\frac{h_{k+1}+h_k}{2}(b\Delta)_k\right.\\
&\quad\left.+\frac{(b\Delta)_N h_N}{2}\right)d\xi+\sum_{i=1}^{N}\int_{x_{i-1}}^{x_i}\mathcal{G}_\xi(x,\xi)\left(\int_0^1(\Upsilon-\Upsilon^I)(s)ds\right)d\xi. \qquad (3.5.15)
\end{aligned}$$

Therefore, from Lemma3.5.1 and Theorem3.5.2, (3.5.15) becomes

$$\begin{aligned}
\|u-U\|_\infty &\le \max_{i=1,\cdots,N}\left\{\left|\Upsilon_{i-1/2}+(aU)_{\bar{x},i}+\epsilon(U_i)''\right|\min\left\{\frac{h_i}{2},\frac{h_i^2}{8\epsilon}\right\}\right\}\\
&\quad\times\left(\frac{2+2\|a\|_\infty+\|b\|_\infty+\alpha}{\alpha}\right)+(\theta_2+\theta_3+\theta_4+\theta_5)\int_0^1\left|\mathcal{G}_\xi(x,\xi)\right|d\xi.
\end{aligned}$$

Hence

$$\|u-U\|_\infty\le\theta:=\theta_1+\theta_2+\theta_3+\theta_4+\theta_5,$$

where

$$\begin{aligned}
\theta_1 &= \max_{i=1,\cdots,N}\left\{\left|\Upsilon_{i-1/2}+(aU)_{\bar{x},i}+\epsilon(U_i)''\right|\min\left\{\frac{h_i}{2},\frac{h_i^2}{8\epsilon}\right\}\left(\frac{2+2\|a\|_\infty+\|b\|_\infty}{\alpha}+1\right)\right\},\\
\theta_2 &= \frac{1}{\alpha}\max_{i=1,\cdots,N} h_i\left|(a\Delta)_{\bar{x},i}\right|,\\
\theta_3 &= \frac{2}{\alpha}\max_{i=1,\cdots,N}\left|\sum_{k=i}^{N-1}\frac{h_{k+1}-h_k}{2}(b\Delta)_k-\frac{(b\Delta)_N h_N}{2}\right|,\\
\theta_4 &= \frac{1}{6\alpha}\sum_{i=1}^{N} h_i^3\|\Upsilon''\|_{\infty,I_i},\\
\theta_5 &= \frac{2}{\alpha}\max_{i=1,\cdots,N} h_i^2\left\{\|\upsilon'\|_{\infty,I_i}+\|(aU)'\|_{\infty,I_i}+\epsilon\|U\|^{(3)}_{\infty,I_i}\right\}.
\end{aligned}$$

□

3.6 Numerical Results

In this section, we examine the performance of the proposed method and numerically verify the theoretical estimates. We consider a test problem for numerical computations.

Example 3.6.1. *Consider the following convection-diffusion problem [245]*

$$-\epsilon u''(x)-u'(x)=x+\delta_{1/2},\quad u(0)=u(1)=0.$$

Table 3.1: Maximum absolute error ($\hat{E}_N$) and order of convergence ($\hat{P}_N$) for example 3.6.1.

	$\epsilon=10^{-3}$		$\epsilon=10^{-7}$	
N	E_N	$\hat{P}_N$	E_N	$\hat{P}_N$
32	2.73914e-03	1.963	2.74024e-03	1.964
64	7.02162e-04	1.985	7.02190e-04	1.985
128	1.77261e-04	1.962	1.77285e-04	1.962
256	4.54710e-05	1.942	4.54789e-05	1.938
512	1.18318e-05	1.970	1.18620e-05	1.973
1024	3.01941e-06	1.982	3.02003e-06	1.980

Test problem is solved using proposed defect correction method over Bakhvalov-Shishkin mesh. The maximum absolute error and numerical rate of convergence is calculated and tabulated in tables. Table 3.1 presents maximum absolute error and numerical rate of convergence for Example 3.6.1 using proposed method over Bakhvalov-shishkin

Table 3.2: Comparison of maximum absolute error ($\hat{E}_N$) and order of convergence ($\hat{P}_N$), for example 3.6.1, using the proposed defect correction method on layer adapted meshes when $\epsilon = 10^{-05}$.

	Shishkin Mesh		Bakhvalov-Shishkin mesh	
N	$\hat{E}_N$	$\hat{P}_N$	$\hat{E}_N$	$\hat{P}_N$
32	4.78532e-02	1.584	2.74021e-03	1.964
64	1.59538e-02	1.570	7.02189e-04	1.985
128	5.37041e-03	1.590	1.77282e-04	1.962
256	1.783104e-03	1.580	4.54787e-05	1.938
512	5.962051e-04	1.594	1.18619e-05	1.973
1024	1.974065e-04	1.589	3.02003e-06	1.979

mesh. Besides, Table 3.2 presents the comparision of the maximum absolute error and numerical rate of convergence of proposed method over two layer adapted meshes and results over Bakhvalov shishkin mesh are better than Shishkin mesh. Log-log plot for different values of ϵ is shown in Figure 3.1. Figure 3.2 shows the comparision of maximum absolute error over Shishkin mesh and Bakhvalov-Shishkin mesh. Moreover, 3.3 presents the numerical solution for Example 3.6.1 for different values of ϵ.

3.7 Conclusion

A class of singularly perturbed convection-diffusion problem with discontinuous coefficient and point source is solved numerically. The presence of discontinuous data and point source makes the problem stiff. In the limiting case, the solution to the problem exhibits a multiscale character. There are narrow regions where solution derivatives are exponential and exhibit turning point behaviour across discontinuities besides a strong boundary layer. A higher-order defect correction method over Bakhvalov Shishkin mesh is proposed to solve the problem. The mesh has been designed so that most of the mesh points remain in the region with layers. The method is investigated for consistency, stability and convergence. A posteriori error estimates in L_∞ are presented. It provides computable and guaranteed upper bounds for the discretization error. The error estimates of the proposed numerical method satisfy parameter uniform second-order convergence. Numerical experiments corroborate the theoretical findings.

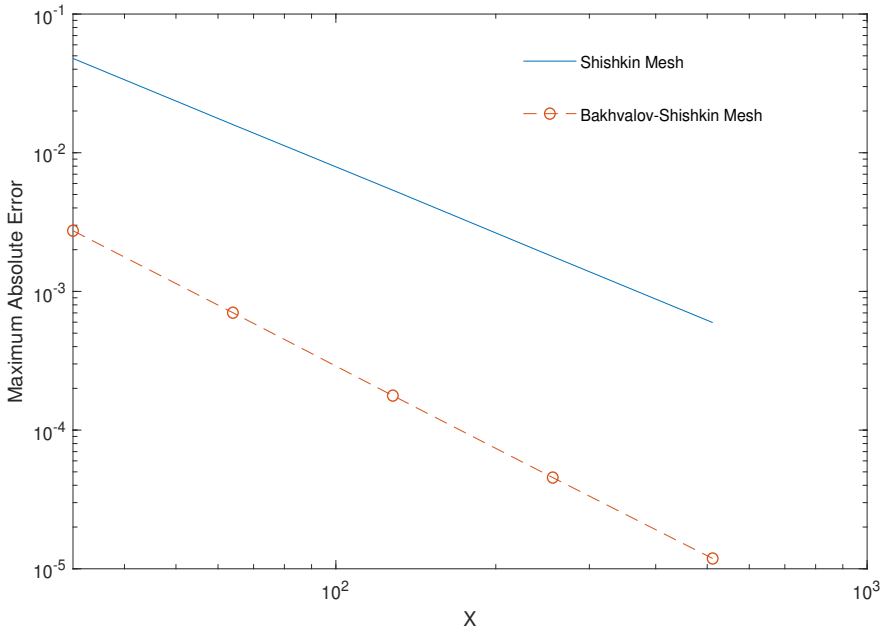

Figure 3.1: Comparison of maximum absolute error ($\hat{E}_N$), for Example 3.6.1, using proposed method over layer adapted meshes.

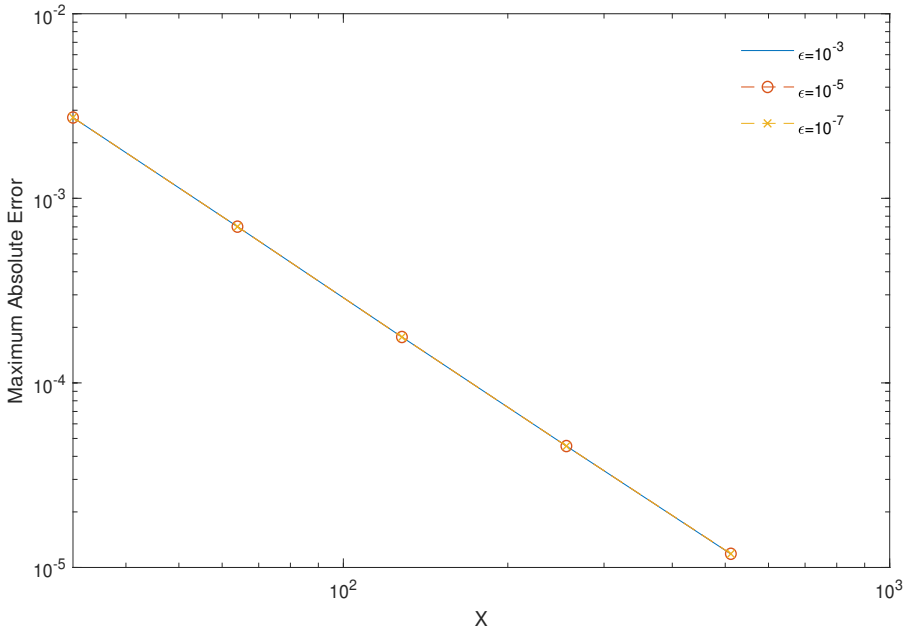

Figure 3.2: Error plot for Example 3.6.1 for different values of ϵ.

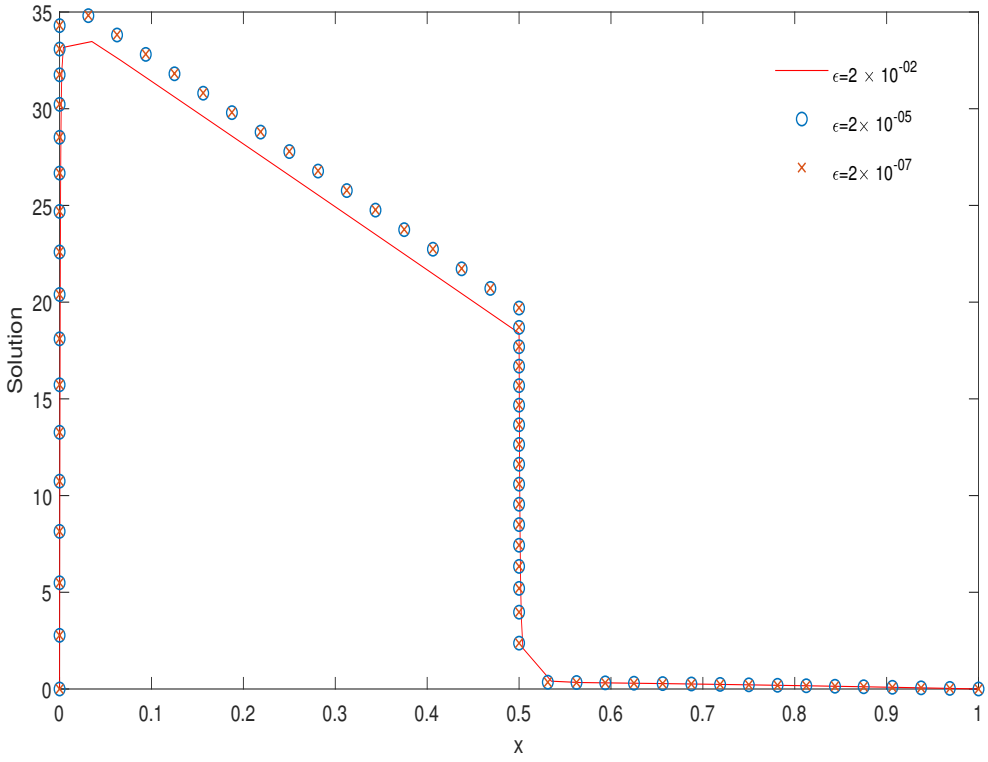

Figure 3.3: Numerical solution to Example 3.6.1 for different values of ϵ.

Chapter 4

Parabolic Convection-Diffusion Problems with a Large Shift

4.1 Introduction

In the previous chapters, we proposed defect correction schemes for different classes of singularly perturbed convection-diffusion problems. This chapter extends our study to a class of singularly perturbed parabolic PDEs.

Singularly perturbed parabolic PDEs with large shift are mathematical problems that arise in various applications, including fluid dynamics, heat transfer, and chemical engineering. These problems are characterised by the presence of a small parameter in the highest-order derivative term, leading to multiple timescales within the system. The interplay between fast and slow dynamics and non-local effects induced by large shifts give rise to complex phenomena such as boundary and interior layers. These layers are regions of rapid variation in the solution, and they can pose significant challenges for numerical solutions. The incorporation of shifts in these equations captures the influence of neighbouring states or events on the current evolution of the system. Shifts add memory-like behaviour to the PDEs, making their analysis and numerical solution more intricate. Standard numerical methods on uniform meshes fail to consistently approximate solutions in these layer regions.

Many researchers have tried to provide consistent numerical approximations to singularly perturbed differential equations with a large shift. In [67], a singularly perturbed differential equation with a large negative shift is solved using an exponentially fitted numerical scheme. The authors divided the original domain into six subdomains: two boundary layer regions, two interior layer regions, and two regular regions. The authors constructed an exponentially fitted numerical scheme on each boundary and interior layer

subdomain and combined it with the solutions on the regular subdomains. The proposed scheme is second-order ϵ-uniform. In [68], a parameter-uniform numerical scheme was presented to solve singularly perturbed parabolic differential equations involving large spatial delay. The numerical scheme combines the weighted average (θ-method) difference approximation on a uniform mesh in time variable and the central difference method on a piecewise uniform spatial mesh. The method is second-order convergent in the temporal direction and almost second-order in the spatial direction. In [276], singularly perturbed reaction-diffusion problems with large spatial delay are solved numerically using the Crank-Nicolson method for the time derivative and a non-standard finite difference method for spatial derivative. The Richardson extrapolation technique is applied to improve convergence order and achieve fourth-order convergence in time and space. In [90], authors solved a class of singularly perturbed parabolic reaction-diffusion problems with a large negative shift and integral boundary condition. Splines are used on a Shishkin mesh to discretize the spatial derivative, and the Crank–Nicolson method resolves the temporal derivative. The method is uniformly convergent to almost second-order in space and time.

In [57], a class of second-order singularly perturbed parabolic differential equations with discontinuous coefficients involving large shifts was dealt with using the implicit Euler and the cubic spline in compression methods for time and spatial dimensions, respectively. The proposed method is second-order accurate in space and first-order accurate in time. In [145], a stabilised central difference method is used to solve singularly perturbed boundary value problems with a large negative shift. The central difference approximations for the derivatives were modified by re-approximating the error terms, leading to a stabilizing effect. In [223], authors presented a computational method for solving a class of differential equations with a negative shift in the differentiated term. The author constructs an exponential spline finite difference scheme using the continuity of its first-order derivative condition at the joint nodes. In [144], authors solved a class of parabolic singularly perturbed initial-boundary value problems with a large shift in the spatial direction. They used a crank-Nicolson scheme on a uniform mesh in time and a standard finite difference scheme on a piecewise uniform mesh for the system of ordinary differential equations obtained in the semi-discretization process. The method is second-order convergent in the temporal direction and almost first-order in the spatial direction. In [183], singularly perturbed differential-difference equations involving small shifts in the reaction terms are solved numerically. Taylor's series approximation approximates the reaction terms. The resulting singularly perturbed boundary value problem was solved using the exponentially fitted operator finite difference method. The author

proves the formulated scheme converges uniformly with linear order before Richardson extrapolation and quadratic order after Richardson extrapolation.

In [199], authors presented exponentially fitted finite difference methods for solving time-dependent singularly perturbed one-dimensional convection-diffusion problems with small shifts. In case shifts are of the order of perturbation parameter, the author expands the terms involving shifts using the Taylor series and devises an exponentially fitted tridiagonal finite difference scheme first-order convergent in time and second-order convergent in space. When the shift parameters are larger than the perturbation parameter, an exponentially fitted scheme is proposed on a special mesh so that the shifts always lie on the nodal points.

In [69], authors constructed a uniformly convergent numerical scheme using the implicit Euler method in the temporal direction and a fitted tension spline method in the spatial direction with uniform meshes to solve a singularly perturbed reaction-diffusion problem with a negative shift. In [56], authors solved singularly perturbed time-dependent differential-difference equations with small shifts. Taylor's series expansion is used to approximate the terms containing shifts. The resulting singularly perturbed parabolic partial differential equation was solved using an implicit Euler method in temporal direction and cubic B-spline collocation method for the resulting system of ordinary differential equations in spatial direction, and an artificial viscosity was introduced in the scheme using the theory of singular perturbations. In [229], a fitted non-polynomial spline approach was applied to solve singularly perturbed problems with negative and positive shifts. In [236], singularly perturbed differential equations with delay and shift were solved numerically using an efficient Haar wavelet collocation method. The authors applied the Taylor series to convert the problem with delay and shift into a new problem without delay and shift and solved the resulting problem using the Haar wavelet collocation method.

Nevertheless, none of the available methods seems appropriate if we scrutinise for a dependable and direction-independent discretization. A fundamental challenge in the numerical solution of the singular perturbation problem is the distinct approximations needed in the slow and fast motion phases.

The analysis of the special methods for singularly perturbed parabolic partial functional differential equations has yet to see much development in the literature. This chapter presents a numerical method to solve singularly perturbed parabolic partial differential equations with a large shift. Besides, the chapter presents rigorous consistency, stability and convergence analysis of the proposed scheme and illustrates numerical results.

4.2 Problem Description

Let $S = D^- \cup D^+ := (0,1) \times (0,T] \cup (1,2) \times (0,T]$, $F := \bar{S}/S$ and for $(x,t) \in S$ consider the nonhomogeneous initial-boundary-value problem

$$\left.\begin{aligned} &u_t(x,t) - \epsilon u_{xx}(x,t) + a(x)u_x(x,t) + b(x)u(x,t) + c(x)u(x-1,t) = g(x,t), \\ &u(x,t) = r_0(x),\ (x,t) \in [0,2] \times \{t=0\}, \\ &u(x,t) = r_1(x,t),\ (x,t) \in [-1,0] \times [0,T], \\ &u(x,t) = r_2(t),\ (x,t) \in \{x=2\} \times [0,T], \end{aligned}\right\} \tag{4.2.1}$$

where $0 < \epsilon \ll 1$, a, b, c and g are sufficiently smooth functions such that $a(x) > \alpha > 0$, $c(x) > 0$, $b(x) \geq 0$. The functions $r_0(x)$, $r_1(x,t)$, and $r_2(t)$ are Hölder continous and satify the following compatibility conditions

$$\left.\begin{aligned} &r_0(0) = r_1(0,0),\ r_0(2) = r_2(0), \\ &\frac{\partial r_1(0,0)}{\partial t} - \epsilon\frac{\partial^2 r_0(0)}{\partial x^2} + a(0)\frac{\partial r_0(0)}{\partial x} + b(0)r_0(0) + c(0)r_1(-1,0) = g(0,0), \\ &\frac{\partial r_2(0)}{\partial t} - \epsilon\frac{\partial^2 r_0(2)}{\partial x^2} + a(2)\frac{\partial r_0(2)}{\partial x} + b(2)r_0(2) + c(2)r_0(1) = g(2,0). \end{aligned}\right\}$$

Under the assumptions above, the solution of (4.2.1) exists and is unique [8, 129]. The simultaneous presence of a small parameter and shift makes the problem stiff. The corresponding degenerate equation obtained by setting $\epsilon = 0$ in (4.2.1) is given by

$$u_t(x,t) + a(x)u_x(x,t) + b(x)u(x,t) + c(x)u(x-1,t) = g(x,t) \tag{4.2.2}$$

which is a hyperbolic partial differential equation. A key difference between (4.2.1) and (4.2.2) is that the former has a second-order derivative. In contrast, the latter contains first-order derivatives and can not satisfy the given initial or boundary data. Consequently, as $\epsilon \to 0$, the solution of the problem exhibits multiscale character and leads to a weak interior layer and a strong boundary layer [166].

Let us rewrite (4.2.1) as

$$Lu(x,t) = G(x,t), \tag{4.2.3a}$$

where

$$Lu = \begin{cases} u_t(x,t) - \epsilon u_{xx}(x,t) + a(x)u_x(x,t) + b(x)u(x,t), & (x,t) \in D^-, \\ u_t(x,t) - \epsilon u_{xx}(x,t) + a(x)u_x(x,t) + b(x)u(x,t) + c(x)u(x-1,t), & (x,t) \in D^+, \end{cases}$$

and

$$G(x,t) = \begin{cases} g(x,t) - c(x)r_1(x-1,t), & (x,t) \in D^-, \\ g(x,t), & (x,t) \in D^+ \end{cases}$$

with

$$\left.\begin{aligned} &u(x,t) = r_0(x), (x,t) \in [0,2] \times \{t=0\}, \\ &u(x,t) = r_1(x,t), (x,t) \in [-1,0] \times [0,T], \\ &u(x,t) = r_2(t), (x,t) \in \{x=2\} \times [0,T], \\ &u(1^-,t) = u(1^+,t),\ u'(1^-,t) = u'(1^+,t). \end{aligned}\right\} \tag{4.2.3b}$$

Following [166, 99], we now establish that the differential operator in (4.2.3) satisfies the following maximum principle.

Lemma 4.2.1. *Let $\psi \in C^0(\bar{S}) \cap C^2(D^- \cup D^+)$ satisfies $\psi(x,t) \geq 0$, $(x,t) \in F$, $L\psi(x,t) \geq 0$ for all $(x,t) \in D^+ \cup D^-$ and $\psi_x(1^+,t) - \psi_x(1^-,t) \leq 0$. Then $\psi(x,t) \geq 0$ for all $(x,t) \in \bar{S}$.*

Proof. Let $(x^i,t^i) \in S$ such that $\psi(x^i,t^i) = \min\limits_{(x,t)\in\bar{S}} \psi(x,t)$ and assume that $\psi(x^i,t^i) < 0$. Then $(x^i,t^i) \notin F$ and $\psi_x(x^i,t^i) = 0,\ \psi_t(x^i,t^i) = 0$ and $\psi_{xx}(x^i,t^i) > 0$.

Case I: If $(x^i,t^i) \in D^-$,

$$L\psi(x^i,t^i) = \psi_t(x^i,t^i) - \epsilon\psi_{xx}(x^i,t^i) + a(x^i)\psi_x(x^i,t^i) + b(x^i)\psi(x^i,t^i) < 0.$$

Case II: If $(x^i,t^i) \in D^+$,

$$\begin{aligned} L\psi(x^i,t^i) &= \psi_t(x^i,t^i) - \epsilon\psi_{xx}(x^i,t^i) + a(x^i)\psi_x(x^i,t^i) + b(x^i)\psi(x^i,t^i) \\ &\quad + c(x^i)\psi(x^i-1,t^i) \\ &= \psi_t(x^i,t^i) - \epsilon\psi_{xx}(x^i,t^i) + a(x^i)\psi_x(x^i,t^i) + b(x^i)\psi(x^i,t^i) \\ &\quad + c(x^i)(\psi(x^i-1,t^i) - \psi(x^i,t^i)) + c(x^i)\psi(x^i,t^i) \\ &= \psi_t(x^i,t^i) - \epsilon\psi_{xx}(x^i,t^i) + a(x^i)\psi_x(x^i,t^i) + (b(x^i) + c(x^i))\psi(x^i,t^i) \\ &\quad + c(x^i)(\psi(x^i-1,t^i) - \psi(x^i,t^i)) < 0. \end{aligned}$$

Case III: If $(x^i,t^i) = (1,t^i)$,

$$\psi_x(x^{i+},t^i) - \psi_x(x^{i-},t^i) > 0.$$

A contradiction to our assumption. Consequently, the required result follows from a contradiction. □

An important application of the maximum principle is establishing the boundedness of the solution. As an immediate consequence, we establish the following uniform stability result.

Lemma 4.2.2. *Let u be the solution of* (4.2.3). *Then*

$$\|u\|_{\infty,\bar{S}} \leq \|u\|_{\infty,F} + \frac{1}{\alpha}\|G\|_{\infty,\bar{S}}\,. \tag{4.2.4}$$

Proof. Define $Y^{\pm} := \|u\|_{\infty,F} + \dfrac{x\,\|G\|_{\infty,\bar{S}}}{\alpha} \pm u,\ x \in [0,2]$.

Case I: If $(x,t) \in D^{-}$,

$$\begin{aligned} LY^{\pm}(x,t) &= \pm u_t - \epsilon Y^{\pm}_{xx} + a(x)\left(\frac{\|G\|_{\infty,\bar{S}}}{\alpha} \pm u_x\right) + b(x)\left(\|u\|_{\infty,F} + \frac{x\,\|G\|_{\infty,\bar{S}}}{\alpha} \pm u\right) \\ &= \pm Lu + a(x)\frac{\|G\|_{\infty,\bar{S}}}{\alpha} + b(x)\left(\|u\|_{\infty,F} + \frac{x\,\|G\|_{\infty,F}}{\alpha}\right) > 0. \end{aligned}$$

Case II: If $(x,t) \in D^{+}$,

$$\begin{aligned} LY^{\pm}(x,t) &= \pm u_t - \epsilon Y^{\pm}_{xx} + a(x)\left(\frac{\|G\|_{\infty,\bar{S}}}{\alpha} \pm u_x\right) + b(x)\left(\|u\|_{\infty,F} + \frac{x\,\|G\|_{\infty,\bar{S}}}{\alpha} \pm u\right) \\ &\quad + c(x)\left(\|u(x-1,t)\|_{\infty,F} + \frac{(x-1)\,\|G\|_{\infty,\bar{S}}}{\alpha} \pm u(x-1,t)\right) \\ &= \pm Lu + a(x)\frac{\|G\|_{\infty,\bar{S}}}{\alpha} + b(x)\left(\|u\|_{\infty,F} + \frac{x\,\|G\|_{\infty,\bar{S}}}{\alpha}\right) \\ &\quad + c(x)\left(\|u(x-1,t)\|_{\infty,F} + \frac{(x-1)\,\|G\|_{\infty,\bar{S}}}{\alpha}\right) > 0. \end{aligned}$$

Case III: If $(x,t) = (1,t)$,

$$[Y^{\pm}_{x}(1,t)] = \pm[u_x](1,t) = 0.$$

The required result (4.2.4) now follows from Lemma 4.2.1. □

Lemma 4.2.3. *Let u be the solution of* (4.2.3)*. Then*

$$\left|\frac{\partial^i u}{\partial t^i}\right| \le C,\ (x,t) \in \bar{S} \ \text{ and } \ i = 0,1,2.$$

Proof. For proof, see [133]. □

4.3 Time Semidiscretization

Let us partition the given time interval $[0,T]$ into K subintervals of uniform mesh width $\Delta t = T/K$, $K > 0$. The mesh in the time direction reads

$$\Gamma^{K}_{t} = \{t_l = lT/K, 0 \le l \le K\}.$$

Applying the implicit Euler method in the time variable, the resulting semidiscretized problem reads

$$L^{\epsilon}_{K}U(x,t_{l+1}) = G(x,t_{l+1});\ 0 \le x \le 2,\ 0 \le l \le K-1 \tag{4.3.1a}$$

subject to the following initial and boundary conditions

$$\left.\begin{aligned} &U(x,0) = r_0(x),\ 0 \le x \le 2,\\ &U(x,t_{l+1}) = r_1(x,t_{l+1}),\ -1 \le x \le 0,\ 0 \le l \le K-1,\\ &U(2,t_{l+1}) = r_2(t_{l+1}),\ 0 \le l \le K-1,\\ &U(1^-,t_{l+1}) = U(1^+,t_{l+1}),\ U_x(1^-,t_{l+1}) = U_x(1^+,t_{l+1}), \end{aligned}\right\} \tag{4.3.1b}$$

where

$$L_K^\epsilon U(x,t_{l+1}) = \begin{cases} -\epsilon\Delta t U_{xx}(x,t_{l+1}) + a(x)\Delta t U_x(x,t_{l+1}) + \hat{b}(x)U(x,t_{l+1}), & 0 < x \le 1,\\ -\epsilon\Delta t U_{xx}(x,t_{l+1}) + a(x)\Delta t U_x(x,t_{l+1}) + \hat{b}(x)U(x,t_{l+1}) & \\ +c(x)\Delta t U(x-1,t_{l+1}), & 1 < x \le 2, \end{cases}$$

and

$$G(x,t_{l+1}) = \begin{cases} \Delta t g(x,t_{l+1}) - \Delta t c(x) r_1(x-1,t_{l+1}) + U(x,t_l), & 0 < x \le 1,\\ \Delta t g(x,t_{l+1}) + U(x,t_l), & 1 < x \le 2. \end{cases}$$

Here, $\hat{b}(x) := \Delta t b(x) + 1$. Next, we establish the following semidiscrete maximum principle to ensure the stability of the method (4.3.1).

Lemma 4.3.1. *Let $P(x,t_{l+1})$ be a sufficiently smooth function such that $P(x,t_{l+1}) \ge 0$ for $x = \{0,2\}$, $L_K^\epsilon P(x,t_{l+1}) \ge 0$, $x \in (0,2)$ and $P_x(1^+,t_{l+1}) - P_x(1^-,t_{l+1}) \le 0$. Then $P(x,t_{l+1}) \ge 0$ for all $x \in [0,2]$.*

Proof. Let $(x^p,t_{l+1}) \in \{(x,t_{l+1}) : x \in [0,2]\}$ and $P(x^p,t_{l+1}) = \min\limits_{x\in[0,2]} P(x,t_{l+1}) < 0$. Clearly, $(x^p,t_{l+1}) \notin F$, $P_x(x^p,t_{l+1}) = 0$ and $P_{xx}(x^p,t_{l+1}) > 0$. Moreover,

Case I: If $x^p \in (0,1)$

$$\begin{aligned} L_K^\epsilon P(x^p,t_{l+1}) &= -\epsilon\Delta t P_{xx}(x^p,t_{l+1}) + a(x^p)\Delta t P_x(x^p,t_{l+1})\\ &\quad +\hat{b}(x^p)P(x^p,t_{l+1}) < 0. \end{aligned}$$

Case II: If $x^p \in (1,2)$

$$\begin{aligned} L_K^\epsilon P(x^p,t_{l+1}) &= -\epsilon\Delta t P_{xx}(x^p,t_{l+1}) + a(x^p)\Delta t P_x(x^p,t_{l+1}) + c(x^p)\Delta t P(x^p-1,t_{l+1})\\ &\quad +\hat{b}(x^p)P(x^p,t_{l+1})\\ &= -\epsilon\Delta t P_{xx}(x^p,t_{l+1}) + a(x^p)\Delta t P_x(x^p,t_{l+1}) + \Delta t(c(x^p)+b(x^p))P(x^p,t_{l+1})\\ &\quad +c(x^p)\Delta t(P(x^p-1,t_{l+1}) - P(x^p,t_{l+1})) + P(x^p,t_{l+1}) < 0. \end{aligned}$$

Case III: If $x^p = 1$

$$P_x(1^+,t_{l+1}) - P_x(1^-,t_{l+1}) > 0.$$

A contradiction to our assumption. Consequently, the required result follows from a contradiction. □

The operator L_K^ϵ satisfies the semidiscrete maximum principle. Consequently, from [166], it follows that $\left\|L_K^\epsilon\right\|_\infty \leq C$ and stability of the method follows. Moreover, the local truncation error at $(l+1)$th time step satisfies $\|e_{l+1}\|_\infty \leq C(\Delta t)^2$. We combine the local error estimates to obtain the following uniform convergence result.

Lemma 4.3.2. *The global discretization error (E_l) at the lth time step satisfies*

$$\|E_l\|_\infty \leq C\Delta t$$

where the constant $C > 0$ is independent of ϵ and Δt.

Proof. The local truncation error at each time step contributes to the estimate for global error. Consequently,

$$\|E_{l+1}\|_\infty \quad = \quad \left\|\sum_{j=1}^{l} e_j\right\|_\infty \leq \|e_1\|_\infty + \|e_2\|_\infty + \cdots + \|e_l\|_\infty \leq C\Delta t.$$

□

This in turn ensures the uniform convergence of the time semidiscretization process. Next, we obtain a priori estimate on the solution of the semidiscretized problem (4.3.1).

Lemma 4.3.3. *Let $U(x, t_{l+1})$ be the solution of* (4.3.1)*. Then*

$$|U(x, t_{l+1})| \leq \max\left\{|U(0, t_{l+1})|, \frac{\|G\|}{\alpha}, |U(2, t_{l+1})|\right\}, \ x \in [0, 2].$$

Proof. Define $P^\pm(x, t_{l+1}) := \max\left\{|U(0, t_{l+1})|, \frac{\|G\|}{\alpha}, |U(2, t_{l+1})|\right\} \pm U(x, t_{l+1})$. Note that $P^\pm(x, t_{l+1}) \geq 0$ for $x \in \{0, 2\}$. Moreover,

Case I: If $x \in (0, 1)$,

$$L_K^\epsilon P^\pm(x, t_{l+1}) = \hat{b}(x) \max\left\{|U(0, t_{l+1})|, \frac{\|G\|}{\alpha}, |U(2, t_{l+1})|\right\} \pm L_K^\epsilon U(x, t_{l+1}) \geq 0.$$

Case II: If $x = 1$,

$$[P_x^\pm](1, t_{l+1}) = \pm[U_x](1, t_{l+1}) = 0.$$

Case III: If $x \in (1, 2)$,

$$\begin{aligned} L_K^\epsilon P^\pm(x, t_{l+1}) \quad &= \quad (c(x) + \hat{b}(x)) \max\left\{|U(0, t_{l+1})|, \frac{\|G\|}{\alpha}, |U(2, t_{l+1})|\right\} \\ &\quad \pm L_K^\epsilon U(x, t_{l+1}) \geq 0. \end{aligned}$$

An application of Lemma 4.3.1 leads us to the required result. □

To obtain sharp bounds on the solution of semidiscretized problem (4.3.1) and its derivatives, we write $U(x, t_{l+1})$ as a sum of regular component $V(x, t_{l+1})$ and singular component $W(x, t_{l+1})$, $U(x, t_{l+1}) := V(x, t_{l+1}) + W(x, t_{l+1})$ [186]. The regular component $V(x, t_{l+1})$ takes the form

$$V(x, t_{l+1}) = \sum_{j=0}^{2} \epsilon^j V_j(x, t_{l+1}),\ x \in (0, 1) \cup (1, 2).$$

For $x \in (0, 2]$, solution of the reduced problem $V_0(x, t_{l+1})$ satisfies

$$\left.\begin{aligned} &a(x)\Delta t(V_0)_x(x, t_{l+1}) + \hat{b}(x)V_0(x, t_{l+1}) + c(x)\Delta t V_0(x-1, t_{l+1}) = g(x, t_{l+1}),\\ &V_0(x, t_{l+1}) = r_1(x, t_{l+1}),\ x \in [-1, 0], \end{aligned}\right\} \tag{4.3.2}$$

and for $x \in (0, 1) \cup (1, 2]$, $V_1(x, t_{l+1})$ satisfies

$$\left.\begin{aligned} &a(x)\Delta t(V_1)_x(x, t_{l+1}) + \hat{b}(x)V_1(x, t_{l+1}) + c(x)\Delta t V_1(x-1, t_{l+1}) = (V_0)_{xx}(x, t_{l+1}),\\ &V_1(x, t_{l+1}) = 0,\ x \in [-1, 0], \end{aligned}\right\} \tag{4.3.3}$$

whereas for $x \in (0, 1) \cup (1, 2)$, $V_2(x, t_{l+1})$ satisfies

$$\left.\begin{aligned} &L_K^{\epsilon} V_2(x, t_{l+1}) = (V_1)_{xx}(x, t_{l+1}),\\ &V_2(x, t_{l+1}) = 0,\ x \in [-1, 0],\ V_2(2, t_{l+1}) = 0. \end{aligned}\right\} \tag{4.3.4}$$

Taking into account (4.3.2), (4.3.3) and (4.3.4), the regular component $V(x, t_{l+1})$ of $U(x, t_{l+1})$ satisfies

$$\left.\begin{aligned} &L_K^{\epsilon} V(x, t_{l+1}) = G(x, t_{l+1}),\ x \in (0, 1) \cup (1, 2),\ 0 \le l \le K-1,\\ &V(x, t_{l+1}) = V_0(x, t_{l+1}), x \in [-1, 0],\\ &V(1, t_{l+1}) = V_0(1, t_{l+1}) + \epsilon V_1(1, t_{l+1}) + \epsilon^2 V_2(1, t_{l+1}),\\ &V(2, t_{l+1}) = V_0(2, t_{l+1}) + \epsilon V_1(2, t_{l+1}). \end{aligned}\right\} \tag{4.3.5}$$

On the other hand, the singular component $W(x, t_{l+1})$ of $U(x, t_{l+1})$ satisfies

$$\left.\begin{aligned} &L_K^{\epsilon} W(x, t_{l+1}) = 0,\ x \in (0, 1) \cup (1, 2),\ 0 \le l \le K-1,\\ &W(x, t_{l+1}) = 0,\ x \in [-1, 0],\\ &W(2, t_{l+1}) = r_2(2, t_{l+1}) - V(2, t_{l+1}),\\ &W_x(1^+, t_{l+1}) - W_x(1^-, t_{l+1}) = V_x(1^-, t_{l+1}) - V_x(1^+, t_{l+1}). \end{aligned}\right\} \tag{4.3.6}$$

Let us further write the singular component $W(x, t_{l+1})$ of $U(x, t_{l+1})$ as $W(x, t_{l+1}) := W_1(x, t_{l+1}) + W_2(x, t_{l+1})$ where $W_1(x, t_{l+1})$ and $W_2(x, t_{l+1})$ satisfies

$$\left.\begin{aligned} &L_K^{\epsilon} W_1(x, t_{l+1}) = 0,\ x \in (0, 2),\ 0 \le l \le K-1,\\ &W_1(0, t_{l+1}) = 0,\ x \in [-1, 0],\\ &W_1(2, t_{l+1}) = r_2(2, t_{l+1}) - V(2, t_{l+1}), \end{aligned}\right\} \tag{4.3.7}$$

and

$$\left.\begin{aligned} &L_K^{\epsilon} W_2(x, t_{l+1}) = 0,\ x \in (0,1) \cup (1,2),\ 0 \le l \le K-1 \\ &W_2(x, t_{l+1}) = 0,\ x \in [-1, 0], \\ &W_2(2, t_{l+1}) = 0, \\ &(W_2)_x(1^+, t_{l+1}) - (W_2)_x(1^-, t_{l+1}) = V_x(1^-, t_{l+1}) - V_x(1^+, t_{l+1}), \end{aligned}\right\} \tag{4.3.8}$$

respectively.

Lemma 4.3.4. *For $j = 0, 1, 2, 3$, the regular component V_{l+1} and singular component W_{l+1} of U_{l+1} satisfies*

$$\begin{aligned} &\left|V^j(x, t_{l+1})\right| \le C\epsilon^{2-j},\ x \in (0,1) \cup (1,2), \\ &\left|W_1^j(x, t_{l+1})\right| \le C\epsilon^{-j} \exp\left(\frac{-\alpha(2-x)}{\epsilon}\right),\ x \in (0,1) \cup (1,2), \\ &\left|W_2^j(x, t_{l+1})\right| \le \begin{cases} \epsilon^{-j+1} \exp\left(\dfrac{-\alpha(1-x)}{\epsilon}\right),\ x \in (0,1), \\ \epsilon^{-j+1},\ x \in (1,2). \end{cases} \end{aligned}$$

Proof. For proof, see [271]. □

4.4 The Space Discretization

4.4.1 Mesh Description

The problem (4.2.3) is known to have a primary discontinuity at $x = 1$ [29]. Moreover, the problem's solution exhibits a strong boundary layer at $x = 2$ and a weak interior layer at $x = 1$. For a positive integer $N \ge 8$, we define the mesh Γ_N so that the mesh points are condensing in the boundary and interior layers region. Let us partition the domain $[0, 2]$ as

$$\Gamma_N = [0, 1-\tau] \cup [1-\tau, 1] \cup [1, 1+\tau] \cup [1+\tau, 2-\tau] \cup [2-\tau, 2],$$

where $\tau = \dfrac{2\epsilon\phi \ln N}{\alpha} \le \dfrac{1}{2}$ is the mesh transition parameter and $\phi \ge 3$. Consequently, the non-uniform mesh Γ_N reads

$$\left.\begin{aligned}
&x_0 = 0,\\
&x_i = x_0 + iH_1,\ 1 \le i \le \frac{N}{4},\\
&x_{i+N/4} = x_{N/4} + ih_1,\ 1 \le i \le \frac{N}{4},\\
&x_{i+N/2} = x_{N/2} + ih_2,\ 1 \le i \le \frac{N}{8},\\
&x_{i+5N/8} = x_{5N/8} + iH_2\ 1 \le i \le \frac{N}{4},\\
&x_{i+7N/8} = x_{7N/8} + ih_2,\ 1 \le i \le \frac{N}{8},
\end{aligned}\right\} \tag{4.4.1}$$

where $H_1 = \dfrac{4(1-\tau)}{N}$, $H_2 = \dfrac{4(1-2\tau)}{N}$, $h_1 = \dfrac{4\tau}{N}$ and $h_2 = \dfrac{8\tau}{N}$. Furthermore, we use the notation h_i to denote the step size in different intervals and write

$$h_i = \begin{cases} H_1,\ 1 \le i \le \frac{N}{4}, \\ h_1,\ \frac{N}{4}+1 \le i \le \frac{N}{2}, \\ h_2,\ \frac{N}{2}+1 \le i \le \frac{5N}{8},\ \frac{7N}{8}+1 \le i \le N, \\ H_2,\ \frac{5N}{8}+1 \le i \le \frac{7N}{8}. \end{cases} \tag{4.4.2}$$

4.4.2 The Difference Scheme

For $i \ge 1$, a function $Z_{i,l+1}$ and step size h_i, the forward, backward and central difference approximation to first-order derivatives are defined as

$$D_+Z_{i,l+1} := \frac{Z_{i+1,l+1} - Z_{i,l+1}}{h_{i+1}},\ D_-Z_{i,l+1} := \frac{Z_{i,l+1} - Z_{i-1,l+1}}{h_i} \text{ and } D_0Z_i := \frac{Z_{i+1,l+1} - Z_{i-1,l+1}}{h_{i+1}+h_i}.$$

On the other hand, the second derivative approximation reads

$$D_+D_-Z_{i,l+1} := \frac{2}{h_{i+1}+h_i}\left(\frac{Z_{i+1,l+1} - Z_{i,l+1}}{h_{i+1}} - \frac{Z_{i,l+1} - Z_{i-1,l+1}}{h_i}\right).$$

The upwind operator $L^1_{N,K}$ for probelm (4.3.1) reads

$$L^1_{N,K}Z_{i,l+1} = \begin{cases} Z_{i,l+1}, & i = 0, N, \\ -\epsilon\Delta t D_+D_-Z_{i,l+1} + a_i\Delta t D_-Z_{i,l+1} + \hat{b}_iZ_{i,l+1}, & 1 \le i \le \frac{N}{2}-1, \\ -\epsilon\Delta t D_+D_-Z_{i,l+1} + a_i\Delta t D_-Z_{i,l+1} + \hat{b}_iZ_{i,l+1} + c_i\Delta t Z_{i-\frac{N}{2},l+1}, & \frac{N}{2}+1 \le i \le N-1, \end{cases}$$

and the modified central difference operator $L^0_{N,K}$ reads

$$L^0_{N,K}Z_{i,l+1} = \begin{cases} Z_{i,l+1}, & i = 0, N, \\ L^2_{N,K}Z_{i,l+1}, & 1 \le i \le \frac{N}{2}-1, \\ L^1_{N,K}Z_{i,l+1}, & \frac{N}{2}+1 \le i \le N-1, \end{cases}$$

where $L^2_{N,K}Z_{i,l+1} = -\epsilon\Delta tD_+D_-Z_{i,l+1} + a_i\Delta tD_0Z_{i,l+1} + \hat{b}_iZ_{i,l+1}$ and

$$G^*_{i,l+1} = \begin{cases} \Delta tg_{i,l+1} - \Delta tc_ir_1(i-\frac{N}{2}, l+1) + U_{i,l}, & 1 \le i \le \frac{N}{2}-1, \\ \Delta tg_{i,l+1} + U_{i,l}, & \frac{N}{2}+1 \le i \le N-1. \end{cases}$$

The two-step defect correction method takes the form given below.

First Step: $L^1_{N,K}U^1_{i,l+1} = G^*_{i,l+1}, i \in \{1, \cdots, N-1\}\backslash\{N/2\}$

Second Step: $L^1_{N,K}U_{i,l+1} = (L^1_{N,K} - L^0_{N,K})U^1_{i,l+1} + G^*_{i,l+1}, i \in \{1, \cdots, N-1\}\backslash\{N/2\}$

with

$$\left.\begin{aligned} &D_+U_{N/2,l+1} = D_-U_{N/2,l+1}, \\ &U_{i,0} = (r_0)_i,\ i \in \{1, \cdots, N\}, \\ &U_{i,l+1} = (r_1)_{i,l+1},\ i \in \{-N/2, \cdots, 0\}, \\ &U_{N,l+1} = (r_2)_{N,l+1}. \end{aligned}\right\} \tag{4.4.3}$$

Here, U^1 and U denotes the initial and the corrected approximation, respectively.

Lemma 4.4.1. *Let $Y_{i,l+1}$ be a mesh function such that $Y_{0,l+1} \ge 0$, $Y_{N,l+1} \ge 0$, $L^1_{N,K}Y_{i,l+1} \ge 0$, $i \in \{1, \cdots, N-1\}\backslash\{N/2\}$ and $D_+Y_{N/2,l+1} - D_-Y_{N/2,l+1} \le 0$. Then $Y_{i,l+1} \ge 0,\ i \in \{0, \cdots, N\}$.*

Proof. Let $Z_{i,l+1} \ge 0$ for $i \in \{0, \cdots, N\}$, $L^1_{N,K}Z_{i,l+1} > 0$ for $i \in \{0, \cdots, N\}\backslash\{N/2\}$ and $[D]Z_{N/2,l+1} < 0$. Define

$$\psi := \max\left\{ \frac{-Y_{i,l+1}}{Z_{i,l+1}},\ i \in \{0, \cdots, N\} \right\}.$$

Then there is an $i^* \in \{0, \cdots, N\}$ such that $Y_{i^*,l+1} + \psi Z_{i^*,l+1} = 0$ and $Y_{i,l+1} + \psi Z_{i,l+1} \ge 0$ for $i \in \{0, \cdots, N\}\backslash i^*$. Thus the function $Y_{i,l+1} + \psi Z_{i,l+1}$ attains its minimum at x_{i^*}.

Suppose that Lemma 4.4.1 is false. Then, for $i^* \in \left\{1, \cdots, \frac{N}{2}-1\right\}$

$$\begin{aligned} L^1_{N,K}(Y_{i^*,l+1} + \psi Z_{i^*,l+1}) &= -\epsilon\Delta tD_+D_-(Y_{i^*,l+1} + \psi Z_{i^*,l+1}) + a_{i^*}\Delta tD_-(Y_{i^*,l+1} + \psi Z_{i^*,l+1}) \\ &\quad + \hat{b}_{i^*}(Y_{i^*,l+1} + \psi Z_{i^*,l+1}) \le 0, \end{aligned}$$

and at $i^* = \frac{N}{2}$

$$[D](Y_{i^*,l+1} + \psi Z_{i^*,l+1}) = [D]Y_{i^*,l+1} + \psi[D]Z_{i^*,l+1} > 0.$$

A contradiction and the required result follows. In the case $i^* \in \left\{\frac{N}{2}+1, \cdots, N\right\}$, a similar arguments leads to the desired result. □

Following (2.4.3), we can write the consistency error $\hat{E}$ of the defect correction scheme as

$$\hat{E} = (L^1_{N,K} - L^0_{N,K})(U_{l+1} - U^1_{i,l+1}) + (L^0_{N,K} - L^\epsilon_K)U_{l+1} \tag{4.4.4}$$

where U_{l+1} is the solution of (4.3.1) and $U_{i,l+1}$ is the corrected approximation of (4.4.3).

Lemma 4.4.2. *The difference operator $L^1_{N,K}$ and $L^2_{N,K}$ defined for* (4.3.1) *satisfies*

$$L^1_{N,K}(L^1_{N,K} - L^2_{N,K})Y_{i,l+1} = (L^1_{N,K} - L^2_{N,K})L^1_{N,K}Y_{i,l+1}$$

iff $a_{i-1} = a_i = a_{i+1}$, $b_{i-1} = b_i = b_{i+1}$ *and* $h_{i+1} = h_i = h_{i-1}$.

Proof. Let a_i be a constant. For $i \in \left\{0, 1, \cdots, \frac{N}{4}\right\}$ and an arbitrary mesh

$$(L^1_{N,K} - L^2_{N,K})Y_{i,l+1} \quad = \quad a_i\Delta t(D_- - D_0)Y_{i,l+1} = \frac{-a_ih_{i+1}\Delta t}{2}D_+D_-Y_{i,l+1}.$$

Applying $L^1_{N,K}$ to obtain

$$\begin{aligned} L^1_{N,K}(L^1_{N,K} - L^2_{N,K})Y_{i,l+1} \quad = \quad & \frac{-\epsilon\Delta t}{2(h_i + h_{i+1})}\left[\frac{-\Delta t\left(a_{i+1}h_{i+2}D_+D_-Y_{i+1,l+1} - a_ih_{i+1}D_+D_-Y_{i,l+1}\right)}{h_{i+1}}\right. \\ & \left. - \frac{-\Delta t\left(a_ih_{i+1}D_+D_-Y_{i,l+1} - a_{i-1}h_iD_+D_-Y_{i-1,l+1}\right)}{h_i}\right] \\ & + \frac{a_i\Delta t}{2}\left[\frac{-\Delta t\left(a_ih_{i+1}D_+D_-Y_{i,l+1} - a_{i-1}h_iD_+D_-Y_{i-1,l+1}\right)}{h_i}\right] \\ & + \hat{b}_i\frac{-a_ih_{i+1}\Delta t}{2}D_+D_-Y_{i,l+1}. \end{aligned} \tag{4.4.5}$$

For a constant a_i, b_i and the Shishkin mesh, $a_{i-1} = a_i = a_{i+1}$, $b_{i-1} = b_i = b_{i+1}$ and $h_{i+1} = h_i = h_{i-1}$. It follows that

$$\begin{aligned} L^1_{N,K}(L^1_{N,K} - L^2_{N,K})Y_{i,l+1} \quad = \quad & \frac{-a_ih_{i+1}\Delta t}{2}\left[-\epsilon\Delta tD_+D_-(D_+D_-Y_{i,l+1}) + \Delta tD_+D_-(a_iD_-Y_{i,l+1})\right. \\ & \left. + \hat{b}_iD_+D_-Y_{i,l+1}\right]. \end{aligned} \tag{4.4.6}$$

If we reverse the order of the operator

$$\begin{aligned} (L^1_{N,K} - L^2_{N,K})L^1_{N,K}Y_{i,l+1} \quad = \quad & \left(-\epsilon\Delta tD_+D_-\left(\frac{-a_ih_{i+1}\Delta t}{2}\right) + a_i\Delta tD_-\left(\frac{-a_ih_{i+1}\Delta t}{2}\right)\right. \\ & \left. + \hat{b}_i\left(\frac{-a_ih_{i+1}\Delta t}{2}\right)\right) \\ = \quad & \frac{-a_ih_{i+1}\Delta t}{2}\left[-\epsilon\Delta tD_+D_-(D_+D_-Y_{i,l+1}) + \Delta tD_+D_-(a_iD_-Y_{i,l+1})\right. \\ & \left. + \hat{b}_iD_+D_-Y_{i,l+1}\right]. \end{aligned} \tag{4.4.7}$$

From (4.4.6) and (4.4.7) the required result follows. Similarly, we can obtain the result for $i \in \left\{\frac{N}{4} + 1, \cdots \frac{N}{2}\right\}$. □

Analogous to the solution of semidiscretized problem U_{l+1}, the initial approximation $U^1_{i,l+1}$ admits a representation $U^1_{i,l+1} = V^1_{i,l+1} + W^1_{i,l+1}$ where

$$\begin{aligned} & L^1_{N,K}V^1_{i,l+1} = G^*_{i,l+1},\ i \in \{1, 2, \cdots N-1\}\backslash\{N/2\}, \\ & V^1_{0,l+1} = V_{l+1}(0),\ [D]V^1_{l+1}(x_{N/2}) = [V'_{l+1}](x_{N/2}),\ V^1_{N,l+1} = V_{l+1}(2), \end{aligned}$$

and

$$L^1_{N,K}W^1_{i,l+1} = 0,\ i \in \{1,2,\cdots N-1\}\backslash\{N/2\},$$
$$W^1_{0,l+1} = W_{l+1}(0),\ [D]W^1_{l+1}(x_{N/2}) = -[D]V^1_{l+1}(x_{N/2}),\ W^1_{N,l+1} = W_{l+1}(2).$$

Moreover, the resulting corrected approximation reads

$$\begin{cases} L^1_{N,K}V_{i,l+1} = (L^1_{N,K} - L^0_{N,K})V^1_{i,l+1} + G^*_{i,l+1},\ i \in \{1,2,\cdots N-1\}\backslash\{N/2\}, \\ V_{0,l+1} = V^1_{0,l+1},\ [D]V_{l+1}(x_{N/2}) = [D]V^1_{l+1}(x_{N/2}),\ V_{N,l+1} = V^1_{N,l+1}, \end{cases}$$

and

$$\begin{cases} L^1_{N,K}W_{i,l+1} = -L^0_{N,K}W^1_{i,l+1},\ i \in \{1,2,\cdots N-1\}\backslash\{N/2\}, \\ W_{0,l+1} = W^1_{0,l+1},\ [D]W_{l+1}(x_{N/2}) = -[D]V_{l+1}(x_{N/2}),\ W_{N,l+1} = W^1_{N,l+1}. \end{cases}$$

4.5 Error Analysis

To analyse the truncation error associated with the numerical approximation, we decompose the discrete approximate solution as $U_{i,l+1} = V_{i,l+1} + W_{i,l+1}$ and calculate the error separately. Then, we combine both results and find the error $\left\|U_{l+1} - U_{i,l+1}\right\|_{\infty,d}$. We begin our analysis with the regular component. To obtain consistency error on regular component $L^1_{N,K}(V_{l+1} - V_{i,l+1})$, we will calculate the consistency error $(L^1_{N,K} - L^0_{N,K})(V_{l+1} - V^1_{i,l+1})$, and relative consistency error $(L^0_{N,K} - L^\epsilon_K)V_{l+1}$, separately. Let us define

$$Q_{i,l+1} := \begin{cases} \dfrac{\prod_{j=1}^{i}\left(1+\frac{\alpha}{\epsilon}h_j\right)}{\prod_{j=1}^{N/2}\left(1+\frac{\alpha}{\epsilon}h_j\right)}, & 0 \le i \le \frac{N}{2} \\ \dfrac{\prod_{j=i}^{N-1}\left(1+\frac{\alpha}{\epsilon}h_{j+1}\right)}{\prod_{j=N/2}^{N-1}\left(1+\frac{\alpha}{\epsilon}h_{j+1}\right)}, & \frac{N}{2} \le i \le N. \end{cases}$$

Lemma 4.5.1. *For the mesh function $Q_{i,l+1}$, we have*

$$L^1_{N,K}Q_{i,l+1} \ge \frac{C}{\max(\epsilon, h_i)}Q_{i,l+1},\quad i = \{1,2,\cdots,N-1\}\backslash\{N/2\},$$
$$\textit{and} \qquad (D_+ - D_-)Q_{\frac{N}{2},l+1} \le -C\epsilon^{-1}.$$

Proof. Note that $0 \leq Q_{i,l+1} \leq 1$. Moreover, for $1 \leq i \leq \dfrac{N}{2} - 1$

$$\begin{aligned}
L^1_{N,K} Q_{i,l+1} &= -\epsilon \Delta t D_+ D_- Q_{i,l+1} + a_i \Delta t D_- Q_{i,l+1} + \hat{b}_i Q_{i,l+1} \\
&= -\epsilon \Delta t \left(\frac{\alpha}{\epsilon}\right)^2 \frac{2h_i}{h_i + h_{i+1}} \frac{1}{\left(1 + \frac{\alpha}{\epsilon} h_i\right)} Q_{i,l+1} \\
&\quad + a_i \Delta t \left(\frac{\alpha}{\epsilon}\right) \frac{1}{\left(1 + \frac{\alpha}{\epsilon} h_i\right)} Q_{i,l+1} + \hat{b}_i Q_{i,l+1} \\
&= \left(-2\Delta t \left(\frac{\alpha^2}{\epsilon}\right) + a_i \Delta t \left(\frac{\alpha}{\epsilon}\right) \frac{1}{\left(1 + \frac{\alpha}{\epsilon} h_i\right)} + \hat{b}_i\right) Q_{i,l+1} \\
&= \frac{\alpha \Delta t}{\alpha h_i + \epsilon} \left(a_i - \frac{2\alpha}{\epsilon}(\alpha h_i + \epsilon) + \hat{b}_i \frac{\epsilon + h_i \alpha}{\alpha \Delta t}\right) Q_{i,l+1} \\
&\geq \frac{C}{\max(\epsilon, h_i)} Q_{i,l+1} > 0.
\end{aligned}$$

At $i = N/2$, $h^+_{N/2} = \hbar = h^-_{N/2}$ and in that case

$$\begin{aligned}
(D_+ - D_-) Q_{\frac{N}{2},l+1} &= \left(\frac{-\alpha}{\epsilon}\left(\frac{1}{1 + \frac{\alpha}{\epsilon}\hbar}\right) - \frac{\alpha}{\epsilon}\left(\frac{1}{1 + \frac{\alpha}{\epsilon}\hbar}\right)\right) Q_{\frac{N}{2},l+1} \\
&\leq \frac{-\alpha}{\epsilon}\left(\frac{2}{1 + \frac{\alpha}{\epsilon}\hbar}\right) \\
&\leq \frac{-C}{\epsilon} < 0.
\end{aligned}$$

Similarly, for $\dfrac{N}{2} + 1 \leq i \leq N - 1$

$$\begin{aligned}
L^1_{N,K} Q_{i,l+1} &= -\epsilon \Delta t D_+ D_- Q_{i,l+1} + a_i \Delta t D_- Q_{i,l+1} + \hat{b}_i Q_{i,l+1} + c_i \Delta t Q_{i-\frac{N}{2},l+1} \\
&= -\epsilon \Delta t \left(\frac{\alpha}{\epsilon}\right)^2 \frac{2h_i}{h_i + h_{i+1}} \frac{1}{\left(1 + \frac{\alpha}{\epsilon} h_i\right)} Q_{i,l+1} + a_i \Delta t \left(\frac{\alpha}{\epsilon}\right) \frac{1}{\left(1 + \frac{\alpha}{\epsilon} h_i\right)} Q_{i,l+1} \\
&\quad + \hat{b}_i Q_{i,l+1} + c_i \Delta t Q_{i-\frac{N}{2},l+1} \\
&= \left(-2\Delta t \left(\frac{\alpha^2}{\epsilon}\right) + a_i \Delta t \left(\frac{\alpha}{\epsilon}\right) \frac{1}{\left(1 + \frac{\alpha}{\epsilon} h_i\right)} + \hat{b}_i\right) Q_{i,l+1} + c_i \Delta t Q_{i-\frac{N}{2},l+1} \\
&= \frac{\alpha \Delta t}{\alpha h_i + \epsilon} \left(a_i - \frac{2\alpha}{\epsilon}(\alpha h_i + \epsilon) + \hat{b}_i \frac{\epsilon + h_i \alpha}{\alpha \Delta t}\right) Q_{i,l+1} + c_i \Delta t Q_{i-\frac{N}{2},l+1} \\
&\geq \frac{C}{\max(\epsilon, h_i)} Q_{i,l+1} > 0. \qquad (4.5.1)
\end{aligned}$$

□

Next, we use Lemma 4.4.1, 4.4.2 and 4.5.1 and the argument following Chapter 2 to obtain the error bounds on the regular and singular components.

Lemma 4.5.2. *The regular component V_{l+1} of the solution U_{l+1} and its corrected approximation $V_{i,l+1}$ satisfies*

$$|L^1_{N,K}(V_{l+1} - V_{i,l+1})| \leq \begin{cases} Ch_i^2 & \text{for } 1 \leq i \leq \frac{N}{2} - 1, \\ Ch_i & \text{for } \frac{N}{2} + 1 \leq i \leq N - 1. \end{cases}$$

Proof. Referring to representation (4.4.4), we can write

$$|L^1_{N,K}(V_{l+1} - V_{i,l+1})| = |(L^1_{N,K} - L^0_{N,K})(V_{l+1} - V^1_{i,l+1})| + |(L^0_{N,K} - L^\epsilon_K)V_{l+1}|.$$

Following Lemma 2.5.1 and Lemma 2.5.2 it follows that

$$|(L^1_{N,K} - L^0_{N,K})(V_{l+1} - V^1_{i,l+1})| \leq Ch_i^2, \ i \in \{1, \cdots N-1\}\backslash\{N/2\}$$

and

$$|(L^\epsilon_k - L^0_{N,K})V_{l+1}| \leq \begin{cases} Ch_i^2 \left(\epsilon \left\|V^{(4)}_{l+1}\right\|_\infty + \left\|V^{(3)}_{l+1}\right\|_\infty\right) & \text{for } 1 \leq i \leq \frac{N}{2} - 1, \\ Ch_i \left(\epsilon \left\|V^{(3)}_{l+1}\right\|_\infty + \left\|V^{(2)}_{l+1}\right\|_\infty\right) & \text{for } \frac{N}{2} + 1 \leq i \leq N - 1. \end{cases}$$

□

Next we estimate the error in the singular component of the solution.

Lemma 4.5.3. *The singular component W_{l+1} of the solution U_{l+1} and its corrected approximation $W_{i,l+1}$ satisfies*

$$|L^1_{N,K}(W_{l+1} - W_{i,l+1})| \leq \begin{cases} CN^{-2} & \text{for } 1 \leq i \leq \frac{N}{2} - 1, \\ Ch_i\epsilon^{-1} & \text{for } \frac{N}{2} + 1 \leq i \leq N - 1. \end{cases}$$

Proof. For $i \in \left\{1, \cdots, \frac{N}{2} - 1\right\}$, we can write

$$|L^1_{N,K}|(W_{l+1} - W_{i,l+1})| = |L^1_{N,K}(W_{l+1} - W^1_{i,l+1})| + |L^1_{N,K}(W^1_{i,l+1} - W_{i,l+1})|.$$

Proceeding in a similar manner as in Lemma 2.5.4, it follows that

$$|L^1_{N,K}(W_{l+1} - W^1_{i,l+1})| \quad = \quad |L^1_{N,K}W_{l+1}| \leq CN^{-(\phi-1)},$$

and

$$|L^1_{N,K}(W^1_{i,l+1} - W_{i,l+1})| \quad = \quad |L^0_{N,K}W^1_{i,l+1}| \leq CN^{-(\phi-1)}.$$

Moreover, for $i \in \left\{\frac{N}{2} + 1, \cdots, N - 1\right\}$, Lemma 4.3.4 and Lemma 2.5.4 leads to

$$|L^1_{N,K}(W_{l+1} - W_{i,l+1})| \leq C\epsilon^{-1}h_i.$$

□

Lemma 4.5.4. *Let $U(x, t_{l+1})$ be the solution of* (4.3.1) *and $U_{i,l+1}$ be its approximation. Then, for $i = N/2$*

$$\left|(D_+ - D_-)(U_{i,l+1} - U(x, t_{l+1}))\right| \leq \frac{Ch_i}{\epsilon^2}.$$

Proof. The proof is straightforward if we consider

$$\begin{aligned}
\left|(D_+ - D_-)(U_{i,l+1} - U(x, t_{l+1}))\right| &= |(D_+ - D_-)(U(x, t_{l+1}))| \\
&\leq \left|\left(D_+ - \frac{d}{dx}\right)U(x, t_{l+1})\right| + \left|\left(D_- - \frac{d}{dx}\right)U(x, t_{l+1})\right| \\
&\leq \frac{1}{2}h^-_{N/2}\max_{x\in(0,1)}\left|\frac{d^2U(x, t_{l+1})}{dx^2}\right| + \frac{1}{2}h^+_{N/2}\max_{x\in(1,2)}\left|\frac{d^2U(x, t_{l+1})}{dx^2}\right| \\
&\leq C\hbar\max_{x\in(0,1)\cup(1,2)}\left|\frac{d^2U(x, t_{l+1})}{dx^2}\right| \\
&\leq \frac{C\hbar}{\epsilon^2}.
\end{aligned}$$

□

Lemma 4.5.5. *The solution U_{l+1} of the problem* (4.3.1) *and its corrected approximation $U_{i,l+1}$ satisfies*

$$|U_{l+1} - U_{i,l+1}| \leq CN^{-2}(\log N)^3 \text{ for } i \in \{0, 1, \cdots, N\}.$$

Proof. Collecting results from Lemma 4.5.2, Lemma 4.5.3 and Lemma 4.5.4 to write

$$|L^1_{N,K}(U_{l+1} - U_{i,l+1})| \leq \begin{cases} Ch_i^2 & \text{for } 1 \leq i \leq \frac{N}{2} - 1, \\ \dfrac{C\hbar}{\epsilon^2} & \text{for } i = \frac{N}{2}, \\ \dfrac{Ch_i}{\epsilon} & \text{for } \frac{N}{2} + 1 \leq i \leq N - 1. \end{cases}$$

Moreover, L_1-norm stability argument for operator $L^1_{N,K}$ yields

$$\begin{aligned}
\left\|U_{l+1} - U_{i,l+1}\right\|_\infty &\leq \sum_{j=1}^{N-1} C\frac{h_i + h_{i+1}}{2}|L^1_{N,K}(U_{l+1} - U_{i,l+1})| \\
&\leq \sum_{j=1}^{\frac{N}{2}-1} Ch_i^3 + C\hbar\frac{h_{\frac{N}{2}} + h_{\frac{N}{2}+1}}{2} + \sum_{j=\frac{N}{2}+1}^{N-1} Ch_i^2\epsilon^{-1} \\
&\leq CN^{-2}(\log N)^3.
\end{aligned}$$

□

We are now able to state the main result of this chapter, the principle convergence theorem.

Theorem 4.5.6. *Let u be the solution of* (4.2.3) *and $U_{i,l+1}$ be its corrected approximation on $\Gamma_N \times \Gamma_K^t$. Then*

$$\left|u(x_i, t_{l+1}) - U_{i,l+1}\right| \leq C(\Delta t + N^{-2}(\log N)^3).$$

Proof. The proof follows from Lemma 4.3.2, Lemma 4.5.5 and the triangle inequality. □

4.6 Numerical Results

This section presents numerical results for two test examples. The exact solution of the problem is not available for comparison. Therefore, we estimate the error using the double mesh principle[166]. For given values of N and K, the maximum absolute error $\hat{E}_{N,K}$ is given by

$$\hat{E}_{N,K} = \max_{(x_i,t_l)\in\Gamma_N\times\Gamma_K^t} |U_{N,K}(x_i, t_{l+1}) - U_{2N,2K}(x_i, t_{l+1})|,$$

where $U_{N,K}(x_i, t_{l+1})$ and $U_{2N,2K}(x_i, t_{l+1})$ are the computed numerical solutions on $\Gamma_N \times \Gamma_K^t$ and $\Gamma_{2N}\times\Gamma_{2K}^t$, respectively. Whereas the numerical order of convergence $\hat{P}_{N,K}$ is calculated using

$$\hat{P}_{N,K} = \log_2\left(\frac{\hat{E}_{N,K}}{\hat{E}_{2N,2K}}\right).$$

Example 4.6.1. *Consider the following parabolic convection-diffusion problem with large shift*

$$\begin{aligned}
&u_t(x,t) - \epsilon u_{xx}(x,t) + u_x(x,t) + \exp xu(x,t) + xu(x-1,t) = 10x(1-x)^3,\ (x,t) \in (0,2)\times(0,2]\\
&u(x,0) = 0,\ x \in [0,2]\\
&u(x,t) = x,\ (x,t) \in [-1,0]\times[0,2]\\
&u(2,t) = 0,\ t \in [0,2].
\end{aligned}$$

Example 4.6.2. *Consider the following parabolic convection-diffusion problem with large shift*

$$\begin{aligned}
&u_t(x,t) - \epsilon u_{xx}(x,t) + u_x(x,t) + 5u(x,t) + u(x-1,t) = t^3x(2-x),\ (x,t) \in (0,2)\times(0,2]\\
&u(x,0) = 0,\ x \in [0,2]\\
&u(x,t) = \tfrac{5}{4}t^2x,\ (x,t) \in [-1,0]\times[0,2]\\
&u(2,t) = 0,\ t \in [0,2].
\end{aligned}$$

Test examples are solved numerically using the proposed defect correction method over a non-uniform mesh. The maximum absolute error and order of convergence are obtained numerically for $K = N$ and tabulated in the form of Tables 4.1 and 4.3 for Example 4.6.1 and Example 4.6.2, respectively. Moreover, Table 4.2 and Table 4.4 presents the

Table 4.1: Maximum absolute error ($\hat{E}_{N,K}$) and order of convergence ($\hat{P}_{N,K}$) for Example 4.6.1 when $K = N$.

ϵ	N= 32	64	128	256	512
10^{-2}	1.4203e-03	5.2890e-04	1.9967e-04	8.0218e-05	3.1218e-05
	1.42	1.40	1.31	1.36	1.37
10^{-4}	1.4212e-03	5.3819e-04	2.0985e-04	8.0893e-05	3.2781e-05
	1.40	1.35	1.37	1.30	1.34
10^{-6}	1.6015e-03	6.2932e-04	2.3989e-04	8.8801e-05	3.3093e-05
	1.34	1.39	1.44	1.41	1.39
10^{-8}	2.7203e-03	9.8332e-04	3.8124e-04	1.3006e-04	4.7056e-05
	1.46	1.36	1.56	1.46	1.41
10^{-10}	2.7206e-03	9.8351e-04	3.8264e-04	1.4019e-04	4.9610e-05
	1.46	1.36	1.46	1.49	1.42

Table 4.2: Maximum absolute error ($\hat{E}_{N,K}$) and order of convergence ($\hat{P}_{N,K}$) for Example 4.6.1 when $K = N^2$.

	$\epsilon = 2 \times 10^{-3}$		$\epsilon = 2 \times 10^{-5}$	
N	$E_{N,K}$	$P_{N,K}$	$E_{N,K}$	$P_{N,K}$
32	3.0834e-04	1.84	3.0839e-04	1.81
64	8.6081e-05	1.90	8.7498e-05	1.92
128	2.2952e-05	1.87	2.2996e-05	1.86
256	6.2671e-06	1.83	6.2931e-06	1.73
512	1.8913e-06	1.89	1.8901e-06	1.80

maximum absolute error and corresponding order of convergence when $K = N^2$ to justify the spatial order of convergence for Example 4.6.1 and Example 4.6.2, respectively. The surface plot of solution for Examples 4.6.1 and 4.6.2 are displayed in Figures 4.1 and 4.3, respectively. Moreover, Figures 4.2 and 4.4 present the solution for different time t. In addition the log-log plots of errors are given in Figures 4.5 and 4.6 for Examples 4.6.1 and 4.6.2, respectively.

4.7 Conclusion

The chapter presents a defect correction method based on finite difference discretizations over a non-uniform mesh for parabolic partial differential equations with a large shift.

Table 4.3: Maximum absolute error ($\hat{E}_{N,K}$) and order of convergence ($\hat{P}_{N,K}$) for Example 4.6.2 when $K = N$.

ϵ	N= 32	64	128	256	512
10^{-2}	2.4246e-02	7.8278e-03	2.5659e-03	8.2137e-04	2.7808e-04
	1.63	1.60	1.64	1.56	1.59
10^{-4}	2.5267e-02	8.266e-03	2.6382e-03	8.3496e-04	2.8916e-04
	1.61	1.64	1.65	1.52	1.58
10^{-6}	2.5445e-02	8.3159e-03	2.6842e-03	8.4029e-04	2.9411e-04
	1.61	1.63	1.67	1.51	1.60
10^{-8}	2.5488e-02	8.3169e-03	2.6905e-03	8.4109e-03	2.9486e-04
	1.61	1.62	1.67	1.51	1.59
10^{-10}	2.5493e-02	8.3176e-03	2.6937e-03	8.4147e-03	2.9491e-04
	1.61	1.62	1.67	1.51	1.59

Table 4.4: Maximum absolute error ($\hat{E}_{N,K}$) and order of convergence ($\hat{P}_{N,K}$) for Example 4.6.2 when $K = N^2$.

	$\epsilon = 2 \times 10^{-3}$		$\epsilon = 2 \times 10^{-5}$	
N	$E_{N,K}$	$P_{N,K}$	$E_{N,K}$	$P_{N,K}$
32	4.3467e-03	1.88	4.5138e-03	1.86
64	1.1784e-03	1.93	1.2350e-03	1.92
128	3.0846e-04	1.87	3.2453e-04	1.94
256	8.3853e-04	1.85	8.4073e-04	1.84
512	2.3191e-05	1.82	2.3372e-05	1.82

The proposed defect correction method improves the efficiency of a numerical solution through iterative improvement and generates a stable second-order method in space over a non-uniform mesh. The mesh has been chosen so that most of the mesh points remain in the regions with rapid transitions. Whereas an implicit finite difference scheme is used to discretize the time variable. The proposed numerical method has been analysed for consistency, stability and convergence. Theoretical analysis is performed to obtain consistency and error estimates. The method is uniformly convergent and second-order accurate in space and first-order in time. We do not use asymptotic expansions of discretization errors in our analysis. Numerical results agree with the theoretical estimates and indicate that the defect correction technique can improve accuracy for singular perturbation problems.

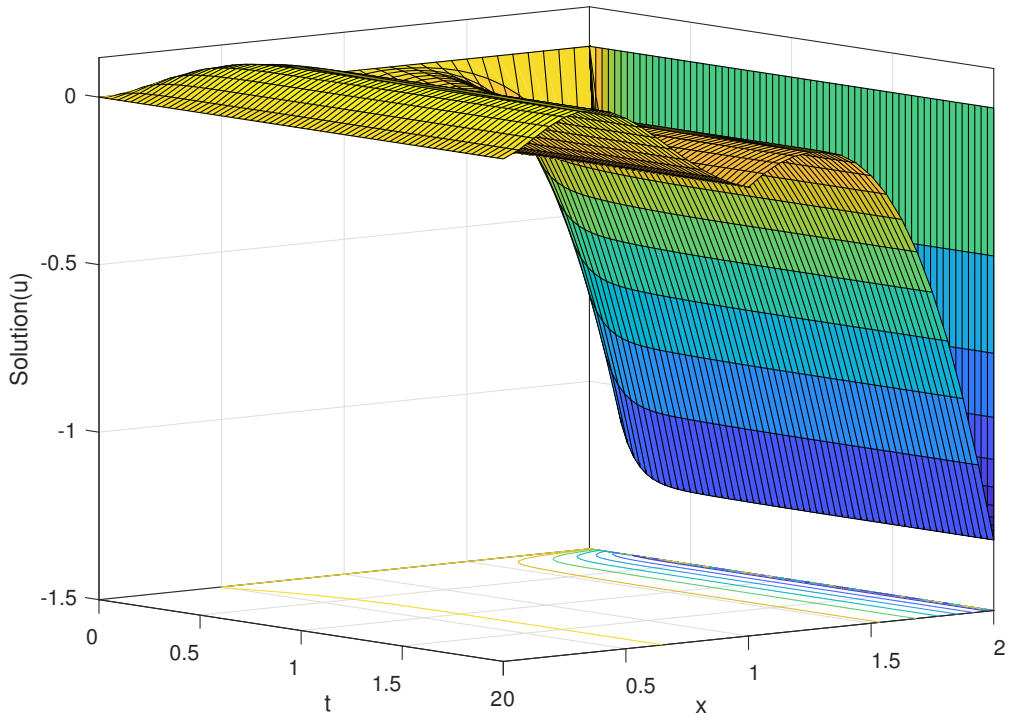

Figure 4.1: Numerical solution to Example 4.6.1 when $K = N = 64$ and $\epsilon = 2 \times 10^{-08}$.

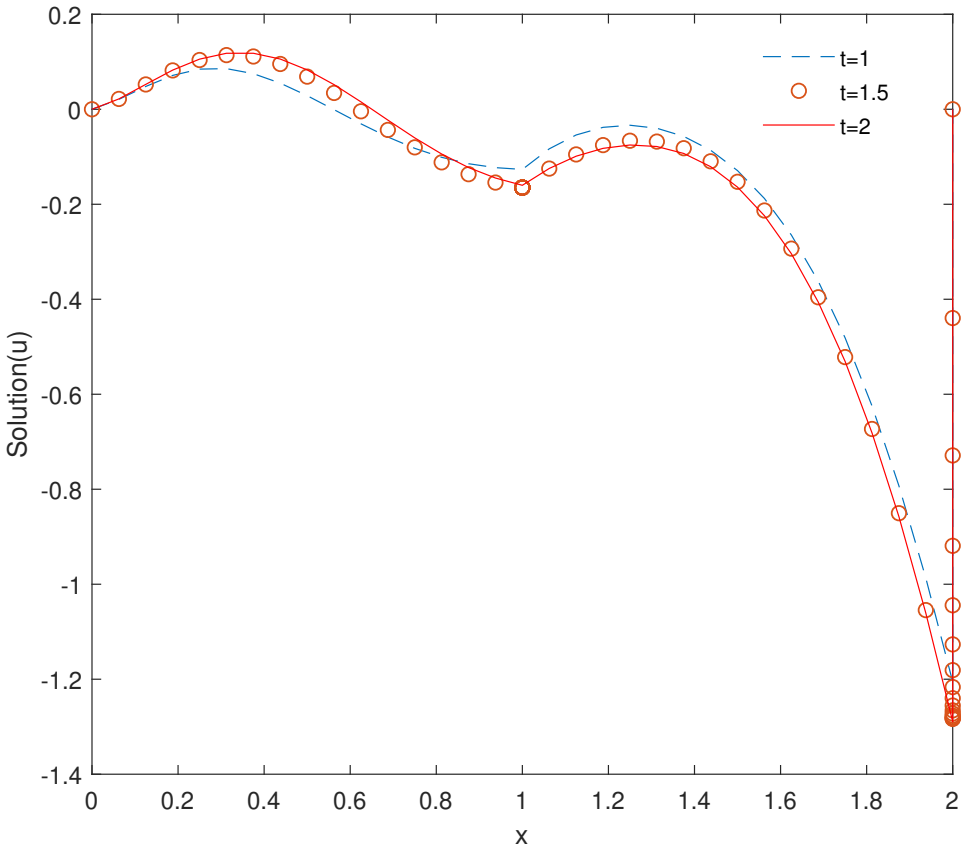

Figure 4.2: Numerical solution to Example 4.6.1 for different t when $\epsilon = 2 \times 10^{-08}$.

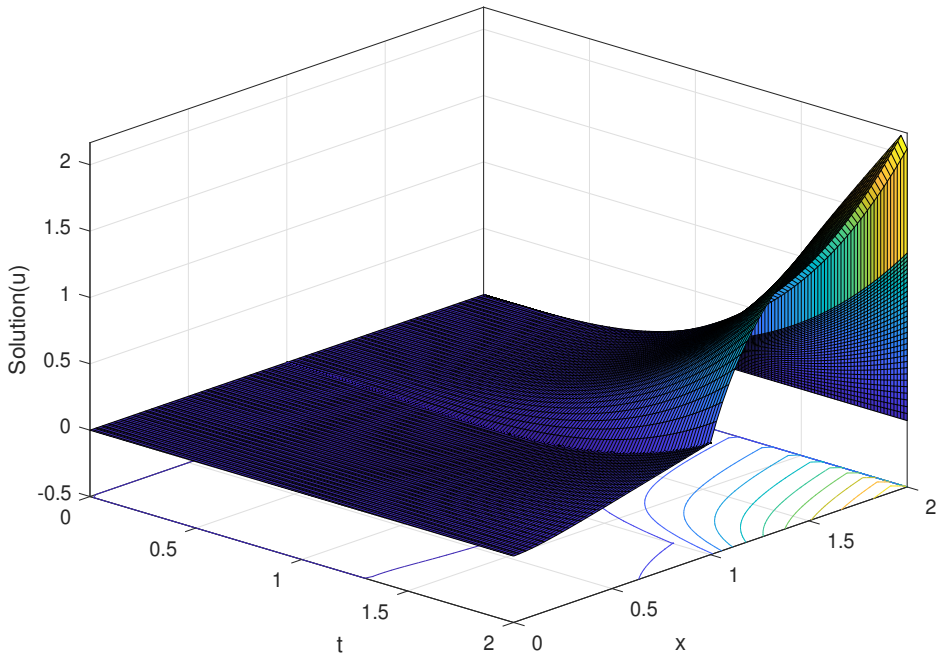

Figure 4.3: Numerical solution to Example 4.6.2 when $K = N = 64$ and $\epsilon = 2 \times 10^{-10}$.

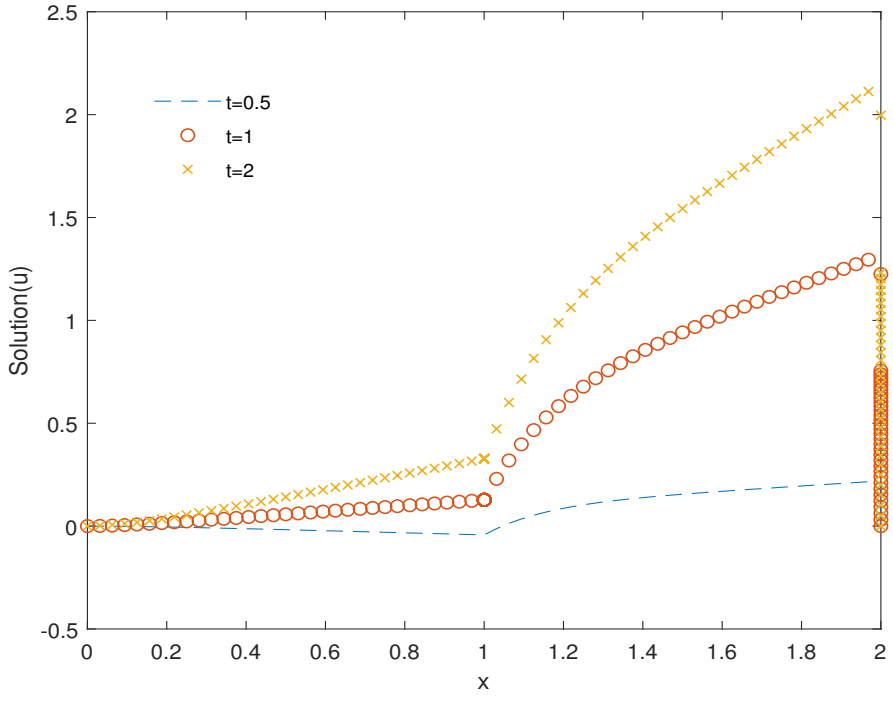

Figure 4.4: Numerical solution to Example 4.6.2 for different t when $\epsilon = 2 \times 10^{-10}$.

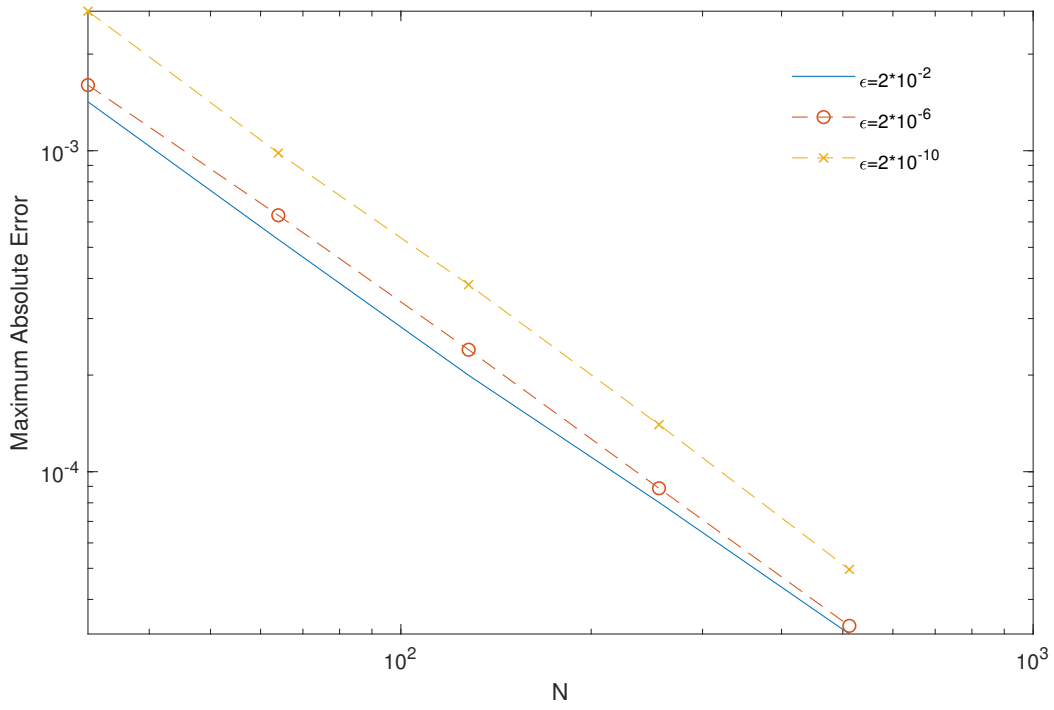

Figure 4.5: Error plot for Example 4.6.1 for different values of ϵ.

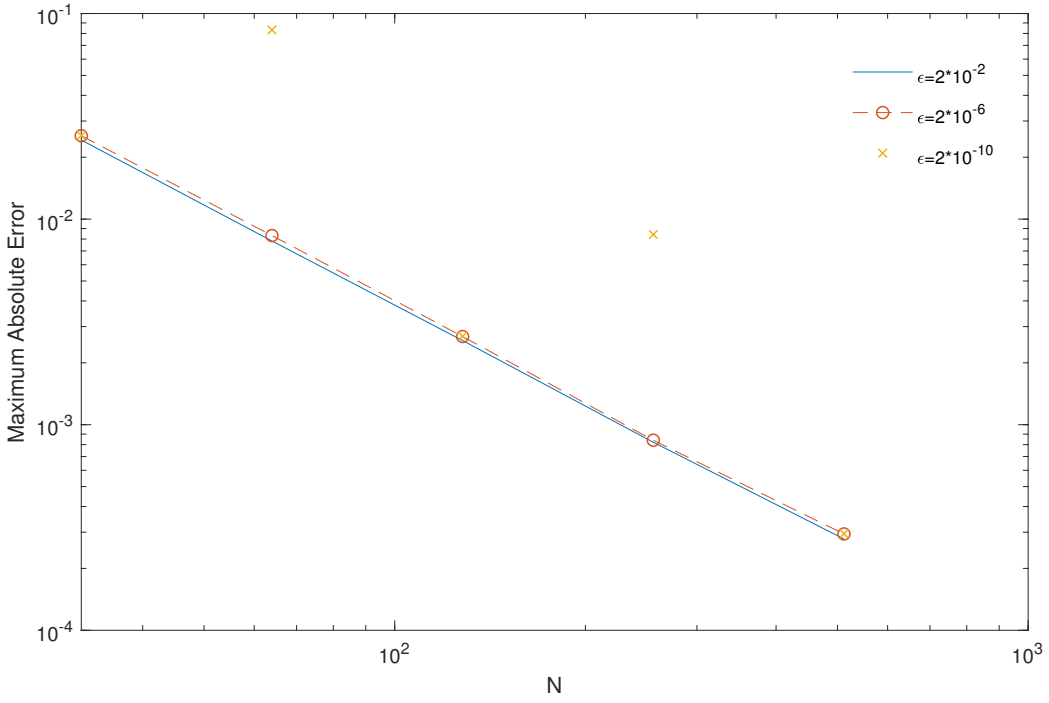

Figure 4.6: Error plot for Example 4.6.2 for different values of ϵ.

Chapter 5

Parabolic Convection-Diffusion Problems with Discontinuous Coefficients and Source

5.1 Introduction

In Chapter 4, we proposed a defect correction scheme for solving singularly perturbed parabolic PDEs with delay. In this chapter, we extend the scope of our work to solve singularly perturbed parabolic PDEs with discontinuous convection coefficients and sources.

Singularly perturbed parabolic PDEs with discontinuous coefficients and sources constitute a challenging class of mathematical models that arise in various fields, including physics, engineering and biology. These equations include time-dependent variables and exhibit sensitivity to small perturbations in the system parameters. The parabolic nature of these PDEs indicates their ability to describe dynamic processes with diffusion-like behaviour, where quantities such as temperature, concentration, or population density evolve over time and space. However, what sets them apart is the presence of discontinuous coefficients and source terms, which introduce additional complexity to the problem.

These problems involve an arbitrary small parameter that multiplies the highest-order derivative in the equation, leading to stiffness in the mathematical model. The solution to such problems exhibits strong interior layers across the discontinuity and demonstrates turning point behaviour [209, 19]. The solution varies exponentially in relatively small spatial regions and short time intervals called layer regions and slowly elsewhere. This multiscale behavior makes it challenging to accurately compute it with traditional numerical methods [166, 253]. Numerical discretization of singularly perturbed differential equations is burdened with difficulties. For example, the finite difference method

[97, 96] and the finite element method [277, 278, 279, 127, 128] require a mesh to approximate solutions. In fact, the discrete solutions obtained using standard Galerkin or centered finite difference methods exhibit oscillatory behavior for small discretization parameters [99]. However, layer-adapted meshes seem promising in the discretization of such equations, leading to growing interest in their generation [209].

Many researchers have studied parabolic singular perturbation problems with discontinuous coefficients and sources and proposed various numerical methods for their solution. For example, in [133], the author proposed two upwind difference schemes on non-uniform meshes to solve a convection-diffusion problem with a concentrated source and discontinuous convection coefficient. In [74], the author examined a convection-diffusion problem with a discontinuous convection coefficient using an upwind scheme over a piecewise uniform mesh. In [213], researchers constructed a numerical method based on piecewise uniform meshes for parabolic differential equations with discontinuous data. They presented a hybrid difference scheme to solve a convection-diffusion problem with a discontinuous convection coefficient and established almost second-order convergence. In [191], the authors propose another hybrid method for solving a parabolic convection-diffusion problem with a discontinuous convection coefficient.

In contrast, the author in [221] presents a hybrid difference scheme over Shishkin mesh for a class of reaction-convection-diffusion problems with a discontinuous source. In [41], the author used a hybrid difference scheme to solve parabolic convection-diffusion problems with a discontinuous convection coefficient and obtained almost second-order convergence. The authors in [169] constructed an implicit upwind finite difference scheme on Shishkin-type meshes to solve parabolic convection-diffusion problems with a discontinuous convection coefficient. In [36], the authors presented a uniformly convergent method to solve a two-point boundary value problem with discontinuous data. In [224], researchers used a hybrid difference scheme to analyse a second-order ordinary differential equation with a discontinuous convection coefficient subject to mixed-type boundary conditions. In [50], researchers analysed a parabolic convection-diffusion problem with a degenerating convective term and a discontinuous source. They considered a second-order convection-diffusion Robin-type problem with a discontinuous source term in [171]. In [42], the author studied a two-parameter singularly perturbed parabolic convection-diffusion problem with non-smooth data. In [57], the author uses the computational method for a class of second-order singularly perturbed parabolic differential equations with discontinuous coefficients involving large negative shifts. The formulated method comprises the implicit Euler and the cubic spline in compression methods for time and spatial dimensions, respectively. Furthermore, [131, 130] solved parabolic delay

differential equations with discontinuous convection coefficients using finite difference discretization over Shishkin mesh.

In [295], authors proposed a nonsymmetric interior penalty Galerkin (NIPG) finite element method to solve convection-dominated-diffusion problems with discontinuous coefficients. In [232], authors proposed a nonsymmetric discontinuous Galerkin finite element technique with interior penalties (NIPG) to solve singularly perturbed convection–diffusion problem with a discontinuous source term. In [16], authors examined a weakly coupled system of two reaction-diffusion equations with discontinuous source terms. They used a numerical method based on finite elements over the Shishkin and Bakhvalov-Shishkin mesh to derive an error estimate in the energy norm. In [270], the author used a standard numerical method with piecewise linear interpolation on Shishkin mesh to solve a weakly coupled system of a singularly perturbed problem for second-order ordinary differential-difference equations with discontinuous convection coefficients and source terms. In [43], authors solved a coupled system of second-order singularly perturbed differential equations of reaction–diffusion type with discontinuous source term subject to Dirichlet boundary conditions using a classical finite difference scheme in conjunction with Shishkin mesh and Bakhvalov mesh. Despite significant progress in this area, the solution of parabolic singular perturbation problems with discontinuous coefficients and sources remains a challenging problem. Thus, developing efficient and accurate methods for solving such problems is important and continues to attract attention from the scientific community.

The theory and the area of numerical approximation for time-dependent singular perturbation problems with discontinuous coefficient terms still need to be developed. This chapter presents a parameter uniform numerical method to solve such a class of singularly perturbed parabolic partial differential equations. Moreover, the chapter presents rigorous consistency, stability and convergence analysis of the proposed method and illustrates numerical results to support theoretical estimates.

5.2 Problem Description

Let $\Omega = (0,1) = \Omega^- \cup \Omega^+$, $\Omega^- = (0,c)$, $\Omega^+ = (c,1)$, $\mathcal{D} = \mathcal{D}^- \cup \mathcal{D}^+ = \Omega \times (0,T]$ and $\hat{F} := \bar{\mathcal{D}}/\mathcal{D}$. Consider the parabolic problem

$$\left.\begin{aligned} &Lu(x,t) = \epsilon u_{xx}(x,t) + a(x)u_x(x,t) - b(x)u(x,t) - u_t(x,t) = g(x,t),\\ &u(x,0) = r_0(x),\ (x,t) \in \bar{\mathcal{D}},\\ &u(0,t) = r_1(t),\ t \in (0,T],\\ &u(1,t) = r_2(t),\ t \in (0,T], \end{aligned}\right\} \tag{5.2.1}$$

where $0 < \epsilon \ll 1$ is the perturbation parameter, $b(x)$ is a sufficiently smooth function such that $b(x) \geq \beta \geq 0$ on $\bar{\mathcal{D}}$, the convection coefficient $a(x)$ and the source term $g(x)$ are sufficiently smooth functions on $\Omega^- \cup \Omega^+$ satisfying

$$|[a](c)| \leq C, \quad |[g](c)| \leq C. \tag{5.2.2}$$

Moreover, the solution $u(x,t)$ to the problem (5.2.1) satisfies the interface conditions

$$[u](c) = 0, \quad \left[\frac{\partial u}{\partial x}\right](c) = 0. \tag{5.2.3}$$

Here $[u]$ denotes the jump of u at the point of discontinuity, written as

$$[u](c,t) = u(c^+,t) - u(c^-,t).$$

Due to a discontinuity in the convection coefficient at $x = c$, the solution to the problem (5.2.1) has an interior layer of width $O(\epsilon)$ in the neighbourhood of $x = c$ [77]. To accentuate the occurrence of the strong interior layer, we consider the case

$$\left.\begin{aligned} -a_1^* < a(x) < -a_1 < 0, \quad & x < c, \\ a_2^* > a(x) > a_2 > 0, \quad & x > c, \end{aligned}\right\} \tag{5.2.4}$$

and write $\alpha = \min\{a_1, a_2\}$. Furthermore, the functions $r_0(x)$, $r_1(t)$ and $r_2(t)$ are Hölder continuous and satisfy the compatibility conditions

$$\left.\begin{aligned} & r_0(0) = r_1(0), \ r_0(1) = r_2(0), \\ & \epsilon\frac{\partial^2 r_0(0)}{\partial x^2} + a(0)\frac{\partial r_0(0)}{\partial x} - b(0)r_0(0) - \frac{\partial r_1(0)}{\partial t} = g(0,0), \\ & \epsilon\frac{\partial^2 r_0(1)}{\partial x^2} + a(1)\frac{\partial r_0(1)}{\partial x} - b(1)r_0(1) - \frac{\partial r_2(0)}{\partial t} = g(1,0). \end{aligned}\right\}$$

The operator L in (5.2.1) satisfies the following continuous minimum principle.

Lemma 5.2.1. *Let $\psi \in C^0(\bar{\mathcal{D}}) \cap C^2(\mathcal{D}^- \cup \mathcal{D}^+)$ satisfies $\psi(x,t) \leq 0$, $(x,t) \in \hat{F}$, $[\psi_x](c,t) \geq 0$, $t > 0$ and $L\psi(x,t) \geq 0$ for all $(x,t) \in \mathcal{D}^- \cup \mathcal{D}^+$. Then $\psi(x,t) \leq 0$, $(x,t) \in \bar{\mathcal{D}}$.*

Proof. Let $\psi(x,t) > 0$ for $(x,t) \in \bar{\mathcal{D}}$, $q(x,t)$ be a function such that

$$\psi(x,t) = e^{-(\alpha(x)|x-c|)/2\epsilon} q(x,t), \quad \text{and} \quad \alpha(x) = \begin{cases} a_1(x), & x < c, \\ a_2(x), & x > c. \end{cases}$$

Let $(x_s,t_s) \in \bar{\mathcal{D}}$ and $q(x_s,t_s) = \max\limits_{(x,t)\in\bar{\mathcal{D}}} q(x,t)$ hence $q_x(x_s,t_s) = 0$, $q_t(x_s,t_s) = 0$ and $q_{xx}(x_s,t_s) < 0$. Moreover, if

Case I: If $s \in \mathcal{D}^- \cup \mathcal{D}^+$

$$L\psi(x_s,t_s) = \begin{cases} \epsilon\psi_{xx}(x_s,t_s) + a_1(x_s)\psi_x(x_s,t_s) - b(x_s)\psi(x_s,t_s) - \psi_t(x_s,t_s) < 0, \ (x_s,t_s) \in \mathcal{D}^-, \\ \epsilon\psi_{xx}(x_s,t_s) + a_2(x_s)\psi_x(x_s,t_s) - b(x_s)\psi(x_s,t_s) - \psi_t(x_s,t_s) < 0, \ (x_s,t_s) \in \mathcal{D}^+. \end{cases}$$

Case II: If $s = (c, t^*)$

$$[\psi_x](c,t^*) = [q_x](c,t^*) - \left[\frac{(a_1+a_2)}{2\epsilon}\right] q(c,t^*) < 0.$$

A contradiction to the assumption and the required result follows from a contradiction.

□

A direct application of the minimum principle guides us to the following stability estimate.

Lemma 5.2.2. *Let u be the solution of* (5.2.1)*. Then*

$$\|u\|_{\bar{\mathcal{D}}} \leq \|u\|_{\infty,\hat{\Gamma}} + \frac{1}{\beta}\|g\|_{\infty,\bar{S}}, \quad \text{where } \beta = \min\left\{\frac{a_1}{c}, \frac{a_2}{1-c}\right\}.$$

Proof. Define barrier functions $Y^\pm$ as

$$Y^\pm = \begin{cases} -\|u\|_{\infty,\hat{\Gamma}} - \dfrac{x\|g\|}{\beta c} \pm u(x,t), \ x \leq c, \\ -\|u\|_{\infty,\hat{\Gamma}} - \dfrac{(1-x)\|g\|}{\beta(1-c)} \pm u(x,t), \ x > c. \end{cases}$$

Case I: If $(x,t) \in \mathcal{D}^-$

$$\begin{aligned} LY^\pm(x,t) &= \epsilon Y^\pm_{xx}(x,t) + a_1(x)Y^\pm_x(x,t) - b(x)Y^\pm(x,t) - Y^\pm_t(x,t) \\ &= \pm\epsilon u_{xx}(x,t) + a_1(x)\left(-\frac{\|g\|}{\beta c} \pm u_x(x,t)\right) - b(x,t)\left(-\|u\|_{\infty,\hat{\Gamma}} - \frac{x\|g\|}{\beta c} \pm u(x,t)\right) \\ &\quad \mp u_t(x,t) \\ &= a_1(x)\left(-\frac{\|g\|}{\beta c}\right) - b(x,t)\left(-\|u\|_{\infty,\hat{\Gamma}} - \frac{x\|g\|}{\beta c}\right) \pm Lu(x,t) \geq 0. \end{aligned}$$

Case II: If $(x,t) \in \mathcal{D}^+$

$$\begin{aligned} LY^\pm(x,t) &= \epsilon Y^\pm_{xx}(x,t) + a_2(x)Y^\pm_x(x,t) - b(x)Y^\pm(x,t) - Y^\pm_t(x,t) \\ &= \pm\epsilon u_{xx}(x,t) + a_2(x)\left(\frac{\|g\|}{\beta(1-c)} \pm u_x(x,t)\right) - b(x,t)\Big(-\|u\|_{\infty,\hat{\Gamma}} \\ &\quad -\frac{(1-x)\|g\|}{\beta(1-c)} \pm u(x,t)\Big) \mp u_t(x,t) \\ &= a_2(x)\left(\frac{\|g\|}{\beta(1-c)}\right) - b(x,t)\left(-\|u\|_{\infty,\hat{\Gamma}} - \frac{(1-x)\|g\|}{\beta(1-c)}\right) \pm Lu(x,t) \geq 0. \end{aligned}$$

Case III: If $x = c$

$$[Y^\pm_x](c,t) = [u_x](c,t) = 0.$$

The required result now follows from Lemma 5.2.1. □

5.3 Time Semidiscretization

Let us split the given interval $[0, T]$ into K subintervals of length $\Delta t = T/K$, $K \in \mathbb{Z}^+$. The resulting mesh becomes

$$\Gamma_t^K = \{t_l = l\Delta t, l = 0, 1, 2, \cdots K\}.$$

An application of the implicit Euler scheme leads to the semidiscrete problem

$$L_K^\epsilon U(x, t_{l+1}) = G(x, t_{l+1});\ 0 \le x \le 1,\ 0 \le l \le K-1 \tag{5.3.1a}$$

such that

$$\left.\begin{aligned} &U(x,0) = r_0(x),\ 0 \le x \le 1,\\ &U(0, t_{l+1}) = r_1(t_{l+1}),\ 0 \le l \le K-1,\\ &U(1, t_{l+1}) = r_2(t_{l+1}),\ 0 \le l \le K-1,\\ &U(c^-, t_{l+1}) = U(c^+, t_{l+1}),\ U_x(c^-, t_{l+1}) = U_x(c^+, t_{l+1}), \end{aligned}\right\} \tag{5.3.1b}$$

where

$$L_K^\epsilon U(x, t_{l+1}) = \epsilon\Delta t U_{xx}(x, t_{l+1}) + a(x)\Delta t U_x(x, t_{l+1}) - \hat{b}(x)U(x, t_{l+1}),\ x \in D^- \cup D^+,$$

and

$$G(x, t_{l+1}) = \Delta t g(x, t_{l+1}) - U(x, t_l),\ x \in D^- \cup D^+.$$

Here, $\hat{b}(x) := 1 + b(x)\Delta t$. Next, we set up the semidiscrete minimum principle. The operator L_K^ϵ satisfies the semidiscrete minimum principle ensuring that the method (5.3.1) is stable.

Lemma 5.3.1. *Let $R(x, t_{l+1})$ be a sufficiently smooth function for $x \in [0, 1]$. If $R(x, t_{l+1}) \le 0$, $x = \{0, 1\}$, $L_K^\epsilon R(x, t_{l+1}) \ge 0$, $x \in \Omega^- \cup \Omega^+$ and $[R(c, t_{l+1})] \ge 0$. Then $R(x, t_{l+1}) \le 0$, $\forall x \in \Omega$.*

Proof. Let $(s, t_{l+1}) \in \{(x, t_{l+1}) : x \in [0, 1]\}$ and $R(s, t_{l+1}) = \max\limits_{x\in[0,1]} R(x, t_{l+1}) > 0$. Consequently, $R_x(s, t_{l+1}) = 0$, $R_t(s, t_{l+1}) = 0$, $R_{xx}(s, t_{l+1}) < 0$ and $(s, t_{l+1}) \notin \hat{F}$.

Case I: If $s \in \Omega^- \cup \Omega^+$

$$L_K^\epsilon R(s, t_{l+1}) = \epsilon\Delta t R_{xx}(s, t_{l+1}) + a(s)\Delta t R_x(s, t_{l+1}) - \hat{b}(s)R(s, t_{l+1}) < 0.$$

Case II: If $s = c$

$$R_x(s^+, t_{l+1}) - R_x(s^-, t_{l+1}) < 0.$$

A contradiction to the assumption and the result follows. □

Lemma 5.3.2. *The solution $U(x, t_{l+1})$ of semidiscretized problem* (5.3.1) *satisfies*

$$|U(x, t_{l+1})| \leq \max\left\{|U(0, t_{l+1})|, \frac{\|G\|}{\alpha}, |U(1, t_{l+1})|\right\}, \ x \in [0, 1].$$

Proof. Let $Y^{\pm}(x, t_{l+1}) := -\max\left\{|U(0, t_{l+1})|, \frac{\|G\|}{\alpha}, |U(1, t_{l+1})|\right\} \pm U(x, t_{l+1})$. Note that $Y^{\pm}(x, t_{l+1}) \leq 0$ for $x \in \{0, 1\}$. Moreover,

Case I: If $x \in \Omega^- \cup \Omega^+$

$$\begin{aligned} L_K^{\epsilon} Y^{\pm}(x, t_{l+1}) &= \epsilon Y^{\pm}_{xx}(x, t_{l+1}) + a(x) Y^{\pm}_{x}(x, t_{l+1}) - b\hat{(x)} Y^{\pm}(x, t_{l+1}) - Y^{\pm}_{t}(x, t_{l+1}) \\ &= \hat{b}(x) \max\left\{|U(0, t_{l+1})|, \frac{\|G\|}{\alpha}, |U(1, t_{l+1})|\right\} \pm L_K^{\epsilon} U(x, t_{l+1}) \geq 0. \end{aligned}$$

Case II: If $x = c$

$$[Y^{\pm}_{x}](c, t_{l+1}) = \pm[U_x](c, t_{l+1}) \geq 0.$$

The required result follows from Lemma 5.3.1. □

From [166], it follows that $\left\|L_K^{\epsilon}\right\|_{\infty} \leq C$ and the stability of the method is immediate. Moreover, it is easy to follow that the local truncation error satisfies $\|e_{l+1}\|_{\infty} \leq C(\Delta t)^2$. Combine local error estimates to obtain the following estimate for the global discretization error ($\hat{E}_l$).

Lemma 5.3.3. *The global discretization error $\hat{E}_l$ at the lth time step satisfies*

$$\left\|\hat{E}_l\right\|_{\infty} \leq C\Delta t$$

where the constant $C > 0$ is independent of ϵ and Δt.

As a result, uniform convergence is achieved using the temporal semidiscretization process. To get sharp bounds on the solution of the semidiscretized problem (5.3.1), we express U_{l+1} as a sum of smooth component V_{l+1} and singular component W_{l+1}, writing $U_{l+1} := V_{l+1} + W_{l+1}$. Furthermore, the smooth component V_{l+1} takes the form

$$V(x, t_{l+1}) = V_0(x, t_{l+1}) + \epsilon V_1(x, t_{l+1}) + \epsilon^2 V_2(x, t_{l+1}),$$

where $V_0(x, t_{l+1})$ is the solution of the reduced problem

$$\left.\begin{aligned} &a(x)\Delta t(V_0)_x(x, t_{l+1}) - \hat{b}(x)V_0(x, t_{l+1}) = G(x, t_{l+1}), \ x \in \Omega^- \cup \Omega^+, \\ &V_0(0, t_{l+1}) = r_1(t_{l+1}), \end{aligned}\right\} \tag{5.3.2}$$

$V_1(x, t_{l+1})$ satisfies

$$\left.\begin{aligned} &a(x)\Delta t(V_1)_x(x, t_{l+1}) - \hat{b}(x)V_1(x, t_{l+1}) = -(V_0)_{xx}(x, t_{l+1}), \ x \in \Omega^- \cup \Omega^+, \\ &V_1(0, t_{l+1}) = 0, \end{aligned}\right\} \tag{5.3.3}$$

and $V_2(x, t_{l+1})$ satisfies

$$\left.\begin{aligned} &L_K^{\epsilon} V_2(x, t_{l+1}) = -(V_1)_{xx}(x, t_{l+1}),\ x \in \Omega^- \cup \Omega^+, \\ &V_2(0, t_{l+1}) = 0,\ V_2(1, t_{l+1}) = 0. \end{aligned}\right\} \tag{5.3.4}$$

Thus, the smooth component V_{l+1} of U_{l+1} satisfies

$$\left.\begin{aligned} &L_K^{\epsilon} V(x, t_{l+1}) = G(x, t_{l+1}),\ x \in \Omega^- \cup \Omega^+,\ 0 \le l \le K-1, \\ &V(0, t_{l+1}) = r_1(t_{l+1}), \\ &V(c^-, t_{l+1}) = V_0(c^-, t_{l+1}) + \epsilon V_1(c^-, t_{l+1}) + \epsilon^2 V_2(c^-, t_{l+1}), \\ &V(c^+, t_{l+1}) = V_0(c^+, t_{l+1}) + \epsilon V_1(c^+, t_{l+1}) + \epsilon^2 V_2(c^+, t_{l+1}), \\ &V(1, t_{l+1}) = r_2(t_{l+1}). \end{aligned}\right\} \tag{5.3.5}$$

The singular component W_{l+1} of U_{l+1}, on the other hand, satisfies

$$\left.\begin{aligned} &L_K^{\epsilon} W(x, t_{l+1}) = 0,\ x \in \Omega^- \cup \Omega^+,\ 0 \le l \le K-1, \\ &W(0, t_{l+1}) = 0,\ W(1, t_{l+1}) = 0, \\ &[W(c, t_{l+1})] = -[V(c, t_{l+1})],\ [W_x(c, t_{l+1})] = -[V_x(c, t_{l+1})]. \end{aligned}\right\} \tag{5.3.6}$$

Lemma 5.3.4. *Let $V(x, t_{l+1})$ be the solution of* (5.3.2)-(5.3.5) *and $W(x, t_{l+1})$ be the solution of* (5.3.6)*. Then, for each integer $0 \le q \le 3$ and $x \in (0, 1)$*

$$\begin{aligned} &\|V(x, t_{l+1})\| \le C,\ \|V^q(x, t_{l+1})\|_{\bar{D}\setminus\{c\}} \le C\epsilon^{2-q}, \\ &|[V(c, t_{l+1})]|, |[V_x(c, t_{l+1})]|, |[V_{xx}(c, t_{l+1})]| \le C, \\ &|W^q(x, t_{l+1})| \le \begin{cases} \epsilon^{-q} \exp\left(\dfrac{-\alpha(c-x)}{\epsilon}\right), & x \in \{0\} \cup \Omega^-, \\ \epsilon^{-q} \exp\left(\dfrac{-\alpha(x-c)}{\epsilon}\right), & x \in \Omega^+ \cup \{1\}. \end{cases} \end{aligned}$$

Proof. Apply the arguments given in [77] to each of the subinterval $\Omega^- \cup \Omega^+$ separately, and the proof follows. □

5.4 The Space Discretization

5.4.1 Mesh Description

The solution to the problem (5.2.1) exhibits a strong interior layer in the neighbourhood of $x = c$ [77]. Thus, we construct a mesh Γ_N that condenses the points around $x = c$. For that, we use the Bakhvalov-Shishkin mesh to discretize the domain in the spatial direction. Let τ_1 and τ_2 be the mesh transition parameters defined as

$$\tau_1 = \min\left\{\frac{c}{2}, \tau_0 \epsilon \log N\right\},\ \tau_2 = \min\left\{\frac{1-c}{2}, \tau_0 \epsilon \log N\right\},$$

where $\tau_0 = \dfrac{\phi}{\epsilon}$ and $\phi \geq 3$. Note that if $\tau_1 = \dfrac{c}{2}$ and $\tau_2 = \dfrac{1-c}{2}$, the mesh is uniform. Divide the spatial domain Γ_N into four subintervals as

$$\Gamma_N = [0, c-\tau_1] \cup [c-\tau_1, c] \cup [c, c+\tau_2] \cup [c+\tau_2, 1]. \tag{5.4.1}$$

The subintervals $[0, c-\tau_1]$ and $[c+\tau_2, 1]$ contain $N/4$ mesh points, each placed uniformly such that $x_0 = 0$, $x_{N/4} = c-\tau_1$, $x_{3N/4} = c+\tau_2$, and $x_N = 1$. However, the other two intervals, $[c-\tau_1, c]$ and $[c, c+\tau_2]$, have the same number of mesh points. The mesh is generated nonuniformly by a continuous, monotonically increasing, piecewise differentiable mesh-generating function $\Phi(t) = \begin{cases} \Phi_L(t), & t \in [\frac{1}{4}, \frac{1}{2}], \\ \Phi_R(t), & t \in [\frac{1}{2}, \frac{3}{4}] \end{cases}$ such that

$$\Phi_L\left(\frac{1}{4}\right) = -\log N, \quad \Phi_R\left(\frac{3}{4}\right) = \log N, \quad \Phi_L\left(\frac{1}{2}\right) = 0, \quad \text{and} \quad \Phi_R\left(\frac{1}{2}\right) = 0.$$

The resulting mesh reads

$$x_i = \begin{cases} 4(c-\tau_1)t_i, & i = 0, \cdots, N/4, \\ c + \epsilon\tau_0\Phi_L(t_i), & i = N/4+1, \cdots, N/2, \\ c + \epsilon\tau_0\Phi_R(t_i), & i = N/2+1, \cdots, 3N/4, \\ (c+\tau_2) + 4\left(i - \dfrac{3N}{4}\right)\left(\dfrac{1-c-\tau_2}{N}\right), & i = 3N/4+1, \cdots, N, \end{cases} \tag{5.4.2}$$

where $t_i = \frac{i}{N}$. Let $h_i := x_i - x_{i-1},\ i = 1, \cdots N$ denotes the mesh width. Then in the smooth region, the width of coarse uniform mesh is

$$h_i = \begin{cases} H_L = \dfrac{4(c-\tau_1)}{N}, & i = 1, \cdots N/4, \\ H_R = \dfrac{4(1-c-\tau_2)}{N}, & i = 3N/4, \cdots N, \end{cases} \tag{5.4.3}$$

and in the layer region, mesh width satisfies

$$h_i = \begin{cases} h_i \geq h_{i+1}, & i = N/4+1, \cdots, N/2-1, \\ h_i \leq h_{i+1}, & i = N/2+1, \cdots, 3N/4-1. \end{cases} \tag{5.4.4}$$

In the layer region, consider the mesh-characterising functions

$$\psi_L(t) = 1 - 4\left(1 - N^{-1}\right)\left(\frac{1}{2} - t\right), \quad \text{and,} \quad \psi_R(t) = 1 - 4\left(1 - N^{-1}\right)\left(t - \frac{1}{2}\right), \tag{5.4.5}$$

related to Φ_L and Φ_R by relation $\Phi_L = \log \psi_L$ and $\Phi_R = -\log \psi_R$, respectively. Moreover, the mesh-characterising functions satisfies $\psi_L\left(\frac{1}{4}\right) = N^{-1}$, $\psi_L\left(\frac{1}{2}\right) = 1$, $\psi_R\left(\frac{1}{2}\right) = 1$, and $\psi_R\left(\frac{3}{4}\right) = N^{-1}$. For uniform mesh $h_i = h_{i+1} := \hbar$.

Lemma 5.4.1. *The step size h_i of Γ_N satisfies $h_i \leq CN^{-1}$ for $i \in \{1, \cdots N\}$.*

Proof. If $1 \leq i \leq \dfrac{N}{4}$ and $\dfrac{3N}{4} \leq i \leq N$, the proof is evident. For $i \in \left\{\dfrac{N}{4}+1, \cdots, \dfrac{3N}{4}\right\}$, it follows from 2.3.1 that $h_i \leq \dfrac{4\epsilon}{\alpha}$ and the result follows. □

5.4.2 The Difference Scheme

For $i \geq 0$, a function $Y_{i,l+1}$ and mesh width h_i the forward, backward and central difference approximation to first-order derivatives are defined as

$$\left.\begin{aligned} D_+Y_{i,l+1} &:= \frac{Y_{i+1,l+1} - Y_{i,l+1}}{h_{i+1}},\ D_-Y_{i,l+1} := \frac{Y_{i,l+1} - Y_{i-1,l+1}}{h_i} \\ \text{and } D_0Y_i &:= \frac{Y_{i+1,l+1} - Y_{i-1,l+1}}{h_{i+1}+h_i}. \end{aligned}\right\}$$

At the same time, a difference approximation for a second-order derivative reads

$$D_+D_-Y_{i,l+1} := \frac{2}{h_{i+1}+h_i}\left(\frac{Y_{i+1,l+1} - Y_{i,l+1}}{h_{i+1}} - \frac{Y_{i,l+1} - Y_{i-1,l+1}}{h_i}\right).$$

The upwind operator for problem (5.3.1) takes the form

$$L^1_{N,K}Y_{i,l+1} = \begin{cases} Y_{i,l+1}, & i = 0, N, \\ \epsilon\Delta t D_+D_-Y_{i,l+1} + a_i\Delta t D_-Y_{i,l+1} - \hat{b}_iY_{i,l+1}, & 1 \leq i \leq \frac{N}{2}-1, \\ \epsilon\Delta t D_+D_-Y_{i,l+1} + a_i\Delta t D_+Y_{i,l+1} - \hat{b}_iY_{i,l+1}, & \frac{N}{2}+1 \leq i \leq N-1. \end{cases} \tag{5.4.6}$$

Moreover, the modified central difference operator $L^0_{N,K}$ reads

$$L^0_{N,K}Y_{i,l+1} = \begin{cases} Y_{i,l+1}, & i = 0, N, \\ L^2_{N,K}Y_{i,l+1}, & 1 \leq i \leq \frac{N}{4},\ \frac{3N}{4}+1 \leq i \leq N-1, \\ L^1_{N,K}Y_{i,l+1}, & \frac{N}{4}+1 \leq i \leq \frac{N}{2}-1,\ \frac{N}{2}+1 \leq i \leq \frac{3N}{4}, \end{cases} \tag{5.4.7}$$

where $L^2_{N,K}Y_{i,l+1} = \epsilon\Delta t D_+D_-Y_{i,l+1} + a_i\Delta t D_0Y_{i,l+1} - \hat{b}_iY_{i,l+1}$ and $G_{i,l+1} = g(x_i, t_{l+1}) - Y_{i,l}$, $i \in \{1, \cdots, N-1\}\backslash\{N/2\}$. The two step defect correction scheme takes the form

First Step: $L^1_{N,K}U^1_{i,l+1} = G_{i,l+1}$, $i \in \{1, \cdots, N-1\}\backslash\{N/2\}$.

Second Step: $L^1_{N,K}U_{i,l+1} = (L^1_{N,K} - L^0_{N,K})U^1_{i,l+1} + G_{i,l+1}$, $i \in \{1, \cdots, N-1\}\backslash\{N/2\}$,

such that

$$\left.\begin{aligned} &D_+U_{N/2,l+1} = D_-U_{N/2,l+1},\ l \in \{1, \cdots, K-1\}, \\ &U_{i,0} = (r_0)_i,\ i \in \{1, \cdots, N\}, \\ &U_{1,l+1} = (r_1)_{l+1},\ l \in \{1, \cdots, K-1\}, \\ &U_{N,l+1} = (r_2)_{N,l+1},\ l \in \{1, \cdots, K-1\}. \end{aligned}\right\} \tag{5.4.8}$$

Here, U^1 and U represent the initial and the corrected approximation of (5.3.1), respectively. Following (2.4.3), the consistency error $\hat{E}$ of the defect correction scheme reads

$$\hat{E} = \left(L^1_{N,K} - L^0_{N,K}\right)\left(U_{l+1} - U^1_{i,l+1}\right) + \left(L^0_{N,K} - L^\epsilon_K\right)U_{l+1}, \tag{5.4.9}$$

where U_{l+1} is a solution to (5.3.1) and $U^1_{i,l+1}$ denotes initial approximation to (5.4.8).

Lemma 5.4.2. *Let $P_{i,l+1}$ be a mesh function. If $P_{0,l+1} \le 0$, $P_{N,l+1} \le 0$, $L^1_{N,K}P_{i,l+1} \ge 0$, $i \in \{1, \cdots, N-1\}\backslash\{N/2\}$ and $D_+P_{N/2,l+1} - D_-P_{N/2,l+1} \ge 0$. Then $P_{i,l+1} \ge 0$, $i \in \{1, \cdots, N\}$.*

Proof. Let $P_{i,l+1} = \max\limits_{x_i \in \Gamma_N, t_{l+1} \in \Gamma^K_t} P_{i,l+1} > 0$. Then

$$D_-P_{i,l+1} = 0, \quad D_+P_{i,l+1} = 0, \quad \text{and} \quad D_-D_+P_{i,l+1} < 0.$$

Case I: If $1 \le i \le \dfrac{N}{2} - 1$

$$L^1_{N,K}P_{i,l+1} = \epsilon\Delta t D_+D_-P_{i,l+1} + a_i\Delta t D_-P_{i,l+1} - \hat{b}_iP_{i,l+1} < 0.$$

Case II: If $i = \dfrac{N}{2}$

$$[D](P_{i,l+1}) < 0, \text{ since } P_{i,l+1} > 0.$$

Case III: If $\dfrac{N}{2} + 1 \le i \le N - 1$

$$L^1_{N,K}P_{i,l+1} = \epsilon\Delta t D_+D_-P_{i,l+1} + a_i\Delta t D_+P_{i,l+1} - \hat{b}_iP_{i,l+1} < 0.$$

Consequently, the result follows from a contradiction. □

Next, we establish that operators $L^1_{N,K}$ and $L^1_{N,K} - L^2_{N,K}$ commute.

Lemma 5.4.3. *The difference operators $L^1_{N,K}$ and $L^1_{N,K} - L^2_{N,K}$, defined by* (5.4.6) *and* (5.4.7)*, satisfies*

$$L^1_{N,K}(L^1_{N,K} - L^2_{N,K})Y_{i,l+1} = (L^1_{N,K} - L^2_{N,K})L^1_{N,K}Y_{i,l+1}$$

iff $a_{i-1} = a_i = a_{i+1}$, $b_{i-1} = b_i = b_{i+1}$ and $h_{i+2} = h_{i+1} = h_i = h_{i-1}$.

Proof. For $1 \le i \le \dfrac{N}{4}$, observe that

$$\begin{aligned}(L^1_{N,K} - L^2_{N,K})Y_{i,l+1} &= -a_i\Delta t(D_- - D_0)Y_{i,l+1} \\ &= \frac{-a_i}{2}\Delta t h_{i+1}D_+D_-Y_{i,l+1}. \end{aligned} \tag{5.4.10}$$

Apply $L^1_{N,K}$ to (5.4.10), and if $h_{i-1} = h_i = h_{i+1} = h_{i+2}$, $b_{i-1} = b_i = b_{i+1}$ and $a_{i-1} = a_i = a_{i+1}$, then

$$\begin{aligned} L^1_{N,K}(L^1_{N,K} - L^2_{N,K})Y_{i,l+1} &= \epsilon\Delta t D_+D_-\left(\frac{-a_i}{2}\Delta t h_{i+1}D_+D_-Y_{i,l+1}\right) + a_i\Delta t D_-\left(\frac{-a_i}{2}\Delta t h_{i+1}D_+D_-Y_{i,l+1}\right) \\ &\quad -\hat{b}_i\left(\frac{-a_i}{2}\Delta t h_{i+1}D_+D_-Y_{i,l+1}\right) \\ &= \frac{-a_i}{2}\Delta t h_{i+1}\left(\epsilon\Delta t D_+D_-(D_+D_-Y_{i,l+1}) + a_i\Delta t D_-(D_+D_-Y_{i,l+1})\right. \\ &\quad \left.-\hat{b}_i(D_+D_-Y_{i,l+1})\right). \end{aligned}$$

If we reverse the order of the operator

$$\begin{aligned} (L^1_{N,K} - L^2_{N,K})L^1_{N,K}Y_{i,l+1} &= \frac{-a_i}{2}\Delta t h_{i+1}D_+D_-\left(\epsilon\Delta t D_+D_-Y_{i,l+1} + a_i\Delta t D_-Y_{i,l+1} - \hat{b}_iY_{i,l+1}\right) \\ &= \frac{-a_i}{2}\Delta t h_{i+1}\left(\epsilon\Delta t D_+D_-(D_+D_-Y_{i,l+1}) + a_i\Delta t D_-(D_+D_-Y_{i,l+1})\right. \\ &\quad \left.-\hat{b}_i(D_+D_-Y_{i,l+1})\right). \end{aligned}$$

Similarly, if $\frac{3N}{4} + 1 \le i \le N-1$

$$(L^1_{N,K} - L^2_{N,K})Y_{i,l+1} = a_i\Delta t(D_+ - D_0)Y_{i,l+1} = \frac{a_i}{2}\Delta t h_iD_+D_-Y_{i,l+1}. \tag{5.4.11}$$

Apply $L^1_{N,K}$ to (5.4.11), and if $h_{i-1} = h_i = h_{i+1} = h_{i+2}$, $b_{i-1} = b_i = b_{i+1}$, then

$$\begin{aligned} L^1_{N,K}(L^1_{N,K} - L^2_{N,K})Y_{i,l+1} &= \epsilon\Delta t D_+D_-\left(\frac{a_i}{2}\Delta t h_{i+1}D_+D_-Y_{i,l+1}\right) + a_i\Delta t D_+\left(\frac{a_i}{2}\Delta t h_{i+1}D_+D_-Y_{i,l+1}\right) \\ &\quad -\hat{b}_i\left(\frac{a_i}{2}\Delta t h_{i+1}D_+D_-Y_{i,l+1}\right) \\ &= \frac{a_i}{2}\Delta t h_i(\epsilon\Delta t D_+D_-(D_+D_-Y_{i,l+1}) + a_i\Delta t D_+(D_+D_-Y_{i,l+1}) \\ &\quad -\hat{b}_i(D_+D_-Y_{i,l+1})). \end{aligned}$$

If we reverse the order of the operator

$$\begin{aligned} (L^1_{N,K} - L^2_{N,K})L^1_{N,K}Y_{i,l+1} &= \frac{a_i}{2}\Delta t h_{i+1}D_+D_-\left(\epsilon\Delta t D_+D_-Y_{i,l+1} + a_i\Delta t D_+Y_{i,l+1} - \hat{b}_iY_{i,l+1}\right) \\ &= \frac{a_i}{2}\Delta t h_{i+1}\left(\epsilon\Delta t D_+D_-(D_+D_-Y_{i,l+1}) + a_i\Delta t D_+(D_+D_-Y_{i,l+1})\right. \\ &\quad \left.-\hat{b}_i(D_+D_-Y_{i,l+1})\right). \end{aligned}$$

Hence, the required result follows. □

Let us decompose solution $U_{i,l+1}$ into regular and singular components to bound the consistency error as

$$U^1_{i,l+1} = V^1_{i,l+1} + W^1_{i,l+1}, \quad i = 0, 1, \ldots, N. \tag{5.4.12}$$

The regular component $V^1_{i,l+1}$ is defined as

$$V^1(x_i, t_{l+1}) = \begin{cases} V^1_L(x_i, t_{l+1}), & 0 \le i \le \dfrac{N}{2} - 1, \\ V^1_R(x_i, t_{l+1}), & \dfrac{N}{2} + 1 \le i \le N, \end{cases} \tag{5.4.13}$$

which is the first approximation to the left and right of the point of discontinuity $x = c$ of the regular component V_{l+1} of the semidiscretized solution U_{l+1} to (5.3.1). Similarly, for singular component, we write

$$W^1(x_i, t_{l+1}) = \begin{cases} W^1_L(x_i, t_{l+1}), & 0 \le i \le \dfrac{N}{2} - 1, \\ W^1_R(x_i, t_{l+1}), & \dfrac{N}{2} + 1 \le i \le N, \end{cases} \tag{5.4.14}$$

such that the size of the jump $|[V^1(c, t_{l+1})]|$ determines the amplitude of the jump $W^1_R(x_i, t_{l+1}) - W^1_L(x_i, t_{l+1})$. Using the regular and singular components, we can bound the consistency error within and outside the layer region. Here, $V^1_L(x_i, t_{l+1})$ and $V_R(x_i, t_{l+1})$ satisfies

$$\left.\begin{aligned} &L^1_{N,K} V^1_L(x_i, t_{l+1}) = G(x_i, t_{l+1}),\ i = 1, \ldots, \tfrac{N}{2} - 1, \\ &V^1_L(0, t_{l+1}) = V_{l+1}(0),\ V^1_L(x_{N/2}, t_{l+1}) = V_{l+1}(c^-), \end{aligned}\right\} \tag{5.4.15}$$

and

$$\left.\begin{aligned} &L^1_{N,K} V^1_R(x_i, t_{l+1}) = G(x_i, t_{l+1}),\ i = \tfrac{N}{2} + 1, \ldots, N - 1, \\ &V^1_R(x_{N/2}, t_{l+1}) = V_{l+1}(c^+),\ V^1_R(x_N, t_{l+1}) = V_{l+1}(1). \end{aligned}\right\} \tag{5.4.16}$$

Similarly, W^1_L and W^1_R satisfies

$$\left.\begin{aligned} &L^1_{N,K} W^1_L(x_i, t_{l+1}) = 0,\ i = 1, \cdots, \tfrac{N}{2} - 1, \\ &L^1_{N,K} W^1_R(x_i, t_{l+1}) = 0,\ i = \tfrac{N}{2} + 1, \cdots, N - 1, \\ &W^1_L(0, t_{l+1}) = W_{l+1}(0),\ W^1_R(N, t_{l+1}) = W_{l+1}(1), \\ &W^1_R(x_{N/2}, t_{l+1}) + V^1_R(x_{N/2}, t_{l+1}) = W^1_L(x_{N/2}, t_{l+1}) + V^1_L(x_{N/2}, t_{l+1}), \\ &D_- W^1_R(x_{N/2}, t_{l+1}) + D_- V^1_R(x_{N/2}, t_{l+1}) = D_+ W^1_L(x_{N/2}, t_{l+1}) + D_+ V^1_L(x_{N/2}, t_{l+1}). \end{aligned}\right\} \tag{5.4.17}$$

Moreover, the corrected approximation $V_L(x_i, t_{l+1})$, $V_R(x_i, t_{l+1})$, $W_L(x_i, t_{l+1})$ and $W_R(x_i, t_{l+1})$ satisfies

$$\left.\begin{aligned} &L^1_{N,K} V_L(x_i, t_{l+1}) = (L^1_{N,K} - L^0_{N,K}) V^1_L(x_i, t_{l+1}) + G(x_i, t_{l+1}),\ i = 1, \cdots, \tfrac{N}{2} - 1, \\ &V_L(0, t_{l+1}) = V^1_L(0, t_{l+1}),\ V_L(x_{N/2}, t_{l+1}) = V^1_L(x_{N/2}, t_{l+1}), \end{aligned}\right\} \tag{5.4.18}$$

$$\left.\begin{aligned} &L_{N,K} V_R(x_i, t_{l+1}) = (L^1_{N,K} - L^0_{N,K}) V^1_R(x_i, t_{l+1}) + G(x_i, t_{l+1}),\ i = \tfrac{N}{2} + 1, \cdots, N - 1, \\ &V_R(x_{N/2}, t_{l+1}) = V^1_R(x_{N/2}, t_{l+1}),\ V_R(x_N, t_{l+1}) = V^1_R(x_N, t_{l+1}), \end{aligned}\right\} \tag{5.4.19}$$

and

$$\left.\begin{aligned}
&L^1_{N,K}W_L(x_i,t_{l+1}) = -L^0_{N,K}W^1_L(x_i,t_{l+1}),\ i=1,\cdots,\tfrac{N}{2}-1,\\
&L^1_{N,K}W_R(x_i,t_{l+1}) = -L^0_{N,K}W^1_R(x_i,t_{l+1}),\ i=\tfrac{N}{2}+1,\cdots,N-1,\\
&W_L(1,t_{l+1}) = W^1_L(1,t_{l+1}),\ W_R(N,t_{l+1}) = W^1_R(N,t_{l+1}),\\
&W_R(x_{N/2},t_{l+1}) + V_R(x_{N/2},t_{l+1}) = W_L(x_{N/2},t_{l+1}) + V_L(x_{N/2},t_{l+1}),\\
&D_-W_R(x_{N/2},t_{l+1}) + D_-V_R(x_{N/2},t_{l+1}) = D_+W_L(x_{N/2},t_{l+1}) + D_+V_L(x_{N/2},t_{l+1}).
\end{aligned}\right\} \tag{5.4.20}$$

Following [191], define mesh functions on $\Gamma_N = \{x_i\}_0^N$ as

$$R_{i,l+1} = \prod_{k=1}^{i}\left(1+\frac{\alpha h_k}{\epsilon}\right),\ 1\le i\le\frac{N}{2}, \tag{5.4.21}$$

and

$$Q_{i,l+1} = \prod_{k=1}^{N-i}\left(1+\frac{\alpha h_k}{\epsilon}\right),\ \frac{N}{2}\le i\le N-1 \tag{5.4.22}$$

with the usual convention $R_0 = 1$ and $Q_N = 1$. It is easy to follow that

$$R_{\frac{N}{4},l+1} = Q_{\frac{3N}{4},l+1} \le CN^{-\phi}. \tag{5.4.23}$$

Lemma 5.4.4. *For some constant C,*

$$\begin{aligned}
-L^1_{N,K}R_{i,l+1} &\ge \frac{C}{\epsilon+\alpha h_i}R_{i,l+1},\ 1\le i\le\frac{N}{2}-1,\ \text{and}\\
-L^1_{N,K}Q_{i,l+1} &\ge \frac{C}{\epsilon+\alpha h_{i+1}}Q_{i,l+1},\ \frac{N}{2}+1\le i\le N-1.
\end{aligned}$$

Moreover, for $i=\frac{N}{2}$

$$\left(D_+Q_{\frac{N}{2},l+1} - D_-R_{\frac{N}{2},l+1}\right) \le \frac{-C}{\alpha}.$$

Proof. Since $R_{i,l+1} - R_{i-1,l+1} = \dfrac{\alpha h_i}{\epsilon}R_{i,l+1}$ and $a_i < -a_1 \le -\alpha$,

$$\begin{aligned}
-L^1_{N,K}R_{i,l+1} &= -\left(\epsilon\Delta t D_+D_-R_{i,l+1} + a_i\Delta t D_-R_{i,l+1} - \hat{b}_iR_{i,l+1}\right)\\
&= -\left(\epsilon\Delta t\left(\frac{2}{h_{i+1}+h_i}\left(\frac{\alpha}{\epsilon}R_{i+1,l+1} - \frac{\alpha}{\epsilon}R_{i,l+1}\right) + a_i\Delta t\left(\frac{\alpha}{\epsilon}R_{i,l+1}\right) - \hat{b}_iR_{i,l+1}\right)\right)\\
&= \frac{-2\alpha\Delta t}{h_i+h_{i+1}}\left(R_{i+1,l+1} - R_{i,l+1}\right) - a_i\frac{\alpha\Delta t}{\epsilon}R_{i-1,l+1} + \hat{b}_iR_{i,l+1}\\
&\ge \frac{-\alpha\Delta t}{\epsilon}R_{i-1,l+1}\left[\frac{\alpha h_i}{h_i+h_{i+1}} + a_i\right] \ge \frac{C}{\epsilon+\alpha h_i}R_{i,l+1}.
\end{aligned}$$

For $i > \frac{N}{2}$, it follows that

$$(Q_{i+1,l+1} - Q_{i,l+1}) = \frac{-\alpha h_{N-i}}{\epsilon}Q_{i+1,l+1} \ \text{ and } \ a_i > \alpha_2 \ge \alpha.$$

Hence

$$\begin{aligned}
-L^1_{N,K}Q_{i,l+1} &= -\left(\epsilon\Delta t D_+D_-Q_{i,l+1} + a_i\Delta t D_+Q_{i,l+1} - \hat{b}_iQ_{i,l+1}\right)\\
&= -\left(\epsilon\Delta t\left(\frac{2}{h_{i+1}+h_i}\left(\frac{\alpha}{\epsilon}Q_{i+1,l+1} - \frac{\alpha}{\epsilon}Q_{i,l+1}\right) + a_i\Delta t\left(\frac{\alpha}{\epsilon}Q_{i+1,l+1}\right) - \hat{b}_iQ_{i,l+1}\right)\right)\\
&= \frac{-2\alpha\Delta t}{h_i+h_{i+1}}\left(Q_{i+1,l+1} - Q_{i,l+1}\right) - a_i\frac{\alpha\Delta t}{\epsilon}Q_{i+1,l+1} + \hat{b}_iQ_{i,l+1}\\
&\geq \frac{\alpha\Delta t}{\epsilon}Q_{i+1,l+1}\left[a_i - \frac{\alpha h_i}{h_i+h_{i+1}}\right] \geq \frac{C}{\epsilon+\alpha h_{N-i}}Q_{i,l+1}.
\end{aligned}$$

Moreover, if $i = \frac{N}{2}$

$$\begin{aligned}
\left(D_+Q_{\frac{N}{2},l+1} - D_-R_{\frac{N}{2},l+1}\right) &= \left(\frac{-\alpha h_{\frac{N}{2}}}{\epsilon+\alpha h_{\frac{N}{2}}} - \frac{\alpha h_{\frac{N}{2}}}{\epsilon+\alpha h_{\frac{N}{2}}}\right)\prod_{k=1}^{\frac{N}{2}}\left(1+\frac{\alpha h_k}{\epsilon}\right)\\
&= \left(\frac{-2\alpha h_{\frac{N}{2}}}{\epsilon+\alpha h_{\frac{N}{2}}}\right)\prod_{k=1}^{\frac{N}{2}}\left(1+\frac{\alpha h_k}{\epsilon}\right) \leq \frac{-C}{\alpha} < 0.
\end{aligned}$$

□

If $\mathcal{S}$ denotes the space of grid functions s_k, it follows from [74, 77] that

$$\|s_k\|_\infty \leq C\left\|L^1_{N,K}s_k\right\|_{1,d}. \tag{5.4.24}$$

5.5 Error Analysis

Let us next calculate the consistency error for regular and singular components separately. Then, we combine both results and find the error $\left\|U_{l+1} - U_{i,l+1}\right\|_\infty$. We begin our analysis with the regular component. To obtain consistency error on regular component $L^1_{N,K}(V(x,t_{l+1}) - V(x_i,t_{l+1}))$, we calculate the consistency error corresponding to the upwind difference scheme consisting of modified central difference consistency error $(L^1_{N,K} - L^0_{N,K})(V(x,t_{l+1}) - V^1(x_i,t_{l+1}))$ and relative consistency error $L^K_\epsilon V(x,t_{l+1}) - L^0_{N,K}V(x_i,t_{l+1})$ separately.

Lemma 5.5.1. *Let $V(x,t_{l+1})$ and $V^1(x_i,t_{l+1})$ be the regular components of the semidiscretized solution $U(x,t_{l+1})$ and initial solution $U^1(x_i,t_{l+1})$, respectively. Then for each $x_i \in \Gamma_N\backslash\{N/2\}$,*

$$(L^1_{N,K} - L^0_{N,K})(V(x,t_{l+1}) - V^1(x_i,t_{l+1})) \leq Ch_i^2,\ i \in \{1,\cdots,N\}\backslash\{N/2\}. \tag{5.5.1}$$

Proof. Note that for $\frac{N}{4}+1 \leq i \leq \frac{N}{2}-1$ and $\frac{N}{2}+1 \leq i \leq \frac{3N}{4}$, $L^1_{N,K} = L^0_{N,K}$. Hence

$$\left.\begin{aligned}
(L^1_{N,K} - L^0_{N,K})(V(x,t_{l+1}) - V^1_L(x_i,t_{l+1})) = 0,\ \frac{N}{4}+1 \leq i \leq \frac{N}{2}-1,\\
(L^1_{N,K} - L^0_{N,K})(V(x,t_{l+1}) - V^1_R(x_i,t_{l+1})) = 0,\ \frac{N}{2}+1 \leq i \leq \frac{3N}{4}.
\end{aligned}\right\} \tag{5.5.2}$$

Now, for $1 \le i \le \dfrac{N}{4}$, assumption of Lemma 5.4.3 holds true. Consequently,

$$\begin{aligned}
L^1_{N,K}(L^1_{N,K} - L^0_{N,K})(V_{l+1} - V^1_L(x_i, t_{l+1})) &= (L^1_{N,K} - L^0_{N,K})L^1_{N,K}(V_{l+1} - V^1_L(x_i, t_{l+1})) \\
&= a_i \Big[D_- \left(L^1_{N,K} V_{l+1} - L^1_{N,K} V_L(x_i, t_{l+1}) \right) \\
&\quad - D_0 \left(L^1_{N,K} V_{l+1} - L^1_{N,K} V_L(x_i, t_{l+1}) \right) \Big] \\
&= \frac{-a_i}{2h_i} \Big[\left((L^1_{N,K} V_{l+1})_{i+1} - 2(L^1_{N,K} V_l)_i \right. \\
&\quad \left. + (L^1_{N,K} V_{l+1})_{i-1} \right) - \left((L^K_\epsilon V_{l+1})_{i+1} \right. \\
&\quad \left. - 2(L^K_\epsilon V_{l+1})_i + (L^K_\epsilon V_{l+1})_{i-1} \right) \Big] \\
&= \frac{-\alpha}{2H_L} \Big[\left(L^1_{N,K} V_{l+1} - L^K_\epsilon V_{l+1} \right)_{i+1} - 2 \left(L^1_{N,K} V_{l+1} \right. \\
&\quad \left. - L^K_\epsilon V_{l+1} \right)_i + \left(L^1_{N,K} V_{l+1} - L^K_\epsilon V_{l+1} \right)_{i-1} \Big].
\end{aligned}$$

Following Lemma 2.5.1, we obtain

$$\begin{aligned}
|L^1_{N,K}(L^1_{N,K} - L^0_{N,K})(V_{l+1} - V^1_L(x_i, t_{l+1}))| &= \left| \frac{\alpha}{2H_L} \left(\frac{-\epsilon}{6H_L^2} \left[\int_{x_i}^{x_{i+1}} \left(V^{(4)}_{l+1}(\xi + h) - 2V^{(4)}_{l+1}(\xi) \right. \right. \right. \right. \\
&\quad \left. + V^{(4)}_{l+1}(\xi - h) \right) (x_{i+1} - \xi)^3 d\xi - \int_{x_{i-1}}^{x_i} \left(V^{(4)}_{l+1}(\xi + h) \right. \\
&\quad \left. - 2V^{(4)}_{l+1}(\xi) + V^{(4)}_{l+1}(\xi - h) \right) (\xi - x_{i-1})^3 d\xi \Big] \\
&\quad + \int_{x_{i-1}}^{x_i} \left(V^{(2)}_{l+1}(\xi + h) - 2V^{(2)}_{l+1}(\xi) + V^{(2)}_{l+1}(\xi - h) \right) \\
&\quad \left. \times (\xi - x_{i-1}) \right) \Big|.
\end{aligned}$$

An application of the fundamental theorem of calculus yields

$$\left| L^1_{N,K} \left(L^1_{N,K} - L^0_{N,K} \right) \left(V(x, t_{l+1}) - V^1_L(x_i, t_{l+1}) \right) \right| \le C H_L^2 \left(\epsilon \left\| V^{(6)}_{l+1} \right\|_\infty + \left\| V^{(4)}_{l+1} \right\|_\infty \right). \tag{5.5.3}$$

Similarly, for $\dfrac{N}{2} + 1 \le i \le N - 1$, it follows that

$$\left| L^1_{N,K} \left(L^1_{N,K} - L^0_{N,K} \right) \left(V(x, t_{l+1}) - V^1_R(x_i, t_{l+1}) \right) \right| \le C H_R^2 \left(\epsilon \left\| V^{(6)}_{l+1} \right\|_\infty + \left\| V^{(4)}_{l+1} \right\|_\infty \right). \tag{5.5.4}$$

Define barrier function $Y_{i,l+1} := C{h_i}^2 (x_i - 3)$. Next, we apply Lemma 5.4.2 with boundary points x_1, $x_{\frac{N}{4}}$, $x_{\frac{3N}{4}+1}$, and x_{N+1}.

Case I: For $1 \le i \le \dfrac{N}{4}$

$$\begin{aligned}
L^1_{N,K} Y_{i,l+1} &= \epsilon D_+ D_- Y_{i,l+1} + a_i D_- Y_{i,l+1} - \hat{b}_i Y_{i,l+1} \\
&= \frac{2\epsilon}{h_i + h_{i+1}} \left[\frac{C h_i^2 (x_{i+1} - x_i)}{h_{i+1}} - \frac{C h_i^2 (x_i - x_{i-1})}{h_i} \right] + a_i \left[C h_i (x_i - x_{i-1}) \right] \\
&\quad - \hat{b}_i \left[C h_i^2 (x_i - 3) \right] \\
&= \frac{\epsilon}{H_L} \left[\frac{C H_L^2 (x_{i+1} - x_i)}{H_L} - \frac{C H_L^2 (x_i - x_{i-1})}{H_L} \right] + a_i \left(C H_L (x_i - x_{i-1}) \right) \\
&\quad - \hat{b}_i (C H_L^2 (x_i - 3)) \ge C H_L^2.
\end{aligned} \tag{5.5.5}$$

Case II: For $\frac{3N}{4} \leq i \leq N-1$

$$\begin{aligned} L^1_{N,K}Y_{i,l+1} &= \epsilon D_+D_-Y_{i,l+1} + a_iD_+Y_{i,l+1} - \hat{b}_iY_{i,l+1} \\ &= \frac{2\epsilon}{h_i+h_{i+1}}\left[\frac{Ch_i^2(x_{i+1}-x_i)}{h_{i+1}} - \frac{Ch_i^2(x_i-x_{i-1})}{h_i}\right] + a_i\left[Ch_i(x_{i+1}-x_i)\right] \\ &\quad -\hat{b}_i\left[Ch_i^2(x_i-3)\right] \\ &= \frac{\epsilon}{H_R}\left[\frac{CH_R^2(x_{i+1}-x_i)}{H_R} - \frac{CH_R^2(x_i-x_{i-1})}{H_R}\right] + a_i\left(CH_R\left(x_{i+1}-x_i\right)\right) \\ &\quad -\hat{b}_i(CH_R^2(x_i-3)) \geq CH_R^2. \end{aligned} \tag{5.5.6}$$

Therefore, for a suitable choice of constant C, from (5.5.3), (5.5.4), (5.5.5) and (5.5.6), it follows that

$$(L^1_{N,K} - L^0_{N,K})(V(x,t_{l+1}) - V^1(x_i,t_{l+1})) \leq Ch_i^2, \quad i \in \{1,\cdots,N\}\backslash\{N/2\}.$$

□

Lemma 5.5.2. *The error due to the regular component $V(x,t_{l+1})$ of the solution $U(x,t_{l+1})$ to the semidiscretized problem* (5.3.1) *satisfies*

$$\left|L^K_\epsilon V(x,t_{l+1})_i - L^0_{N,K}V(x_i,t_{l+1})\right| \leq \begin{cases} C\hbar^2\left(\epsilon\left\|V^{(4)}(x_i,t_{l+1})\right\|_\infty + \left\|V^{(3)}(x_i,t_{l+1})\right\|_\infty\right), \\ 1 \leq i \leq \frac{N}{4},\ \frac{3N}{4}+1 \leq i \leq N-1, \\ Ch_i\left(\epsilon\left\|V^{(3)}(x_i,t_{l+1})\right\|_\infty + \left\|V^{(2)}(x_i,t_{l+1})\right\|_\infty\right), \\ \frac{N}{4}+1 \leq i \leq \frac{N}{2}-1, \\ Ch_{i+1}\left(\epsilon\left\|V^{(3)}(x_i,t_{l+1})\right\|_\infty + \left\|V^{(2)}(x_i,t_{l+1})\right\|_\infty\right), \\ \frac{N}{2}+1 \leq i \leq \frac{3N}{4}. \end{cases} \tag{5.5.7}$$

Proof. For $1 \leq i \leq \frac{N}{4}$ and $\frac{3N}{4}+1 \leq i \leq N-1$, it follows that

$$\begin{aligned} \left|L^0_{N,K}(V(x_i,t_{l+1})) - L^K_\epsilon V(x,t_{l+1}))_i\right| &= \left|\frac{a_i\Delta t}{4\hbar}\left[\left\|V^{(3)}(x_i,t_{l+1})\right\|_\infty \frac{(x_{i+1}-x_i)^3}{3} + \left\|V^{(3)}(x_i,t_{l+1})\right\|_\infty\right.\right. \\ &\quad \left.\times\frac{(x_i-x_{i-1})^3}{3}\right] + \frac{\epsilon\Delta t}{6\hbar^2}\left[\left\|V^{(4)}(x_i,t_{l+1})\right\|_\infty \frac{(x_{i+1}-x_i)^4}{3}\right. \\ &\quad \left.\left. + \left\|V^{(4)}(x_i,t_{l+1})\right\|_\infty \frac{(x_i-x_{i-1})^4}{3}\right]\right| \\ &\leq C\hbar^2\left(\epsilon\left\|V^{(4)}(x_i,t_{l+1})\right\|_\infty + \left\|V^{(3)}(x_i,t_{l+1})\right\|_\infty\right) \end{aligned}$$

and for $\frac{N}{4}+1 \le i \le \frac{N}{2}-1$

$$\begin{aligned}
\left|L^0_{N,K}(V(x_i,t_{l+1})) - L^K_\epsilon V(x_i,t_{l+1}))_i\right| &= \left|\frac{a_i\Delta t}{h_i}\int_{x_{i-1}}^{x_i} V^{(2)}(\xi,t_{l+1})(\xi-x_{i-1})d\xi - \frac{\epsilon\Delta t}{h_i+h_{i+1}}\right.\\
&\quad \times\left[\frac{1}{h_{i+1}}\int_{x_i}^{x_{i+1}} V^{(3)}(\xi,t_{l+1})(x_{i+1}-\xi)^2 d\xi\right.\\
&\quad \left.\left.-\frac{1}{h_i}\int_{x_{i-1}}^{x_i} V^{(3)}(\xi,t_{l+1})(\xi-x_{i-1})^2 d\xi\right]\right|\\
&= \left|\frac{a_i\Delta t}{h_i}\left\|V^{(2)}(x_i,t_{l+1})\right\|_\infty (x_i-x_{i-1})^2 - \frac{\epsilon\Delta t}{6(h_i+h_{i+1})}\right.\\
&\quad \times\left[\frac{1}{h_{i+1}}\left\|V^{(3)}(x_i,t_{l+1})\right\|_\infty \frac{(x_{i+1}-x_i)^3}{3}\right.\\
&\quad \left.\left.-\frac{1}{h_i}\left\|V^{(3)}(x_i,t_{l+1})\right\|_\infty \frac{(x_i-x_{i-1})^3}{3}\right]\right|\\
&\le Ch_i\left(\epsilon\left\|V^{(3)}(x_i,t_{l+1})\right\|_\infty + \left\|V^{(2)}(x_i,t_{l+1})\right\|_\infty\right).
\end{aligned}$$

Moreover, if $\frac{N}{2}+1 \le i \le \frac{3N}{4}$

$$\begin{aligned}
\left|L^0_{N,K}(V(x_i,t_{l+1})) - L^K_\epsilon V(x,t_{l+1}))_i\right| &= \left|\frac{a_i\Delta t}{h_{i+1}}\int_{x_i}^{x_{i+1}} V^{(2)}(\xi,t_{l+1})(\xi-x_i)d\xi - \frac{\epsilon\Delta t}{h_i+h_{i+1}}\right.\\
&\quad \times\left[\frac{1}{h_{i+1}}\int_{x_i}^{x_{i+1}} V^{(3)}(\xi,t_{l+1})(x_{i+1}-\xi)^2 d\xi\right.\\
&\quad \left.\left.-\frac{1}{h_i}\int_{x_{i-1}}^{x_i} V^{(3)}(\xi,t_{l+1})(\xi-x_{i-1})^2 d\xi\right]\right|\\
&= \left|\frac{a_i\Delta t}{h_{i+1}}\left\|V^{(2)}(x_i,t_{l+1})\right\|_\infty (x_i-x_{i-1})^2 d\xi - \frac{\epsilon\Delta t}{6(h_i+h_{i+1})}\right.\\
&\quad \times\left[\frac{1}{h_{i+1}}\left\|V^{(3)}(x_i,t_{l+1})\right\|_\infty \frac{(x_{i+1}-x_i)^3}{3}\right.\\
&\quad \left.\left.-\frac{1}{h_i}\left\|V^{(3)}(x_i,t_{l+1})\right\|_\infty \frac{(x_i-x_{i-1})^3}{3}\right]\right|.
\end{aligned}$$

Consequently, we have

$$\left|L^0_{N,K}(V(x_i,t_{l+1})) - L^K_\epsilon V(x,t_{l+1}))_i\right| \le Ch_{i+1}\left(\epsilon\left\|V^{(3)}(x_i,t_{l+1})\right\|_\infty + \left\|V^{(2)}(x_i,t_{l+1})\right\|_\infty\right)$$

and the required result follows. □

Lemma 5.5.3. *The error due to the singular component $W(x,t_{l+1})$ of the solution $U(x,t_{l+1})$ and its corrected approximation $W(x_i,t_{l+1})$ satisfies*

$$\left|L^1_{N,K}(W(x,t_{l+1})_i - W(x_i,t_{l+1}))\right| \le \begin{cases} CN^{-(\phi-1)}, & 1 \le i \le \frac{N}{4}-1,\ \frac{N}{2}+1 \le i \le \frac{3N}{4}-1,\\ CN^{-(\phi-2)}, & i = \frac{N}{4}, \frac{3N}{4},\\ CN^{-1}\epsilon^{-1}, & \frac{N}{4}+1 \le i \le \frac{N}{2}-1,\ \frac{3N}{4}+1 \le i \le N-1. \end{cases} \tag{5.5.8}$$

Proof. For $1 \le i \le \frac{N}{4}$, we may write

$$\begin{aligned}\left|L^1_{N,K}(W(x,t_{l+1}) - W_L(x_i,t_{l+1}))\right| &= \left|L^1_{N,K}(W(x,t_{l+1}) - W^1_L(x_i,t_{l+1}))\right| + \left|L^1_{N,K}(W^1_L(x_i,t_{l+1})\right. \\ &\quad \left. - W_L(x_i,t_{l+1}))\right|.\end{aligned}$$

Consider the first addend and the result for the second addend will follow analogously. For $1 \le i < \frac{N}{4}$

$$\begin{aligned}\left|L^1_{N,K}(W(x,t_{l+1}) - W^1_L(x_i,t_{l+1}))\right| &= \left|L^1_{N,K}(W(x,t_{l+1}))\right| \\ &\le R_{i+1,l+1}\left|\frac{4\epsilon\Delta t}{h_i^2} - \frac{4\alpha\Delta t}{h_i}\right| \\ &\le CNR_{i+1,l+1} \\ &\le CN^{-(\phi-1)}. \end{aligned} \tag{5.5.9}$$

For $i = \frac{N}{4}$

$$\begin{aligned}\left|L^1_{N,K}(W(x,t_{l+1}) - W^1_L(x_i,t_{l+1}))\right| &\le R_{\frac{N}{4}+1}\left|\frac{4\epsilon\Delta t}{h_i^2} - \frac{4\alpha\Delta t}{h_i^2}\right| \\ &\le CN^{-(\phi-2)}. \end{aligned} \tag{5.5.10}$$

Similarly, for $1 \le i < \frac{N}{4}$

$$\begin{aligned}\left|L^1_{N,K}(W^1_L(x_i,t_{l+1}) - W_L(x_i,t_{l+1}))\right| &= \left|L^1_{N,K}W_L(x_i,t_{l+1})\right| = \left|L^0_{N,K}W_L(x_i,t_{l+1})\right| \\ &\le R_{i+1,l+1}\left|\frac{4\epsilon\Delta t}{h_i^2} - \frac{2\alpha\Delta t}{h_i}\right| \\ &\le CN^{-(\phi-1)}. \end{aligned} \tag{5.5.11}$$

For $i = \frac{N}{4}$

$$\left|L^1_{N,K}(W^1_L(x_i,t_{l+1}) - W_L(x_i,t_{l+1}))\right| = \left|L^0_{N,K}W_L(x_i,t_{l+1})\right| = 0. \tag{5.5.12}$$

Hence

$$\left|L^1_{N,K}(W(x,t_{l+1}) - W_L(x_i,t_{l+1}))\right| \le \begin{cases} CN^{-(\phi-1)}, & 1 \le i \le \frac{N}{4}, \\ CN^{-(\phi-2)}, & i = \frac{N}{4}. \end{cases} \tag{5.5.13}$$

Also, for $\frac{N}{4}+1 \le i < \frac{N}{2}$

$$\begin{aligned}\left|L^1_{N,K}(W(x,t_{l+1})-W_L(x_i,t_{l+1}))\right| &= \epsilon\Delta t\left[\frac{1}{h_i+h_{i+1}}\left(\frac{1}{h_{i+1}}\int_{x_i}^{x_{i+1}} W^{(3)}(\xi)(x_{i+1}-\xi)^2 d\xi\right.\right.\\ &\quad \left.\left.-\frac{1}{h_i}\int_{x_{i-1}}^{x_i} W^{(3)}(\xi)(\xi-x_{i-1})d\xi\right)\right] + a_i\Delta t\left[\frac{-1}{h_i}\right.\\ &\quad \left.\times\int_{x_{i-1}}^{x_i} W^{(2)}(\xi)(\xi-x_{i-1})d\xi\right]\\ &\le \frac{C\epsilon^{-1}}{2\alpha}\exp\left(\frac{-\alpha c}{\epsilon}\right)\exp\left(\frac{\alpha x_i}{\epsilon}\right)\left(\exp\left(\frac{\alpha h_{i+1}}{2\epsilon}\right)\right.\\ &\quad \left.\sinh\left(\frac{\alpha h_{i+1}}{2\epsilon}\right)+\exp\left(\frac{\alpha h_i}{2\epsilon}\right)\sinh\left(\frac{\alpha h_i}{2\epsilon}\right)\right)\\ &\le C\epsilon^{-1}N^{-1}. \end{aligned} \tag{5.5.14}$$

Moreover, for $\frac{N}{2}+1 \le i \le \frac{3N}{4}$, we obtain

$$\left|L^1_{N,K}(W(x,t_{l+1})-W_R(x_i,t_{l+1}))\right| \le \begin{cases} CN^{-(\phi-1)}, & \frac{N}{2}+1 \le i \le \frac{3N}{4}-1,\\ CN^{-(\phi-2)}, & i=\frac{3N}{4}, \end{cases} \tag{5.5.15}$$

and for $\frac{3N}{4}+1 \le i \le N-1$

$$\begin{aligned}\left|L^1_{N,K}(W(x,t_{l+1})-W_L(x_i,t_{l+1}))\right| &= \epsilon\Delta t\left[\frac{1}{h_i+h_{i+1}}\left(\frac{1}{h_{i+1}}\int_{x_i}^{x_{i+1}} W^{(3)}(\xi)(x_{i+1}-\xi)^2 d\xi\right.\right.\\ &\quad \left.\left.-\frac{1}{h_i}\int_{x_{i-1}}^{x_i} W^{(3)}(\xi)(\xi-x_{i-1})d\xi\right)\right] + a_i\Delta t\left[\frac{-1}{h_{i+1}}\right.\\ &\quad \left.\times\int_{x_i}^{x_{i+1}} W^{(2)}(\xi)(\xi-x_i)d\xi\right] \le C\epsilon^{-1}N^{-1}. \end{aligned} \tag{5.5.16}$$

The required result now follows from (5.4.14). □

Lemma 5.5.4. *For $i = \frac{N}{2}$, the solution $U(x,t_{l+1})$ to (5.3.1) and its approximation $U(x_i,t_{l+1})$ satisfies*

$$|(D_+ - D_-)(U(x_i,t_{l+1})-U(x,t_{l+1}))| \le \frac{Ch_i}{\epsilon^2}.$$

Proof. Consider

$$\begin{aligned}|(D_+ - D_-)(U(x_i,t_{l+1})-U(x,t_{l+1}))| &= |(D_+ - D_-)(U(x,t_{l+1}))|\\ &\le C\hbar \max_{x\in(0,1)\cup(1,2)}\left|\frac{d^2U(x,t_{l+1})}{dx^2}\right|\\ &\le \frac{C\hbar}{\epsilon^2}. \end{aligned}$$

□

Lemma 5.5.5. *The solution $U(x, t_{l+1})$ and its corrected approximation $U(x_i, t_{l+1})$ over Γ_N satisfies*

$$\|U(x, t_{l+1}) - U(x_i, t_{l+1})\|_\infty \leq CN^{-2},\ i \in \{0, 1, \cdots, N\} \setminus \{N/2\}. \tag{5.5.17}$$

Proof. The result follows from Lemma 5.5.1, Lemma 5.5.2, Lemma 5.5.3, and (5.4.24). □

We are now able to state the main result of this section, the principle convergence theorem. The proof of which follows immediately from Lemma 5.4.1, Lemma 5.5.4, and Lemma 5.5.6.

Lemma 5.5.6. *Let u be the solution of* (5.2.1) *and $U(x_i, t_{l+1})$ be its corrected approximation on $\Gamma_t^K \times \Gamma_N$. Then*

$$|u(x_i, t_{l+1}) - U(x_i, t_{l+1})| \leq C\left(\Delta t + N^{-2}\right). \tag{5.5.18}$$

5.6 Numerical Results

In this section, we examine the performance of the proposed method and numerically verify the theoretical estimates. We consider three test problems for numerical computations.

Example 5.6.1. *Consider the following singularly perturbed parabolic problem*

$$\begin{aligned}
&\epsilon u_{xx} + a(x)u_x - u - u_t = g(x,t),\ (x,t) \in (0,1) \times (0,1],\\
&u(x,0) = 0,\ x \in [0,1],\\
&u(0,t) = 0,\ u(1,t) = 0,\ t \in [0,1],
\end{aligned}$$

where

$$a(x) = \begin{cases} -1, & 0 \leq x \leq 0.5, \\ 1, & 0.5 < x \leq 1, \end{cases} \quad \textit{and} \quad g(x,t) = \begin{cases} 2(1+x^2)t^2, & 0 \leq x \leq 0.5, \\ 3(1+x^2)t^2, & 0.5 < x \leq 1. \end{cases}$$

Example 5.6.2. *Consider the following singularly perturbed parabolic problem*

$$\begin{aligned}
&\epsilon u_{xx} + a(x)u_x - 5u_t = g(x,t),\ (x,t) \in (0,1) \times (0,1],\\
&u(x,0) = 0,\ x \in [0,1],\\
&u(0,t) = 0,\ u(1,t) = 0,\ t \in [0,1],
\end{aligned}$$

where

$$a(x) = \begin{cases} -2, & 0 \leq x \leq 0.5, \\ 3, & 0.5 < x \leq 1, \end{cases} \quad \textit{and} \quad g(x,t) = \begin{cases} 2x\exp(-t)t^2 & 0 \leq x \leq 0.5, \\ 2(1-x)\exp(-t)t^2, & 0.5 < x \leq 1. \end{cases}$$

Example 5.6.3. *Consider the following singularly perturbed parabolic problem [192]*

$$\begin{aligned}
&\epsilon u_{xx} + a(x)u_x - u_t = g(x,t),\ (x,t) \in (0,1)\times(0,1],\\
&u(x,0) = 0,\ x \in [0,1],\\
&u(0,t) = t^2,\ u(1,t) = 0,\ t \in [0,1],
\end{aligned}$$

where

$$a(x) = \begin{cases} -1, & 0 \le x \le 0.5,\\ 1, & 0.5 < x \le 1, \end{cases} \quad \textit{and} \quad g(x,t) = \begin{cases} 2xt & 0 \le x \le 0.5,\\ 2(1-x)t, & 0.5 < x \le 1. \end{cases}$$

Table 5.1: Maximum absolute error ($\hat{E}_{N,K}$) and order of convergence ($\hat{P}_{N,K}$) for Example 5.6.1 when $K = N$.

ϵ	N= 32	64	128	256	512
10^{-2}	1.20142e-02	3.70899e-03	1.14397e-03	3.53190e-04	1.10280e-04
	1.695	1.696	1.695	1.679	1.682
10^{-4}	1.55921e-02	4.80274e-03	1.50387e-03	4.72108e-04	1.46902e-04
	1.698	1.675	1.671	1.684	1.671
10^{-6}	1.561105e-02	4.81489e-03	1.50662e-03	4.75420e-04	1.47612e-04
	1.697	1.676	1.664	1.684	1.672
10^{-8}	1.56231e-02	4.81501e-03	1.50679e-03	4.78193e-04	1.47822e-04
	1.698	1.675	1.655	1.693	1.671
10^{-10}	1.56240e-02	4.81502e-03	1.50680e-03	4.79220e-04	1.48155e-04
	1.698	1.676	1.652	1.693	1.673

Table 5.2: Maximum absolute error ($\hat{E}_{N,K}$) and order of convergence ($\hat{P}_{N,K}$) for Example 5.6.1 when $K = N^2$.

	$\epsilon = 2\times10^{-2}$		$\epsilon = 2\times10^{-5}$	
N	$E_{N,K}$	$P_{N,K}$	$E_{N,K}$	$P_{N,K}$
32	1.37311e-02	1.871	1.69840e-02	1.878
64	3.75390e-03	1.913	4.61863e-03	1.912
128	9.96179e-04	1.884	1.22692e-03	1.895
256	2.69749e-04	1.903	3.29738e-04	1.904
512	7.21204e-05	1.896	8.81049e-05	1.889

Table 5.3: Maximum absolute error ($\hat{E}_{N,K}$) and order of convergence ($\hat{P}_{N,K}$) for Example 5.6.2 when $K = N$.

ϵ	N= 32	64	128	256	512
10^{-2}	1.01220e-04	2.88103e-05	8.51976e-06	2.52150e-06	7.62419e-07
	1.812	1.757	1.756	1.725	1.745
10^{-4}	1.21177e-04	3.57103e-05	1.10398e-05	3.22857e-06	9.72216e-07
	1.762	1.693	1.773	1.731	1.710
10^{-6}	1.21388e-04	3.57840e-05	1.11228e-05	3.31829e-06	9.72831e-07
	1.762	1.685	1.745	1.770	1.725
10^{-8}	1.21390e-04	3.57847e-05	1.11235e-05	3.37215e-06	9.731693e-07
	1.762	1.685	1.721	1.792	1.724
10^{-10}	1.21390e-04	3.57847e-05	1.11236e-05	3.37216e-06	9.73351e-07
	1.762	1.685	1.721	1.792	1.724

Table 5.4: Maximum absolute error ($\hat{E}_{N,K}$) and order of convergence ($\hat{P}_{N,K}$) for Example 5.6.2 when $K = N^2$.

	$\epsilon = 2 \times 10^{-3}$		$\epsilon = 2 \times 10^{-5}$	
N	$E_{N,K}$	$P_{N,K}$	$E_{N,K}$	$P_{N,K}$
32	1.78479e-04	1.945	1.81191e-04	1.938
64	4.63295e-05	2.025	4.72589e-05	1.997
128	1.13821e-05	1.974	1.18351e-05	1.991
256	2.89721e-06	2.086	2.97721e-06	2.090
512	6.82193e-07	2.010	6.99263e-07	1.998

Test examples are solved using an implicit Euler scheme over a uniform mesh in time and a defect correction scheme over a Bakhvalov Shishkin mesh in space. The maximum absolute error and order of convergence are calculated and tabulated in tables. For Examples 5.6.1, 5.6.2 and 5.6.3 the maximum absolute error and order of convergence are tabulated in Tables 5.1, 5.3 and 5.6 for $N = K$. Tables 5.2 and 5.4 present the maximum absolute error and order of convergence for $N = K^2$ and justify the spatial order of convergence. Table 5.7 compares the results obtained using the proposed defect correction method over Bakhvalov-Shishkin mesh in space and an implicit Euler method in time with the hybrid method over shishkin mesh in space and backward euler scheme in time [192]. Besides, Table 5.5 presents a comparison of maximum absolute error obtained using the defect correction scheme over a variety of adaptive meshes developed in the

Table 5.5: Comparison of maximum absolute error ($\hat{E}_{N,K}$) and order of convergence ($\hat{P}_{N,K}$) for Example 5.6.2 when $K = N$ using proposed method on various layer adapted meshes.

	ϵ	N= 32	64	128	256
Vulanovic-Improved	10^{-2}	6.35976e-03	2.55314e-03	1.14821e-03	4.93341e-04
Shishkin mesh [166]		1.316	1.152	1.218	1.231
	10^{-6}	6.37231e-03	2.58429e-03	1.15724e-03	4.96327e-04
		1.302	1.159	1.221	1.229
Shishkin	10^{-2}	1.24896e-04	4.96582e-05	2.14383e-05	9.13216e-06
mesh [158]		1.330	1.211	1.231	1.250
	10^{-6}	1.30943e-04	4.99312e-05	2.16539e-05	9.13583e-06
		1.390	1.205	1.246	1.256
Bakhvalov-Shishkin	10^{-2}	1.01220e-04	2.88103e-05	8.51976e-06	2.52150e-06
mesh		1.812	1.757	1.756	1.725
	10^{-6}	1.21388e-04	3.57840e-05	1.11228e-05	3.31829e-06
		1.762	1.685	1.745	1.770

literature. Numerical solutions are plotted in Figures 5.1 and 5.3 for Examples 5.6.1 and 5.6.2, respectively. Numerical solutions at fixed time levels are plotted in Figures 5.2 and 5.4. Aditionally, log-log plots for errors are shown in Figures 5.5 and 5.6 for Examples 5.6.1 and 5.6.2, respectively.

5.7 Conclusion

A higher-order defect correction method was proposed to solve singularly perturbed parabolic differential equations with discontinuous coefficients over a Bakhvalov Shishkin mesh. The method combines the stability of the lower-order scheme with the convergence of the higher-order less stable scheme and results in a higher-order stable scheme. The method yields highly accurate results for singular perturbation problems avoiding prevalent numerical oscillation in the numerical approximation and is independent of perturbation parameters. We have shown theoretically that the proposed method is first-order convergent in time and second-order convergent in space. Moreover, numerical illustrations are presented for two test examples that demonstrate the efficiency of the scheme. Convergence obtained numerically agrees with theoretical predictions.

Table 5.6: Maximum absolute error ($\hat{E}_{N,K}$) and order of convergence ($\hat{P}_{N,K}$) for Example 5.6.3 when $K = N$.

ϵ	N= 32	64	128	256
10^{-2}	3.06504e-03	1.02247e-03	3.36363e-04	1.10253e-04
	1.583	1.603	1.609	1.673
10^{-4}	3.59544e-03	1.16685e-03	3.70748e-04	1.18631e-04
	1.623	1.654	1.643	1.652
10^{-6}	3.60099e-03	1.19035e-03	3.81538e-04	1.20173e-04
	1.597	1.641	1.666	1.631
10^{-8}	3.60104e-03	1.19083e-03	3.83561e-04	1.20825e-04
	1.596	1.634	1.666	1.658
10^{-10}	3.60105e-03	1.19102e-03	3.84925e-04	1.21152e-04
	1.596	1.629	1.667	1.642

Table 5.7: Comparison of maximum absolute error ($\hat{E}_{N,K}$) and order of convergence ($\hat{P}_{N,K}$), for example 5.6.3, using the proposed method and results in [192].

	Results in [192]		Proposed method	
N	$\epsilon = 10^{-5}$	$\epsilon = 10^{-10}$	$\epsilon = 10^{-5}$	$\epsilon = 10^{-10}$
32	9.9736e-03	9.9737e-03	3.6004e-03	3.6010e-03
	1.279	1.279	1.605	1.596
64	4.1094e-03	4.1095e-03	1.1832e-03	1.1910e-03
	1.220	1.220	1.664	1.629
128	1.7641e-03	1.7641e-03	3.7836e-04	3.8492e-04
	1.094	1.095	1.659	1.667
256	8.2587e-04	8.2580e-04	1.1973e-04	1.20176e-04
	1.057	1.057	1.642	1.641

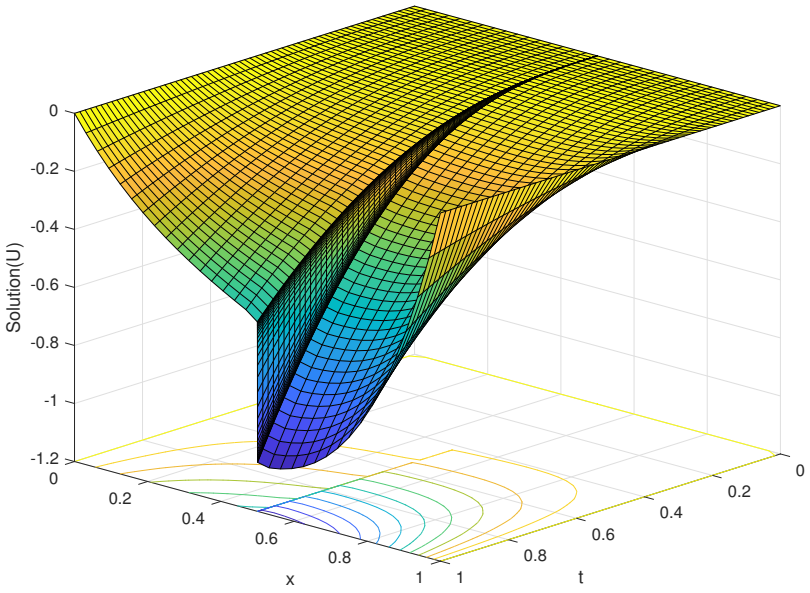

Figure 5.1: Numerical solution to Example 5.6.1 with $K = N = 64$ and $\epsilon = 2 \times 10^{-10}$.

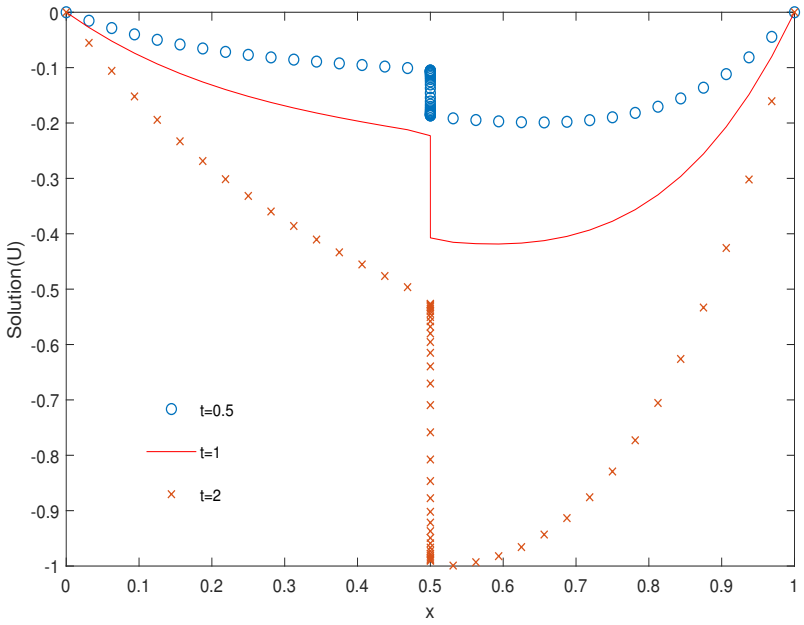

Figure 5.2: Numerical solution to Example 5.6.1 for different t when $K = N = 64$ and $\epsilon = 2 \times 10^{-10}$.

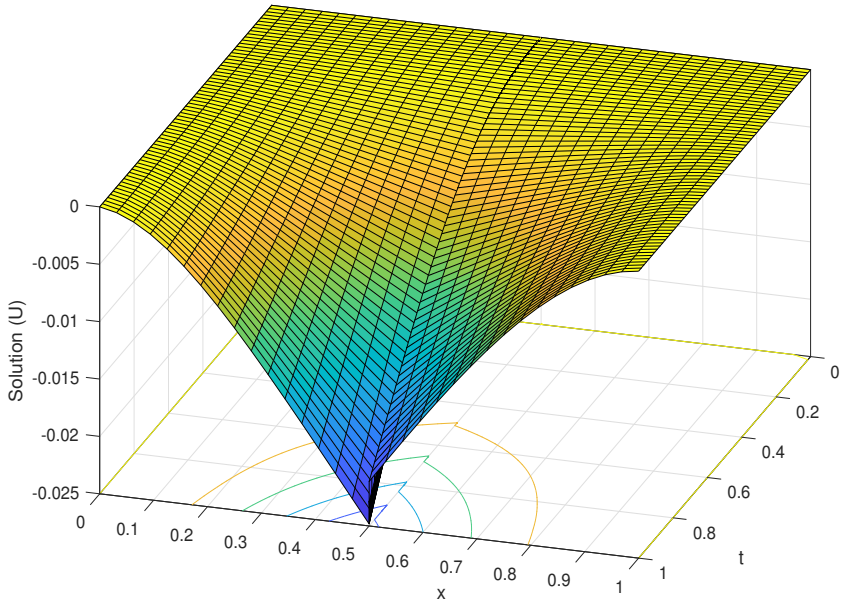

Figure 5.3: Numerical solution to Example 5.6.2 with $K = N = 64$ and $\epsilon = 2 \times 10^{-7}$.

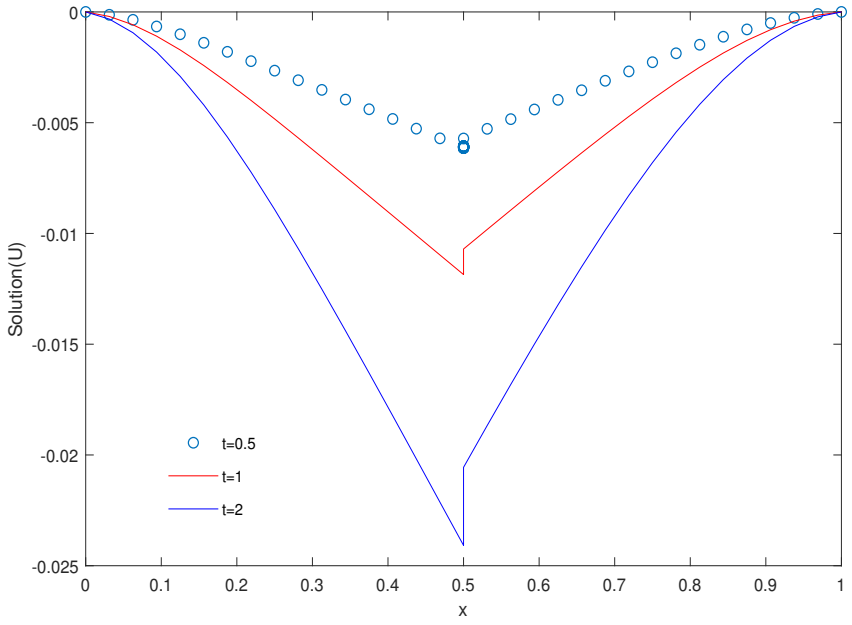

Figure 5.4: Numerical solution to Example 5.6.2 for different t when $K = N = 64$ and $\epsilon = 2 \times 10^{-7}$.

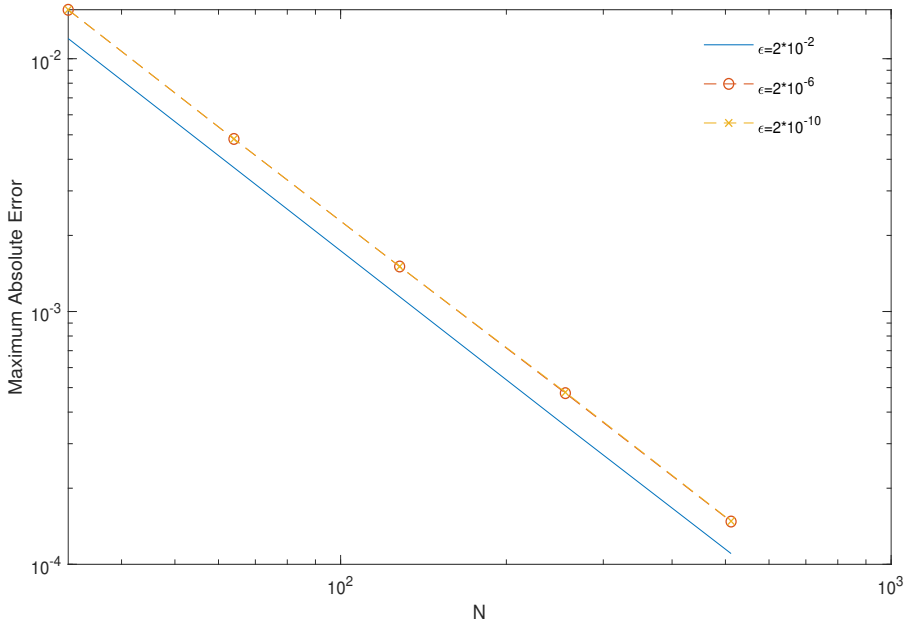

Figure 5.5: Error plot for Example 5.6.1 for different values of ϵ.

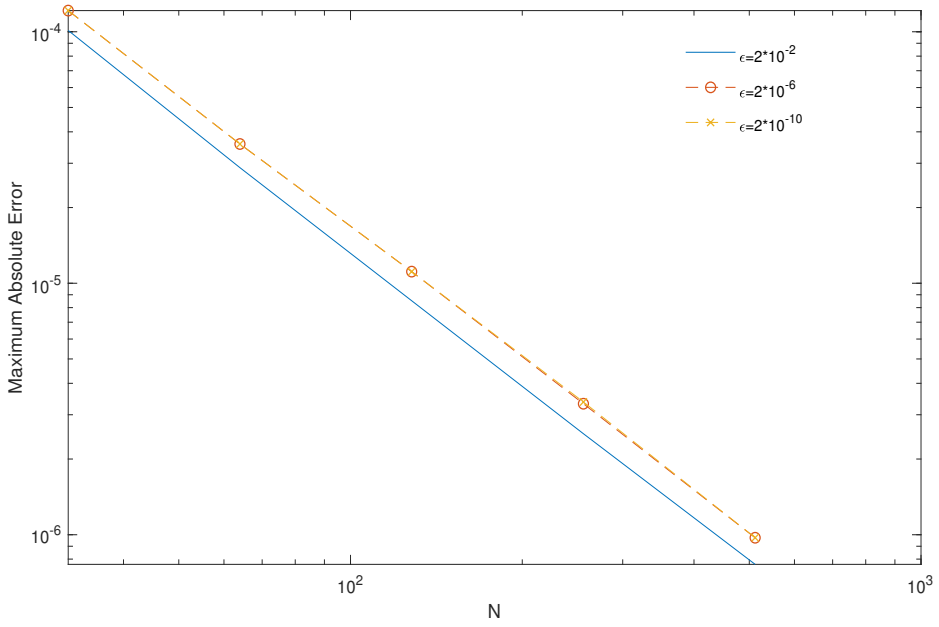

Figure 5.6: Error plot for Example 5.6.2 for different values of ϵ.

Chapter 6

Conclusions and Future Scope

6.1 Summary

This chapter summarises the thesis's primary accomplishments and outlines potential future research directions with possible extensions of the current work. As simple upwinding yields only low accuracy, it is natural to look for higher-order alternatives. This thesis contributes to developing higher-order numerical methods for analysing singularly perturbed convection-diffusion boundary value problems. The numerical method combines a high-order defect correction method based on finite difference approximations with the adaptive mesh refinement strategy to capture the layer behaviour of the solution. The following are some of the thesis's major contributions and important results.

Chapter 2 presents and analyses a higher-order defect correction method to solve a class of singularly perturbed convection-diffusion boundary value problems. The numerical method involves the combination of a first-order upwind difference scheme with the classical central difference method over a non-uniform polynomial Shishkin mesh. The mesh is generated using a mesh-generating function in the layer part and divided uniformly elsewhere. The theoretical and numerical analysis for the proposed method confirms the parameter uniform convergence of order two. The results obtained using the proposed method over the polynomial-Shishkin mesh are superior to other adaptive meshes in the literature and spline collocation methods. Thus, the numerical experience with standard finite difference methods on layer-adapted meshes reveals that the proposed method yields uniformly stable, inverse monotone and highly convergent approximations.

Chapter 3 solves a class of singularly perturbed convection–diffusion problems with discontinuous coefficient and point source. A defect correction scheme consisting of an upwind difference scheme and central difference scheme at all mesh points is proposed to solve the problem. A non-uniform Bakhvalov-Shishkin mesh is considered to discretize

the domain. A robust a posteriori error estimate in the maximum norm is derived. It provides computable and guaranteed upper bounds for the discretisation error. The error estimates of the proposed numerical method satisfy parameter uniform second-order convergence. Numerical experiments complement our theoretical results.

Chapter 4 presents a higher-order numerical method to solve a class of singularly perturbed parabolic convection-diffusion problems with a large shift. The numerical method involves a defect correction scheme on a layer-adapted Shishkin mesh in space and a backward Euler method in time on a uniform mesh. The proposed numerical method is analysed for consistency, stability and convergence. Extensive theoretical analysis is performed to obtain consistency and error estimates. The error estimates of the proposed numerical method satisfy parameter uniform second-order convergence in space and first-order convergence in time. The rigorous numerical analysis of the proposed method on a Shishkin class mesh establishes the supremacy of the proposed scheme.

Chapter 5 proposes a higher-order numerical scheme to solve a class of singularly perturbed parabolic convection-diffusion problems with discontinuous convection coefficient and source. A defect correction scheme is used on a Bakhvalov-Shishkin mesh in space, while a backwards-Euler scheme is used on a uniform mesh in the time variable. The proposed method is unconditionally stable and converges uniformly, independent of the perturbation parameter. The error analysis indicates that the numerical solution is parameter-uniform second-order convergence in space and first-order convergence in time. The comparison of the results of the proposed method on a priori chosen Shishkin mesh, Vulanovic-Improved Shishkin mesh, and the Bakhvalov-Shishkin mesh corroborates the optimal accuracy of the proposed scheme.

6.2 Future Scope

The thesis is primarily concerned with the development and use of extremely accurate adaptive numerical methods for a wide range of singularly perturbed convection-diffusion problems. The use of the defect correction schemes to layer-adapted meshes results in higher-order convergence. In this section, we describe some of the interesting problems to which the thesis's approach/idea can be extended. It might be interesting to think about the following problems for future work.

- Using the defect correction scheme, we can possibly extend the analysis to find the solution of the following coupled system of singularly perturbed parabolic

convection-diffusion problems

$$\left.\begin{aligned} &L\overrightarrow{u}(x,t) = -\mathcal{E}\frac{\partial^2\overrightarrow{u}}{\partial x^2} + \mathcal{A}(x,t)\frac{\partial\overrightarrow{u}}{\partial x} + \frac{\partial\overrightarrow{u}}{\partial t} + \mathcal{B}(x,t) = \overrightarrow{g}(x,t),\ (x,t) \in S = (0,1)\times(0,T),\\ &\overrightarrow{u}(x,0) = \overrightarrow{u}_0(x),\ x \in [0,1],\\ &\overrightarrow{u}(0,t) = 0,\ t \in [0,T],\\ &\overrightarrow{u}(1,t) = 0,\ t \in [0,T]. \end{aligned}\right\}$$

Here $T > 0$, $\mathcal{E} = diag(\epsilon_1, \epsilon_2)$ is a diagonal matrix with small perturbation parameters $0 < \epsilon_1, \epsilon_2 << 1$, $\mathcal{A} = diag(a_1(x), a_2(x))$, $\mathcal{B} = \begin{bmatrix} b_{11} & b_{12} \\ b_{21} & b_{22} \end{bmatrix}$, $\overrightarrow{u} = (u_1, u_2)^T$ and $\overrightarrow{g} = (g_1, g_2)^T$. These types of problems can be traced in modelling various physical phenomenon, particularly in the field of electro analytical chemistry, predator prey population dynamics, modeling of optimal control situations and resistance-capacitor electrical circuits.

- It will be interesting to extend the analysis of the defect-correction method for 2D problems. Consider the following class of 2D time dependent singularly perturbed convection-diffusion problems with turning points

$$\left.\begin{aligned} &Lu = \tfrac{\partial u}{\partial t} + (L_1(t) + L_2(t))u = g,\ (x,z,t) \in D\times(0,T],\\ &u(x,z,0) = f(x,z),\ (x,z) \in D,\\ &u(x,z,t) = 0,\ (x,z,t) \in \partial D\times[0,T], \end{aligned}\right\}$$

where $D = (0,1)^2$ and the operators L_i, $i = 1,2$ and defined by

$$\begin{aligned} L_1(t) &= -\epsilon\tfrac{\partial^2}{\partial x^2} + \hat{a}_1(x,z,t)\tfrac{\partial}{\partial x} + k_1(x,z,t),\\ L_2(t) &= -\epsilon\tfrac{\partial^2}{\partial x^2} + \hat{a}_2(x,z,t)\tfrac{\partial}{\partial x} + k_2(x,z,t). \end{aligned}$$

Here $0 < \epsilon << 1$ is perturbation parameter, reaction term $k_i(x,z,t) \geq 0$ for $i = 1,2$ convection coefficients and given by

$$\begin{aligned} \hat{a}_1(x,z,t) &= -(x - \tfrac{1}{2})a_1(x,z,t),\\ \hat{a}_2(x,z,t) &= -(z - \tfrac{1}{2})a_2(x,z,t), \end{aligned}$$

with a_1 and a_2 such that $a_1(x,z,t) \geq \alpha_i > 0$ for $i = 1,2$ both components of the convective terms has a simple turning point which is located at $x = \frac{1}{2}$ for the first component and at $z = \frac{1}{2}$ for the second one. Such type of problems appears in many fields of applied mathematics and enginnering including hydrodynamic dispersion process, pollution control, soil physics, bio-physics, petroleum engineering and chemical engineering.

- The proposed method can be extended to solve the time-dependent singularly perturbed problem involving a fractional-time derivative with initial–boundary conditions on a rectangular domain $S = (0,1) \times (0,T]$

$$\left.\begin{aligned} &Lu = \mathcal{D}_t^{\alpha} + L_x u = g(x,t),\ (x,t) \in S, \\ &u(x,t) = K_b,\ (x,t) \in \Gamma_b = [0,1] \times \{0\}, \\ &u(x,t) = K_l(t),\ (x,t) \in \Gamma_l = \{(x,t) : x = 0, 0 \le t \le T\}, \\ &u(x,t) = K_r(t),\ (x,t) \in \Gamma_r = \{(x,t) : x = 1, 0 \le t \le T\}. \end{aligned}\right\}$$

  Here $L_x u = -\epsilon u_{xx} + a(x,t)u_x + b(x,t)u(x,t)$, $0 < \epsilon << 1$ is small perturbation parameter and $\bar{S} = S \cup \Gamma$. The operator $\mathcal{D}_t^{\alpha}$ is the Caputo fractional derivative of order $\alpha \in (0,1)$. The coefficients $a(x,t)$ and $b(x,t)$ are assumed to sufficiently smooth. These type of problems model various physical phenomena such as complex systems, including electric conductance of biological systems, glassy and disordered media, anomalous diffusion transport, signal processing, fluid flow in porous materials, acoustic wave propagation in viscoelastic materials, and signal processing.

References

[1] Abbasbandy, S., 2006, "Iterated He's homotopy perturbation method for a quadratic Riccati differential equation," *Appl. Math. Comput.* **175**, 581–589.

[2] Abdallah, N., and Pinaud, O., 2006, "Multiscale simulation of transport in an open quantum system: Resonances and WKB interpolation," *J. Comp. Phys.* **213**, 288–310.

[3] Abrahamsson, L., Keller, H., and Kreiss, H., 1974, "Difference approximations for singular perturbations of systems of ordinary differential equations," *Numer. Math.* **22**, 367–391.

[4] Akulenko, L., 2002, "Higher-order averaging schemes in systems with fast and slow phases," *J. Appl. Math. Mech.* **66**, 153–163.

[5] Allen, D. N. G., and Southwell, R. V., 1955, "Relaxation methods applied to determine the motion, in two dimensions, of a viscous fluid past a fixed cylinder," *Quart. J. Mech. Appl. Math.* **8**, 129–145.

[6] Amore, P., and Aranda, A., 2005, "Improved Lindstedt–Poincaré method for the solution of nonlinear problems," *J. Sound Vib.* **283**, 1115–1136.

[7] Andreev, V. B., 2002, "A priori solution estimates of singularly perturbed TWO-point boundary problems," *Matem. Mod.* **14**, 5–16.

[8] Ansari, A. R., Bakr, S. A., and Shishkin, G. I., 2007, "A parameter-robust finite difference method for singularly perturbed delay parabolic partial differential equations," *J. Comput. Appl. Math.* **205**, 552–566.

[9] Ansari, A., and Hegarty, A., 2003, "Numerical solution of a convection diffusion problem with robin boundary conditions," *J. Comput. Appl. Math.* **156**, 221–238.

[10] Arakeri, J. H., and Shankar, P. N., 2000, "Ludwig Prandtl and boundary layers in fluid flow - How a small viscosity can cause large effects," *Resonance – Journal of Science Education* **5**, 48–63.

[11] Assiff, T. C., and Yen, D. H. Y., 1987, "On the solutions of clamped Reissner-Mindlin plates under transverse loads," *Q. Appl. Math.* **45**, 679–690.

[12] Awrejcewicz, J., Andrianov, I. V., and Manevitch, L. I., 2012, *Asymptotic approaches in nonlinear dynamics: New trends and applications* (Springer Science & Business Media).

[13] Axelsson, O., and Gustafsson, I., 1979, "A modified upwind scheme for convective transport equations and the use of a conjugate gradient method for the solution non-symmetric systems of equations," *IMA J. Appl. Math.* **23**, 321–337.

[14] Axelsson, O., and Layton, W., 1990, "Defect correction methods for convection-dominated convection-diffusion problems," *RAIRO Modél. Math. Anal. Numér.* **4**, 423–455.

[15] Aziz, A., 2014, *The mathematical foundations of the finite element method with applications to partial differential equations* (Academic Press).

[16] Babu, A. R., and Ramanujam, N., 2013, "A FEM for a system of singularly perturbed reaction-diffusion equations with discontinuous source term," *Int. J. Comput. Methods* **10**, 1350057.

[17] Bakhvalov, N. S., 1969, "On the optimization of methods for solving boundary value problems with boundary layers," *Zh. Vychisl. Mat. Mat. Fis.* **9**, 841–859.

[18] Bakhvalov, N., 1969, "The optimization of methods of solving boundary value problems with a boundary layer," *USSR Comput. Math. & Math. Phys.* **9**, 139–166.

[19] Barbu, L., and Moroşanu, G., 2007, *Singularly Perturbed Boundary Value Problems* (Birkhäusar, Basel).

[20] Barrett, J. W., and Morton, K. W., 1980, "Optimal finite element solutions to diffusion-convection problems in one dimension," *Int. J. Numer. Methods Eng.* **15**, 1457–1474.

[21] Barrett, J. W., and Morton, K. W., 1981, "Optimal finite element approximation for diffusion-convection problems," in *Conference on Mathematics of Finite Elements and Their Applications.*

[22] Barrett, J. W., and Morton, K. W., 1981, "Optimal Petrov-Galerkin methods through approximate symmetrization," *IMA J. Numer. Anal.* **1**, 439–468.

[23] Barrett, J. W., and Morton, K. W., 1984, "Approximate symmetrization and petrov-galerkin methods for diffusion-convection problems," *Comput. Methods Appl. Mech. Eng.* **45**, 97–122.

[24] Barrett, K. E., 1974, "The numerical solution of singular-perturbation boundary-value problems," *Quart. J. Mech. Appl. Math.* **27**, 57–68.

[25] Bawa, R. K., 2005, "Spline based computational technique for linear singularly perturbed boundary value problems," *Appl. Math. Comput.* **167**, 225–236.

[26] Beckett, G., and Mackenzie, J. A., 2000, "Convergence analysis of finite difference approximations on equidistributed grids to a singularly perturbed boundary value problem," *Appl. Numer. Math.* **35**, 87–109.

[27] Beckett, M. G., and Mackenzie, J. A., 2001, "On a uniformly accurate finite difference approximation of a singularly perturbed reaction diffusion problem using grid equidistribution," *J. Comput. Appl. Math.* **131**, 381–405.

[28] Belhaq, M., and Lakrad, F., 2000, "Elliptic multiple scales method for a class of autonomous strongly non-linear oscillators," *J. Sound Vib.* **234**, 547–553.

[29] Bellen, A., and Zennaro, M., 2003, *Numerical methods for delay differential equations* (Clarendon Press, Oxford).

[30] Benbachir, S., 2000, "Lindstedt–Poincaré method and periodic families of the Barbanis-Contopoulos Hamiltonian system," *Math. Comput. Simul.* **51**, 579–596.

[31] Bender, C. M., and Orszag, S. A., 1978, *Advanced Mathematical Methods for Scientists and Engineers* (McGraw-Hill, New York).

[32] Berger, A. E., Solomon, J. M., and Ciment, M., 1981, "An analysis of a uniformly accurate difference method for a singular perturbation problem," *Math. Comp.* **37**, 79–94.

[33] Black, F., and Scholes, M., 1973, "The Pricing of Options and Corporate Liabilities," *J. Polit. Econ.* **81**, 637–654.

[34] Boah, D., and Twum, S., 2020, "A review of water quality optimisation models and techniques," *J. appl. math. phys.* **8**, 424–433.

[35] Boffi, D., Brezzi, F., and Fortin, M., 2013, *Mixed finite element methods and applications* (Springer).

[36] Boglaev, I., 2004, "Uniform numerical methods on arbitrary meshes for singularly perturbed problems with discontinuous data," *Appl. Math. Comput.* **154**, 815–833.

[37] Borowitz, S., 1967, *Fundamentals of Quantum Mechanics, Particles, Waves, and Wwave Mechanics* (Benjamin).

[38] Brdar, M., and Zarin, H., 2016, "On graded meshes for a two parameter singularly perturbed problem," *Appl. Math. Comput.* **282**, 97–107.

[39] Brdar, M., and Zarin, H., 2016, "A singularly perturbed problem with two parameters on a Bakhvalov type mesh," *J. Comput. Appl. Math.* **292**, 307–319.

[40] Brezzi, F., and Fortin, M., 2012, *Mixed and hybrid finite element methods* (Springer Science & Business Media).

[41] Cen, Z., 2005, "A hybrid difference scheme for a singularly perturbed convection-diffusion problem with discontinuous convection coefficient," *Appl. Math. Comput.* **169**, 689–699.

[42] Chandru, M., Das, P., and Ramos, H., 2018, "Numerical treatment of two-parameter singularly perturbed parabolic convection diffusion problems with non-smooth data," *Math. Methods Appl. Sci.* **41**, 5359–5387.

[43] Chawla, S., Singh, J., and Urmil, 2022, "An analysis of the robust convergent method for a singularly perturbed linear system of reaction-diffusion type having nonsmooth data," *Int. J. Comput. Methods* **19**

[44] Chen, S. H., Huang, J. L., and Sze, K. Y., 2007, "Multidimensional Lindstedt-Poincaré method for nonlinear vibration of axially moving beams," *J. Sound Vib.* **306**, 1–11.

[45] Cheng, Y., Jiang, S., and Stynes, M., 2022, "Supercloseness of the local discontinuous Galerkin method for a singularly perturbed convection-diffusion problem," , DOI: 10.13140/RG.2.2.10750.87369.

[46] Cheng, Y., and Stynes, M., 2023, "The local discontinuous Galerkin method for a singularly perturbed convection–diffusion problem with characteristic and exponential layers," *Numer. Math.* **154**, 283–318.

[47] Christie, I., Griffiths, D., Mitchell, A., and Zienkiewicz, O., 1976, "Finite element methods for second order differential equations with significant first derivatives," *Int. J. Numer. Meth. Engng.* **10**, 1389–1396.

[48] Chu, C.-C., Graham, I., and Hou, T.-Y., 2010, "A new multiscale finite element method for high-contrast elliptic interface problems," *Math. Comput.* **79**, 1915–1955.

[49] Clavero, C., and Gracia, J., 2004, "HODIE finite difference schemes on generalized Shishkin meshes," *J. Comput. Appl. Math.* **164**, 195–206.

[50] Clavero, C., Gracia, J., Shishkin, G., and Shishkina, L., 2013, "A robust numerical method for a singularly perturbed parabolic convection diffusion problem with a degenerating convective term and a discontinuous right hand side," *Proceedings of ENUMATH* **2011**, 257–266.

[51] Clavero, C., Jorge, J., and Lisbona, F., 2003, "A uniformly convergent scheme on a nonuniform mesh for convection–diffusion parabolic problems," *J. Comput. Appl.Math.* **154**, 415–429.

[52] Clavero, C., and Jorge, J., 2023, "A splitting uniformly convergent method for one-dimensional parabolic singularly perturbed convection-diffusion systems," *Appl. Numer. Math.* **183**, 317–332.

[53] Couchouron, J., Kamenski, M., and Precup, R., 2003, "A nonlinear periodic averaging principle," *Nonlinear Anal.* **54**, 1439–1467.

[54] Coulaud, O., 1997, "Multiple time scales and perturbation methods for high frequency electromagnetic-hydrodynamic coupling in the treatment of liquid metals," *Nonlinear Anal.* **30**, 3637–3643.

[55] Crighton, D. G., and Leppington, F. G., 1973, "Singular perturbation methods in acoustics : diffraction by a plate of finite thickness," *Proceedings of the Royal Society of London. Series A, Mathematical and Physical Sciences* **335**, 313–339.

[56] Daba, I. T., and Duressa, G. F., 2022, "Collocation method using artificial viscosity for time dependent singularly perturbed differential–difference equations," *Math. Comput. Simul.* **192**, 201–220.

[57] Daba, I. T., and Duressa, G. F., 2022, "Computational method for singularly perturbed parabolic differential equations with discontinuous coefficients and large delay," *Heliyon* **8**, e10742.

[58] Das, A., and Natesan, S., 2018, "Higher-order convergence with fractional-step method for singularly perturbed 2d parabolic convection-diffusion problems on shishkin mesh," *Comput. Math. Appl.* **75**, 2387–2403.

[59] Das, P., and Natesan, S., 2012, "Higher order parameter uniform convergent schemes for Robin type reaction diffusion problems using adaptively generated grid," *Int. J. Comput. Methods* **9**, 125–152.

[60] Dessi, D., Mastroddi, F., and Morino, L., 2004, "A fifth-order multiple-scale solution for Hopf bifurcations," *Comput. Struct.* **82**, 2723–2731.

[61] Doedel, E., 1978, "The construction of finite difference approximations to ordinary differential equations," *SIAM J. Numer. Anal.* **15**, 450–465.

[62] Doolan, E., Miller, J., and Schilders, W., 1980, *Uniform numerical methods for problems with initial and boundary layers* (Boole Press).

[63] Dorr, F., 1970, "The numerical solution of singular perturbations of boundary value problems," *SIAM J. Numer. Anal.* **7**, 281–313.

[64] Dorr, F., Parter, S., and Shampine, L., 1973, "Applications of the maximum principle to singular perturbation problems," *SIAM Review* **15**, 43–88.

[65] Douglas, J., and Russell, T., 1982, "Numerical methods for convection-dominated diffusion problems based on combining the method of characteristics with finite element or finite difference procedures," *SIAM J. Numer. Anal.* **19**, 871–885.

[66] Durán, R., Lombardi, A., and Prieto, M., 2012, "Superconvergence for finite element approximation of a convection diffusion equation using graded meshes," *IMA J. Numer. Anal.* **32**, 511–533.

[67] Ejere, A., File, G., Mekuria, M., and Gemechu, T., 2022, "An exponentially fitted numerical scheme via domain decomposition for solving singularly perturbed differential equations with large negative shift," *J. Math.* **2022**, 1–13.

[68] Ejere, A., File, G., Mekuria, M., and Gemechu, T., 2022, "A uniformly convergent numerical scheme for solving singularly perturbed differential equations with large spatial delay," *SN Appl. Sci.* **4**

[69] Ejere, A., Gemechu, T., Mekuria, M., and File, G., 2023, "A tension spline fitted numerical scheme for singularly perturbed reaction-diffusion problem with negative shift," *BMC Res. Notes*, DOI : 10.1186/s13104–023–06361–8.

[70] El-Mistikawy, T., and Werle, M., 1978, "Numerical method for boundary layers with blowing-the exponential box scheme," *AIAA J.* **16**, 749–751.

[71] Eriksson, K., 1994, "An adaptive finite element method with efficient maximum norm error control for elliptic problems," *Math. Models Methods Appl. Sci.* **4**, 313–329.

[72] Ervin, V., and Layton, W., 1989, "An analysis of a defect-correction method for a model convection-diffusion equation," *SIAM J. Numer. Anal.* **26**, 169–179.

[73] Ewing, R. E., 1983, *The Mathematics of Reservoir Simulation* (Society for Industrial and Applied Mathematics, DOI : 10.1137/1.9781611971071).

[74] Farrell, P. A., Hegarty, A. F., Miller, J. J. H., O'Riordan, E., and Shishkin, G. I., 2004, "Global maximum norm parameter-uniform numerical method for a singularly perturbed convection-diffusion problem with discontinuous convection coefficient," *Math. Comput. Modelling* **40**, 1375–1392.

[75] Farrell, P., 1987, "Sufficient conditions for uniform convergence of a class of difference schemes for a singularly perturbed problem," *IMA J. Numer. Anal.* **7**, 459–472.

[76] Farrell, P., 1988, "Sufficient conditions for the uniform convergence of a difference scheme for a singularly perturbed turning point problem," *SIAM J. Numer. Anal.* **25**, 619–643.

[77] Farrell, P., Hegarty, A., Miller, J., O'Riordan, E., and Shishkin, G., 2000, *Robust Computational Techniques for Boundary Layers* (Chapman and Hall/CRC, Boca Raton).

[78] Franz, S., and Linß, T., 2008, "Superconvergence analysis of the Galerkin FEM for a singularly perturbed convection-diffusion problem with characteristic layers," *Numer. Methods Partial Differ. Equ.* **24**, 144–164.

[79] Friedrichs, K. O., 1941, "The mathematical structure of the boundary layer problem," *Fluid Mechanics*, 171–174.

[80] Friedrichs, K., and Wasow, W., 1946, "Singular perturbations of nonlinear oscillations," *Duke Math.* **13**, 367–381.

[81] Fröhner, A., Linß, T., and Roos, H.-G., 2001, "Defect correction on Shishkin-type meshes," *Numer. Algorithms* **26**, 281–299.

[82] Fröhner, A., and Roos, H. G., 2001, "The ε-uniform convergence of a defect correction method on a shishkin mesh," *Appl. Numer. Math.* **37**, 79–94.

[83] G. Babu, G., Prithvi, M., Sharma, K., and Ramesh, V., 2022, "A uniformly convergent numerical algorithm on harmonic (h(l)) mesh for parabolic singularly perturbed convection-diffusion problems with boundary layer," *Differ. Equ. Dyn. Syst.*, 1–14.

[84] Gartland, E., 1987, "Uniform high-order difference schemes for a singularly perturbed two-point boundary value problem," *Math. Comput.* **48**, 551–564.

[85] Gartland, E., 1988, "Graded mesh difference schemes for singularly perturbed two point boundary value problems," *Math. Comput.* **51**, 631–657.

[86] Gayaz, K., and Denys, D., 2017, "On supraconvergence phenomenon for second order centered finite differences on non-uniform grids," *J. Comput. Appl. Math.* **326**, 1–14.

[87] Geetha, N., and Tamilselvan, A., 2018, "Parameter uniform numerical method for fourth order singularly perturbed turning point problems exhibiting boundary layers," *Ain Shams Eng. J.* **9**, 845–853.

[88] Gelu, F. W., and Duressa, G. F., 2023, "A parameter-uniform numerical method for singularly perturbed robin type parabolic convection-diffusion turning point problems," *Appl. Numer. Math.* **190**, 50–64.

[89] Gharibi, Z., and Dehghan, M., 2021, "Convergence analysis of weak galerkin flux-based mixed finite element method for solving singularly perturbed convection-diffusion-reaction problem," *Appl. Numer. Math.* **163**, 303–316.

[90] Gobena, W. T., and Duressa, G. F., 2023, "An efficient numerical approach for solving singularly perturbed parabolic differential equations with large negative shift and integral boundary condition," *Applied Mathematics in Science and Engineering* **31**, 2236769.

[91] Gold, R. R., 1962, "Magnetohydrodynamic pipe flowṖart 1," *J. Fluid Mech.* **13**, 505–512.

[92] Gosse, L., and Mauser, L., 2006, "Multiphase semiclassical approximation of an electron in a one-dimensional crystalline lattice–III. from ab initio models to WKB for Schrödinger-Poisson," *J. Comp. Phys.* **211**, 326–346.

[93] Gowrisankar, S., and Natesan, S., 2014, "Robust numerical scheme for singularly perturbed convection diffusion parabolic initial boundary value problems on equidistributed grids," *Comput. Phys. Commun.* **185**, 2008–2019.

[94] Gracia, J. L., and O'Riordan, E., 2006, "A defect correction parameter-uniform numerical method for a singularly perturbed convection diffusion problem in one dimension," *Numer. Algorithms* **41**, 359–385.

[95] Grossmann, C., Mohanty, R., and Roos, H.-G., 2011, "A direct higher order discretization in singular perturbations via domain split-A computational approach," *Appl. Math. Comput.* **217**, 9302–9312.

[96] Gupta, A., and Kaushik, A., 2021, "A higher-order accurate difference approximation of singularly perturbed reaction-diffusion problem using grid equidistribution," *Ain Shams Eng. J.* **12**, 4211–4221.

[97] Gupta, A., and Kaushik, A., 2021, "A robust spline difference method for robin-type reaction-diffusion problem using grid equidistribution," *Appl. Math. Comput.* **390**, 125597.

[98] Gupta, A., and Kaushik, A., 2022, "A higher-order hybrid finite difference method based on grid equidistribution for fourth-order singularly perturbed differential equations," *J. Appl. Math. Comput.* **68**, 1163–1191.

[99] H.-G., Stynes, M., and Tobiska, L., 2008, *Robust Numerical Methods for Singularly Perturbed Differential Equations* (Springer, Berlin).

[100] He, J., 1999, "Variational iteration method - a kind of non-linear analytical technique: some examples," *Internat. J. Non-Linear Mech.* **34**, 699–708.

[101] He, J., 2002, "Modified Lindstedt-Poincare methods for some strongly non-linear oscillations: Part I: expansion of a constant," *Internat. J. Non-Linear Mech.* **37**, 309–314.

[102] He, J., 2006, "Homotopy perturbation method for solving boundary value problems," *Phys. Lett. A* **350**, 87–88.

[103] He, J., Wan, Y., and Guo, Q., 2004, "An iteration formulation for normalized diode characteristics," *Internat. J. Circuit. Theory. Appl.* **32**, 629–632.

[104] Heading, J., 1962, *An introduction to phase-integral methods* (Methuen, London).

[105] Heinrich, J. C., 1980, "On quadratic elements in finite element solutions of steady-state convection-diffusion equation," *Int. J. Numer. Methods Eng.* **15**, 1041–1052.

[106] Heinrich, J. C., Huyakorn, P. S., Mitchell, A. R., and Zienkiewicz, O. C., 1977, "An upwind finite element scheme for two-dimensional convective transport equations," *Int. J. Numer. Methods Eng.* **11**, 131–143.

[107] Heinrich, J. C., and Zienkiewicz, O. C., 1979, "The finite element method and 'upwinding' techniques in the numerical solution of convection dominated flow problems," in *Finite Element Methods for Convection Dominated Flows*, pp. 105–136.

[108] Hemker, P. W., 1982, *An accurate method without directional bias for the numerical solution of a* 2*-D elliptic singular perturbation problem, in: W. Eckhaus, E.M.de jager (Eds.)* (Theory and Applications of singular perturbations, Lecture Notes in Mathematics Springer, Berlin-New York).

[109] Herceg, D., Surla, K., and Rapajic, S., 1998, "Cubic spline difference scheme on a mesh of Bakhvalov type," *Novi Sad J. Math* **28**, 41–49.

[110] Horssen, W. V., 2001, "On integrating vectors and multiple scales for singularly perturbed ordinary differential equations," *Nonlinear Anal.* **46**, 19–43.

[111] Houston, P., Roggendorf, S., and van der Zee, K. G., 2020, "Eliminating gibbs phenomena: A non-linear petrov–galerkin method for the convection–diffusion–reaction equation," *Comput. Math. Appl.* **80**, 851–873.

[112] Huang, J., Cen, Z., and Xu, A., 2021, "An improved a posteriori error estimation for a parameterized singular perturbation problem," *Appl. Math. Lett.* **114**, 106912.

[113] Il'in, A. M., 1969, "Differencing scheme for a differential equation with a small parameter affecting the highest derivative," *Math. Notes* **6**, 596–602.

[114] Jalaal, M., Ganji, D. D., and Mohammadi, F., 2010, "Heś homotopy perturbation method for two-dimensional heat conduction equation: Comparison with finite element method," *Heat Transfer-Asian Res.* **39**, 232–245.

[115] Kabeto, M. J., and Duressa, G. F., 2022, "Second-order robust finite difference method for singularly perturbed burgers' equation," *Heliyon* **8**, e09579.

[116] Kadalbajoo, M., and Awasthi, A., 2011, "The midpoint upwind finite difference scheme for time-dependent singularly perturbed convection-diffusion equations on non-uniform mesh," *Int. J. Comput. Methods Eng. Sci. Mech.* **12**, 150–159.

[117] Kadalbajoo, M., and Gupta, V., 2010, "A brief survey on numerical methods for solving singularly perturbed problems," *Appl. Math. Comp.* **217**, 3641–3716.

[118] Kadalbajoo, M., and Jha, A., 2013, "A posteriori error analysis for defect correction method for two parameter singular perturbation problems," *J. Appl. Math. Comput.* **42**, 421–440.

[119] Kadalbajoo, M., and Jha, A., 2013, "A posteriori error analysis for defect correction method for two parameter singular perturbation problems," *J. Appl. Math. Comput.* **42**, 421–440.

[120] Kadalbajoo, M., and Patidar, K., 2002, "Spline techniques for solving singularly-perturbed nonlinear problems on nonuniform grids," *J. Optim. Theory Appl.* **114**, 573–591.

[121] Kadalbajoo, M., and Patidar, K., 2003, "Exponentially fitted spline in compression for the numerical solution of singular perturbation problems," *Comput. Math. Appl.* **46**, 751–767.

[122] Kadalbajoo, M., and Patidar, K., 2003, "Singularly perturbed problems in partial differential equations: A survey," *Appl. Math. Comp.* **134**, 371–429.

[123] Kadalbajoo, M., and Yadaw, A., 2008, "B-spline collocation method for a two-parameter singularly perturbed convection–diffusion boundary value problems," *Appl. Math. Comp.* **201**, 504–513.

[124] Kamenskii, M., and Nistri, P., 2003, "An averaging method for singularly perturbed systems of semilinear differential inclusions with analytic semigroups," *Nonlinear Anal.* **53**, 467–480.

[125] Kaplun, S., 1954, "The role of coordinate systems in boundary-layer theory," *Z. Angew. Math. Phys.* **5**, 111–135.

[126] Kaplun, S., and Lagerstrom, P. A., 1957, "Asymptotic expansions of Navier-Stokes solutions for small Reynolds numbers," *J. Math. Mech.*, 585–593.

[127] Kaushik, A., Kumar, V., Sharma, M., and Sharma, N., 2021, "A modified graded mesh and higher order finite element method for singularly perturbed reaction–diffusion problems," *Math. Comput. Simul.* **185**, 486–496.

[128] Kaushik, A., Vashishth, A. K., Kumar, V., and Sharma, M., 2019, "A modified graded mesh and higher order finite element approximation for singular perturbation problems," *J. Comp. Phys.* **395**, 275–285.

[129] Kaushik, A., 2014, "Error estimates for a class of partial functional differential equation with small dissipation," *Appl. Math. Comput.* **226**, 250–257.

[130] Kaushik, A., and Sharma, N., 2020, "An adaptive difference scheme for parabolic delay differential equation with discontinuous coefficients and interior layers," *J. Differ. Equ.* **26**, 1450–1470.

[131] Kaushik, A., and Sharma, N., 2021, "A hybrid finite difference method for singularly perturbed delay partial differential equations with discontinuous coefficient and source," *J. Mar. Sci. Technol.* **30**

[132] Keller, H., 1968, *Numerical Methods for Two-Point Boundary-Value Problems* (Blaisdell Publication Co., Waltham, Massachusetts).

[133] Kellogg, R. B., and Tsan, A., 1978, "Analysis of some difference approximations for a singular perturbation problem without turning points," *Math. Comp.* **32**, 1025–1039.

[134] Kevorkian, J., 1962, *The two variable expansion procedure for the approximate solution of certain non-linear differential equations*, Tech. Rep. (Santa Monica, California).

[135] Kevorkian, J. K., and Cole, J. D., 2013, *Perturbation Methods in Applied Mathematics* (Springer, Berlin).

[136] Khan, H., Bazaz, M. A., and Nahvi, S. A., 2019, "Singular perturbation-based model reduction of power electronic circuits," *IET Circuits Devices Syst.* **13**, 471–478.

[137] Khrustalev, O., and Vernov, S., 2001, "Construction of doubly periodic solutions via the Poincare-Lindstedt method in the case of massless $\phi 4$ theory," *Math. Comput. Simul.* **57**, 239–252.

[138] Kokotovic, P. V., 1984, "Applications of singular perturbation techniques to control problems," *SIAM Review* **26**, 501–550.

[139] Kopteva, N., Madden, N., and Stynes, M., 2005, "Grid equidistribution for reaction diffusion problems in one dimension," *Numer. Algor.* **40**, 305–322.

[140] Kopteva, N., and O'Reordan, E., 2010, "Shishkin meshes in the numerical solution of singularly perturbed differential equations," *Int. J. Numer. Anal. Model.* **7**, 393–415.

[141] Kopteva, N., and Stynes, M., 2001, "A robust adaptive method for a quasi-linear one-dimensional convection-diffusion problem," *SIAM J. Numer. Anal.* **39**, 1446–1467.

[142] Kopteva, N., 2001, "Maximum norm a posteriori error estimates for a one-dimensional convection-diffusion problem," *SIAM J. Numer. Anal.* **39**, 423–441.

[143] Krivec, R., and Mandelzweig, V., 2006, "Quasilinearization method and WKB," *Comput. Phys. Commun.* **174**, 119–126.

[144] Kumar, D., and Kumari, P., 2020, "Parameter-uniform numerical treatment of singularly perturbed initial-boundary value problems with large delay," *Appl. Numer. Math.* **153**, 412–429.

[145] Kumar, N., and Rao, R., 2023, "A second order stabilized central difference method for singularly perturbed differential equations with a large negative shift," *Differ. Equ. Dyn. Syst.* **31**, 787–804.

[146] Kumar, S., Sumit, and Ramos, H., 2021, "Parameter-uniform approximation on equidistributed meshes for singularly perturbed parabolic reaction-diffusion problems with robin boundary conditions," *Appl. Math. Comput.* **392**, 125677.

[147] Kumar, S., Sumit, and Vigo-Aguiar, J., 2022, "A high order convergent numerical method for singularly perturbed time dependent problems using mesh equidistribution," *Math. Comput. Simulation* **199**, 287–306.

[148] Kuzmak, G. E., 1959, "Asymptotic solutions of nonlinear second order differential equations with variable coefficients," *J. Appl. Math. Mech.* **23**, 730–744.

[149] Labovschii, A., 2009, "A defect correction method for the time-dependent Navier-Stokes equations," *Numer Methods Partial Differ. Equ.* **25**, 1–25.

[150] Lagerstrom, P. A., and Casten, R. G., 1972, "Basic concepts underlying singular perturbation techniques," *SIAM Review* **14**, 63–120.

[151] Lagerstrom, P. A., and Cole, J. D., 1955, "Examples illustrating expansion procedures for the Navier-Stokes equations," *J. Ration. Mech. Anal.* **4**, 817–882.

[152] Lakrad, F., and Belhaq, M., 2002, "Periodic solutions of strongly non-linear oscillators by the multiple scales method," *J. Sound Vib.* **258**, 677–700.

[153] Lenbury, Y., 1996, "Singular perturbation analysis of a model for a predator-prey system invaded by a parasite," *Biosystems* **39**, 251–262.

[154] LeVeque, R. J., 2002, *Finite volume methods for hyperbolic problems* (Cambridge University Press).

[155] Levinson, N., 1950, "The first boundary value problem for ε-δ $U + A(X,Y)UX + B(X,Y)UY + C(X,Y)U = D(X,Y)$ for small ε," *Ann. Math.* **51**, 428–445.

[156] Liang, D., and Zhao, W., 1997, "A high-order upwind method for the convection-diffusion problem," *Comput. Methods Appl. Mech. Engrg.* **147**, 105–115.

[157] Lin, C., and Segel, L., 1988, *Mathematics Applied to Deterministic Problems in the Natural Sciences* (Society for Industrial and Applied Mathematics (SIAM, 3600 Market Street, Floor 6, Philadelphia, PA 19104)).

[158] Linß, T., 1999, "An upwind difference scheme on a novel Shishkin type mesh for a linear convection diffusion problem," *J. Comput. Appl. Math.* **110**, 93–104.

[159] Linß, T., 2000, "Analysis of a Galerkin finite element method on a Bakhvalov-Shishkin mesh for a linear convection diffusion problem," *IMA J. Numer. Anal.* **20**, 621–632.

[160] Linß, T., 2000, "Uniform superconvergence of a Galerkin finite element method on Shishkin-type meshes," *Numer. Methods Partial Differ. Equ.* **16**, 426–440.

[161] Linß, T., 2001, "Finite Difference Schemes for Convection-Diffusion Problems with a Concentrated Source and a Discontinuous Convection Field," *Comput. Methods Appl. Math.* **2**, 41–49.

[162] Linß, T., 2001, "Uniform pointwise convergence of finite difference schemes using grid equidistribution," *Computing* **66**, 27–39.

[163] Linß, T., 2003, "Layer-adapted meshes for convection-diffusion problems," *Comput. Methods Appl. Mech. Eng.* **192**, 1061–1105.

[164] Linß, T., 2004, "Error expansion for a first-order upwind difference scheme applied to a model convection-diffusion problem," *IMA J. Numer. Anal.* **24**, 239–253.

[165] Linß, T., 2007, "Layer adapted meshes and FEM for time dependent singularly perturbed reaction diffusion problems," *Int. J. Comput. Sci. Math.* **1**, 259–270.

[166] Linß, T., 2010, *Layer Adapted Meshes for Reaction Convection Diffusion Problems* (Springer, Berlin).

[167] Linß, T., and Kopteva, N., 2010, "A posteriori error estimation for a defect-correction method applied to convection-diffusion problems," *Int. J. Numer. Anal. Model.* **7**, 1–16.

[168] Linß, T., and Stynes, M., 2001, "Numerical methods on Shishkin meshes for linear convection diffusion problems," *Comput. Methods Appl. Mech. Eng.* **190**, 3527–3542.

[169] Linß, T., 2001, "Finite difference schemes for convection-diffusion problems with a concentrated source and a discontinuous convection field," *Comput. Methods Appl. Math.* **2**, 41–49.

[170] Linß, T., and Kopteva, N., 2010, "A posteriori error estimation for a defect-correction method applied to convection-diffusion problems," *Int. J. Numer. Anal. Model.* **7**

[171] Linß, T., and Kopteva, N., 2010, "A posteriori error estimation for a defect-correction method applied to convection-diffusion problems," *Int. J. Numer. Anal. Model.* **7**

[172] Linß, T., 2010, "A posteriori error estimation for a singularly perturbed problem with two small parameters," *Int. J. Numer. Anal. Model.* **7**

[173] Liu, D., and He, W., 2021, "Numerical simulation analysis mathematics of fluid mechanics for semiconductor circuit breaker," *Appl. math. nonlinear sci.* **0**

[174] Liu, H., 2005, "Approximate period of nonlinear oscillators with discontinuities by modified Lindstedt–Poincare method," *Chaos Solit. Fractals* **23**, 577–579.

[175] Lodhi, R. K., and Mishra, H. K., 2018, "Septic b-spline method for second order self-adjoint singularly perturbed boundary-value problems," *Ain Shams Eng. J.* **9**, 2153–2161.

[176] Lubuma, J., and Patidar, K., 2006, "Uniformly convergent non-standard finite difference methods for self-adjoint singular perturbation problems," *J. Comput. Appl. Math.* **191**, 228–238.

[177] Lynch, R., and Rice, J., 1980, "A high-order difference method for differential equations," *Math. Comput.* **34**, 333–372.

[178] Ma, G., and Stynes, M., 2020, "A direct discontinuous galerkin finite element method for convection-dominated two-point boundary value problems," *Numer. Algor.* **83**, 741–765.

[179] Mackenzie, J., 1999, "Uniform convergence analysis of an upwind finite-difference approximation of a convection-diffusion boundary value problem on an adaptive grid," *IMA J. Numer. Anal.* **19**, 233–249.

[180] Majumdar, A., and Natesan, S., 2017, "Alternating direction numerical scheme for singularly perturbed 2d degenerate parabolic convection-diffusion problems," *Appl. Math. Comput.* **313**, 453–473.

[181] Marasco, A., 2000, "Lindstedt-Poincarè method and Mathematica applied to the motion of a solid with a fixed point," *Comput. Math. Appl.* **40**, 333–343.

[182] Mazumder, S., 2015, *Numerical methods for partial differential equations: finite difference and finite volume methods* (Academic Press).

[183] Mekuria, M., and File, G., 2020, "Higher-order uniformly convergent numerical scheme for singularly perturbed differential difference equations with mixed small shifts," *Int. J. Differ. Equ.* **2020**, 1–15.

[184] Mickens, R., 1981, *An introduction to nonlinear oscillations* (CUP Archive).

[185] Miller, J., 1975, "A finite element method for a two point boundary value problem with a small parameter affecting the highest derivative," *Presented to the Seminar, Mathematical Models and Numerical Methods* **3**, 143–146.

[186] Miller, J., O'Riordan, E., and Shishkin, G., 2012, *Fitted Numerical Methods for Singular Perturbation Problems* (World Scientific, Singapore).

[187] Miller, J. J. H., 1997, "Singular perturbation problems in chemical physics : analytic and computational methods,"

[188] Minero, R., Anthonissen, M. J. H., and Mattheij, R. M. M., 2006, "A local defect correction technique for time-dependent problems," *Numer. Methods Partial Differential Equations* **22**, 128–144.

[189] Mohapatra, J., and Natesan, S., 2010, "The parameter-robust numerical method based on defect-correction technique for singularly perturbed delay differential equation with layer behavior," *Int. J. Comput. Methods* **190**, 573–594.

[190] Morton, K., 2010, *Numerical Solution of Convection Diffusion Problems* (Chapman & Hall, London).

[191] Mukherjee, K., and Natesan, S., 2011, "ϵ-uniform error estimate of hybrid numerical scheme for singularly perturbed parabolic problems with interior layers," *Numer. Algorithms* **58**, 103–141.

[192] Mukherjee, K., and Srinivasan, N., 2008, "An efficient numerical scheme for singularly perturbed parabolic problems with interior layer," *Neural, Parallel & Scientific Computations* **16**, 405–417.

[193] Munch, A., and Zuazua, E., 2010, "Numerical approximation of null controls for the heat equation: Ill-posedness and remedies," *Inverse Problems* **26**

[194] Munyakazi, J., 2015, "A uniformly convergent nonstandard finite difference scheme for a system of convection-diffusion equations," *Comp. Appl. Math.* **34**, 1153–1165.

[195] Munyakazi, J., and K.C.Patidar, 2013, "A fitted numerical method for singularly perturbed parabolic reaction-diffusion problems," *Comput. Appl. Math.* **32**, 509–519.

[196] Munyakazi, J., and Patidar, K., 2008, "On Richardson extrapolation for fitted operator finite difference methods," *Appl. Math. Comput.* **201**, 465–480.

[197] Murray, J., 1977, *Lectures on Nonlinear-Differential-Equation Models in Biology* (Clarendon Press).

[198] Nagarajan, S., 2022, "A parameter robust fitted mesh finite difference method for a system of two reaction-convection-diffusion equations," *Appl. Numer. Math.* **179**, 87–104.

[199] Nageshwar Rao, R., and Pramod Chakravarthy, P., 2019, "Fitted numerical methods for singularly perturbed one-dimensional parabolic partial differential equations with small shifts arising in the modelling of neuronal variability," *Differ. Equ. Dyn. Syst.* **27**, 1–18.

[200] Natesan, S., and Bawa, R. K., 2007, "Second-order numerical scheme for singularly perturbed reaction-diffusion robin problems," *J. Numer. Anal. Ind. Appl. Math.* **2**, 177–192.

[201] Navarro, J., 2008, "On the implementation of the Poincaré-Lindstedt technique," *Appl. Math. Comput.* **195**, 183–189.

[202] Nayfeh, A., 1979, *Perturbation Methods* (Wiley, New York).

[203] Nayfeh, A. H., 2011, *Introduction to perturbation techniques* (John Wiley & Sons).

[204] Nhan, T. A., Mai, V. Q., Mohapatra, J., and Hammouch, Z., 2023, "A new upwind difference analysis of an exponentially graded bakhvalov-type mesh for singularly perturbed elliptic convection-diffusion problems," *J. Comput. Appl. Math.* **418**, 114622.

[205] Niederdrenk, K., and Yserentant, H., 1983, "Die gleichmäßige stabilität singulär gestörter diskreter und kontinuierlicher randwertprobleme," *Numer. Math.* **41**, 223–253.

[206] Ning, L., Haiyan, S., Dongwei, G., and Xinlong, F., 2018, "Multiquadric RBF-FD method for the convection-dominated diffusion problems based on Shishkin nodes," *Int. J. Heat Mass Transfer* **118**, 734–745.

[207] Nofel, T., 2014, "Application of the homotopy perturbation method to nonlinear heat conduction and fractional Van der Pol damped nonlinear oscillator," *Appl. Math.* **5**, 852–861.

[208] Oleĭnik, O., 1952, "On boundary problems from equations with a small parameter in the highest derivatives," *Dokl. Akad. Nauk, SSR* **85**, 493–495.

[209] O'Malley, R., 1974, *Introduction to Singular Perturbations* (Academic Press, New York).

[210] O'Malley, R., 2014, *Historical developments in singular perturbations* (Springer).

[211] O'Riordan, E., 1984, "Singularly perturbed finite element methods," *Numer. Math.* **44**, 425–434.

[212] O'Riordan, E., 2016, *Interior Layers in Singularly Perturbed Problems*, Vol. 172, ISBN 978-81-322-3596-5

[213] O'Riordan, E., and Shishkin, G., 2004, "Singularly perturbed parabolic problems with non-smooth data," *J. Comput. Appl. Math.* **166**, 233–245.

[214] Öziş, T., and Yıldırım, A., 2007, "Determination of periodic solution for a $u^{\frac{1}{3}}$ force by He's modified Lindstedt–Poincaré method," *J. Sound Vib.* **301**, 415–419.

[215] Panda, A., and Mohapatra, J., 2023, "On the convergence analysis of efficient numerical schemes for singularly perturbed second order volterra integro-differential equations," *J. Appl. Math. Comput.*, 1–24.

[216] Panda, A., and Mohapatra, J., 2023, "A robust finite difference method for the solutions of singularly perturbed fredholm integro-differential equations," *Mediterr. J. Math.* **20**, 198.

[217] Patidar, K., 2005, "High order fitted operator numerical method for self-adjoint singular perturbation problems," *Appl. Math. Comput.* **171**, 547–566.

[218] Pearson, C. E., 1968, "On a differential equation of boundary layer type," *J. Math. and Phy.* **47**, 134–154.

[219] Pearson, C. E., 1968, "On a nonlinear differential equation of boundary layer type," *J. Math. and Phy.* **47**, 351–358.

[220] Pillai, A. R., 2001, "Fourth-order exponential finite difference methods for boundary value problems of convective diffusion type," *Int. J. Numer.Methods Fluids* **37**, 87–106.

[221] Prabha, T., Chandru, M., and Shanthi, V., 2017, "Hybrid difference scheme for singularly perturbed reaction-convection-diffusion problem with boundary and interior layers," *Appl. Math. Comput.* **314**, 237–256.

[222] Prandtl, L., 1904, *Über Flüssigkeitsbewegung bei sehr kleiner Reibung: in Verhandlungen des III Internationalen Mathematiker-Kongresses* (Teubner, Leipzig).

[223] Prasad, E., Omkar, R., and Phaneendra, D., 2022, "Fitted parameter exponential spline method for singularly perturbed delay differential equations with a large delay," *Comput. Math. Methods.* **2022**, 1–11.

[224] Priyadharshini, R., and Ramanujam, N., 2008, "A hybrid difference scheme for singularly perturbed second order ordinary differential equations with discontinuous convection coefficient and mixed type boundary conditions," *Int. J. Comput. Methods* **05**, 575–593.

[225] Protter, M., and Weinberger, H., 1984, *Maximum Principles in Differential Equations* (Springer-Verlag, New York).

[226] Pudykiewicz, J., 1989, "Simulation of the Chernobyl dispersion with a 3-D hemispheric tracer model," *Tellus B Chem Phys Meteorol* **41**, 391–412.

[227] Pušenjak, R., 2008, "Extended Lindstedt-Poincare method for non-stationary resonances of dynamical systems with cubic nonlinearities," *J. Sound Vib.* **314**, 194–216.

[228] Quinn, J., 2015, "A numerical method for a nonlinear singularly perturbed interior layer problem using an approximate layer location," *J. Comput. Appl. Math.* **290**, 500–515.

[229] Ragula, K., Soujanya, G., and Swarnakar, D., 2023, "Computational approach for a singularly perturbed differential equations with mixed shifts using a non-polynomial spline," *Int. J. Anal. Appl.* **21**, 5.

[230] Rahaman, H., Hasan, M., Ali, A., and Alam, M. S., 2021, "Implicit methods for numerical solution of singular initial value problems," *Appl. math. nonlinear sci.* **6**, 1–8.

[231] Ranjan, K. R., and Gowrisankar, S., 2022, "Uniformly convergent nipg method for singularly perturbed convection diffusion problem on shishkin type meshes," *Appl. Numer. Math.* **179**, 125–148.

[232] Ranjan, K. R., and Gowrisankar, S., 2023, "NIPG method on Shishkin mesh for singularly perturbed convection-diffusion problem with discontinuous source term," *Int. J. Comput. Methods* **20**, 2250048.

[233] Rao, S., and Kumar, M., 2009, "Parameter-uniformly convergent exponential spline difference scheme for singularly perturbed semilinear reaction-diffusion problems," *Nonlinear Anal.* **71**, e1579–e1588.

[234] Rao, S., and Kumar, M., 2010, "A uniformly convergent exponential spline difference scheme for singularly perturbed reaction-diffusion problems," *Neural Parallel Sci. Comput.* **18**, 121–136.

[235] Rashidinia, J., Ghasemi, M., and Mahmoodi, Z., 2007, "Spline approach to the solution of a singularly perturbed boundary value problems," *Appl. Math. Comput.* **189**, 72–78.

[236] Raza, A., and Khan, A., 2022, "Treatment of singularly perturbed differential equations with delay and shift using Haar Wavelet collocation method," *Tamkang J. Math.* **53**, 303–322.

[237] Reinhardt, H.-J., 1981, "A-posteriori error estimates and adaptive finite element computations for singularly perturbed one space dimensional parabolic equations," *North-Holland Math. Stud.* **47**, 213–233.

[238] Reinhardt, H.-J., 1985, "A-posteriori error estimation for finite element modifications of line methods applied to singularly perturbed partial differential equations," *Appl. Numer. Math.* **1**, 145–176.

[239] Ren, Y., and Zhang, H., 2006, "A generalized F-expansion method to find abundant families of Jacobi elliptic function solutions of the (2 + 1)-dimensional Nizhnik-Novikov-Veselov equation," *Chaos Solit. Fractals* **27**, 959–979.

[240] Roos, H.-G., 2006, "Error estimates for linear finite elements on Bakhvalov type meshes," *Appl. Math.* **51**, 63–72.

[241] Roos, H.-G., 2012, "Robust numerical methods for singularly perturbed differential equations: A survey covering 2008-2012," *ISRN Appl. Math.* **2012**, 1–30.

[242] Roos, H.-G., and Linß, T., 1999, "Sufficient conditions for uniform convergence on layer adapted grids," *computing*, 27–45.

[243] Roos, H.-G., and Skalický, T., 1997, "A comparison of the finite element method on Shishkin and Gartland type meshes for convection diffusion problems," *CWI Quaterly* **10**, 277–300.

[244] Roos, H.-G., Teofanov, L., and Uzelac, Z., 2015, "Graded meshes for higher order FEM," *J. Comput. Math.* **33**, 1–16.

[245] Roos, H. G., and Zarin, H., 2003, "The streamline-diffusion method for a convection–diffusion problem with a point source," *J. Comput. Appl. Math.* **150**, 109–128.

[246] Samarskii, A., 1977, *Theory of difference schemes* (Nauka, Moscow).

[247] Schamberg, T., and Heinrichs, W., 2004, "An adaptive refinement method for convection-diffusion problems," pp. 718–719.

[248] Schlichting, H., and Gersten, K., 2003, *Boundary Layer Theory* (Springer-Verlag, Berlin).

[249] Schlissel, A., 1977, "The initial development of the WKB solutions of linear second order ordinary differential equations and their use in the connection problem," *Hist. Math.* **4**, 183–204.

[250] Schmeiser, C., 1990, "A singular perturbation analysis of reverse biased pn-junctions," *SIAM J. Math. Anal.* **21**, 313–326.

[251] Selvakumar, K., and Ramanujam, N., 1996, "Uniform finite difference schemes for singular perturbation problems arising in gas porous electrodes theory," *Indian J. Pure Appl. Math.* **27**, 893–906.

[252] Shahraki, M., and Hosseini, S., 2006, "Comparison of a higher order method and the simple upwind and non-monotone methods for singularly perturbed boundary value problems," *Appl. Math. Comput.* **182**, 460–473.

[253] Sharma, K., and Kaushik, A., 2006, "A solution of the discrepancy occurs due to using the fitted mesh approach rather than to the fitted operator for solving singularly perturbed differential equations," *Appl. Math. Comput.* **181**, 756–766.

[254] Shiromani, R., Shanthi, V., and Ramos, H., 2023, "Numerical treatment of a singularly perturbed 2-d convection-diffusion elliptic problem with robin-type boundary conditions," *Appl. Numer. Math.* **187**, 176–191.

[255] Shishkin, G. I., 1983, "A difference scheme on a non-uniform mesh for a differential equation with a small parameter in the highest derivative," *USSR Comput. Math. Math. Phys.* **23**, 59–66.

[256] Shishkin, G. I., 1988, "A difference scheme for a singularly perturbed equation of parabolic type with discontinuous boundary conditions," *USSR Comp. Math. Math. Phys.* **28**, 1679–1692.

[257] Shishkin, G. I., 1989, "Approximation of the solutions of singularly perturbed boundary-value problems with a parabolic boundary layer," *USSR Comput. Math. & Math. Phys.* **29**, 1–10.

[258] Shivamoggi, B., 2003, "The method of strained coordinates/parameters," in *Perturbation Methods for Differential Equations*, pp. 41–111.

[259] Shooshtari, A., and Zanoosi, A. P., 2010, "A multiple times scale solution for nonlinear vibration of mass grounded system," *Appl. Math. Model.* **34**, 1918–1929.

[260] Singh, M. K., and Natesan, S., 2018, "Richardson extrapolation technique for singularly perturbed system of parabolic partial differential equations with exponential boundary layers," *Appl. Math. Comput.* **333**, 254–275.

[261] Singh, S., and Kumar, D., 2023, "Parameter uniform numerical method for a system of singularly perturbed parabolic convection-diffusion equations," *Math. Comput. Simulation* **212**, 360–381.

[262] Singh, S., Kumar, D., and Vigo-Aguiar, J., 2023, "A robust numerical technique for weakly coupled system of parabolic singularly perturbed reaction–diffusion equations," *J. Math. Chem.* **61**, 1313–1350.

[263] Skinner, L., 2011, *Singular perturbation theory* (Springer Science & Business Media).

[264] Smith, G., 1985, *Numerical Solution of Partial Differential Equations : Finite Difference Methods* (Oxford Applied Mathematics and Computing Science Series).

[265] Stahara, S., Crisalli, A., and Spreiter, J., 1980, "Evaluation of a strained-coordinate perturbation procedure-nonlinear subsonic and transonic flows," in *18th Aerospace Sciences Meeting*, p. 339.

[266] Steele, C., 1976, "Application of the WKB method in solid mechanics," *Mech. Today* **3**, 243–295.

[267] Stojanović, M., 2003, "A uniformly accurate finite elements method for singular perturbation problems," *Glas. Mat.* **38**, 185–197.

[268] Stynes, M., and O'Riordan, E., 1991, "An analysis of a singularly perturbed two-point boundary value problem using only finite element techniques," *Math. Comput.* **56**, 663–675.

[269] Stynes, M., and Roos, H. G., 1997, "The midpoint upwind scheme," *Appl. Numer. Math.* **23**, 361–374.

[270] Subburayan, V., 2016, "A robust computational method for system of singularly perturbed differential difference equations with discontinuous convection coefficients," *Int. J. Comput. Methods* **13**, 1641008.

[271] Subburayan, V., and Ramanujam, N., 2021, "Uniformly convergent finite difference schemes for singularly perturbed convection diffusion type delay differential equations," *Differ. Equ. Dyn. Syst.* **29**, 139–155.

[272] Sun, G., and Stynes, M., 1994, "Finite element methods on piecewise equidistant meshes for interior turning point problems," *Numer. Algor.* **8**, 111–129.

[273] Sun, G., and Stynes, M., 1995, "Finite element methods for singularly perturbed higher order elliptic two point boundary value problems ii: convection diffusion type," *IMA J. Numer. Anal.* **15**, 197–219.

[274] Surla, K., and Jerković, V., 1990, *An exponentially fitted quadratic spline difference scheme on a non-uniform mesh* (Univ. u Novom Sadu Zb. Rad. Prirod. Mat. Fak. Ser. Mat.).

[275] Surla, K., and Uzelac, Z., 1997, "A spline difference scheme on a piecewise equidistant grid," *ZAMM* **77**, 901–909.

[276] Tiruneh, A. A., Derese, G. A., and Ayele, M. A., 2023, "Singularly perturbed reaction-diffusion problem with large spatial delay via non-standard fitted operator method," *Research in Mathematics* **10**, 2171698.

[277] Toprakseven, Ş., 2021, "Superconvergence of a modified weak Galerkin method for singularly perturbed two-point elliptic boundary-value problems," *Calcolo* **59**, 1.

[278] Toprakseven, Ş., 2022, "Optimal order uniform convergence in energy and balanced norms of weak Galerkin finite element method on Bakhvalov-type meshes for nonlinear singularly perturbed problems," *Comput. Appl. Math.* **41**, 377.

[279] Toprakseven, Ş., and Zhu, P., 2023, "Error analysis of a weak Galerkin finite element method for two-parameter singularly perturbed differential equations in the energy and balanced norms," *Appl. Math. Comput.* **441**, 127683.

[280] Van-Dyke, M., 1964, *Perturbation Methods in Fluid Dynamics* (Academic Press, New York).

[281] Veldhuizen, M., 1978, "Higher order methods for a singularly perturbed problem," *Numer. Math.* **30**, 267–279.

[282] Verhulst, F., 2005, *Methods and applications of singular perturbations: boundary layers and multiple timescale dynamics* (Springer Science & Business Media).

[283] Versteeg, H., and Malalasekera, W., 2007, *An Introduction to Computational Fluid Dynamics* (Pearson).

[284] Vishik, M., and Lyusternik, L., 1957, "Regular degeneration and boundary layer for linear differential equations with a small parameter multiplying the highest derivatives," *Usp. Mat. Nauk* **12**, 3–122.

[285] Visik, M., and Lyusternik, L., 1957, "On elliptic equations containing small parameters in the terms with higher derivatives," *Dokl. Akad. Nauk, SSR* **113**, 734–737.

[286] Visik, M., and Lyusternik, L., 1957, "Regular degeneration and boundary layer for linear differential equations with small parameter," *Uspekhi Mat. Nauk* **12**, 3–122.

[287] Vulanović, R., 1983, "On a numerical solution of a type of singularly perturbed boundary value problem by using a special discretisation mesh," *Rev. Res. Math. Ser. Univ. Novi Sad* **13**, 187–201.

[288] Vulanović, R., 2001, "A priori meshes for singularly perturbed quasilinear two point boundary value problems," *IMA J. Numer. Anal.* **21**, 349–366.

[289] Vulanović, R., and Hovhannisyan, G., 2006, "A posteriori error estimates for one-dimensional convection-diffussion problems," *Comput. Math. Appl.* **51**, 915–926.

[290] Vulanović, R., and Teofanov, L., 2013, "A modification of the shishkin discretization mesh for one dimensional reaction diffusion problems," *Appl. Math. Comp.* **220**, 104–116.

[291] Wang, D., and Zhang, H., 2005, "Further improved F-expansion method and new exact solutions of konopelchenko-dubrovsky equation," *Chaos Solit. Fractals* **25**, 601–610.

[292] Wang, S., 1997, "An a posteriori error estimate for finite element approximations of a singularly perturbed advection-diffusion problem," *J. Comput. Appl. Math.* **87**, 227–242.

[293] Wang, Y., Meng, X., and Li, Y., 2021, "The finite volume element method on the shishkin mesh for a singularly perturbed reaction-diffusion problem," *Comput. Math. Appl.* **84**, 112–127.

[294] Xenophontos, C., Franz, S., and Ludwig, L., 2016, "Finite element approximation of convection diffusion problems using an exponentially graded mesh," *Comput. Math. Appl.* **72**, 1532–1540.

[295] Yadav, R. P., Rai, P., and Sharma, K. K., 2023, "NIPG finite element method for convection-dominated diffusion problems with discontinuous data," *Int. J. Comput. Methods* **20**, 2350001.

[296] Yadav, S., and Rai, P., 2023, "A parameter uniform higher order scheme for 2d singularly perturbed parabolic convection-diffusion problem with turning point," *Math. Comput. Simulation* **205**, 507–531.

[297] Zhang, B., Chen, S., and Zhao, J., 2014, "A posteriori error estimation based on conservative flux reconstruction for nonconforming finite element approximations to a singularly perturbed reaction–diffusion problem on anisotropic meshes," *Appl. Math. Comput.* **232**, 1062–1075.

[298] Zhang, J., and Liu, X., 2019, "Superconvergence of finite element method for singularly perturbed convection-diffusion equations in 1-D," *Appl. Math. Lett.* **98**, 278–283.

[299] Zhang, Z., 2002, "Finite element superconvergence approximation for one-dimensional singularly perturbed problems," *Numer. Methods Partial Differ. Equ.* **18**, 374–395.

[300] Zheng, Q., Zheng, X., and Liu, Y., 2014, "Uniform second order hybrid schemes on Bakhvalov-Shishkin mesh for quasilinear convection diffusion problems," *Adv. Mat. Res.* **871**, 135–140.

[301] Zienkiewicz, O., Gallagher, R., and Hood, P., 1975, "Newtonian and non-Newtonian viscous impompressible flow. temperature induced flows and finite elements solutions. the mathematics of finite elements and applications," *Academic Press, London*, 235–267.

List of Publications

1. Aditya Kaushik, Manju Sharma, Aastha Gupta and Monika Choudhary, Iterative analytic approximation to one-dimensional nonlinear reaction–diffusion equations, Mathematical Methods in the Applied Sciences, 44, 12152– 12168 (2021). **SCIE, IF 3.007**

2. Aditya Kaushik and Monika Choudhary, A higher-order uniformly convergent defect correction method for singularly perturbed convection-diffusion problems on an adaptive mesh, Alexandria Engineering Journal, 61, 9911-9920 (2022) **SCIE, IF 6.626**.

3. Monika Choudhary and Aditya Kaushik, A uniformly convergent defect correction method for parabolic singular perturbation problems with a large delay, Journal of Applied Mathematics and Computing, 69, 1377–1401 (2023). **SCIE, IF 2.196**.

4. Aditya Kaushik and Monika Choudhary, A higher-order defect correction method over an adaptive Bakhvalov-Shishkin mesh for advection-diffusion equations, Iranian Journal of Science, 47, 1221–1232 (2023) (2023). **SCIE, IF 1.70**

5. Monika Choudhary and Aditya Kaushik, A uniformly convergent defect correction method for parabolic singular perturbation problems with discontinuous convection coefficient and source term, International Journal of Computational Methods, https://doi.org/10.1142/S0219876223500172, (2023). **SCIE, IF 1.70**

Papers presented in International Conferences

1. “A defect correction method for singularly perturbed convection-diffusion problem on Shishkin mesh", International Conference on Innovations in Physical Sciences, Chaudhary Charan Singh University, Meerut. August 09-11, 2019.

2. “The parameter uniform defect correction method on a novel Shishkin-type mesh for linear singularly perturbed convection-diffusion problem", International Conference on Integrated Interdisciplinary Innovations in Engineering, Panjab University, Chandigarh. August 28-30, 2020.